WIRELESS SENSOR NETWORKS BASED MONITORING OF SLOPE STABILITY OVER OLD UNDERGROUND COAL WORKINGS

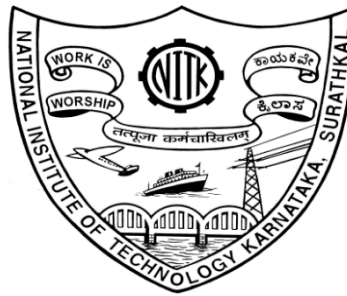**Thesis**

Submitted in partial fulfillment of the requirements for the degree of
DOCTOR OF PHILOSOPHY

by

Kumar Dorthi

Reg. No. MN14F03

DEPARTMENT OF MINING ENGINEERING

NATIONAL INSTITUTE OF TECHNOLOGY KARNATAKA

SURATHKAL, MANGALORE – 575025, INDIA

May, 2019

I hereby *declare* that the Research Thesis entitled "Wireless Sensor Networks based Monitoring of Slope Stability over Old Underground Coal workings," which is being submitted to the National Institute of Technology Karnataka, Surathkal in partial fulfillment of the requirements for the award of the Degree of Doctor of Philosophy in Department of Mining Engineering is a *bonafide report of the research work carried out by me*. The material contained in this Research Thesis has not been submitted to any University or Institution for the award of any degree.

Kumar Dorthi,

Reg. No.148023MN14F03,

Department of Mining Engineering

Place: NITK, Surathkal

Date:

CERTIFICATE

This is to *certify* that the Research Thesis entitled "Wireless Sensor Networks based Monitoring of Slope Stability over Old Underground Coal workings," submitted by Kumar Dorthi (Register Number: 148023MN14F03) as the record of the research work carried out by him, is *accepted as the Research Thesis submission* in partial fulfillment of the requirements for the award of the degree of Doctor of Philosophy.

Research Guide(s)

(Name and signature with Date and Seal)

Chairman-DRPC

(Signature with Date and Seal)

ACKNOWLEDGEMENTS

ABSTRACT

Coal is primary energy source in India for generation of electricity and other industrial uses. Though Indian coal industry is one of the oldest in the world, but still India is importing coal for domestic needs. In order to increase the production of coal, many approaches are being used such as shortwall, highwall longwall mining etc. One of them is conversion of the old underground workings where coal is blocked in the form pillars into opencast projects. In the olden days, coal seams were developed using bord & pillar method of working and due to various technical reasons like strata control or fire, these were either partially depillared or not depillared yet and the panels were closed permanently. The coal left out was supposed to be a permanent loss of natural resource. Such panels are being extracted using surface mining methods. But, there are some problems in conversion of underground galleries into opencast projects like the stability of slopes and collapse of partitions due to the moment of Heavy Earth Moving Machinery (HEMM). Factors leading to the stability of old underground workings include material properties of the partition/cover, thickness of cover/partition, movement of machinery, dimensions of old workings and relative position of the underground workings to the mine bench as the bench progresses. These factors may lead to slope failures and cause damage to equipment and loss of human lives. Monitoring of stability of partition and slope is required over old underground galleries. Partition and slope monitoring is generally carried out with conventional methods. In many of the cases, the data is acquired and analyzed in off-line. In such type of monitoring, the physical presence of a person is required at the site, the readout units are physically connected to the base units and generally, such monitoring can be done only during daylight. On the other hand, the wireless-based instrumentation like Slope Stability Radar (SSR) can monitor slope moments effectively but these are highly technology-based and very expensive.

In order to address this ambiguity and to get real-time data to study the dynamic behavior of workings, a low cost, state of the art Zigbee based Wireless Data Acquisition System (WDAQ) was developed. It consists of sensing unit, Wireless DAQ and base station. Institute of Electrical and Electronics Engineers (IEEE)

802.15.4 standard of Zigbee wireless communication network was used for collecting and sending data from monitoring point to base station. Field investigations were carried out in two large opencast mines where conversion of old galleries are being done in southern India. In total, 144 locations were monitored, at each location data was captured for about 5hours to 8hours. A conventional data logger was used with the similar set of sensors for validation of zigbee based WDAQ. The variation between Zigbee based WDAQ and data logger is around 10.27% to 13.30% which says zigbee based WDAQ data is very reliable.

Numerical modeling approach was used for simulating field conditions and to assess the influence of geometrical dimensions, rock properties and external load on the stability of old underground coal workings. Geometrical dimensions includes gallery width, gallery height, pillar width, partition thickness, slope angle and berm width. Regression analysis was carried out to evaluate the influence and relative significance of various parameters.

Regression analysis results revealed that external load was found to be the most influencing parameter on the stability of old underground galleries. Pillar width and gallery width were found to be second and third most important parameters. Partition thickness was found to be the fourth most influencing parameter. Gallery height, Slope angle and berm width were found to be fifth, sixth and seventh most important parameters respectively considered in this study. Density of sandstone was found to be eighth most important parameter and followed by compressive strength of sandstone. Similarly, density and compressive strength of coal was found to be tenth and eleventh position to influence the stability of old galleries.

Further analysis was carried out for developing design guidelines for safe extraction of old galleries. Design guidelines were developed based on FOS which was determined using Mohr-Coulomb theory in numerical modeling studies.

In this study, FOS was categorized as unsafe, moderately safe and highly safe. If FOS was more than '2.0', the model considered as highly safe. If FOS was in between '1.5'

to '2.0', the model considered as moderately safe. If FOS is below '1.5', it was considered as unsafe. Therefore, the design guidelines recommended that the partition thickness with respect to the slope angle for different gallery widths, pillar widths, gallery heights, berm width, rock properties, external load was based on FOS of "highly safe" and "moderately safe".

Finally, a user-friendly software was developed to use the guidelines in simple way. The software takes input as geometrical dimensions, rock properties and external load. Optimum partition thickness, slope angle and FOS are output parameters for given input.

ACRONYMS

ADC	Analog to Digital Conversion
ANOVA	Analysis of Variance
CIL	Coal India Limited
FEM	Finite Element Method
FOS	Factor of Safety
GUI	Graphical User Interface
GSM	Global System for Mobile
GPS	Global Positioning System
GPRS	General Packet Radio Service
GSI	Geological Survey of India
HEMM	Heavy Earth Moving Machinery
ICT	Information and Communication Technology
IDE	Integrated Development Environment
IEA	International Energy Agency
IEEE	Institute of Electrical and Electronics Engineers
ISM	Industrial Scientific and Medical radio
ISRM	International Society for Rock Mechanics
LiDAR	Light Detection and Ranging
LVDT	Linear Variable Differential Transformer
OC	Opencast
RGOCP-I	Ramagundam Opencast Project-I
RGOCP-III	Ramagundam Opencast Project-III
SCCL	The Singareni Collieries Company Limited
SPSS	Statistical Package for Social Sciences
SSR	Slope Stability Radar
TDR	Time Domain Reflectometry
UG	Underground
USB	Universal Serial Bus
USN	Ubiquitous Sensor Network

ACRONYMS

WDAQ	Wireless Data Acquisition System
Wi-Fi	Wireless Fidelity
WSN	Wireless Sensor Networks

LIST OF CONTENTS

LIST OF FIGURES

LIST OF TABLES

INTRODUCTION

Coal is the prime source for generation of electrical power in many countries including in India. It is the second largest fuel in terms of energy consumption (Fig. 1.1). Coal provides 30.1% of global primary energy needs and generates over 40% of the world's electricity. It is also used in the production of over 70% of the world's steel and it is more than any other fuel (BP statistical review, 2017). The International Energy Agency (IEA) estimates that global electricity demand could double between 2009 and 2035 as more people get basic access to electricity around the world and household energy consumption grows in the developing world.
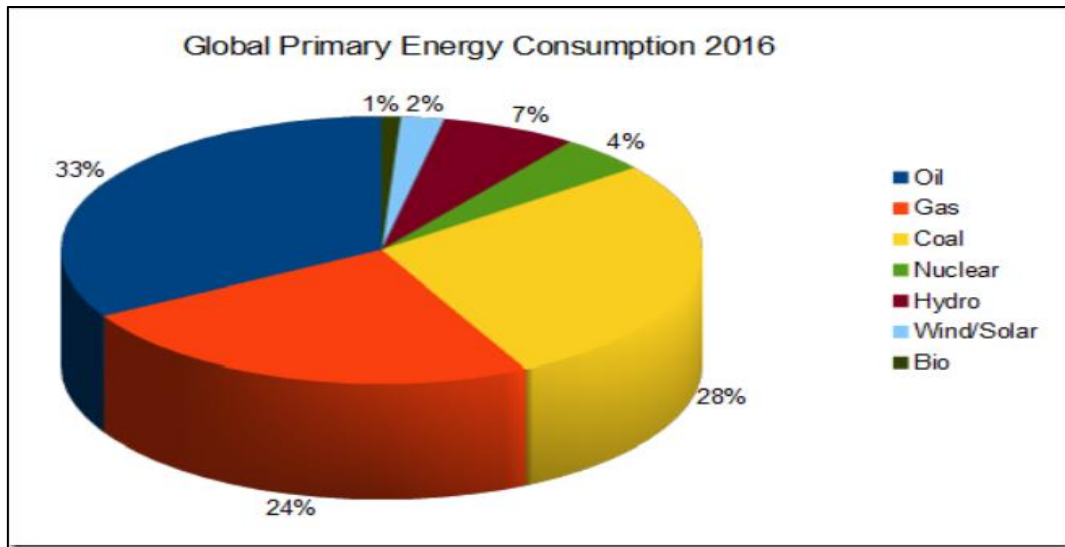
Fig. 1.1 Global primary energy consumption in 2017-18 (BP statistical, 2018)

During the same period, global steel demand is likely to go up by around 60%, as a result of rapid urbanization in Asia and the increase in steel consumption by the construction sector. Present scenario shows that with growing energy demand around the world, coal continues to play an important role in the global energy mix up to 2035. In India, commercial primary energy consumption has grown by about 700% in the last four decades. The current *per capita* commercial primary energy consumption

in India is 606.1kgoe/year in 2013 and it is expected to increase up to 1250 kgoe/year by 2031-32 due to increasing population, expanding economy and improved quality of life. By the year 2031-32, projected coal demand and total energy requirements are shown in Fig. l.2. Coal has been the most important source of energy for power generation in India. It accounts for 52% of the country's energy need and around 66% of power generation. The majority of coal output is consumed by (71%) power sector and 7% by steel sector and the remaining for different sectors like cement, fertilizers, chemicals, paper and other medium and small-scale industries (Energy Statistics, 2017).
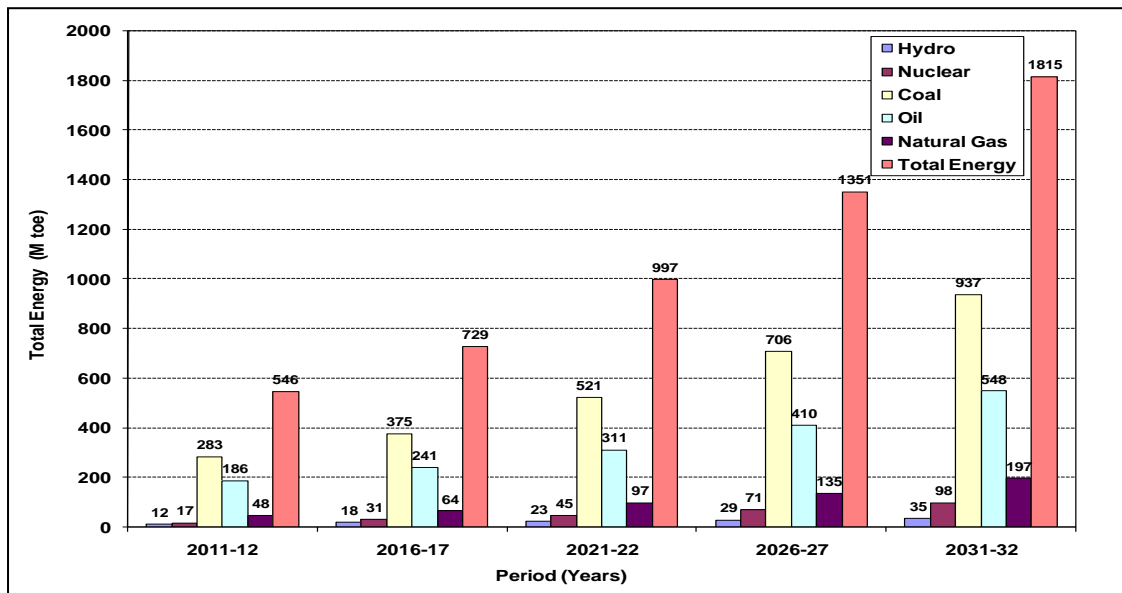
Fig. 1.2 Projected demand of total energy requirement in India (Energy Statistics, 2017)

Coal is extracted by both surface and underground coal mining methods. Surface mining is a form of mining in which the top soil and the rock covering the mineral deposits are removed. Surface mining carried out when the deposits are found closer to the surface. Underground mining is carried out when mineral deposits are located at greater depth. Room and pillar, longwall mining, short wall mining, blasting gallery are methods of underground coal mining. Open pit mining is a very cost-effective mining method allowing a high level of mechanization and large production and productivity. Opencast method of mining leads the coal production in India and has a

share of more than 93.91% (Fig. 1.3). Further, the productivity of opencast mines is much higher as compared to the underground mines.
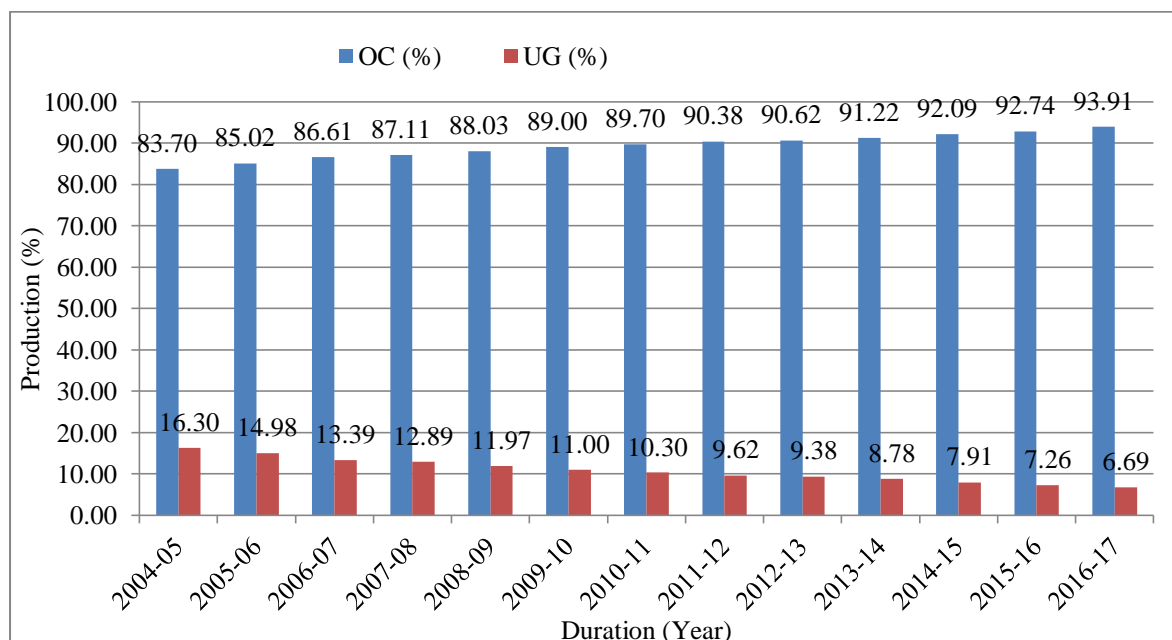
Fig. 1.3 Coal production in India (Coal Statistics, 2016-17)

Demand for coal has been increasing day by day to meet the requirements of various industries. Demand and supply gap has been increasing every year gradually. In this process, conversion of old underground coal workings where coal is left in the form of pillars and roof is carried out to meet the demand and supply gap to certain extent. These reserves in India are of shallow to medium depth. Extraction of such coal seams was initially done by bord and pillar method of mining. However, many panels were abandoned after development and no depillaring operations were undertaken due to unscientific methods of mining and some geo-technical/strata control problems. In some cases, even the depillaring was done, still a large quantity of coal was left as supporting pillars.

Prasad (1986) stated that in Jharia coalfields alone about 800Mt of coking coal was blocked in the form of supporting pillars and also in the roof. There are nearly 3.0 to 3.5 billion tons of coal reserves in standing pillars in India (Mahto, 2015).

3

Opencast mining methods have been adopted to extract the coal which is in the form of pillars and roof in old underground coal workings. There are some problems associated with the conversion of old underground coal workings into opencast mines. In some projects, the coal blocked in old workings is being extracted, but due to lack of specific technical guidelines, there were many accidents like falling down of men and machinery into the underground galleries and failure of slopes over old underground workings. Factors leading to the stability of old underground workings include material properties of the partition/cover, thickness of cover/partition, movement of machinery, dimensions of old workings and relative position of the underground workings to the mine bench as the bench progresses. These factors may lead to slope failures and cause damage to equipment and loss of human lives.

Monitoring of stability of partition and slope is required over old underground galleries. The selection of a monitoring system is based on its reliability and capabilities. It requires a thorough understanding of displacement patterns that result from generally occurring mechanisms of failure. Different methods are available for monitoring slope in open cast mines. These methods are classified into subsurface and surface monitoring methods and are used to measure both geometrical and physical parameters such as distance changes between points / deformation, tilt angles, borehole profiles, stresses and ground-water pressures etc. Monitoring of slope is generally carried out with conventional methods earlier. In conventional methods of monitoring, different instruments used directly or indirectly are wireline extensometer, inclinometer, borehole extensometer, settlement gauge, tilt meter, pore pressure gauge, rainfall gauge, crack meter, etc.

The recent and emerging technologies used to monitor slopes are Automated Total station, LIDAR (Light Detection and Ranging) scanning, Global Positioning System (GPS), Time Domain Reflectometery (TDR), Digital Photogrammetry, High-resolution micro-seismic monitoring and Slope Stability Radar (SSR). In many of the cases, the data is acquired and analyzed in off-line. Physical presence of the person is required at the site and the readout units are physically connected to the base units and generally such monitoring can be done only during day light. On the other hand, the

wireless based instrumentation like Slope Stability Radar (SSR) can monitor slope moments effectively but these are highly technology based and very expensive.

In order to address this ambiguity and to get real-time data for online data analysis and display to study the dynamic behavior of partition and slopes, a data acquisition and analysis system with advanced wireless technology is required. Developments in Information and Communications Technology (ICT) supports the connection, collection and analysis of data through sensing and interfacing with wireless data communication systems can be used to make revolution in real time data monitoring systems in mines.

Wireless Sensor Network (WSN) of low-complexity, low power consumption, low-cost and two-way communication, is an effective approach for the real-time monitoring of partition and slope instabilities over old underground coal workings during surface mining operations. This network has the capability to provide real-time data through Internet. It can also be used to issue warnings ahead of failure time through the early warning system. It allows the operation to continue to mine and to monitor optimizing extraction while maintaining the safety of personnel and equipment in opencast mines.

1.1 Research Problem Statement

Stability of benches over old underground workings is a big challenge when mined with opencast mining methods, because slope or partition failure causes damage to equipment and loss of human lives. There are many parameters that influence the stability of benches over old underground workings such as material properties of the cover / partition, thickness of cover / partition, movement of machinery, dimensions of the old workings and relative position of the underground workings to the mine bench as the bench progresses. An optimum design methodology is, therefore, essential for maintaining stable partition/cover and optimum slope over old underground workings.

It is aimed to propose a set of instrumentation for monitoring and also proposing state-of-the-art and cost-effective Wireless Sensor Networks (WSNs) for real-time monitoring of partition and slope deformation over old underground workings. The study considered the different parameters such as weight of machinery, partition thickness and gallery dimensions using filed investigations as well as numerical modeling approach. Finally, guidelines are developed for safe extraction of coal from old underground workings and also to optimize slope angles and partition cover.

1.2 Objectives of the Study

Major objectives of research work are as follows:

1. To develop state-of-the-art Wireless Sensor Networks (WSNs) based system for monitoring the deformation/strain in partition/cover and slopes over the old underground workings.

2. To identify and assess the influence of various parameters which affect the stability of old underground workings on surface workings using numerical modeling along with field investigations. The parameters considered are:
   - Width of gallery
   - Height of gallery
   - Partition thickness
   - Berm width
   - Width of pillar
   - Rock properties

3. To assess the influence of moment of Heavy Earth Moving Machinery (HEMM) on the stability of workings.

4. To develop design guidelines for safe extraction of coal blocked under old underground workings using surface mining methods and also to develop a user-friendly comprehensive software package.

1.3 Organization of the Thesis

The thesis is divided into five major chapters.

Chapter-1 gives a brief introduction to the research topic giving the background information. Introduction includes coal production and consumption in India, various coal mining methods, problems associated with the conversion of old underground galleries with surface mining operations, Conventional instruments for slope monitoring systems and also gives an outline of the background to the research problem along with objectives.

Chapter-2 provides a comprehensive review of the literature. It includes the review of related work carried out by various researchers in this area of research. Literature related to the studies describing the coal production, different conversion methods of old underground galleries, problems with conversion methods, conventional slope stability monitoring systems, wireless sensor networks and its applications and numerical modeling and regression analysis are discussed in this chapter.

Chapter-3 deals with the methodology adopted for the research study and details of field investigations. Field instrumentation adopted and details of the field monitoring programme are given in this chapter. Numerical modeling studies using Ansys software for simulation and analysis to assess the influence of various geometrical parameters are described. Regression analysis using Statistical Package for the Social Sciences (SPSS) software is discussed in this chapter.

Chapter-4 describes the results obtained from field investigations and numerical modeling studies. SPSS based regression analysis for field and numerical modeling data as the parametric study is discussed. Further, design guidelines recommended for safe extraction of old underground galleries and details of self-developed software for design guidelines in a simple manner are presented in this chapter.

Chapter-5 gives significant conclusions drawn from the research carried out and recommendations for the future work.

A novel approach to adopt state-of-the-art Wireless Sensor Networks (WSNs) based system for monitoring the deformation/strain in the partition and slope over the old underground coal workings as an innovation is presented in the thesis.

REVIEW OF LITERATURE

This chapter deals with a brief review on coal mining, conversion of old underground workings into surface mine, problems associated with conversion, factors influencing slope stability over old underground coal workings, conventional slope monitoring systems, Wireless Sensor Networks(WSNs) and numerical modeling methods.

2.1 Coal Mining in India

Coal is an ignitable dark rock comprising predominantly of carbonized plant matter, which can be utilized as fuel. India is the third largest producer of coal in the world after China and United States. Coal is widely used in Indian power industry to generate electricity. It has significant contribution in industrialization and contributes a total of 55% of commercial energy production in India (Hussain and Aquil, 2014). According to the Geological Survey of India, a cumulative total of 315.148 billion tonnes of geological resources of coal have been estimated so far in the country as on 01.04.2017 (Geological Survey of India, 2017). Coal reserves in different states of the country and coal producing companies are shown in Table 2.1 and Figure 2.1 respectively. Coal deposits are located in the Lower Gondwana sediments and the early Tertiary sediments. Major Gondwana coalfield spreads in the states of Uttar Pradesh, Jharkhand, Odisha, Madhya Pradesh, Chattisgarh, West Bengal, Maharashtra and Telangana states. While minor ones are located in Singrimari area of Garo Hills, Himalayan foot hills of Darjeeling district of Bengal west state and Arunachal Pradesh. Tertiary coal constitutes a small portion of the total coal resources occurring in north-eastern states of Assam, Meghalaya, Arunachal Pradesh and Nagaland.

Table 2.1 State-wise break-up of Indian coal resources (Geological Survey of India, 2017)

State	Inventory of Geological Reserves of Coal in India (Mt)
Jharkhand	83,439.52
Odisha	77,284.84
Chhattisgarh	56,661.16
West Bengal	31,667.22
Madhya Pradesh	27,673.20
Telangana	21,464.31
Maharashtra	12,259.16
Andhra Pradesh	1,580.70
Bihar	1,353.50
Uttar Pradesh	1,061.80
Meghalaya	576.48
Assam	525.01
Nagaland	410.45
Sikkim	101.23
Arunachal Pradesh	90.23
Total	**315,148.81**
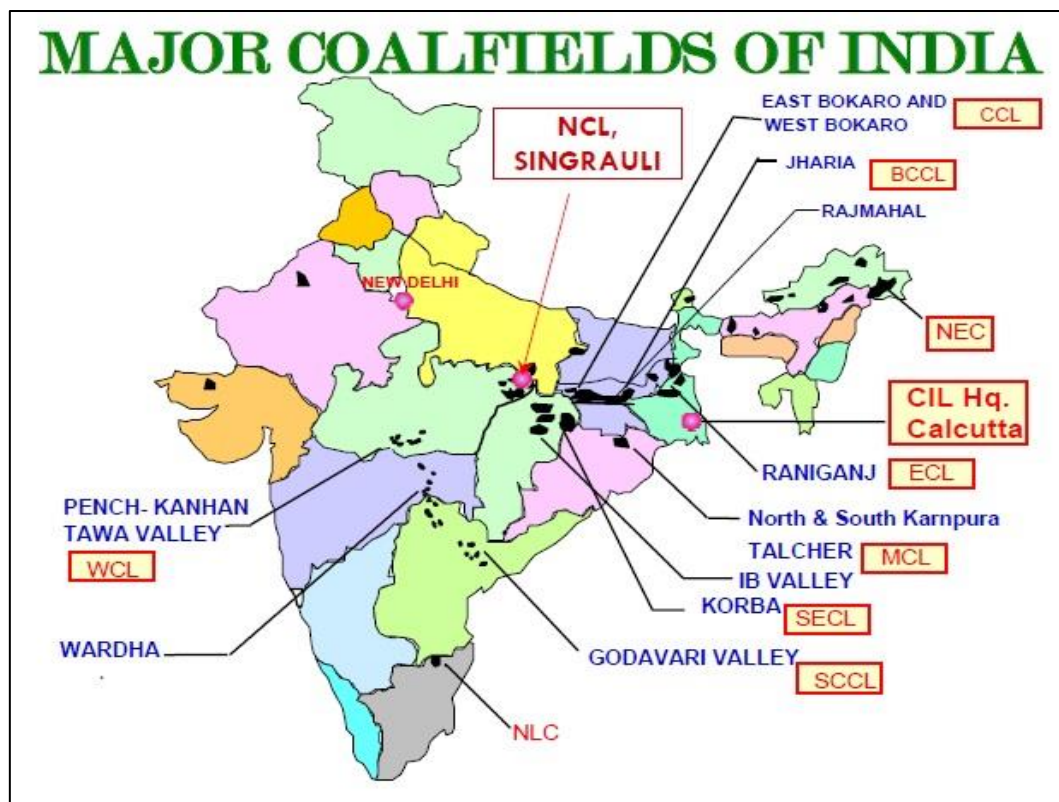
Fig. 2.1 Major coalfields of India (Courtesy: Maps of India)

Surface mining and underground mining are two mining methods to extract coal. There are five main methods of surface mining for extraction of coal such as strip mining, open-pit mining, and highwall mining.

Strip mining: It is the removal of soil and rock (overburden) above a layer or seam (particularly coal), followed by the removal of the exposed mineral. The common strip-mining techniques are classified as area mining or contour mining on the basis of the deposit geometry and type. The cycle of operations for both techniques consists of vegetation clearing, soil removal, drilling and blasting of overburden (if needed), stripping, removal of the coal and reclamation.

Open-pit mining: It is also known as opencast mining and open-cut mining. It is a process of digging out rock or minerals from the earth by their elimination from an open pit.

Highwall mining: Highwall mining is a method of mining, originated from auger mining that involves the use of a remote-controlled mining machine, which is driven into a coal seam to extract the coal. This method is often used to access coal left behind from previous mining operations or when difficult geological conditions restrict the use of other mining methods. Coal is extracted from the base of a cliff (a highwall) using horizontal or inclined drilling to create holes in the coal seam left in barriers of highwall of opencast mine.

Underground mining is carried out when minerals deposits are located at a depth far beneath the ground to be extracted with surface mining. Bord and pillar, longwall mining, short wall mining and continuous mining are methods of underground coal mining.

Bord and pillar method of mining involves the driving of a series of narrow headings in coal seam parallel to each other. These headings are connected by cross headings so as to form pillars for subsequent extraction either partially or completely. Ideally,

the pillar should be square but they are sometimes rectangular or of rhombus shape and the galleries surrounding the pillars are invariably of the square cross-section.

Longwall mining: It is a highly productive underground coal mining method where a long wall of coal is mined in a single slice, typically of thickness 0.6 m to 1.0 m. Long wall mining is used to create longwall mining face by driving a roadway at right angles between two roadways that forms of the sides of the longwall block, with one rib of this new roadway forming the longwall face. Maximum block of coal is being extracted by this method.

Shortwall mining: It is similar to longwall mining but with shorter face length, with the aim of controlling the caving nature of the overlying upper strata, the load on support and the overall operation of the supports applied at the face.

Continuous mining: Continuous mining machine cuts or rips coal from the face and loads it onto conveyors or into shuttle cars in a continuous operation. Thus, the drilling and blasting operations are eliminated, along with the necessity for working several headings in order to have a heading available for loading at all times.

Year-wise comparison between opencast and underground coal production in India for the last decade is given in Table 2.2. It shows that India has produced about 662.792Mt of coal in the year 2016-17 compared to 639.23Mt in the year 2015-16. It has been observed that there is a 48.21% increase in coal production from opencast mines and 28.87% decrease in coal production from underground mines for the period 2004-05 to 2016-17. It can be also observed that the production of coal in opencast projects had been increased by around 30-40Mt during the period 2004-05 to 2009-10 and 2014-15 to 2016-17. The rate of increase of coal production from opencast mines has decreased by around 5-15Mt during the period 2010-11 to 2013-14.

In underground projects, coal production decreased by 2-3Mt for the period 2004-05 to 2006-07 and it remained consistent till 2009-10 and later, it has decreased by almost 2-4Mt each year (Fig. 2.2). Compared to underground mining methods,

surface mining results maximum extraction of the deposits leaving minimum in the in-situ. Hence, the production and productivity of surface mining projects will be very high. The projected demand for coal in 2016-17 was 838.68Mt and indigenous supply was only 662.792Mt. Demand and supply gap was 175Mt and it is expected to increase further. Out of the total coal production during the period 2016-2017, about 93% production came from opencast mining (Provisional Coal Statistics, 2016-17).

Opencast mines are shrinking day by day due to exhaustion of virgin coal. Extraction of coal by Underground mining is very uneconomical. In future, there will not be any virgin coal seam for opencast mining and the only alternative for coal production will be by open casting of developed pillars of underground mines. There are nearly 3 to 3.5 Bt of coal reserves in standing pillars in the country. In Singareni Collieries Company Limited (SCCL), there are 19 opencast mines and mostly working on developed pillars of old underground mines (Satynarayana, 2012). Upcoming opencast projects are being planned on old underground mines and future of mining will be very challenging for engineers.

Table 2.2 Trends in production of coal from opencast and underground mines (Provisional Coal Statistics, 2016-17)

Year	Open Cast (OC)					Under Ground (UG)					All India Raw Coal	
	Production(Mt)			OC share in(%) all India	OC growth in (%) in all India	Production(Mt)			UG share in(%) all India	UG growth in (%) in all India	Production (Mt)	Growth (%)
	CIL	SCCL	All India			CIL	SCCL	All India				
2004-05	276.534	22.329	320.266	83.700	7.290	47.041	12.974	62.349	16.300	-0.640	382.615	5.920
2005-06	297.572	23.427	346.074	85.020	8.060	45.817	12.711	60.965	14.980	-2.220	407.039	6.380
2006-07	317.591	25.831	373.134	86.610	7.820	43.322	11.876	57.698	13.390	-5.360	430.832	5.850
2007-08	335.918	27.959	398.182	87.110	6.710	43.541	12.645	58.900	12.890	2.080	457.082	6.090
2008-09	359.771	32.459	433.785	88.030	8.940	43.959	12.087	58.972	11.970	0.120	492.757	7.800
2009-10	387.997	38.460	473.519	89.000	9.160	43.262	11.969	58.523	11.000	-0.760	532.042	7.970
2010-11	391.303	39.705	477.839	89.700	0.910	40.018	11.628	54.855	10.300	-6.270	532.694	0.120
2011-12	397.445	41.573	487.993	90.380	2.120	38.393	10.638	51.957	9.620	-5.280	539.950	1.360
2012-13	414.423	41.593	504.195	90.620	3.320	37.777	11.597	52.207	9.380	0.480	556.402	3.050
2013-14	426.300	39.921	516.117	91.220	2.360	36.113	10.548	49.649	8.780	-4.900	565.766	1.680
2014-15	459.191	42.333	563.970	92.090	9.270	35.043	10.203	48.465	7.910	-2.380	612.230	8.250
2015-16	504.969	49.727	592.822	92.740	5.120	33.785	10.653	46.408	7.260	-4.240	639.230	4.380
2016-17	527.897	50.017	618.445	93.910	4.320	31.477	9.515	44.347	6.690	-4.440	662.792	3.690

CIL- Coal India Limited, SCCL - The Singareni Collieries Company Limited.
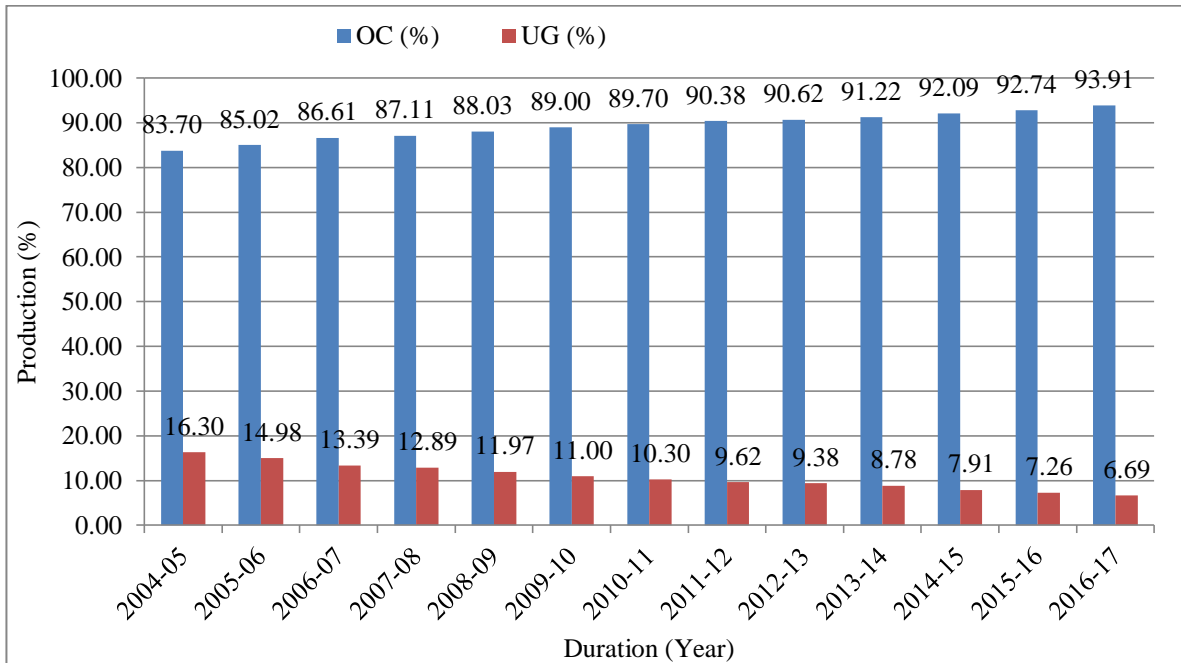
Fig. 2.2 Year wise coal production from opencast and underground mines in India

2.2 Conversion of Old Underground Workings into Surface Mines

Conversion of old underground mine into surface mine is carried out in a series of steps. It starts with a preliminary survey of the area and finally the extraction of pillars is undertaken. The steps in the process are as follows:

- Off-set survey and recording of partings
- Extraction of locked-up coal

Off-set survey and recording of partings: The detailed off-set survey has to be conducted and the position of workings including disturbances and falls should be clearly demarcated on the plan for the conversion of the underground mine into opencast mine. The steps in the survey are as follows:

- Identifying the location of parting
- Marking the position of underground galleries

Identifying the location of parting: Whenever the parting in the overburden reaches to a critical zone, the gallery junctions are marked in the field and demarcated with plan

parting on the play cards. After demarcation, drilling is done to ascertain proved parting and is recorded. Based on the proved parting, zones are demarcated in the field.

Marking the position of underground galleries: Underground galleries are marked on the surface with stone dust before drilling activity (Fig. 2.3). The marking is done in order to prevent the bogging down of the partition due to the movement of the HEMM over the partitions.

Extraction of locked-up coal

After the survey and marking of galleries, extraction of coal from pillars is carried out. Collapsing of bords method and Preservation of the working methods are the two basic methods for extraction of coal from pillars.

Fig. 2.3 Correlation of surface workings with old underground galleries

Collapsing of bords method: This method works only if all the bords collapse during blasting when considering the dead load of blasted inter-burden, it should cause the top coal over the bords to fail. In addition, toe damage at the bottom of the blastholes and cratering should assist in the collapse of the top coal into the working. The sequence of mining operations is shown schematically in Figure 2.4.

The blastholes will be drilled into the interburden to the top coal left over the bords, ensuring collapse during blasting. After blasting, dragline removes the broken overburden by leaving few centimeters above the coal seam to ensure that large quantity of coal should not get mixed up with waste rock. The dozer dozes the remaining material to dragline and prepares the top surface of the coal for drilling. After drilling into the pillars,

the blasted coal is loaded with a shovel. In some cases, to remove the coal along the floor, ripping is done if the blasting of the pillars not fragmented till the floor.

1. Overburden drilling   2. Dragline removes overburden   3. Dozer cleans to top of coal
4. Drilling pillars   5. Coaling   6. Ripping bottom coal
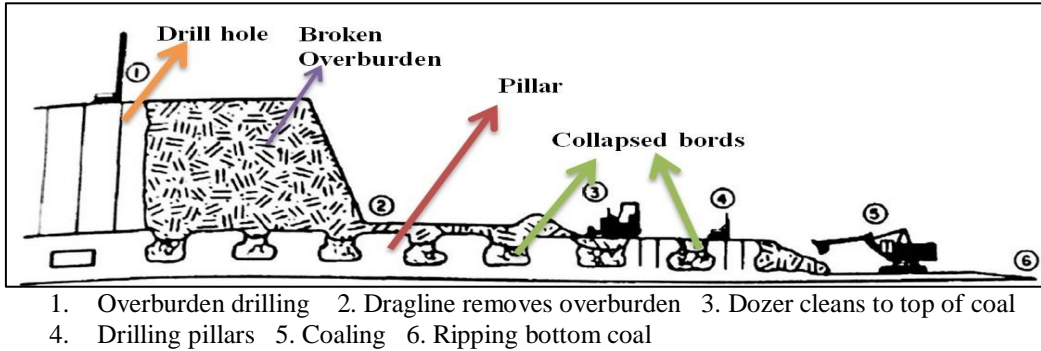
Fig. 2.4 Sequence of operations in the method of collapsing of bords (Morris and Clough, 1985)

***Preservation of the working methods*:** The main purpose of attempting to preserve the workings is to minimize waste dilution of coal. A thin coal roof may not be able to support the dead weight of broken overburden. Therefore, the only way that the workings could be kept open, would be leaving a protective beam of intact overburden over the workings. The sequence of mining operations is shown schematically in Figure 2.5. The overburden is drilled to above the roof of the bords and blasted, leaving some partition above coal. Dragline removes the broken overburden. The dozer dozes overburden beam until the top of coal seam is exposed. It prepares the top surface of the coal seam for drilling. After drilling the coal seam, the blasted coal is loaded. Sometimes ripping may be required as discussed in the previous method.

1. Overburden drilling 2. Dragline removes overburden 3. Stripping of Siltstone (overburden) beam

4.Drilling coal seam   5. Coaling   6. Ripping bottom coal
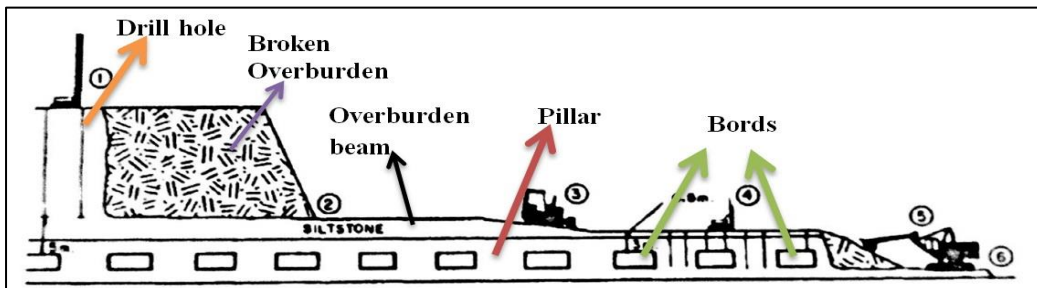
Fig. 2.5 Sequence of operations in the method of preservation of working method (Morris and Clough, 1985)

2.2.1 Problems associated with the conversion of old underground galleries

Opencast mining over old underground voids is rife with high potential risks. A large network of galleries poses a threat of collapse. Further, rock pieces can move away from underground walls. Gradual attrition can result in voids becoming significantly larger over a period of time. The potential for voids to migrate vertically and break through to the pit floor poses another major challenge. In case, a relatively thin pillar of coal has been left between the unfilled void and the pit floor or road as the pit is developed, the pillar may eventually give way into the empty void below or heavy equipment or blasting may cause the pillar to collapse. In case people or equipment fall into these voids or it collapses, serious injury or death may occur.

The major problems associated with the conversion are as follows.
- Collapsing of parting into the galleries (Bogging down of men and machinery).
- Extraction of workings leads to rock displacement and destroys slope integrity (Watters et al., 1989).
- Development of new discontinuities which loosens rock mass lead to slope failures and even alter the inclination of some critical surfaces (Morris and Clough, 1985).
- Fire due to spontaneous heating. The exposure of the coal seam to oxygen from the atmosphere generally leads to fire and loss of coal.
- Contamination of coal due to mixing with overburden.

2.2.2 Influence of old underground galleries on the stability of opencast mine

There is limited information available for extraction of coal from old underground workings using surface mining method or the influence of underground excavations on open pit slope stability.

Conversion of old underground galleries into open pit mines leads to the modification of existing structures or alternatively the developments of new discontinuities that loosen the rock mass and even alter the inclination of some critical surfaces(Morris and Clough, 1985).

Finite element analysis was used to investigate the effect of pit extractions on pillar stability since the presence of open pit extractions changed the stress distribution in pillars adjacent to the highwall and resulted in complete failure of a single pillar in underground workings (Morris and Clough, 1986). Presence of extraction, permitting rock displacement within individual benches over a period of time destroys slope integrity (Walton et al., 1989).

Physical models were used to predict ground movement in opencast mines above existing underground voids and monitored the behavior of slopes during progressive extractions. Equivalent material modeling was constructed for a section of rock mass having old workings to study the behavior of slopes. Further, the purpose was to study the extent to which the locked coal could be extracted and analyzed the behavior of the dip side and rise side slopes in the simulated section of the rock mass of the mine (Singh and Singh, 1992). Other factors that affect the stability of slopes are berm width (Sastry and Ram Chandar, 2014) and width of the gallery (Ram Chandar and Gowtham Kumar, 2014; Ram Chandar et al., 2015).

There is no research has been done for maintaining optimum partition/cover thickness and slope angle for safe extraction of old underground coal workings.

2.3 Slope Stability Monitoring Systems

Slope stability is a critical safety and production issue for surface mining. Monitoring systems, ranging from simple piezometers to highly sophisticated systems like RADAR are deployed to predict impending instabilities and failures. A review of the available monitoring systems used in slope management and highlight their major advantages and shortcomings are discussed.

2.3.1 Classification of slope stability monitoring systems

Slope monitoring in opencast mines is done by different methods. These methods are classified into three sections, namely, visual inspection, sub-surface and surface monitoring methods (Fig. 2.6). The classification of the slope monitoring systems depends on the parameters that are monitored by the system (Girard et al., 1998; Little, 2006; Ashkan Vaziri et al., 2010).

The monitoring system is used to measure both geometrical and physical parameters such as the distance between points, tilt angles, borehole profiles, stresses and ground-water pressures. Deformations or movements of the structure could be calculated from the measurements at different times (Chrzanowski, 1994; Ding et al., 1995).
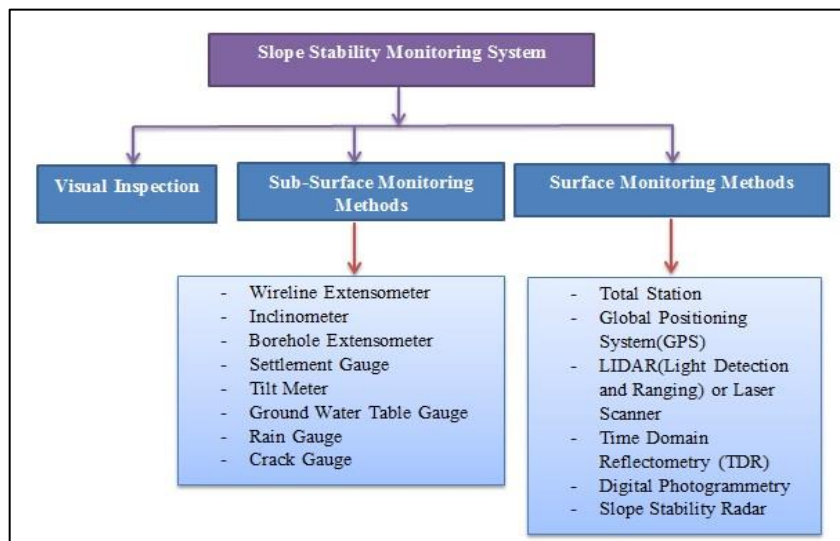
Fig. 2.6 Classification of slope monitoring techniques

2.3.1.1 Visual inspection

Visual inspection of the slope is done by routine walkover of the pit, access ways, high walls and crest that are close to potentially dangerous working areas. The last visit observations are compared with the latest one and the changes are recorded (Girard et al., 1998).

2.3.1.2 Surface monitoring methods

Surface monitoring methods can be further classified into different methods that measure the displacements at discrete points and over a large area of slopes. The recent and emerging technologies used to monitor the slope continuously are Total Station, Global Positioning System (GPS), LIDAR (Light Detection and Ranging) or Laser Scanner, Time Domain reflectometry (TDR), Digital Photogrammetry and Slope Stability Radar (SSR).

Total station: It is also known as a surveying method. It is used to monitor over a large area where access to the slope is dangerous. Target prisms situated close by regions of expected unsteadiness on the pit inclines with at least one control focuses for survey stations constitute a network (Girard et al., 1998; Girard and McHugh, 2000). Total stations must be found sufficiently near to the pit crest for good observation of all prisms and they should likewise be situated on the totally stable ground (Fig. 2.7). Electronic Distance Measurement (EDM) is the main component, which ranges from 2.7 km to 4.3 km. The measurement accuracy is in between 5 mm to 10 mm for every km. Changes that have happened, computed by the software with respect to the initial location of targets. Vertical and horizontal angles are measured with an electronic theodolite. Direction of reference is considered as vertical upward (peak) for vertical angle measurement. Accuracy of angle measurement fluctuates from 2 to 6 seconds.

There are many factors which influence the accuracy of total station such as atmospheric factors like fog and dust, human mistakes, harm to prism or movement of the survey station and blunders created by instrument or reflector set-up errors (Ding et al., 1998; Wilkins et al., 2003).

Fig. 2.7 Schematic diagram of surveying network (Girard et al., 1998)

Global Positioning System (GPS): GPS is the suitable technology used for monitoring of slopes, landslides and civil engineering sites (Sakurai and Shimizu, 2003). It is a potential tool for opencast slope monitoring.

The GPS technology used at Xiaowan, China consists of the GMAS, the GPS receivers, the data link component and data processing center (Chen et al., 2005). Integration of GPS with other monitoring instruments like total station, geographical information system and global navigation satellite system had achieved up to sub-centimeter level of accuracy (Bond et al., 2003; Casademont et al., 2004; Bond et al., 2007; Wang et al., 2010; Wheaton et al., 2012; Francioni et al., 2015). The disadvantage in using GPS for slope monitoring is expensive of installing a GPS receiver at every checking point. Accuracy relies upon components including environmental impacts and recipient quality. Leica Geosystems Inc., Motorola, Position & Navigation Systems Business, Novatel Inc., Philips Semiconductors etc., are some of the manufacturing companies of GPS.

Laser Scanner: Monitoring of every potential failure block at every location on a mine slope with survey network is impractical but a new generation of laser scanner range finders detects deformation over expansive ranges has incompletely tended to this issue. The laser scanner is an active, independent estimation technology that produces digital models of mine slopes without reflector prisms. The scanner detects displacement by comparing successive scans of the slope face (McHugh et al. 2006). A modern scanner

called SiteMonitor was initially developed by 3D Laser Mapping Ltd, UK and used in old coal mine waste tips in South Wales, UK (Fig. 2.8). It can observe displacements as small as 10mm within distance of 1000m. It also stores and analyses a minimum of 9,000 measurements per second to get a detailed, accurate and continuous record of the slope profile. The system can be worked in both automatic and manual modes. Operating distance is 2,500m with 50mm accuracy. The system can do continuous remote scanning for 24 hours at locations and collect displacement information of several points on daily basis. The software is used to detect slope deformation based on new readings from instruments and initial measurements. Advanced Laser scanner was used at Kumba Iron Ore and De Beers Kimberley diamond mine in South Africa to improve slope monitoring (Hunter, 2006). Unlike the survey system of slope monitoring, laser scanner monitors large slope face rapidly without the use of prism at an operating distance of 2,500m. Laser scanner is portable and easy to move around the mine area. Also, the risk involved in installing prisms on unstable slope face is eliminated. However, compared to the radar monitoring system, laser scanner is not commonly used for slope monitoring because of lower accuracy (Reeves et al., 2001).

Fig. 2.8 Schematic diagram of laser scanner (Hunter, 2006)

Time Domain Reflectometry (TDR): It is an electronic instrument where a cable tester connected to a coaxial cable installed in a borehole, emits a stepped voltage pulse. Rock or soil mass improvements distort the cable link interface, changing the cable link impedance and the reflected waveform of the voltage pulse (Fig. 2.9). Time delay between a transmitted stroke and the observation from a cable deformity determines the damage

23

location. The sign, length and magnitude of the observed pulse tell the type and severity of the cable deformation (Kane et al., 1996; Kane and Beck, 1999).

The usage of TDR was extended to geotechnical survey and monitoring of unstable slopes typically by burying coaxial cables in the underground (Dowding et al., 1989). While current TDR implementations can detect the exact depth of cable movement due to slope movement, the magnitude and orientation of slope movement are not found absolutely (Kane et al., 2007; Singer et al., 2010).
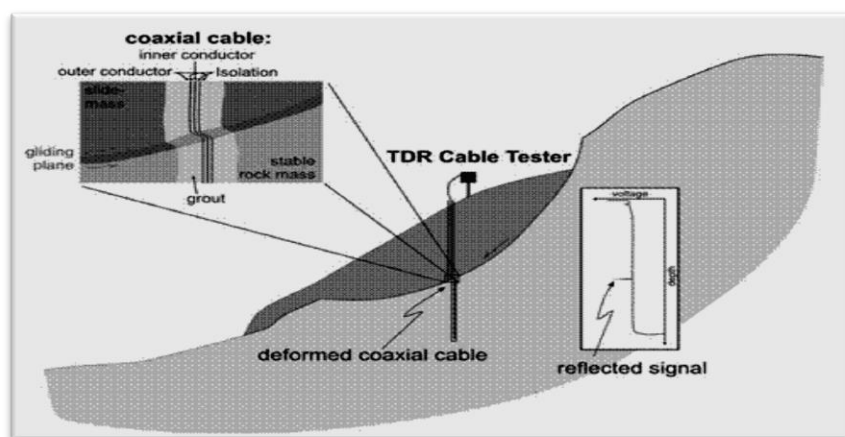
Fig. 2.9 Computer-aided data acquisition form TDR system (Kane and Beck, 1999)

Digital Photogrammetry: This works in light of the rule that, when an object is captured from two unique areas (Fig. 2.10), diverse observable pathways from every area are gotten. The observable pathways for the object from every area are intersected mathematically to produce a three-dimensional picture of the object. These pictures are then stacked onto programming which builds up a three-dimensional picture of the face. From the three dimensional picture, the area of the issues, dikes, joints and failure planes are acquired (Patikova, 2004). The procedure can be reused at standard interim to empower the distinguishing proof of new failure planes and along these lines recognize potential zones of failures (Little, 2006). The upsides of the photogrammetry can be labour saving and it gives the total information of deformation in slope face. It is inexpensive and helps in real-time measurements.
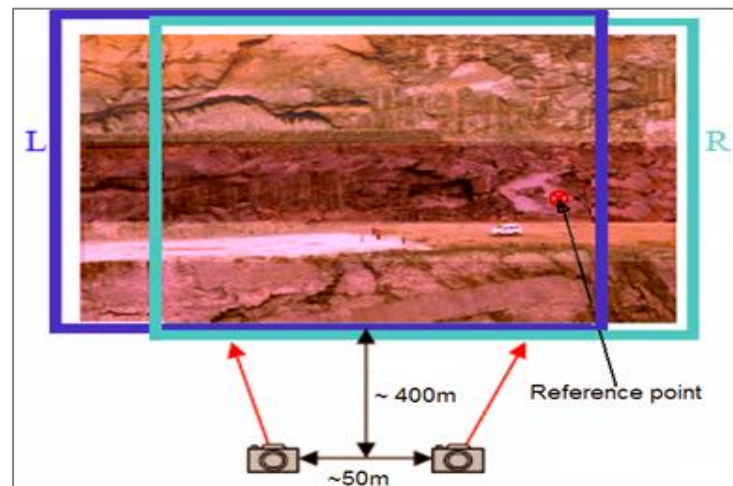
Fig. 2.10 Schematic diagram of digital photogrammetry (Little, 2006)

Radar-based slope stability monitoring systems: Radar refers to "Radio Detection and Ranging". The primary purpose of radar is to measure altitude, range, speed of an object. Nowadays, apart from military use, RADAR has found applications in many areas such as the measurement of meteorological detection of precipitation, detection of speeding traffic, slope stability monitoring etc. The most common types of RADAR used for monitoring of slope of open pit mines are Synthetic Aperture Radar, Slope Stability Radar (SSR), Movement and Surveying Radar (MSR) and IBIS-M Slope Monitoring Radar, etc.

Synthetic Aperture Radar (SAR): SAR is used to find surface disturbances or changes in surface (Girard et al. 1998). It can generate elevation maps and surface change maps by comprising two or more images of an area. It can be extended to study earthquakes, landslides, ground subsidence etc. It operates effectively in all weather conditions (Berardinoa et al., 2003; Singhroy and Molch, 2004).

Slope Stability Radar (SSR): SSR is a technology used for measuring slope deformation (Fig. 2.11). It can measure with sub-millimeter precision and gives a large area of coverage irrespective of atmospheric conditions (Reeves et al., 2001; Harries et al., 2003; McHugh et al. 2006; Yu et al., 2013). In 2010, GroundProbe introduced another slope monitoring equipment called the Work Area Monitoring (WAM). WAM uses a high-resolution camera and radar technology to allow a work production crew to quickly select an area to monitor. If the displacement is detected on the mine slope, the machine alerts

the mining personnel via wireless Personal Alerts (PALS) by displaying text messages and audio alerts.

Fig. 2.11 A view of slope stability radar (Reeves et al., 2001)

Movement and Surveying Radar (MSR): A contemporary of the SSR called the MSR-200 was introduced into the market in January, 2006 by Reutech Radar Mining, a division of Reutech Ltd., South Africa. The MSR provides fully geo-referenced surveying information thus allowing areas that are not hitherto accessible to be surveyed. This ability is made possible because the system is incorporated with a fully integrated total station, which is a surveying instrument that allows the MSR to be accurately geo-referenced. MSR is capable of measuring 3-D information of the slope surface and can also find the amount of material removed. MSR has been utilized in Africa, South America, United States of America, Europe, Indonesia, Papa New Guinea and Australia. Specifically, it had been used by Anglo Gold Ashanti in its Navachab open-pit mine in Namibia, Sadiola Gold mine in Mali and Sunrise Dam Gold mine in Australia.

IBIS-M Slope Monitoring Radar: The IBIS-M has the capacity to continuously measure mine wall movements with sub-millimeter accuracy (Fig. 2.12). It has the highest spatial resolution of 0.5m x 4.4m at 1km and the greatest operating distance of 4,000m compared with other slope monitoring radars currently available. Other unique features of the IBIS-M are its self-powered operation with a combination of solar panels and batteries, utilizing a diesel generator only as a back-up. It operates remotely through a wireless radio link.

Like the MSR and the SSR, the IBIS-M operates in all weather conditions (Farina et al., 2011; Farina and Coli, 2013).

Fig. 2.12 A view of IBIS-M slope monitoring radar (Farina and Coli, 2013)

2.3.1.3 Sub-surface monitoring methods

In this method of slope monitoring, different instruments are used directly or indirectly like wireline extensometer, inclinometer, borehole extensometer, settlement gauge, tilt meter, groundwater table gauge, rain gauge, crack gauge, etc. These instruments are used to measure both geometrical and physical parameters such as a change in between points, tilt angles, borehole profiles, stresses and ground-water pressures (Kayesa, 2006; Nunoo et al., 2015).

Piezometer: It is a device which measures the pressure of groundwater at a specific point. It is a valuable tool for evaluating the effectiveness of mine dewatering programs and the effects of seasonal variations. Water pressure data is essential for maintaining safe slopes since water behind a rock slope will decrease the resisting forces and will increase the driving forces on potentially unstable rock masses (Girard et al., 1998).

Borehole extensometer: An extensometer is used to measure the change in the length of specific objects. Borehole extensometers are specifically designed to fit easily in a standard size borehole (Fig. 2.13). Extensometers of this type are best used to monitor known structural features which will have a major influence on slope stability. These

instruments are fairly expensive when compared to other instrumentation options (Girard et al., 1998).
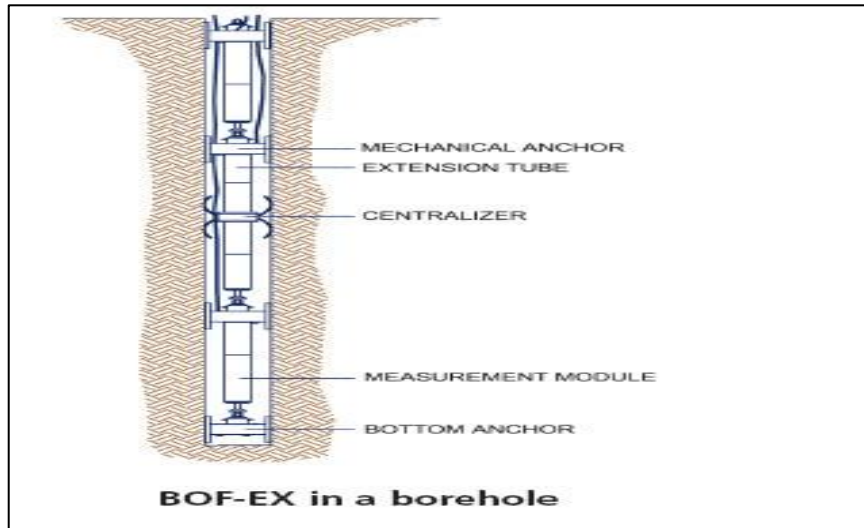
Fig. 2.13 Schematic diagram of borehole extensometer

Inclinometer is an instrument for measuring angles of slope, elevation or depression of an object with respect to gravity (Fig. 2.14). Information collected from inclinometers can be used to locate shear zones, determine whether shearing is planar or rotational and determine whether movement along a shear zone is constant, accelerating, or decelerating (Kliche, 1999; Abramson et al., 2002).
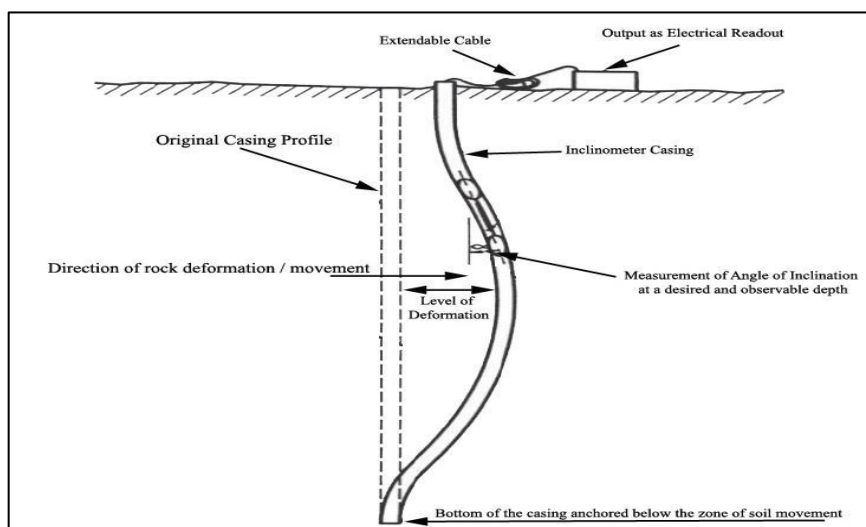
Fig. 2.14 Typical inclinometer system (Abramson et al., 2002)

2.3.1.4 Overview of slope monitoring systems

Monitoring of slope movement remains the necessity and most reliable procedure to detect slope instability. Apart from visual inspection, conventional monitoring equipment provides information of a small number of locations on the mine slope. Conventional monitoring tools are crucial and precarious to install at many surface mines where steep high-walls and improper bench limit to access the unstable locations above the working floor. Relocating monitoring equipment from one location to another is a difficult process, time-consuming and dangerous on unstable slopes. Sub surface monitoring systems require physical presence of the person at the site and the readout units which are physically connected to the base units and generally such monitoring can be done only during day light.

Comparison of slope stability monitoring systems considering different parameters such as accuracy, range, coverage, update rate, deployment etc., are discussed in Table 2.3. It can be observed from the table that total station has better accuracy compared to the other instruments. Total station is costly and skilled persons are required for conducting surveys. LiDAR scanner has better accuracy than GPS and Total station. LiDAR is ineffective during heavy rain, fog, smoke etc. and involves high cost of installation. TDR has low accuracy than other instruments and difficult to install. TDR can only locate the shear plane. It cannot provide the direction of movement. Photogrammetry has a greater scope but affected by weather conditions (Winds, clouds, haze etc.). Seasonal conditions affect the aerial photographs, i.e., snow cover will obliterate the targets and give a false ground impression. Radar-based systems such as SSR, SAR are being used to monitor the broad area through rain, dust, smoke and operate during both day and night. They provide accurate results, but they are high-cost and require a skilled person for operating in the field.

Table 2.3 Summary of slope stability monitoring systems

Technology	Accuracy	Slope Coverage	Update Rate	Range	Deployment	All Weather	Advantages	Disadvantages
Robotic Total Stations	~1 cm	Discrete Points	Twice/day	2000m	Difficult	No	Automatic operation. Long-term displacement trend.	Damaged prisms are difficult to replace. Data is affected by atmospheric variation in temperature and pressure.
Global Positioning System(GPS)	~1 cm	Discrete Points	~Seconds	4000m-20000m	Difficult	Yes	Easy automation. Less labour intensive.	High cost of installation. Satellite Signals can be obstructed.
Laser	~1 cm	Broad	~Seconds	900 m	Easy	No	Portable, continuous and automatic operation. Identifying long-term displacement.	Time-consuming in scanning. Cannot provide early warning of failure.
Time Domain Reflectometry(TDR)	~10 cm	Discrete Points	~Seconds	100m	Difficult	Yes	Rapid and remote monitoring. Low cost. Covers great depth.	Cable must be destroyed before displacement can be located. Cannot determine the magnitude and direction of slope.
Digital Photogrammetry	~1 cm	Broad	Hours	<150 m	Moderate	No	Reduced time of field work. Labor saving.	Recorded data is affected by dust and haze.
Slope Stability Radar(SSR)	± 0.2 mm	Broad	~Minutes	850 m	Easy	Yes	Continuous and automatic operation. Geo-referencing is possible	Expensive to procure and maintain. Uncontrollable down-time.

2.4 Wireless Sensor Networks (WSNs)

Slope monitoring in real-time is the prime necessity as large opencast mines are planned. WSN is the emerging technology used for real-time monitoring (Dave et al., 2013, Baronti et al., 2007). It is composed of sensor nodes, coordinator or sink node and base station (Fig. 2.15).
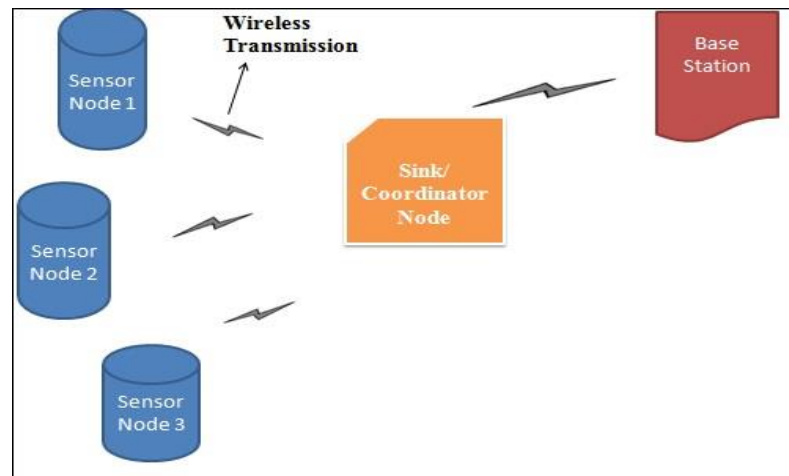
Fig. 2.15 Structure of Wireless Sensor Networks (WSNs)

Sensor node consists of sensing unit, microcontroller unit, transceiver unit and battery unit (Fig. 2.16). Sensing unit is collection of sensors and detects changes in its environment. Identification of suitable sensors is an essential requirement to monitor and detect slope instabilities. It requires detailed knowledge about slope failure phenomena along with the parameters that trigger slope failures. Basic geological data, geo-technical parameters and groundwater characteristics are used for selection of sensors. The most important parameters to be monitored for slopes or landslides are the changes in deformation, strain, stress, moisture content, pore pressure and rainfall (Ali et al., 2012; Ramesh, 2014).
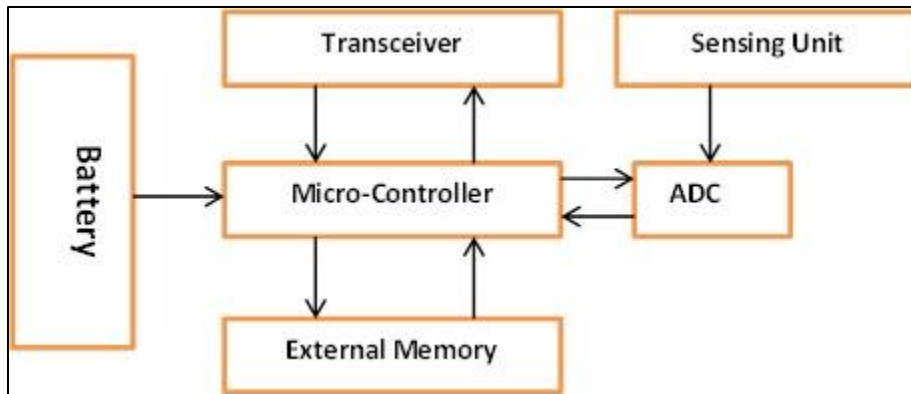
Fig. 2.16 Structure of sensor node

Microcontroller consists of Central Processing Unint (CPU) along with memory and programmable input/output peripherals and it has features like small size, low power utilization and ease of programming and an embedded ADC. It is used to process the sensor data, executes the communication protocols, signal processing and controls the sensors. Transceiver unit is used to transmit the processed data from micro controller to the sink or coordinator node. Sensor nodes in the network are communicated through transceiver unit. There are many technologies available like Bluetooth, Wi-Fi, GSM, Zigbee etc., used for transmitting data among nodes. Battery unit provides the electrical power to the sensing unit, microcontroller and transceiver unit.

Coordinator or sink node is used to gather, integrate and distribute the data from multiple sensor nodes and sent to the base station. It is also used to process the sensor data, executes the communication protocols, signal processing and controls the sensors.

Base station is also called as display unit and located in the field. It is responsible for receiving the data coming from coordinator and display the data either in analog or digital format. It consists of database server and analysis station, which performs data analysis and issue an alarm type signal incase of emergency.

2.4.1 Zigbee

Zigbee is developed and oriented to wireless network consisting of low-cost devices (Baronti et al., 2007). Zigbee transmission distance is over 10-100 m and the operating frequency band is ISM frequency band of 868 MHz, 915 MHz and 2.45 GHz respectively. Universal industrial and medical standard frequency band in the world is 2.45 GHz, providing 16 channels and transmission speed of 250 kbps (Dave et al., 2013). A total of 65,356 number of devices are allowed in the network. Zigbee consists of transmitter and receiver. Higher amount of data with higher speed is sent through Zigbee. It does not require an external signal for communication, so Zigbee technologies can be used anywhere even in forests, hill stations and industrial applications etc. In Zigbee, the transmitter sends a signal to the receiver without any delay. Receiver automatically receives a signal from the transmitter without any data loss. Here, Human interaction is not necessary for sending or receiving data as it is wireless technology (ShizhuangLin et al., 2007). Alliance of Zigbee represents a network, security and application layers whereas IEEE 802.15.4 represents physical and media access control layers (Fig. 2.17).
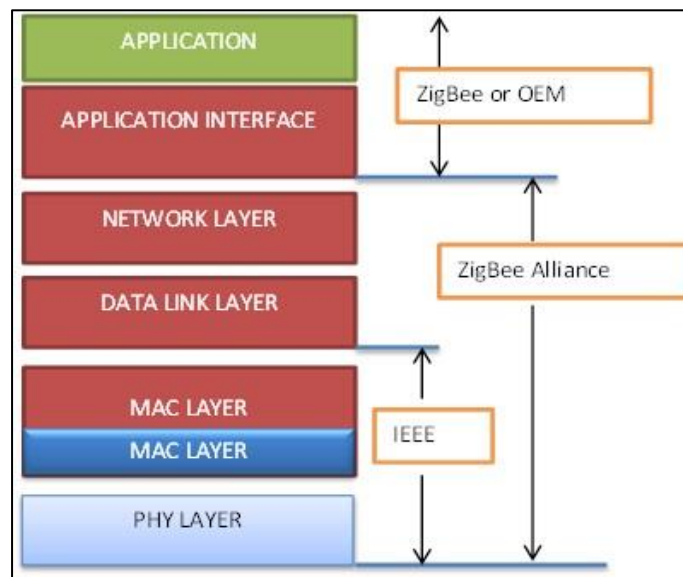
Fig. 2.17 A view of zigbee protocol stack (ShizhuangLin et al., 2007)

33

Physical Layer: This layer does modulation and demodulation operations upon transmitting and receiving signals respectively.

MAC Layer: It is a portion of Data Link Layer (DLL). This layer is responsible for reliable transmission of data by accessing different networks with the carrier sense multiple access collision avoidance (CSMA).

Network Layer: This layer takes care of all network related operations such as network setup, end device connection and disconnection to network, routing, device configurations, etc.

Application Layer: It is the effective interface of the Zigbee system to its end users.

2.4.1.1 Zigbee topologies

ZigBee supports only star, cluster and mesh topology (Somani and Patel, 2012; Kasraoui et al., 2013).

Star: It consists of coordinator at the center of network and number of end devices are connected to coordinator directly (Fig. 2.18). End devices communicate only with the coordinator and not with other end devices. Exchange of information between end devices takes place via coordinator only.

Cluster: It consists of a coordinator, router and end devices as represented in the form of a tree where all the nodes are linked up (Fig. 2.18). End devices are linked directly to the coordinator and the routers. Every end device can interact with its parent nodes i.e. router and coordinator. End device directly interacts with other devices only through its parent node. Disadvantage is that if parent node becomes disabled, children of the disabled parent node cannot interact with other devices.
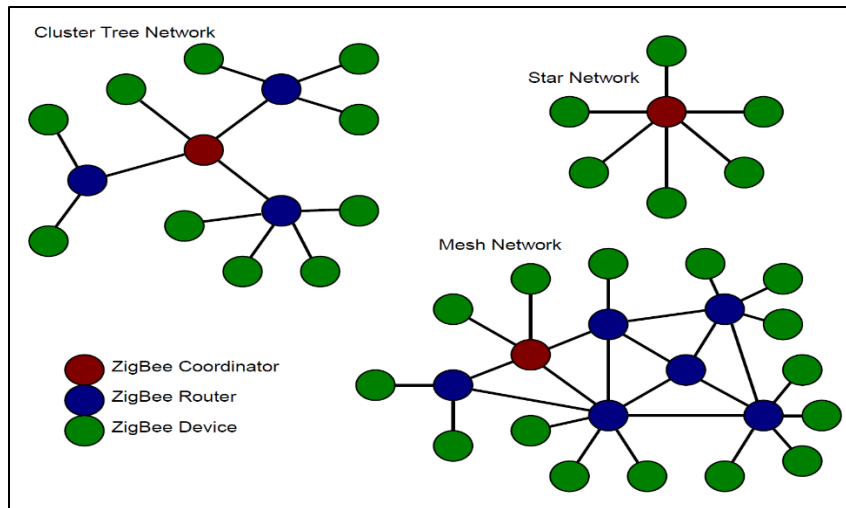
Fig. 2.18 A view of zigbee devices and network topologies

Mesh: It consists of a coordinator, routers and one or more end devices. The coordinator sends data to any device in the network. If the device or node is not in range, a message will be sent to an adjacent node which will then forward it to the endpoint. It covers a larger range while using only a fraction of the power. It has the ability of growing or shrinking depending on user requirement. It is a self-healing network i.e. during transmission of data, if any of the route fails, the node will find another route to reach the destination.

2.4.2 Comparison of wireless technologies

Zigbee technology has many advantages than other wireless technologies. The comparison among various wireless technologies is shown below Table 2.4.

Table 2.4 Comparison of various wireless technologies

Technology / Features	ZigBee	Wifi	Bluetooth	Cellular Network (GSM)
Power Profile	Years	Hours	Days	Days
Range (m)	10-100	1-100	1-10	1000
Nodes	64500	32	7	1
Latency (s)	3ms-1s	3s	10s	600ms
Extendibility	Yes	Yes	No	Yes
Data Rate	250Kb/s	11Mb/s	1Mb/s	128Kb/s
Security	High	Medium	Low	Medium
Cost	Low	High	Low	High
Application	Remote control, battery-operated products, sensors	Internet browsing, PC networking, file transfers	Wireless USB, handset, headset	Transmission of voice, data and others.

2.4.3 WSN applications

WSNs have been used in many areas like environmental monitoring, industrial automation, agriculture, disaster control, automotive, landslide prediction, structure health monitoring (Akyildiz et al., 2002; Desai and Jain, 2007; Pakzad et al., 2008).

WSN has been effectively used for real-time monitoring of landslides. Some are discussed below:

Zan et al., (2002) have developed a real-time monitoring system for landslide detection. Geophones, laser diastimeter, pressure transducer and rain gauge sensors were used to measure the parameters like seismic noise, ground displacement, piezometric level and rainfall. Based on landslide bodies, incline metric tubes used rather than borehole for installation of instruments. The system was tested on a sample landslide according to standard civil protection procedures. The entire system was capable of managing landslide area and it consisted of data acquisition card which collects data recorded by the sensors on the landslide.

Hsu-Yang Kung et al., (2006) have designed and developed Drought Forecast and Alert System (DFAS), which is a 4-tier system framework composed of Mobile Users (MUs), Ecology Monitoring Sensors (EMSs), Integrated Service Server (ISS), and Intelligent Drought Decision System (ID2S). DFAS monitored and collected all spatial and temporal ground surface information by using wireless sensor networks and network camera. MDA300 (Mote Data Acquisition) and MTS420 (Mote Sensor Board) sensors were used to sense soil moisture, air temperature, humidity, air pressure and GPS coordinate. The collected environmental drought data include the soil and air moisture, air temperature, the location of sensor devices, and 24-hour monitored drought images, which were sent and stored back to the rear database through wired/wireless network or third-generation mobile system.

A network of sensor columns was simulated for monitoring of slope on hills (Fig. 2.19). Each column included four types of sensors such as geophones, strain gages, pore pressure transducers and reflectometers. Sensor network uses a collection of instruments to detect such movements and collectively estimate the displacements of sensor nodes embedded in the hill under observation (Terzis et al., 2006).
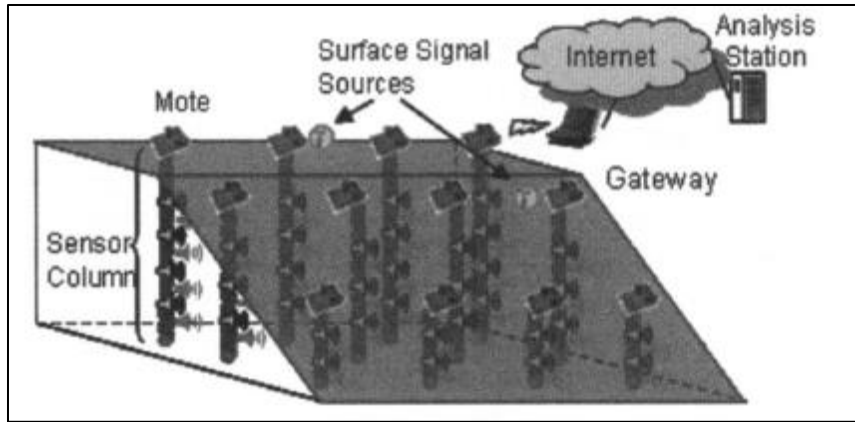
Fig. 2.19 Slope stability warning system (Terzis et al., 2006)

Kalyana T et al., (2006), proposed two distributed clustering and multi-hop routing protocols, Clustering and Multi-hop protocol (CAMP) and Heed with Beacon Vector Routing (HBVR) to reduce redundant communication from neighbor sensors so that it leads to increase the lifetime and decrease energy consumption of Wireless Sensor Network used in landslide prediction (Fig. 2.20).
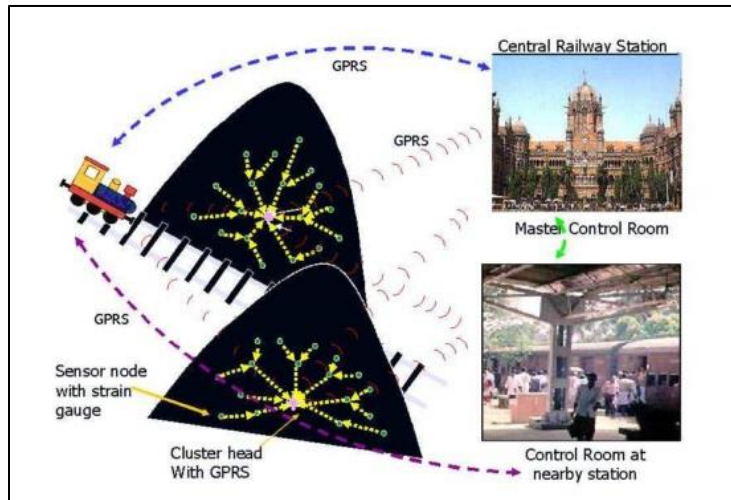
Fig. 2.20 A view of landslide prediction system (Kalyana T et al., 2006)

WSN was deployed for prediction of landslide in the rocky mountain regions of Konkan Railway. Strain gauge was installed on the surface of the rock to measure strain in the rock due to build up pressure (Prakshep et al., 2007). Evan Andrew Garich (2007) had developed a wireless sensor node, which could be deployed for remote monitoring of soil conditions. Soil moisture probes and soil tilt sensors were used and combined with low power, wireless data transmitters to form a self-configuring network of soil monitoring sensors. Ubiquitous Sensor Network (USN) technology was developed to replace existing wired-based measuring system for monitoring slopes (Kyoon-Tai Kim and Jae-Goo Han, 2008).

Ramesh, (2009) has carried out a research in estimating the chance of occurrence of landslides by using wireless sensor networks. The design, development and implementation of a Wireless Sensor Network for real-time monitoring were discussed. The actual deployment of the test bed was in the Idukki district of the Southern state of Kerala, India, a region known for its heavy rainfall, steep slopes, and frequent landslides. The geophysical sensors considered for the in-situ measurements were pore pressure transducers, soil moisture sensors, geophones, stain gauges and tilt meters.

A prototype model of early warning system was developed for different types of landslide using WSN (Fig. 2.21) (Azzam et al., 2010). Jiang Tiantian and Yang Zhanyong (2011) and Raj kumar et al., (2012) have developed prototype model based on Zigbee based wireless sensor network for monitoring the gas concentration, temperature, humidity in the coal mines.

Ali et al., (2012) carried out research on the deployment of WSN interfaced with suitable sensors for slope monitoring. The system was designed to collect the data from the sensors, transmit it to the base station, present the data with graphical representation and interprets it so that a suitable level of warning can be declared. A sensor network for

landslide monitoring was simulated at Tongji University, Shanghai. It was tested and given significant results (Scaioni et al., 2012).
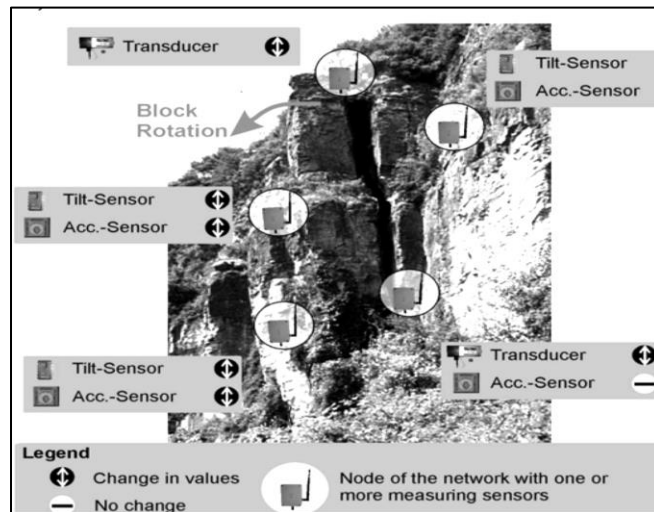
Fig. 2.21 Prototype model for slope stability monitoring (Azzam et al., 2010)

The study of Wireless Sensor Network (WSN) was made for slope stability monitoring. IEEE standard of ZigBee was used for wireless communication network. Signal transmission of WSN was tested against environmental factors such as temperature and humidity (Dave et al., 2013).

Wireless Sensor Networks (WSNs) technology is the recent emerging technology for monitoring of slopes, structures, landslides and environment etc. This network has the capability to provide real-time and online analysis of data. It can also be used to issue warnings ahead of time, using the Early warning system (Kumar and Ram Chandar, 2016). Kumar and Ram Chandar (2017) have proposed ZigBee based wireless sensor network for monitoring slopes in opencast mine. In this, ZigBee technology and GPRS are used for internal nodes monitoring and remote monitoring respectively (Fig. 2.22).
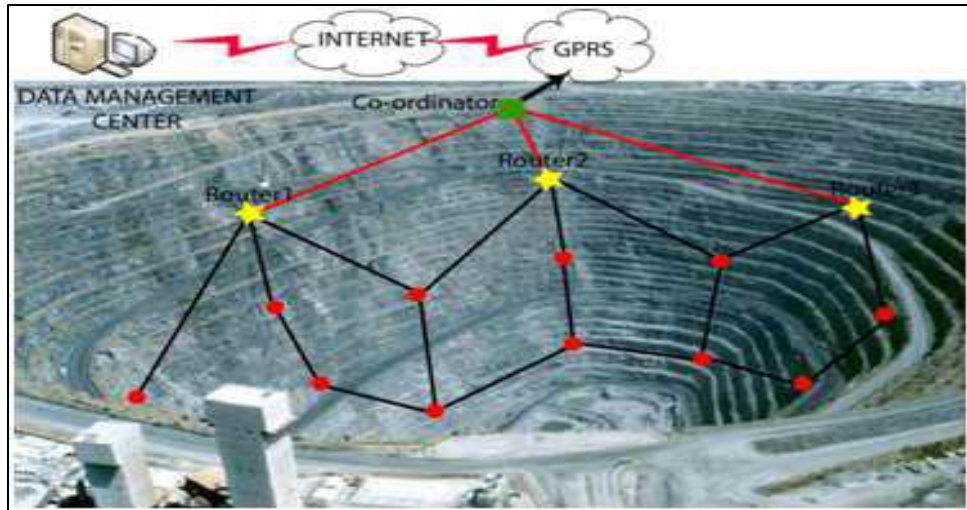
Fig. 2.22 The framework of real time monitoring system (Kumar and Ram
chandar, 2016)

2.5 Modeling

Modeling is the process of representing a model which includes its construction and
working. It gives information about how something will behave without actually testing it
in real life. It is used by scientists and engineers for prediction or understanding of a
phenomenon/system by its replication (Tolk et al., 2010).

There are three major types of modeling as briefed below.

2.5.1 Physical modeling

Physical Modeling or Equivalent Material Modeling (EMM) has been in use probably
since 1936 to understand the influence of geological features on the response of rock
mass in openings, underground excavations and stability of pillars (Azizi et al., 2013).
The parameters to be simulated are geometry, stress, strain, displacement, deformation
modulus, Poisson's ratio, volume, force, density, friction coefficient, cohesion,

compressive strength and boundary strength. An equivalent material has been plaster, paraffin, Vaseline, Portland cement, gypsum, lime, plaster, etc. with fillers like sand, mica, chalk, clay, talc, mica dust, etc. The model that is constructed with these materials is then put under scaled test conditions in the laboratory and the parameters required are measured. However, in practice it is seldom possible to attain perfect simulation (Azizi et al., 2013).

2.5.2 Analytical modeling

It is a mathematical modeling technique used for simulating, explaining, and making predictions about the mechanisms involved in complex physical processes.

Since analytical modeling is the construction and solving of a set of mathematical equations, their scope is limited in the number of parameters to be associated and it becomes cumbersome to govern number of parameters and by establishing their inter-relationships in the equation.

2.5.3 Numerical modeling

The numerical modeling approach came into existence due to the cumbersomeness of the construction of the physical model and the limited application of the analytical problem to multivariable systems.

Numerical models are the computer programs that attempt to represent the mechanical response of rock mass subjected to a set of initial conditions such as in situ stresses/strain, boundary conditions and induced changes such as slope excavation. These numerical models divide the rock mass into zones. Each zone is assigned a material model and

properties. The material models are idealized stress/strain relations that describe the material behavior (Eberhardt, 2003).

Numerical modeling can assist a mining engineer in designing underground and as well as opencast excavations and support systems. If extensive geotechnical data is given, the complete predictions of deformations, stability and support loads can be made. Numerical method has found wide applications in slope stability study of open pit mines. This widespread use is related to their ability to model the irregular structure, non-linear, non-homogeneous and anisotropic nature of rock strata.

Numerical methods commonly used to analyze the complex problems in many branches of engineering are:

     1. Continuum methods

          a. Finite Difference Method (FDM)

          b. Finite Element Method (FEM)

          c. Boundary Element Method (BEM)

     2. Discrete methods

          a. Discrete Element Method (DEM)

          b. Discrete Fracture Network (DFN) method

     3. Hybrid continuum/discrete models

          a. Hybrid FEM/BEM

          b. Hybrid FEM/DEM

          c. Other hybrid models

Continuum methods: The most notable continuum numerical methods are Finite Difference Method (FDM), Finite Element Method (FEM) and Boundary Element Method (BEM). The Finite Difference Method (FDM) is one of the oldest and widely-applied numerical methods for solving the partial differential equations that found their

application in the rock mechanics. The general principle of the method is replacing the partial derivatives of the function by the finite differences defined over a certain interval in the coordinate directions (Perrone and Kao, 1975).

The Finite Element Method (FEM) is an alternative to the finite difference method and is the numerical method for finding approximate solutions to the boundary value problems for differential equations (Clough, 1960). The general principle is to divide the domain of the problem into smaller sub-domains called finite elements, do the local approximation inside each finite element, perform the finite element assembly and find the solution of the global matrix equation. After the finite element assembly is performed, the algebraic system of equations on a global level is obtained. One of the mostly used advantages of FEM is a possibility of representing heterogeneous rocks, where it is possible to assign different material properties to different finite elements.

Boundary element method (BEM) is a numerical computational method for solving partial differential equations where the solution of weak form is obtained globally through an integral statement. The basic principle of BEM is, using the given boundary conditions, to fit boundary values into the integral equation. The main advantage of the BEM is a reduction of model dimensions by 1, so for 2D BEM problems, the boundary elements are 1D lines that can be constant, linear or quadratic. In the 3D case, the boundary elements are 2D elements.

Discrete methods: The discontinuum methods are Discrete Element Method (DEM) and Discrete Fracture Network (DFN). The DEM was developed in the field of the rock mechanic applications for modeling the discontinuous behavior (Cundall, 1971). The method is primarily defined as the computational approach that can simulate finite displacements and rotations of discrete bodies including their detachment. The main strength of the approach is the fact that the real discontinuities can be simulated, as well

as representing the rock blocks which move and interact with each other including the fragmentation process etc.

An alternative DEM for fluid flowing fractured rock masses is the Discrete Fracture Network (DFN) method that simulates fluid flow through connected fracture networks, with the matrix permeability either ignored or approximated by simple means. The stress and deformation of the fractures are generally ignored as well. This method is conceptually attractive for simulating fluid flow in fractured rocks when the permeability of the rock matrix is low compared to that of the fractures and has wide applications in groundwater flow for civil engineering, reservoir simulation in petroleum engineering and heat energy extraction in geothermal engineering.

Hybrid models are increasingly being adopted in rock slope analysis. The main types of hybrid models are the hybrid BEM/FEM, DEM/BEM models. These models have been used for a considerable time in underground rock engineering including coupled boundary finite element and coupled boundary-distinct element solutions.

Different numerical programs available for modeling rock mechanics problems are given in Table 2.5.

2.5.3.1 ANSYS software

ANSYS is a general purpose software, used to simulate interactions of all disciplines of physics, structural, vibration, fluid dynamics, heat transfer and electromagnetic for engineers. ANSYS can work integrated with other used engineering software on the desktop by adding CAD and FEA connection modules. With the development of computer techniques and the theory of generalized plastic mechanics of soil, the FEM Program such as ANSYS, make great progress in nonlinear finite element techniques. Its

Table 2.5 Numerical programmes used for rock mechanics problems

Program	Source	Type
ANSYS	ANSYS, Inc.	3D FEM
ABAQUS	ABAQUS, Inc	3D FEM
ALGOR	ALGOR, Inc.	3D FEM
BESOL/MINAP_97	Mining stress system	2D BEM
BESOL/MS	Mining stress system	3D BEM
CSIR-Minap32	CSIR Miningtel	2D BEM
DIGS	CSIR Miningtel	2D BEM
Examine 3D	Rocscience Inc.	3D FEM
FLAC	Itasca Consulting Group Inc.	2D FDM
FLAC 3D	Itasca Consulting Group Inc.	3D FDM
Map3D	Mine Modeling Ltd	3D BEM
MINNIFT	CSIR Miningtel	3D BEM
MINISIM-W	CSIR Miningtel	3D BEM
PFC2D	Itasca Consulting Group Inc.	2D DEM
PFC3D	Itasca Consulting Group Inc.	3D DEM
Phase	Rocscience Inc.	3D DEM
3.DEC	Itasca Consulting Group Inc.	3D BEM
WAVE	CSIR Miningtel	2D-3D FDM
Plaxis	Plaxis BV	2D-3D FEM
NISA	EMRC	3D FEM

pre-processing and post-processing become more and more convenient and the derived parameters such as Safety Factor and Error Estimation can be directly obtained.

ANSYS has many applications including aerospace and defense, automotive, construction, healthcare, material and chemical processing, slope stability etc., which are described below:

The analysis of rock slope stability of a mine was carried out using with ANSYS software. Stresses, strain, element displacement vectors, plastic state of slope and safety factors were calculated (Zheng et al., 2005).

Marconcin et al., (2010) have done a study on steel-concrete composite beams to simulate their structural behavior, with emphasis on the beam –slab interface using ANSYS. Jingsui et al, (2011) have carried out studies on prestressed anchorage method to supervise high rock slope of hydropower project based on numerical simulations using ANSYS.

The stability problems of rock moving zone slope in Sanyou Limestone mine were simulated using elastic-plastic finite element theory by ANSYS software (Rui and Fangwei, 2012). A systematic study was taken up using numerical modeling approach using ANSYS software to assess the influence of width of a gallery of highwall on the stability of highwall (Ram Chandar and Gowtham Kumar, 2014).

Guangming et al., (2014) used numerical modeling approach combined with the GAMBIT and ANSYS structure analysis to assess the slope stability of open-pit to underground mining. A numerical model of underwater wellhead stability analysis in deep-water drilling was established using the pile element and nonlinear spring element of ANSYS (Wei et al., 2015). Numerical modeling based on ANSYS was done to assess the performance of a Flat Plate Solar Collector (FPSC) with different types of working fluid, double distilled water (DDW) and Alumina nanofluids (Hawwash et al., 2017).

INVESTIGATIONS

This chapter gives the details of field investigations carried out to assess the influence of partition and slope stability over old underground coal workings while converting into opencast mines. Deformation and strain were monitored in partition and slope using Zigbee based Wireless Data Acquisition System (WDAQ) and a conventional data logger during field investigations and a large amount of data was generated. Numerical modeling studies were carried out to simulate the field conditions and also to generate more cases, which were not possible in the field. Design, development and deployment of Zigbee based Wireless Data Acquisition System (WDAQ), conventional data logger, numerical modeling studies using ANSYS workbench software and regression analysis using Statistical Package for the Social Sciences (SPSS) software are discussed in this chapter.

3.1 Zigbee based Wireless Data Acquisition System

Zigbee based WDAQ was developed and implemented for monitoring of stability of partition and slope over old underground coal workings. Development and deployment of Zigbee based WDAQ are discussed in the following sections.

3.1.1 Development of wireless data acquisition system

Zigbee based wireless data acquisition system was developed for monitoring of slope and partition over old underground coal workings. It consists of three components, namely sensing unit, Wireless DAQ and base station (Fig. 3.1).

3.1.1.1 Sensing unit

After a detailed review of literature, suitable geophysical sensors required for monitoring deformation and strain in partition and slopes were selected. Sensing unit is responsible for gathering data from the field and to send the data to the Wireless DAQ. The sensors used for this purpose were Linear Variable Differential Transformer (LVDT) and strain gauge.
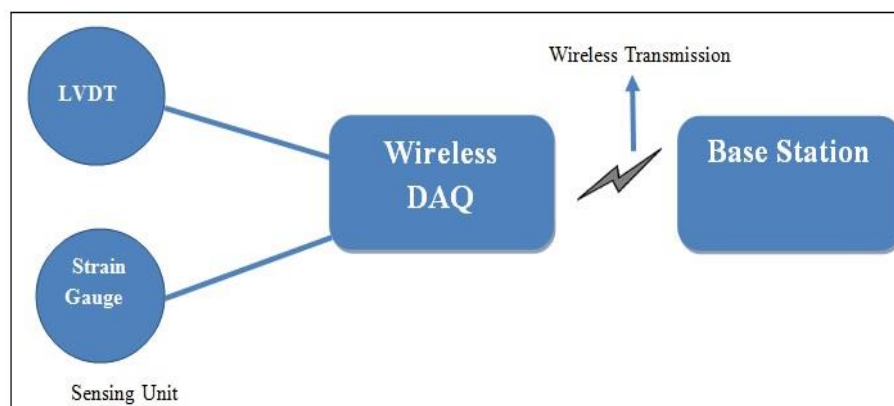
Fig. 3.1 Block diagram of zigbee based wireless data acquisition system

Linear Variable Differential Transformer (LVDT): It is inductive type devices that measures linear deformation. These sensors consist of three coils (i.e. a primary and two secondary) wound around a hollow tube. A moveable ferromagnetic core (armature) is connected to the object being measured and slides along the tube. The excitation signal (AC reference voltage) is applied to the primary winding which in turn induces an EMF signal into the two adjacent secondary windings. LVDT is categorized based on range of operation, type of armature and excitation supply (AC or DC).

AC LVDT was selected for measuring deformation in slope and partition (Fig. 3.2). AC LVDTs are excited by a AC voltage having frequency between 50 hertz and 25 KHz with 2.5 KHz as a nominal value. The carrier frequency is generally selected to be at least 10 times greater than the highest expected frequency of the core motion. AC-operated LVDT's are generally smaller in size and more accurate than DC versions which is provided with onboard oscillator, carrier amplifier and demodulator circuitry.

49

Fig. 3.2 A view of AC LVDT being used in the field

AC LVDT's are able to tolerate the extreme variations in operating temperature than the DC LVDT. These AC LVDTs are the more economically priced displacement transducers. Housed in stainless steel body, they are a combination of ruggedness and high performance. These sensors are used in applications where deformations ranging from fraction of a mm to a few cm. Specification of AC LVDT are as follows:

Winding Configuration	:	Inductive LVDT
Excitation	:	1 to 10V rms, 2Khz
Resolution	:	0.01 mm.
Full Stroke Range	:	±50mm/ 0~100mm
Temperature range	:	upto 60ºC
Temp Coeff(% FSR)	:	Zero:< 0.01% per ºC
Senstivity	:	<0.025%per ºC
Housing dia.	:	22mm
Core rod dia.	:	6 to 6.35mm
Spring Return	:	Optional Internal spring return
Termination	:	Standard: 4 Core Screened PVC insulated-3m

Strain gauge: Strain is defined as the amount of deformation per unit length, a material experience due to an applied force. There are mechanical, optical, acoustical, pneumatic

or electrical instruments used to measure strain of an object. However, these strain gauges offer certain limitations like low resolutions and they are bulky and difficult to use. Further, capacitance and inductance-based strain gauges were introduced but these device's sensitivity to vibration, their mounting requirements and circuit complexity restricted their usage. Next are the photoelectric gauges. These gauges use a light beam, two fine gratings and a photocell detector to generate an electrical current proportional to strain. A photoelectric gauge can be as short as 1/16 inch but its usage proves to be extremely costly and the device is very delicate.

The first bonded, metallic wire-type strain gauge was introduced(Fig.3.3). This type strain gauge consists of an insulating flexible backing which supports a metallic foil pattern. The gauge is attached to the object by a suitable adhesive. As the object is deformed, the foil is deformed, causing its electrical resistance to change. This resistance change, usually measured using a Wheatstone bridge, is related to the strain by the quantity known as the gauge factor. As the load applied to the surface, it gets strained and experiences a change in length. This resulting change in length is conveyed to the resistor and the corresponding strain is measured in terms of electrical resistance of the foil wire, which varies linearly with strain. The metallic foil-type strain gauge is selected for measuring strain in partition and slope. Specifications of strain gauge are given as follows:

Resistance	:	$120 \, \Omega$
Bridge excitation supply	:	5V
Guage Factor (GF):	:	0.1000 to 1.0000
Noise	:	+/- 10 microstrain jumping will be permissible for dynamic strain measurement

Fig. 3.3 A view of strain gauge being used in the field

3.1.1.2 Wireless DAQ

The main objective of Wireless DAQ is to acquire data from sensing unit and to process the same. Finally, processed data sent to the base station. It consists of Atmega328 microcontroller, LVDT module, Strain gauge module, Zigbee transceiver, Battery and Memory card (SD card) (Fig. 3.4).
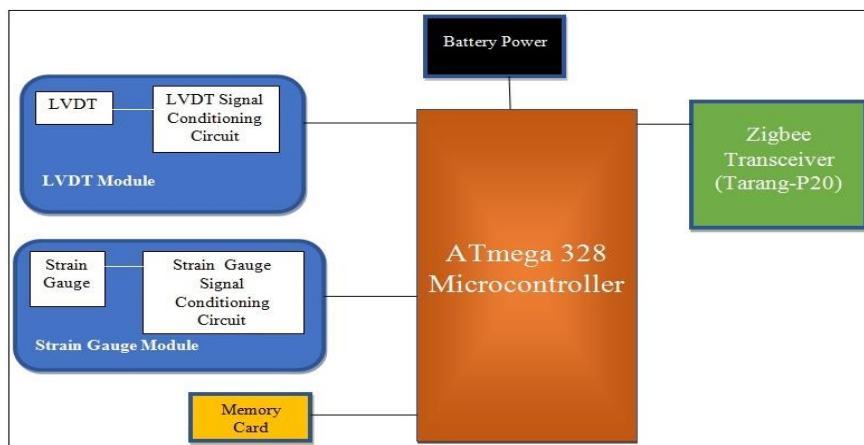
Fig. 3.4 Components of wireless DAQ

Microcontroller: Microcontroller is an integrated circuit, which includes a processor, memory and input/output (I/O) peripherals on a single chip. ATmega328 microcontroller is used for developing Wireless DAQ. Atmega328 microcontroller has the following features:

- High Performance, Low Power Atmel AVR 8-Bit Microcontroller Family
- Up to 20 MIPS Throughput at 20MHz
- 32 KB flash memory, 32 x 8 General Purpose Working Registers
- 6-channel 10-bit ADC in PDIP Package
- IO and Packages
  - 23 Programmable I/O Lines
  - 28-pin PDIP, 32-lead TQFP, 28-pad QFN/MLF and 32-pad QFN/MLF
- Operating Voltage
  - 1.8 - 5.5V
- Temperature Range
  - -40 °C to 85 °C
- Power Consumption
  - Active Mode: 0.2mA
  - Power-down Mode: 0.1μA
  - Power-save Mode: 0.75μA (Including 32kHz RTC)
- Special Features
  - Power-on Reset and Programmable Brown-out Detection
  - Internal Calibrated Oscillator
  - External and Internal Interrupt Sources
  - Six Sleep Modes: Idle, ADC Noise Reduction, Power-save, Power-down, Standby and Extended Standby

Atmega328 microcontroller is a single chip microcontroller and configuration is given in Figure 3.5. It is small and low-cost computer built for the purpose of dealing with specific tasks. The description of Atmega328 pin configuration as follows:

VCC   :Digital supply voltage.

GND   :Ground.
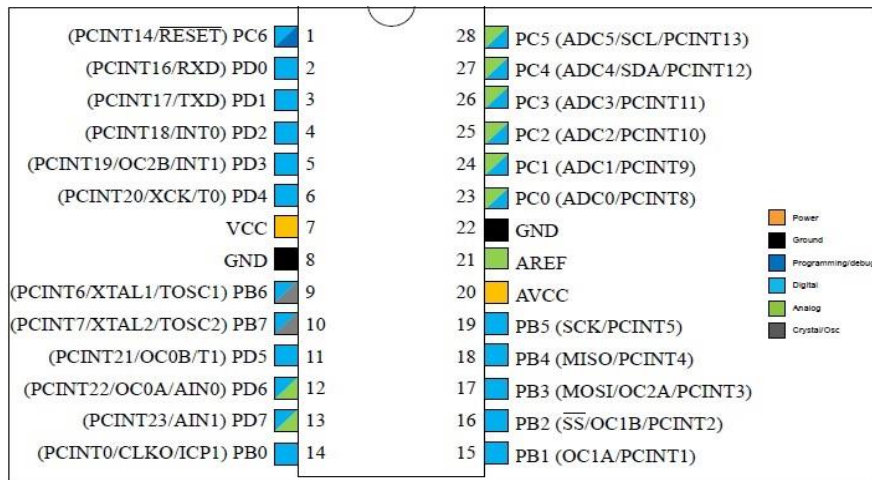
Fig. 3.5 Microcontroller (Atmega328) pin configuration

Port B (PB7:0), Port C (PC5:0) and Port D (PD7:0) are 8-bit bi-directional I/O ports with internal pull-up resistors. The Port B, Port C and Port D output buffers have symmetrical drive characteristics with both high sink and source capability. As inputs, The Port B, Port C and Port D pins that are externally pulled low will source current if the pull-up resistors are activated. The Port B, Port C and Port D pins are tri stated when a reset condition becomes active, even if the clock is not running.

PC6/RESET: If the RSTDISBL Fuse is programmed, PC6 is used as an I/O pin. The electrical characteristics of PC6 differ from those of the other pins of Port C. If the RSTDISBL Fuse is unprogrammed, PC6 is used as a Reset input. A low level on this pin for longer than the minimum pulse length will generate a Reset, even if the clock is not running. Shorter pulses are not guaranteed to generate a Reset.

AVCC: AVCC is the supply voltage pin for the A/D Converter, PC3:0 and ADC7:6. It should be externally connected to VCC even if the ADC is not used. If the ADC is used, it should be connected to VCC through a low-pass filter. Note that PC6...4 use digital supply voltage, VCC.

AREF: AREF is the analog reference pin for the A/D Converter.

ADC7:6 (TQFP and QFN/MLF Package Only): In the TQFP and QFN/MLF package, ADC7:6 serves as analog input to the A/D converter. These pins are powered from the analog supply and serve as 10-bit ADC channels.

LVDT module: LVDT module consists of 4-wire LVDT and signal conditioner (Fig. 3.6). The 4-wire LVDT is an electromechanical transducer used for measuring linear displacement. It consists of a primary winding energized by an external sine wave reference source and two secondary windings connected in the series having opposed configuration. The output voltage across the series of secondary increases as the core is moved from the center. The direction of movement is detected by measuring the phase of the output.

Signal conditioner consists of operational amplifier (µA741) which energizes the LVDT coil, sense the LVDT output voltages and produce a DC output voltage (VOUT) proportional to core position. Operational amplifier (µA741) has a sine wave oscillator and a power amplifier to drive the LVDT. Two synchronous demodulation stages are available for decoding the primary and secondary voltages. A decoder determines the ratio of the output signal voltage to the input drive voltage (A/B). A filter stage and output amplifier are used to scale the resulting output.
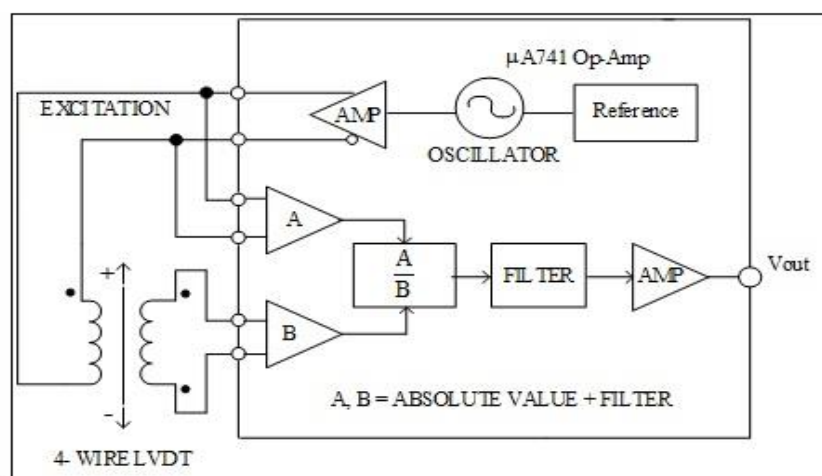
Fig. 3.6 Block diagram of LVDT signal conditioner

Strain gauge module: Strain gauge module consists of a quarter-Wheatstone bridge and amplifier (Fig. 3.7). The strain gauge sensor is connected to form a quarter-Wheatstone bridge circuit. Wheatstone bridge is a divided bridge circuit used for the measurement of dynamic electrical resistance. The output voltage of the Wheatstone bridge circuit is expressed in millivolt output per volt input. The output of the quarter - Wheatstone bridge (voltage signal) is given to an amplifier to the increase measurement resolution and improve signal-to-noise ratio. The output signal (V_{out}) of the amplifier is then sent to the ATmega 328 microcontroller.
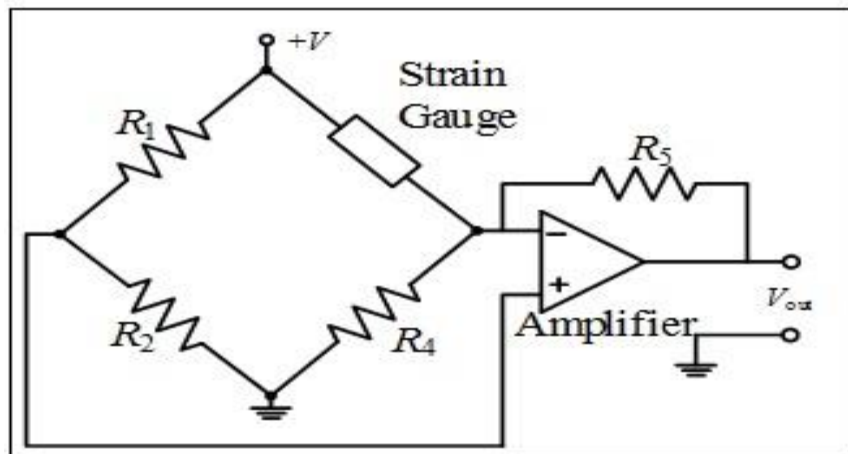
Fig. 3.7 Block diagram of strain gauge signal conditioner

Zigbee transceiver: Tarang-P series modules are designed with low to medium transmit power and for high-reliability wireless networks. It has following features:

- Supply Voltage (VCC): 3.3 to 3.6V
- Operating Frequency: ISM 2.4GHz
- RF Data Rate: 250Kbps
- Operating Temperature: -40 to 85 ºC
- Supported Network Topologies: - Mesh/Star
- Transmission Range: up to 500m Lin of Site(LOS)

Zigbee Tarang P series is used for wireless transmission. It is used to transmit the sensed data to Base Station (BS). The circuit connection with Atmega328 microcontroller is

given in Figure 3.8. Microcontroller was operated with a set of commands programmed in it, for obtaining the strain and deformation under the field conditions. The programming code was written in Integrated Development Environment (IDE) for operating Wireless DAQ. IDE is a software suite that consolidates the basic tools to write and test software. Typically, an IDE contains a code editor, compiler or interpreter and a debugger that are accessed through Graphical User Interface (GUI). IDE supports object-oriented software development packages (such as CPP, Java etc.,).
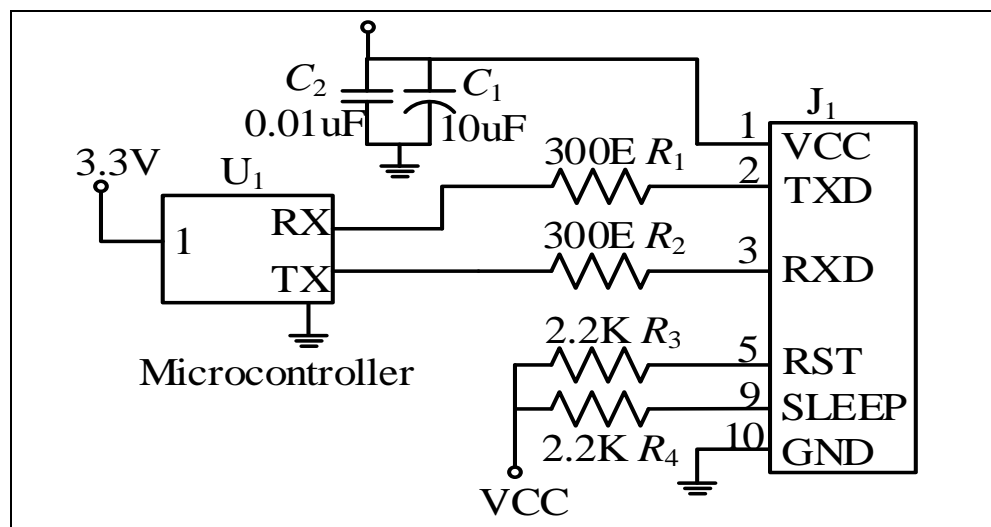
Fig. 3.8 Block diagram of tarang P20 with atmega328 microcontroller

User-friendly software is developed and named as 'Wireless Slope Monitoring System (WISMS)' using Integrated Development Environment (IDE). It consists of four modules such as LVDT module, strain gauge module, Analog-to-Digital Converter (ADC) module and zigbee module. These modules are run parallel to acquire, process and transmit sensed data from monitoring point to base station. LVDT module and strain module have a code for acquiring deformation and strain respectively. ADC module converts the sensed data into system understandable format for processing. Zigbee module is responsible for sending and receiving the data from wireless DAQ to base station and vice versa. Wireless DAQ was programmed to store the sensed data in memory card (SD card) at monitoring point to avoid data loss in case of wireless signal failure and also to send to the base station to store the data in data base.

3.1.1.3 Base station

Base Station (BS) was equipped with display unit (laptop) and Zigbee receiver. Zigbee receiver receives the data (deformation and strain) from Wireless DAQ and is connected to display unit via Universal Serial Bus (USB) port. Data is captured continuously at the rate of 1 sample per 2 seconds and there is an option to change the sampling rate based on field requirements. Data is displayed in four columns such as time, date, strain(microstrain) and deformation (mm) in WISMS software. Data is stored in the database and can be analyzed as per the requirement. The data can be represented in other file formats like .txt, .doc and .xlsx. The working and flow of data of Zigbee based Wireless DAQ is given in the flowchart (Fig.3.9).

To assess the reliability of the Wireless DAQ, uniaxial compressive strength experiment was carried out on different rock samples. Two strain gauges were fixed along the longitudinal axis of the rock sample, one was connected to the data logger and other remotely with Wireless DAQ. Similarly, one LVDT was connected to the data logger and another to the Wireless DAQ. Deformation and strain values of both units were found to be similar, indicating the Wireless DAQ is giving a reliable data (Fig.3.10).
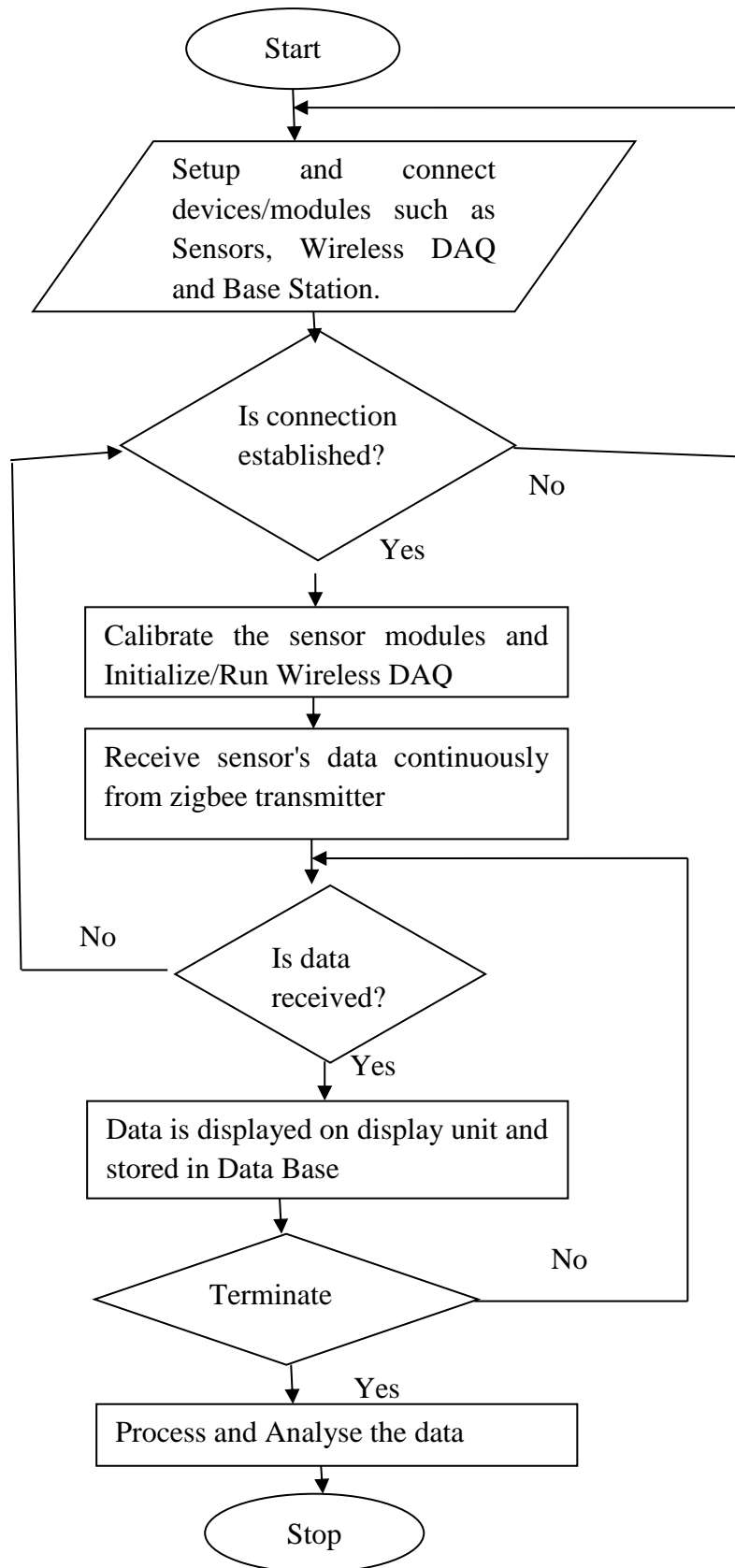
Fig. 3.9 Flow chart for working of zigbee based Wireless Data Acquisition
   System (WDAQ)

Fig.3.10 Validation of zigbee based WDAQ with laboratory testing

3.2 Field Investigations

Field investigations were carried out in Ramagundam Opencast Project-I (RGOCP-I) and Ramagundam Opencast Project-III (RGOCP-III) of The Singareni Collieries Company Limited, Ramagundam in Peddapalli District of Telangana State in three phases.

Phase-I studies were carried out in RGOCP-III in the month of May/June 2016. Deformation and strain were monitored in partition using Zigbee based Wireless DAQ and conventional data logger. Phase-II studies were carried out in RGOCP-I and RGOCP-III in the month of Nov/Dec, 2016. Deformation and strain were monitored in partition and slope using Zigbee based Wireless DAQ and conventional data logger. Numerical modeling studies were carried out and compared with field investigations. Inorder to get more data, phase-III studies were carried out in RGOCP-I and RGOCP-III in the month of Feb/March, 2017. Partition and slope were monitored based on Zigbee based Wireless DAQ and conventional data logger. In total, 144 locations were monitored, at each location data was captured about 5hours to 8hours. The detailed description is discussed in the following sections.

3.2.1 Case study1-Ramagundam opencast project-I

Ramagundam Opencast Project-I (RGOCP-I) is located in South Godavari Valley Coalfields (Fig. 3.11). It is covering a total area of 3.76 sq. km. The area lies between 18º 39' 07'' and 18º 41' 05'' N and longitude 79º 32' 37''E to 79º 33' 53'' E. The nearest Railway station is Ramagundam on Kazipet to Nagpur section of South Central Railway and is about 18km in north direction to the mine. A view of mine is given in Figure 3.12.

RGOCP-I is conversion of GDK 9, GDK 9A and GDK 10 (Block A&B) incline underground mines. Benching method is adopted in this mine to remove Over Burden (OB) and to extract coal as discussed in the previous section. The excavation of OB is done by dragline of capacity 24/96 and Shovel-Dumper combination. Shovels ranging from 3.0 to 12.0cu.m coupled with suitable number of 100t/60t/35t capacity dumpers.

Salient features of RGOCP-I expansion project:

Mining operations commenced during year	:	2008-09
Mineable reserves	:	61.151Mt
Total OB estimated to be handled	:	355.53 M. Cu.m
Stripping Ratio (Coal in Te: OB in CuM)	:	1: 5.81
Maximum depth of quarry	:	240m
Average Gradient	:	1 in 5.0 to 10.0
Total life of mine	:	14 years
Mining Technology	:	Shovel-Dumper combination and Dragline

Fig. 3.11 Satellite view of Ramagundam Opencast Project-I (RGOCP-I)

Fig. 3.12 A view of Ramagundam Opencast Project-I (RGOCP-I)

3.2.2   Case study2-Ramagundam opencast project-III

Case Study-2 was carried out in Ramagundam Opencast Project-III (RGOCP-III). It is located in South Godavari Valley Coalfields (Fig. 3.13). The nearest Railway station is Ramagundam on Kazipet to Nagpur section of South Central Railway and is about 16 km in north direction to the mine. The mine is located between latitudes from North 18° 35' 19" to 18° 50' 03" and East Longitude 79° 27' 30" to 79° 37' 30" forming part of a survey of India topo sheet No. 56 N/5, 56 N/9, 56 N/10. The general direction and full dip of the seams are North 76° East and 9° respectively. Mine has a lease hold area of about 13.93 Sq. km and a view of the mine is shown in Fig. 3.14.

Benching method is adopted in this mine to remove the OB and to extract the coal. 150mm diameter blastholes are drilled with wagon drills and fragmented using chemical energy in the form of blasting. Fragmented material is loaded with the help of shovels and transported to the dump yard in dumpers in case of OB and transported to the coal handling plant in case of coal. RGOCP-III is conversion of old GDK-6, 6B & 7 incline underground mines. It was proposed to extract both coal and OB with Shovel-Dumper combination. 4 no. of 12-15 m^3 hydraulic shovels along with 64 no. of 100t capacity dumpers are deployed for removal of OB.

Salient features of the RGOCP-III extension project:

Mining operations commenced during year	:	2008-09
Total OB	:	490.04 M. Cum.
Average stripping ratio	:	1:6.02
Total life of mine	:	21 years
Maximum depth of quarry	:	280m
Average gradient	:	1 in 4.5 to 1 in 7.0
Mining Technology	:	Shovel-Dumper combination and Dragline

Fig. 3.13 Satellite view of Ramagundam Opencast Project-III (RGOCP-III)

Fig. 3.14 A view of Ramagundam Opencast Project-III (RGOCP-III)

During filed investigations, old underground coal workings were identified based on correlation survey. After detailed survey, marking is done to identify galleries and pillars in the field. Gallery width of 4.2m, gallery height of 3.0m, pillar width of 30.5m and bench height of 8m were found during correlation survey in the field. Partition or overburden of different thicknesses and slope angles were considered for monitoring to obtain deformation and strain based on Zigbee based WDAQ and conventional data logger.

During phase-I studies, monitoring was done only in partition whereas during phase-II and phase-III studies monitoring was done in partition and along the slope. In total, 144 locations were monitored, at each location data was captured about 5hours to 8hours. The details of field monitoring are given in Table 3.1. Deployment and monitoring of stability of partition and slope over old underground coal workings based Zigbee based WDAQ and conventional data logger is discussed in the following sections.

Table 3.1 The details of partition and slope monitoring in the field

Method of Monitoring	Sensors Used	Location of Monitoring		Total Number of Data Sets	Monitoring Hours at each location (hours)	Sampling Rate	Mining Operation
		Partition	Slope				
Zigbee based WDAQ	LVDT and Strain Gauge	left, right corners and center of partition above the gallery	toe, crest and in between toe and crest of slope (not scaled)	144	5-8	1 sample per 2 seconds	Shovel-Dumper operation (HEMM)
Conventional Data Logger						3 samples per second	

3.2.3   Investigations with zigbee based WDAQ

Sensors were installed as per International Society for Rock Mechanics and Rock Engineering (ISRM) suggested methods at different monitoring points, namely A, B and C in partition and along the slope above old underground galleries. In case of partition monitoring, point 'A' was the left edge of the gallery whereas point 'B' and 'C' were above the center and the right edge of the gallery respectively (Fig. 3.15).
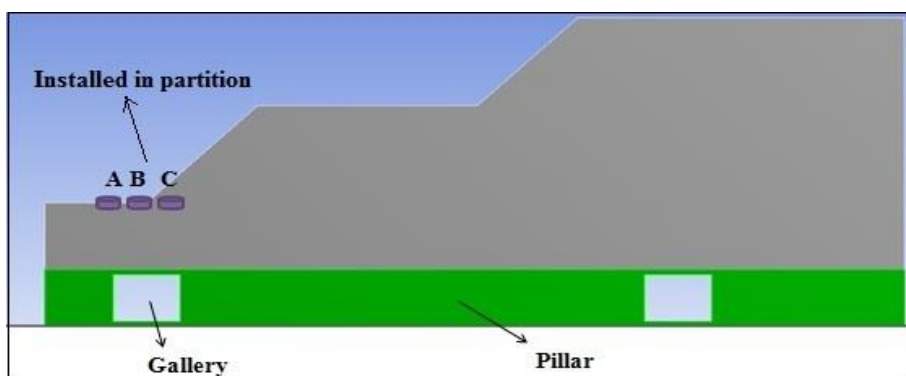
Fig. 3.15 Monitoring points in the partition

In case of slope monitoring, point 'E' was the toe of the slope above the gallery whereas point 'F' and 'G' were above the approximately near the center based on the accessibility and the crest of slope respectively (Fig. 3.16). Strain gauge of 120Ω and LVDT of range 50mm were installed in the partition and slope above old underground galleries of height 3m and width 4.2m by digging a pit of 15cm x 15cm x 15cm in the overburden (Fig. 3.17).
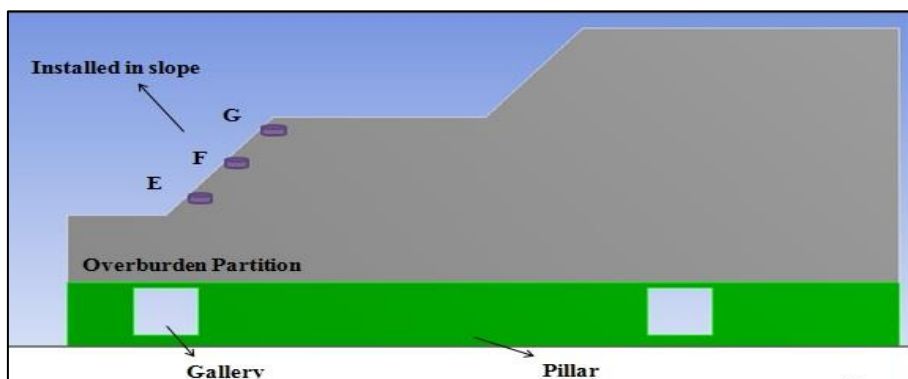
Fig. 3.16 Monitoring points along the slope (not to scale)

66

LVDT and strain gauge sensors were connected to Wireless DAQ. Wireless DAQ consisits of LVDT module, strain gauge module, Atmega328 microcontroller, ADC module and Zigbee module. LVDT and strain gauge modules are to capture the LVDT and strain gauge sensors data and to convert into the signal (sensed data) using signal conditioner (Figs.3.17 and 3.18).

Atmega328 microcontroller captured the data continuously from LVDT and strain gauge modules. The collected data was converted into a system understandable format using ADC. Further, sensor's data was processed and sent to the based station by using Zigbee (Tarang-P20) wireless medium. Zigbee was used to construct a wireless sensor environment while monitoring the partition and slope movement. The measured data from various sensors displayed at the base station which was located in the field. Zigbee wireless receiver at base station was used to collect data from the wireless DAQ and to display the data on the laptop screen (Fig. 3.19).

Fig. 3.17 Monitoring of deformation and strain due to the movement of HEMM using zigbee based WDAQ
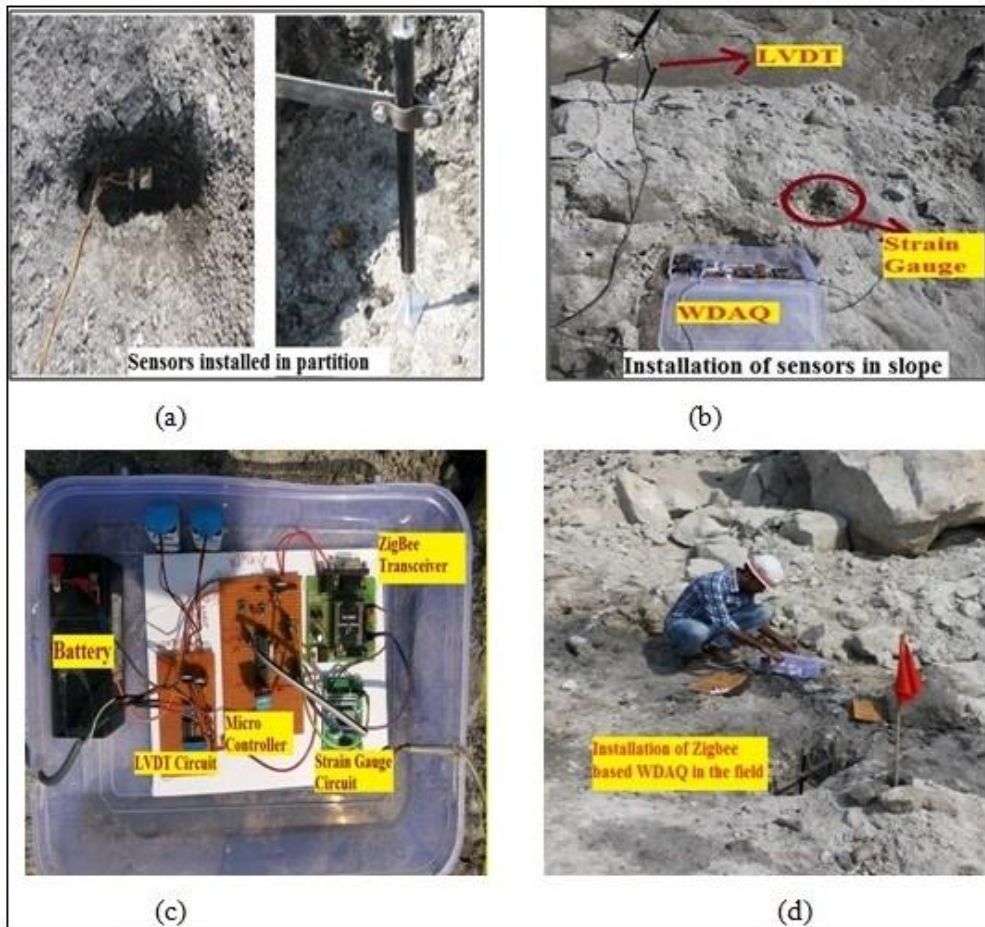
Fig. 3.18 Monitoring of partition and slope using zigbee based WDAQ

Fig. 3.19 A view of base station in the field

Wireless Slope Monitoring System (WISMS) is a user-friendly software and it has Graphical User Interface (GUI). GUI consists title bar, menu bar and space for displaying of sensor's data (Fig. 3.20). Title bar displays the title of software. Menu bar consists of different menu's like File, Edit, Connection and View. 'File' menu is used to perform operations such as open, save, print and close operations on the file where data is stored. Edit menu consists of copy, delete operations. 'View' menu is used for representing data in various forms like Hexadecimal, Octal formats etc. Connection menu consists of operations like open connection, close connection, transmit and receive of data among various devices. WISMS gets initialized when wireless zigbee receiver connected using USB to the display unit (laptop). The automatic detection of zigbee wireless transmitter is done and data will be received continuously once the connection established.

Fig. 3.20 Display of strain and deformation in the software WISMS

Partition monitoring: Partition thicknesses of 4.12m, 5.91m, 6.86m, 7.91m, 10.21m and 12.10m were considered and sensors were installed at different locations in partition. A large quantity of data (deformation and strain) was generated continuously in Zigbee based WDAQ. At each location, data was generated at 1 sample per 2

seconds. Data was collected for about minimum of 5 hours and in some cases, upto 8 hours per day. In total, 72 locations were monitored and from which minimum, maximum and average values of deformation and strain at each location were obtained as shown Table 3.2 and 3.3.

Table 3.2 Variation in deformation at different monitoring points for the different partition thicknesses using zigbee based WDAQ

Partition Thickness (m)	Deformation (mm)								
	Monitoring Point-A			Monitoring Point-B			Monitoring Point-C		
	Min.	Max.	Avg.	Min.	Max.	Avg.	Min.	Max.	Avg.
4.12	0.03	2.01	1.02	0.05	2.41	1.23	0.02	1.94	0.98
5.91	0.01	1.92	0.96	0.04	2.21	1.12	0.01	1.88	0.94
6.86	0.01	1.81	0.91	0.01	1.89	0.95	0.01	1.68	0.84
7.91	0.01	1.60	0.8	0.01	1.77	0.89	0.01	1.54	0.77
10.21	0.01	1.41	0.71	0.01	1.62	0.81	0.01	1.35	0.68
12.10	0.01	1.36	0.68	0.01	1.58	0.79	0.01	1.29	0.65

Table 3.3 Variation in strain at different monitoring points for different partition thicknesses using zigbee based WDAQ

Partition Thickness (m)	Strain ($\mu\varepsilon$)								
	Monitoring Point-A			Monitoring Point-B			Monitoring Point-C		
	Min.	Max.	Avg.	Min.	Max.	Avg.	Min.	Max.	Avg.
4.12	1	350	175.5	1	387	194.0	1	342	171.5
5.91	1	289	145.0	1	312	156.5	1	283	142.0
6.86	1	285	143.0	1	296	148.5	1	280	140.5
7.91	1	284	142.5	1	289	145.0	1	282	141.5
10.21	1	281	141.0	1	284	142.5	1	276	138.5
12.10	1	280	140.5	1	282	141.5	1	274	137.5

Slope monitoring: Slope angles of 49°, 65°, 64°, 70°, 62° and 68° and respective partition thicknesses of 5.82m, 5.91m, 6.26m, 6.47m, 6.86m and 6.95m were monitored using Zigbee based WDAQ. Sensors were installed at different locations in slope. In total, 72 locations were monitored, at each location, data was captured for about 5hours to 8hours per day. Minimum, maximum and average values of deformation and strain were obtained from huge amount of data points monitored at each location and tabulated in Table 3.4 and 3.5.

70

Table 3.4 Variation in deformation at different monitoring points for different slope
angle using zigbee based WDAQ

Slope Angle (Degrees)	Partition Thickness (m)	Deformation(mm)								
		Monitoring Point-E			Monitoring Point-F			Monitoring Point-G		
		Min.	Max.	Avg.	Min.	Max.	Avg.	Min.	Max.	Avg.
49	5.82	0.01	1.90	0.96	0.01	1.86	0.94	0.01	1.76	0.89
65	5.91	0.01	1.88	0.95	0.01	1.84	0.93	0.01	1.74	0.88
64	6.26	0.01	1.81	0.91	0.01	1.79	0.90	0.01	1.71	0.86
70	6.47	0.01	1.65	0.83	0.01	1.62	0.82	0.01	1.55	0.78
62	6.86	0.01	1.52	0.77	0.01	1.48	0.75	0.01	1.45	0.73
68	6.95	0.01	1.46	0.74	0.01	1.39	0.70	0.01	1.31	0.66

Table 3.5 Variation in strain at different monitoring points for different slope angles
using zigbee based WDAQ

Slope Angle (Degrees)	Partition Thickness (m)	Strain (µε)								
		Monitoring Point-E			Monitoring Point-F			Monitoring Point-G		
		Min.	Max.	Avg.	Min.	Max.	Avg.	Min.	Max.	Avg.
49	5.82	1	185	93.0	1	156	78.5	1	132	66.5
65	5.91	1	182	91.5	1	153	77.0	1	129	65.0
64	6.26	1	176	88.5	1	147	74.0	1	123	62.0
70	6.47	1	158	79.5	1	144	72.5	1	120	60.5
62	6.86	1	149	75.0	1	133	67.0	1	99	50.0
68	6.95	1	140	70.5	1	129	65.0	1	91	46.0

3.2.4 Investigations with conventional data logger

In order to validate the data obtained using Zigbee based WDAQ, the same location
points were monitored by conventional data logger with a similar set of sensors
simultaneously. Data logger (AH391) is a 4 Channel mainframe cabinet and it is
designed to house up to 4 no. of measurement modules either for strain measurement
or displacement measurement (Fig. 3.21).

Strain measurement module (AM422) is designed for dynamic measurement using a
strain gauge-based bridge. AC LVDT (AM321) measurement module is designed to
give an analog output proportional to the displacement of an LVDT. ADQM is a 16-
channel high-frequency NI- DAQ module designed to accept 16 no's of analog I/P for

fast acquisition of measured Input. It is powered by USB interface of PC to which it is connected (Fig.3.22).

Fig. 3.21 Conventional data logger used in the field

Data logger has display at the front panel and interface for connecting sensors at the back panel (Fig.3.23). Sensors were installed in slope and partition and connected through wire to conventional data logger (Fig. 3.24). Partition and slope were continuously monitored and the data was captured and displayed with the help of software. "ADsof" software was used to process the data. It was capable of capturing the strain gauge data and LVDT data continuously (Fig. 3.25 and 3.26).

Fig. 3.22 Installation of data logger
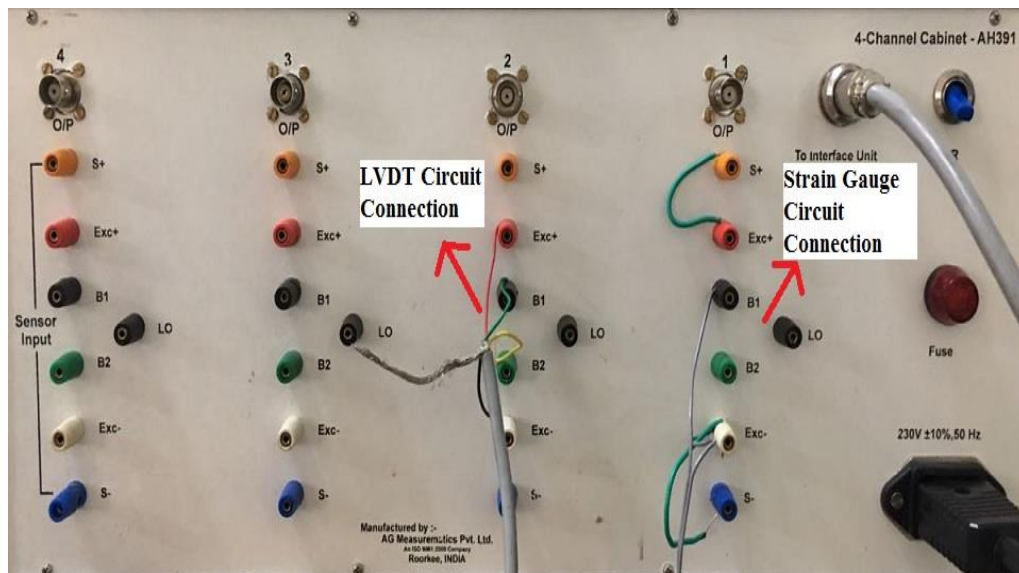
Fig. 3.23 Circuit connection for sensors at back panel of data logger

Fig. 3.24 Connection of sensors to the data logger in the field

Fig. 3.25 A view of software module of conventional data logger

74

Fig. 3.26 Display of strain and deformation in software of data logger

Partition monitoring: Partition thicknesses of 4.12m, 5.91m, 6.86m, 7.91m, 10.21m and 12.10m were considered as similar to the Zigbee based WDAQ. Sensors were installed at different locations in partition and data (deformation and strain) was generated continuously. 72 locations were monitered and data was generated at the rate of 3 samples per second. At each location, data was captured about 5hours to 8hours. Minimum, maximum and average values of deformation and strain at each location are given in Table 3.6 and 3.7.

Table 3.6 Variation in deformation at different monitoring points for the different partition thickness using Data Logger

Partition Thickness (m)	Deformation (mm)								
	Monitoring Point-A			Monitoring Point-B			Monitoring Point-C		
	Min.	Max.	Avg.	Min.	Max.	Avg.	Min.	Max.	Avg.
4.12	0.01	1.69	0.85	0.02	2.31	1.17	0.01	1.64	0.83
5.91	0.01	1.60	0.81	0.01	1.96	0.99	0.01	1.53	0.77
6.86	0.01	1.56	0.79	0.01	1.81	0.91	0.01	1.39	0.70
7.91	0.01	1.42	0.72	0.01	1.68	0.85	0.01	1.22	0.62
10.21	0.01	1.26	0.64	0.01	1.52	0.77	0.01	1.19	0.60
12.10	0.01	1.20	0.61	0.01	1.46	0.74	0.01	1.15	0.58

Table 3.7 Variation in strain at different monitoring points for different partition
thickness using Data Logger

Partition Thickness(m)	Strain (με)								
	Monitoring Point-A			Monitoring Point-B			Monitoring Point-C		
	Min.	Max.	Avg.	Min.	Max.	Avg.	Min.	Max.	Avg.
4.12	1	293	147.0	3	331	167.0	1	275	138.0
5.91	1	241	121.5	3	267	135.0	1	234	117.5
6.86	1	237	119.5	2	242	122.0	2	225	113.5
7.91	2	230	116.0	2	236	119.0	2	224	113.0
10.21	2	225	113.5	2	233	117.5	2	220	111.0
12.10	1	220	110.5	2	229	115.5	2	218	110.0

Slope monitoring: Slope angles of 49º, 65º, 64º, 70º, 62º and 68º and respective partition thicknesses of 5.82m, 5.91m, 6.26m, 6.47m, 6.86m and 6.95m were monitored using conventional data logger along with Zigbee based WDAQ. In slope, 72 locations were monitored and data was generated at the rate of 3 samples per second. Data was captured for 5hours to 8hours at each location. Minimum, maximum and average values of deformation and strain from collected data at each location are given in Table 3.8 and 3.9.

Table 3.8 Variation in deformation at different monitoring points for different slope
angles using Data Logger

Slope Angle (Degrees)	Partition Thickness (m)	Deformation(mm)								
		Monitoring Point-A			Monitoring Point-B			Monitoring Point-C		
		Min.	Max.	Avg.	Min.	Max.	Avg.	Min.	Max.	Avg.
49	5.82	0.01	1.65	0.83	0.01	1.63	0.82	0.01	1.61	0.81
65	5.91	0.01	1.63	0.82	0.01	1.62	0.82	0.01	1.58	0.80
64	6.26	0.01	1.58	0.80	0.01	1.56	0.79	0.01	1.52	0.77
70	6.47	0.01	1.44	0.73	0.01	1.41	0.71	0.01	1.39	0.70
62	6.86	0.01	1.36	0.69	0.01	1.35	0.68	0.01	1.32	0.67
68	6.95	0.01	1.31	0.66	0.01	1.29	0.65	0.01	1.27	0.64

Table 3.9 Variation in strain at different monitoring points for different slope angles using Data Logger

Slope Angle (Degrees)	Partition Thickness (m)	Strain (με)								
		Monitoring Point-A			Monitoring Point-B			Monitoring Point-C		
		Min.	Max.	Avg.	Min.	Max.	Avg.	Min.	Max.	Avg.
49	5.82	1	172	86.50	1	152	76.50	1	138	69.50
65	5.91	1	168	84.50	1	146	73.50	1	135	68.00
64	6.26	1	154	77.50	1	135	68.00	1	126	63.50
70	6.47	1	149	75.00	1	126	63.50	1	116	58.50
62	6.86	1	140	70.50	1	118	59.50	1	110	55.50
68	6.95	1	138	69.50	1	115	58.00	1	108	54.50

3.3 Numerical Modeling

Numerical modeling approach was adopted to assess the stability of old underground workings while converting into surface mining operations. Numerical modeling was carried out in two phases.

In the first phase, modeling studies were carried out exactly based on the field conditions. In the second phase, assessment of the influence of geometrical dimensions such as partition thickness, gallery width, gallery height, pillar width, slope angle and berm width, rock properties and external load was carried out. The ANSYS Workbench software was used to develop the models by simulating the field conditions. The model consists of two distinct regions such as coal seam and overburden. Coal seam includes two galleries (gallery1 and gallery2) and a pillar. Overburden consists of partition thickness, slope, berm and benches (Fig. 3.27).

Input parameters like rock properties, bench configuration and old gallery dimensions for modeling were collected during the field visits. The properties of coal and sandstone are given in Table 3.10. These parameters were used for developing models using ANSYS workbench software.
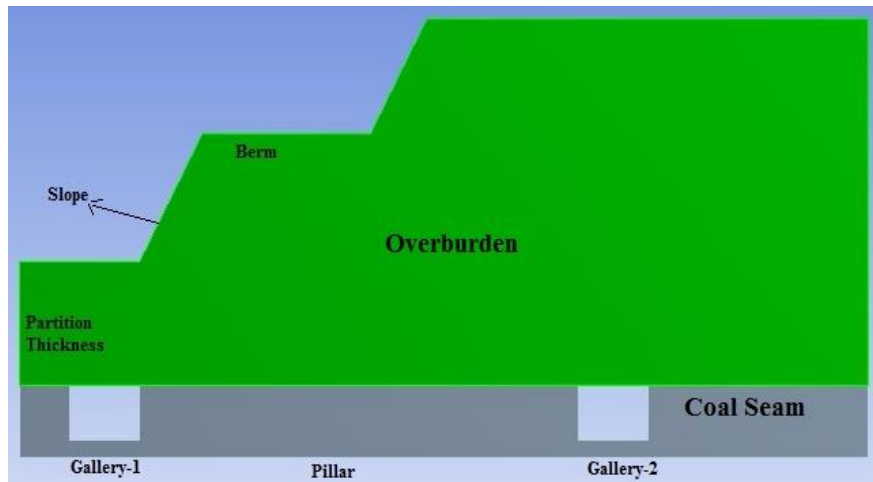
Fig. 3.27 Overview of simulation model

Table 3.10 Rock properties used in the models

Property	Overburden	Coal
Young's Modulus (GPa)	25	3
Density (kg/m^3)	2450	1500
Poisson's Ratio	0.25	0.22
Tensile Yield Strength (MPa)	3.9	0.23
Compressive Yield Strength (MPa)	40	25

3.3.1 Modeling with ANSYS workbench

The ANSYS Workbench platform is the backbone for delivering a comprehensive and integrated simulation system (Fig. 3.28). The workbench is used for the analysis of model development and simulations for getting higher productivity from integrated applications leveraging common and compatible data models.

Modeling with ANSYS workbench is carried out in a series of steps. Firstly, **Ansys workbench > static structural is sklected**. The static structural components are shown in the Figure 3.29. **Engineering Data** allows to define different material properties to be used in the models.
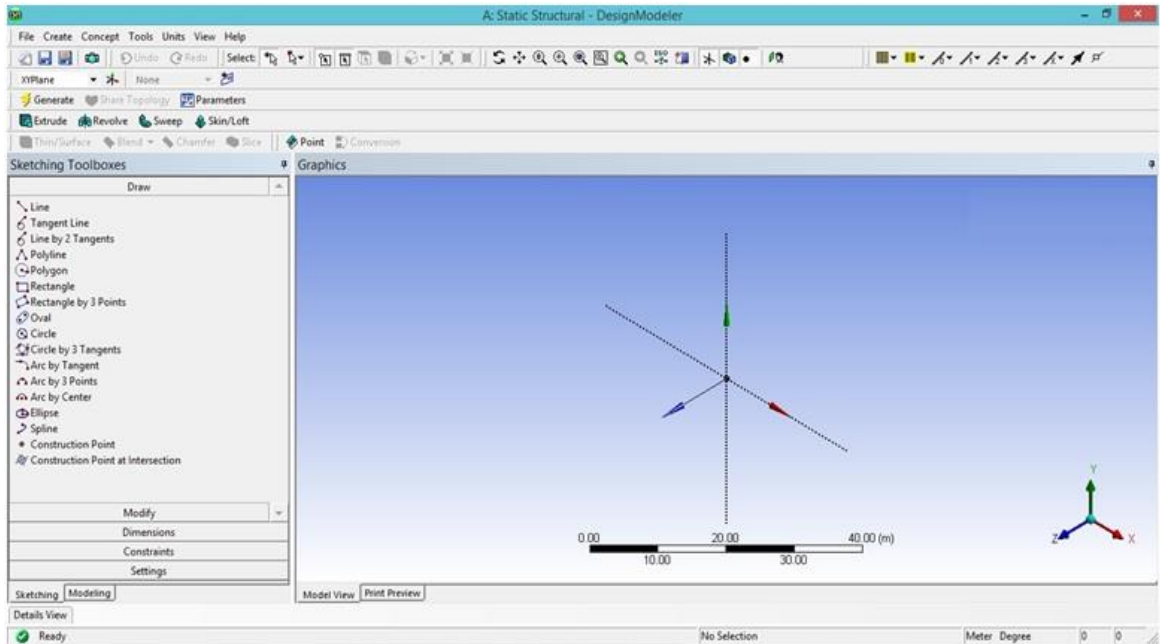
Fig. 3.28 Graphical user interface of ANSYS workbench

Geometry is used to sketch the model and to assign respective material properties to different materials. Meshing is done with the option **Model.** Loading, boundary conditions and supports are defined by using the **Setup** option. By the **Solution** option, output parameters are defined. Graphical representation, tabular form of output data is defined by using the **Results** option. The detailed explanation is given in the following sections.

Fig. 3.29 Static structural components of ANSYS workbench

A simple sketch in 2D is created in any one of X,Y or Z plane for the creation of any model in ANSYS using the option of **Sketching** as in the Figure 3.30.
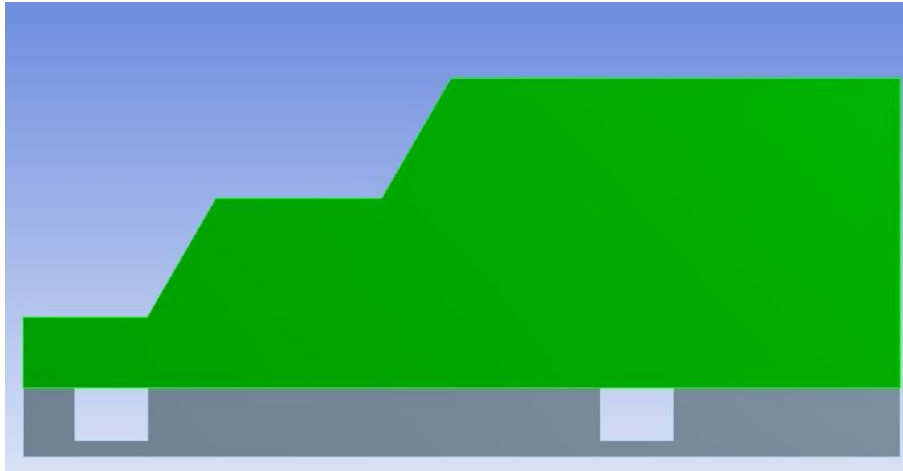
Fig. 3.30 2D sketch of the model in ANSYS workbench

After the 2D sketch is created, the different sections of the model can be extruded to the required width separately to convert the model into 3D using the option of **Extrude**. After defining the details under **Extrude**, the sections must be stopped from merging with other sections using the option **Tools > Freeze**. This should be carried out for all the sections in the model to finally get the 3D model as shown in Figure 3.31. Once the required 3D model is created, the next step is a simulation of the model. The simulation is carried out in the following steps.
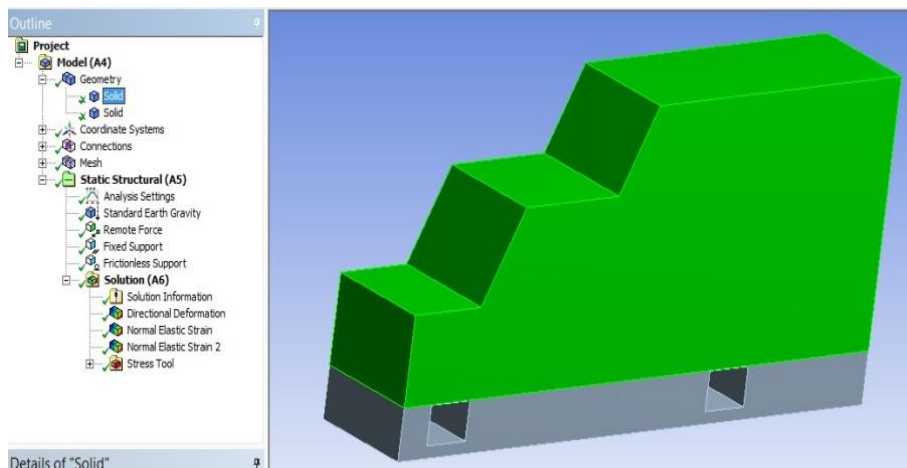
Fig. 3.31 3D model in ANSYS workbench

Specifications and assignment of rock properties: The materials to be modeled in ANSYS Workbench should be specified with the required physical, mechanical,

thermal or electromagnetic properties as per the scope of the modeling object. This is done with the option **Engineering Data** on the toolbar as shown in the Figures 3.32 and 3.33. After the specification of rock properties, these are assigned to various sections of the model. Firstly, select the required section to assign the properties under **Project > Model > Geometry**. When details of the geometry are displayed, choose the rock type from the drop-down menu under **Definition > Material**. The section selected is highlighted in green as shown in the Figure 3.34.

Fig. 3.32 Coal properties incorporated in ANSYS workbench

Fig. 3.33 Overburden properties incorporated in ANSYS workbench
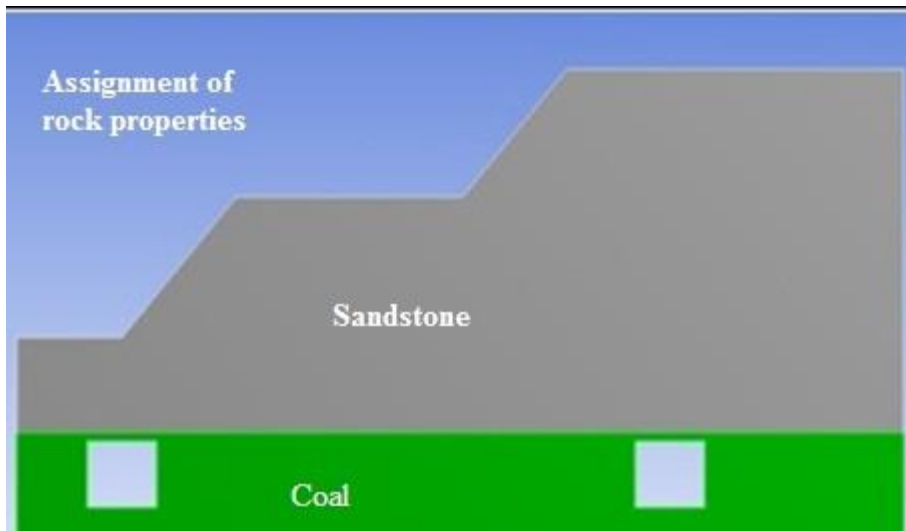
Fig. 3.34 Assignment of rock properties to the model

Meshing of model: This is the most crucial part of the construction of the model. ANSYS provides an advantage of auto-mesh generation for amateur users. The mesh must be as small as possible around the area of observation and the element size must be **Fine**. A correct balance must be struck between the speed of computation due to the size of the element and the accuracy of the result required. In this case, **Tetrahedrones mesh** was chosen by default and the transition of the mesh when crossing from one solid to the other must be **Slow/Smooth**. A mesh generated model is shown in the Figure 3.35.
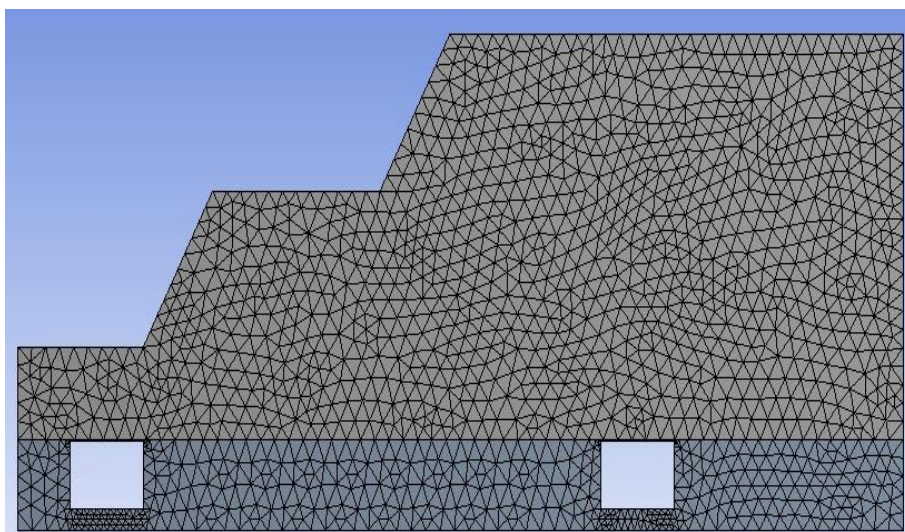
Fig. 3.35 Meshing in ANSYS workbench

Applying loading condition to the model: In this stage, the forces, loads, environmental conditions and boundary conditions are applied. For the simulation of this model, the following loading conditions were imposed on the model.

Gravitational force: The gravity can be applied to the model in the **Model** option of **Static Structural** from **Environment > Inertial > Standard Earth Gravity.** The gravitational force acts along the center of gravity of the combined mass. The application of gravity is shown in the Figure 3.35.
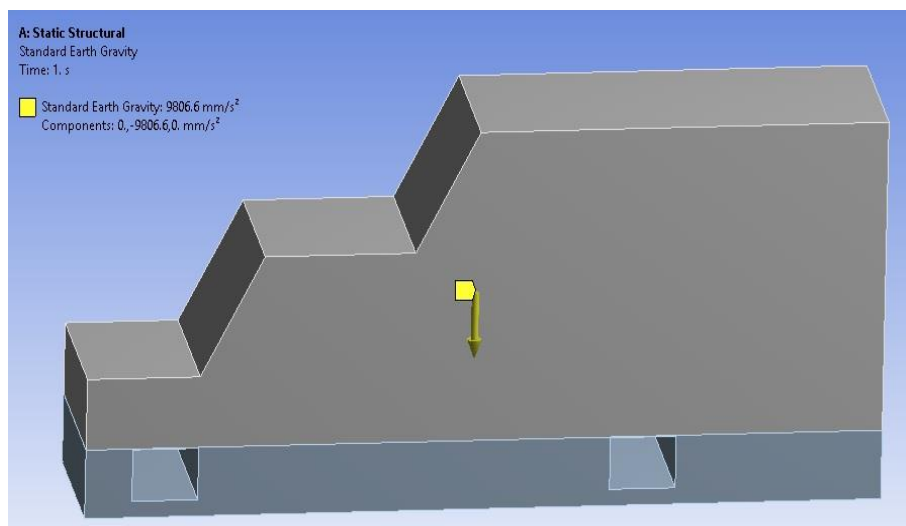
Fig. 3.36 Standard earth gravity on a model

External load due to HEMM: HEMM load was placed at the center of the surface above the gallery. Stress exerted by HEMM was taken as 3.7×10^6 N. The load due to HEMM is chosen from the option, **Environmental > Loads > Remote Force**.

The face on which the load was applied, direction of the force and the coordinates at which the force acting was specified (Fig. 3.37).
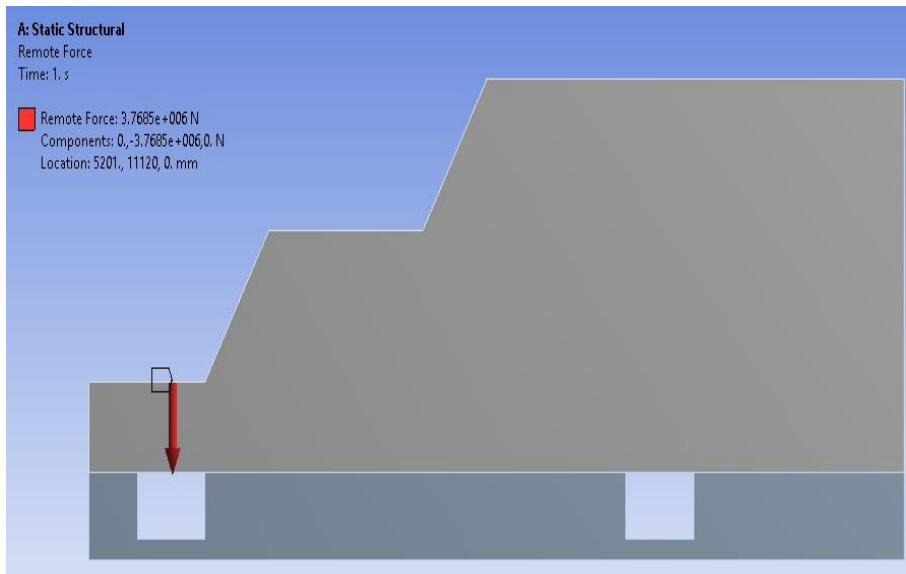
Fig. 3.37 External load applied to the model

Specifying supports on the model: A rigid support was applied to the base of the model as shown in the Figure 3.38. The support is chosen from **Environmental > Supports > Fixed Supports**. Frictionless supports were applied to the sides of the model as shown in the Figure 3.39. The support is chosen from **Environmental > Supports > Frictionless Support.**
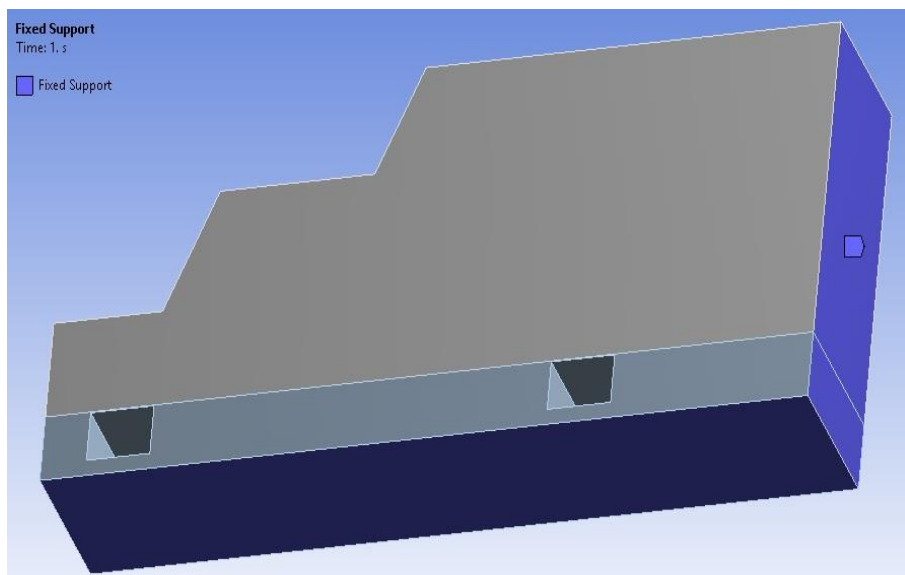
Fig. 3.38 Fixed support applied to the model

84
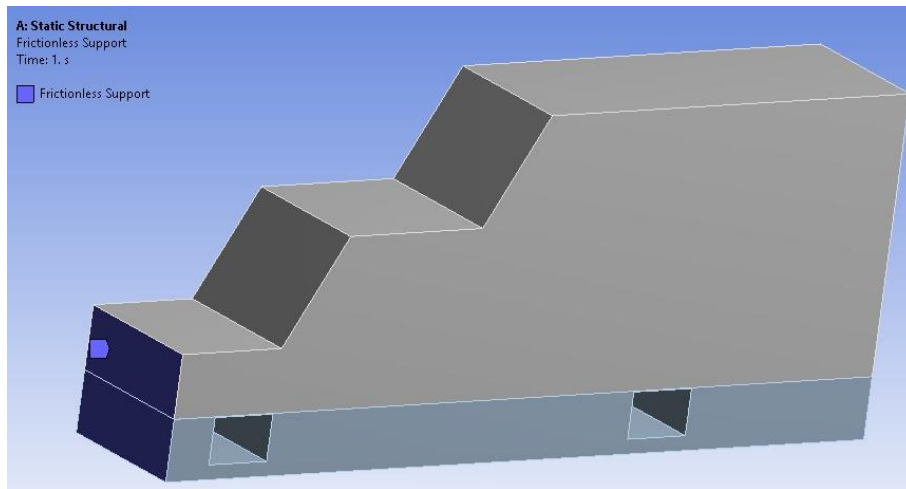
Fig. 3.39 Applying frictionless supports in the model

Specifying the output results: The Final step is to select the result parameters. The result parameters can be chosen from a variety of options ranging from stress, strain to displacements and FOS. Once the loads are applied and the supports assigned, the desired results can be selected from the list of results. The list of results can be obtained under the **Solution** tab of the project tree. Solution tab allows us to select the options **Deformation** and also allows us to select sub-choices of deformation like **Total Deformation**, **Directional Deformation**, etc.

Finally, for obtaining the results, **Solve** button is clicked upon and the values of the parameters are obtained by selecting **Probe** and then clicking on the desired point. After processing, a multicolored model is obtained which would be showing the vertical deformation and strain of the model (Fig. 3.40 and 3.41).
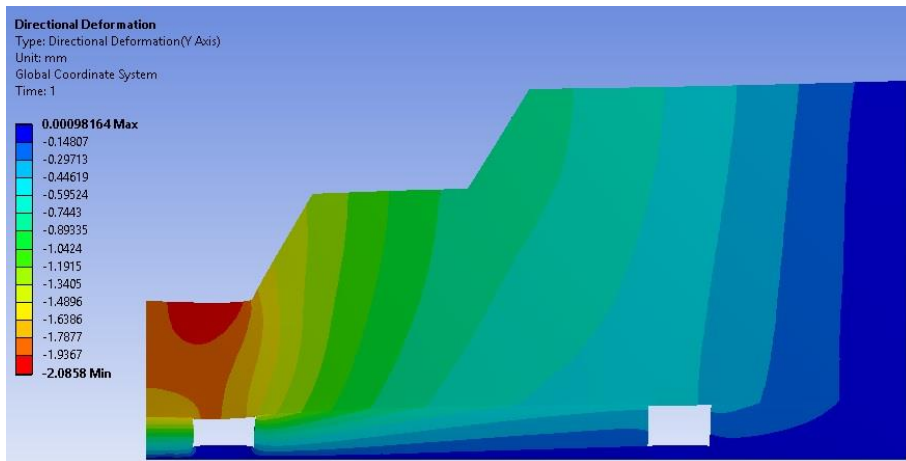
Fig. 3.40 Variation in deformation in ANSYS workbench
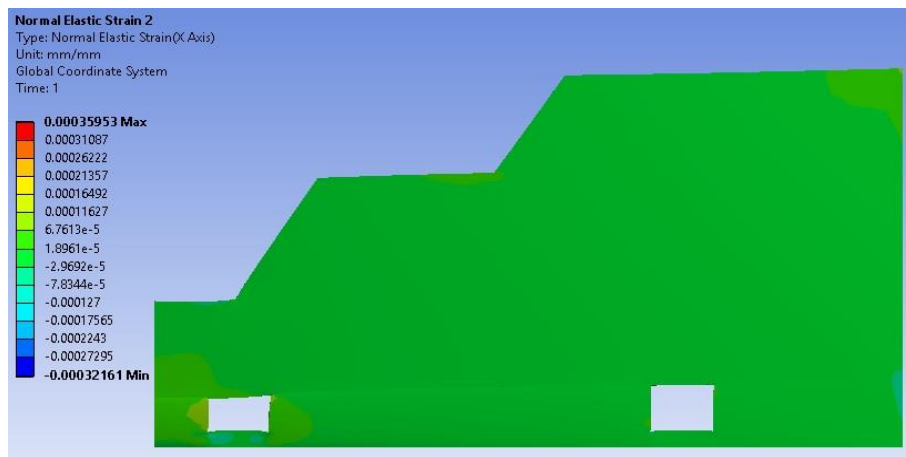
Fig. 3.41 Variation in strain in ANSYS workbench

In this study, Factor of Safety (FOS) was calculated due to the load caused by the movement of HEMM. FOS is determined using Mohr-Coulomb theory for brittle materials, which is also known as internal friction theory. The theory states that the failure occurs when the maximum, middle and minimum principal stresses at the same point equal or exceed their respective stress limits.

$$\frac{\sigma_1}{S_{\text{tensile limit}}} + \frac{\sigma_3}{S_{\text{compressive limit}}} < 1 \quad \text{------------- (3.1)}$$

Where $\sigma_1 > \sigma_2 > \sigma_3$; σ_3 and the compressive strength limit must be entered as positive values. This theory is used to calculate the FOS mainly because the compressive

strength is usually much greater than the tensile strength for sandstone, of which this theory takes a direct account. FOS values are in the form of colored contours that are indexed on the left top corner of the model shown in Fig. 3.42.
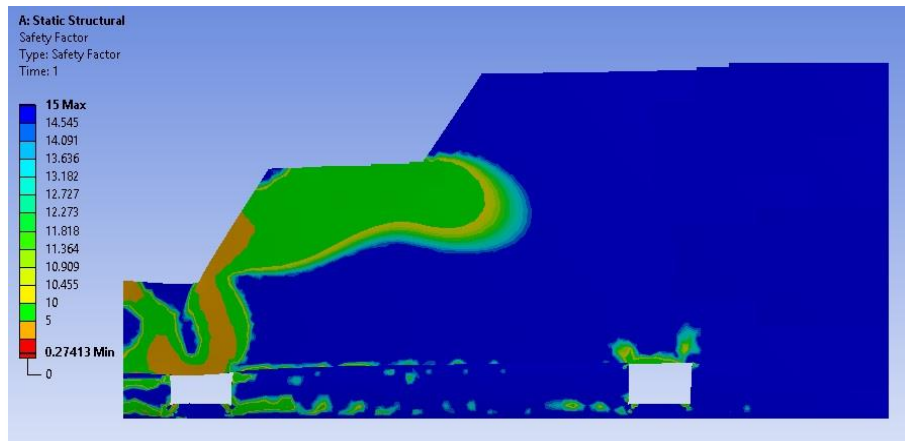
Fig. 3.42 Variation in FOS in ANSYS workbench

3.3.2   Details of numerical modeling study

This section consists two phases. In the first phase, modeling of field condition is discussed. In the second phase, modeling of influence of geometrical dimensions, rock properties and external load on the stability of old underground galleries is carried out.

3.3.2.1 Modeling of field conditions

Modeling of field cases was carried out to validate the data generated by Zigbee based WDAQ and conventional data logger during field investigations. Gallery width of 4.2m, gallery height of 3.0m, pillar width of 30.5m and coal seam thickness of 4.0m were taken for modeling as per field conditions. Rock properties and other bench configurations like berm width and bench height were collected during field studies. Partition thickness and slope angles over old underground galleries were varied by keeping other parameters as constant as per field conditions.

Models developed for partition thicknesses of 4.12m, 5.91m, 6.86m, 7.91m, 10.21m and 12.10 and the results of ANSYS model for different partition thicknesses are shown in the Figure 3.43.
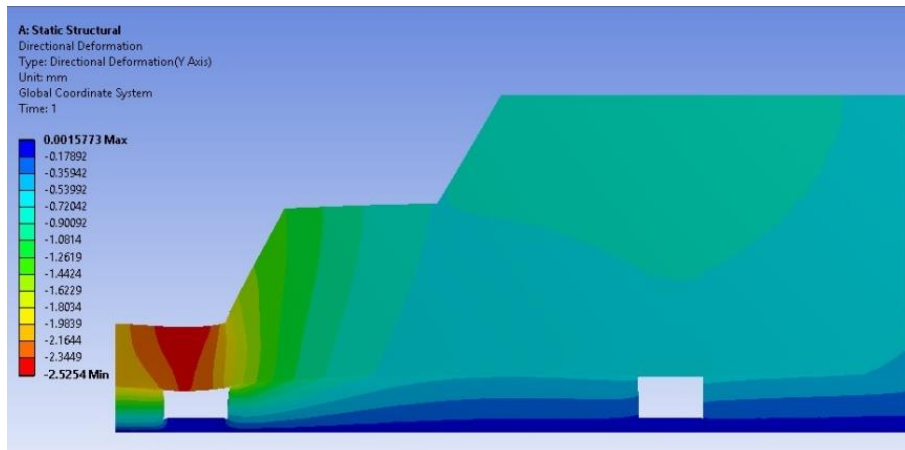
Fig. 3.43A Variation of deformation in partition thickness of 4.12m
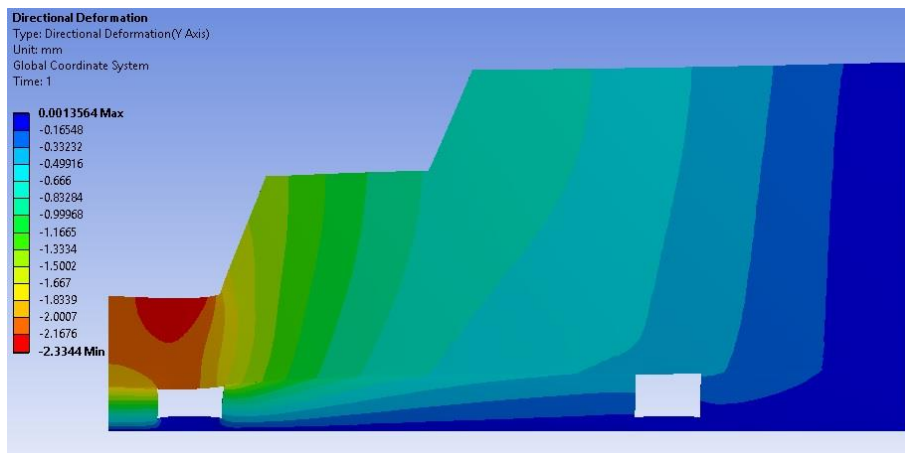
Fig. 3.43B Variation of deformation in partition thickness of 5.91m
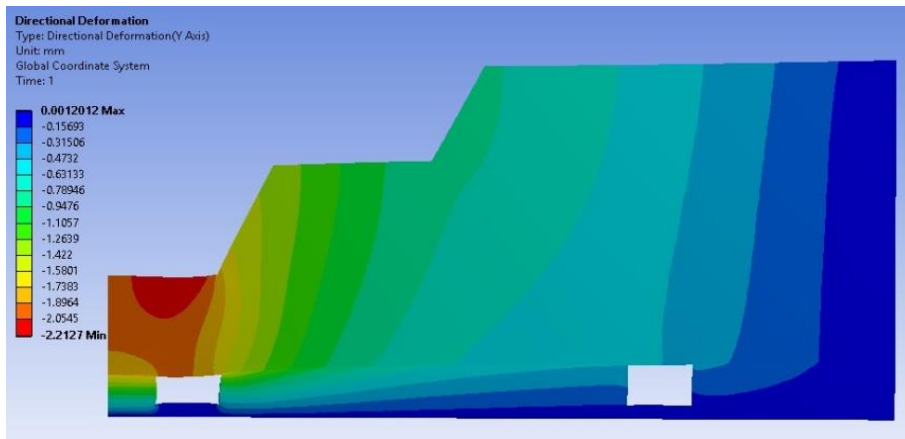
Fig. 3.43C Variation of deformation in partition thickness of 6.86m
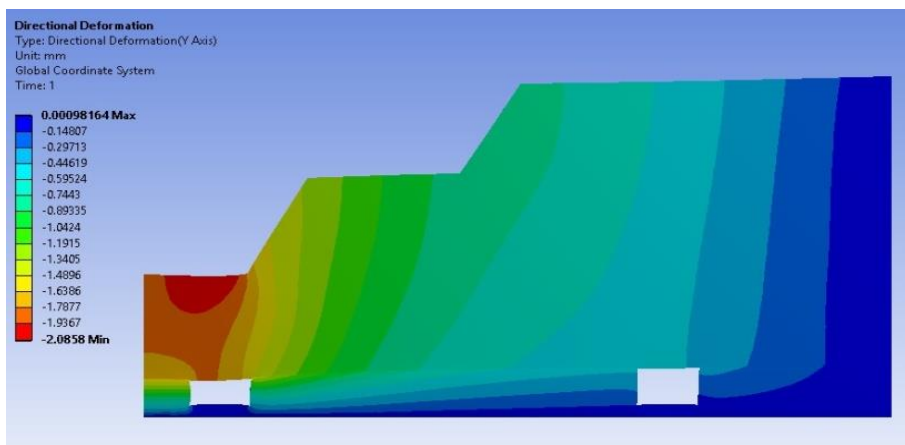
Fig. 3.43D Variation of deformation in partition thickness of 7.91m
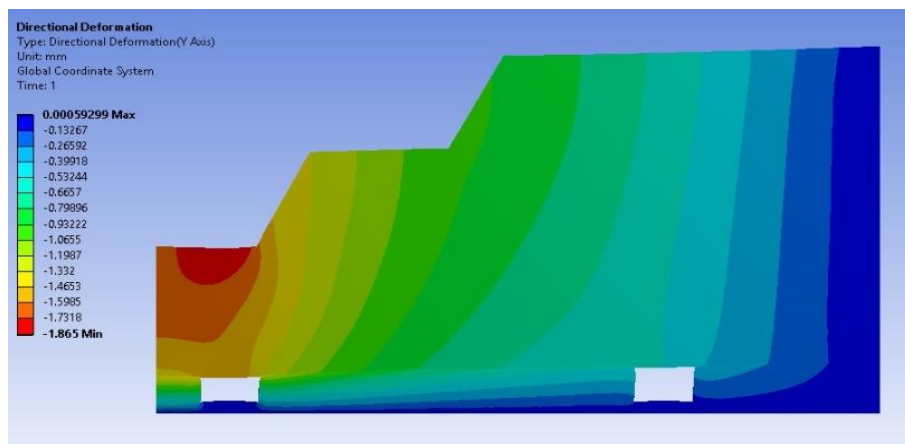
Fig. 3.43E Variation of deformation in partition thickness of 10.21m
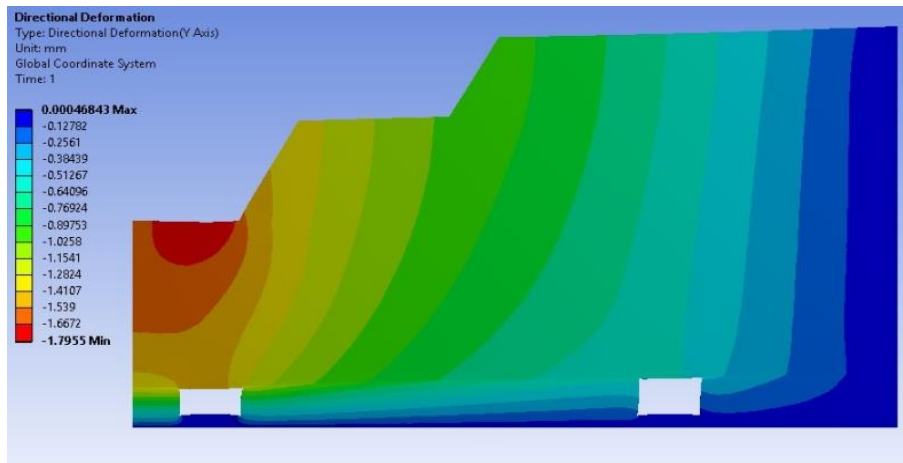
Fig. 3.43F Variation of deformation in partition thickness of 12.10m

Fig. 3.43 Modeling of partition thickness based on field conditions

Deformation values at monitoring points 'A', 'B' and 'C' for different partition thicknesses above the old underground galleries are obtained from models and given in Table 3.11.

Table 3.11 Variation in deformation at different monitoring points in partition using numerical modeling

Partition thickness(m)	Deformation(mm)		
	Monitoring Point-A	Monitoring Point-B	Monitoring Point-C
4.12	2.50	2.52	2.49
5.91	2.30	2.33	2.28
6.86	2.08	2.21	2.04
7.91	1.98	2.08	2.01
10.21	1.79	1.86	1.74
12.10	1.68	1.79	1.69

Models were developed for different slope angles with similar field conditions same as Zigbee based WDAQ and Data logger. Slope angles of 49°, 65°, 64°, 70°, 62° and 68° and partition thicknesses of 5.82m, 5.92m, 6.26m, 6.47m, 6.86m and 6.95m respectively, were considered for this study based on field conditions. The results of ANSYS model for different partition thicknesses are shown in the Figure 3.44.
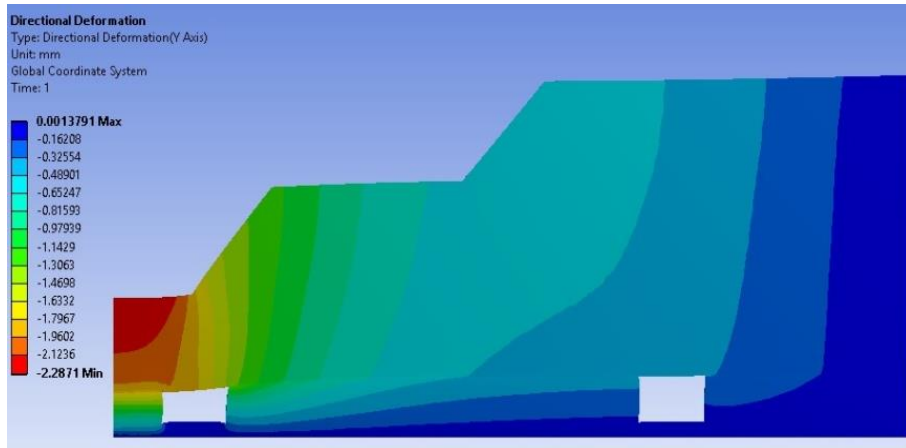
Fig. 3.44A Variation of deformation in slope of angle of 49º
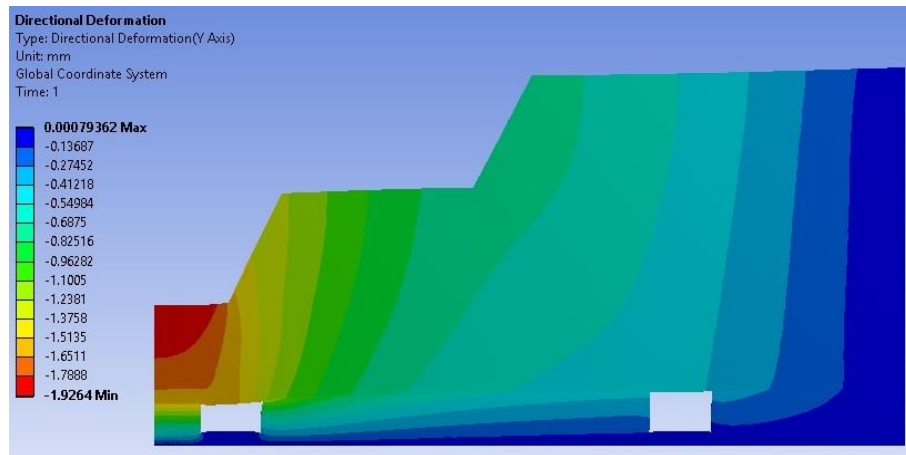
Fig. 3.44B Variation of deformation in slope of angle of 62º
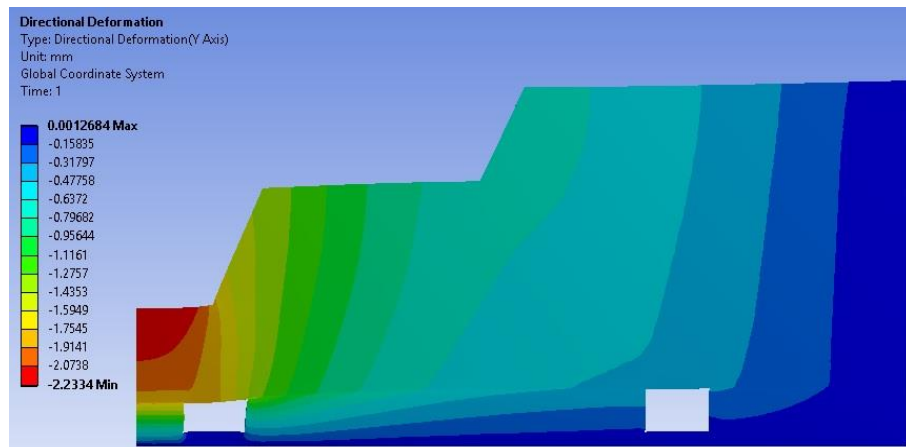
Fig. 3.44C Variation of deformation in slope of angle of 64º
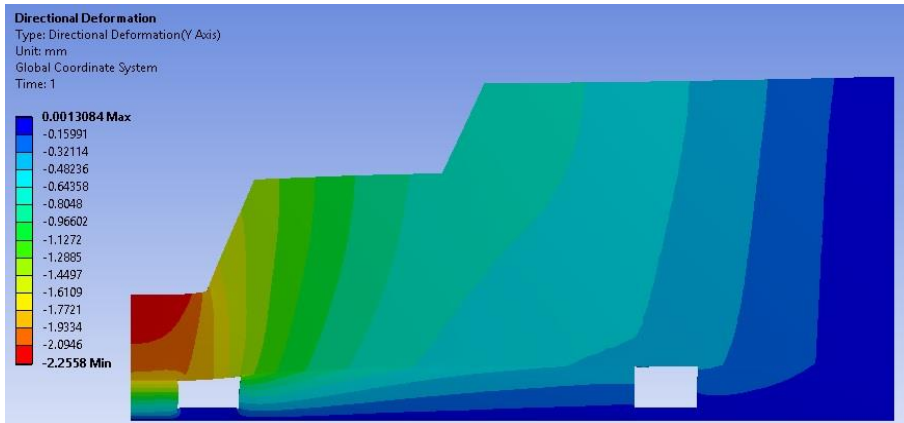
Fig. 3.44D Variation of deformation in slope of angle of 65°
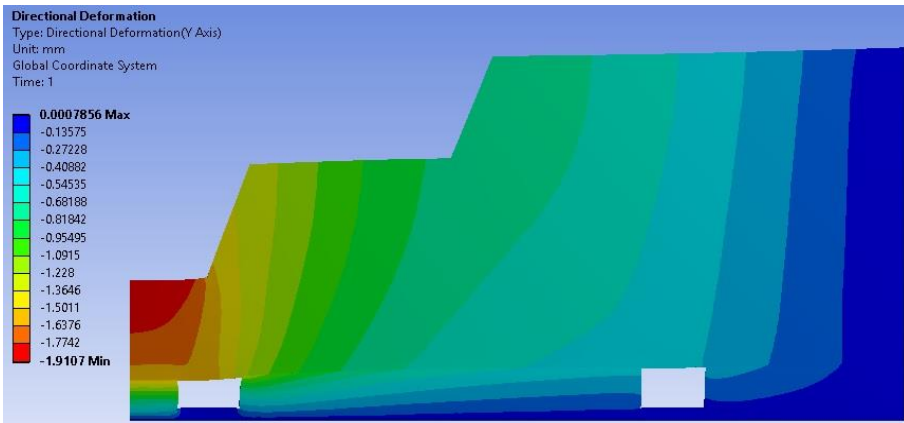
Fig. 3.44E Variation of deformation in slope of angle of 68°
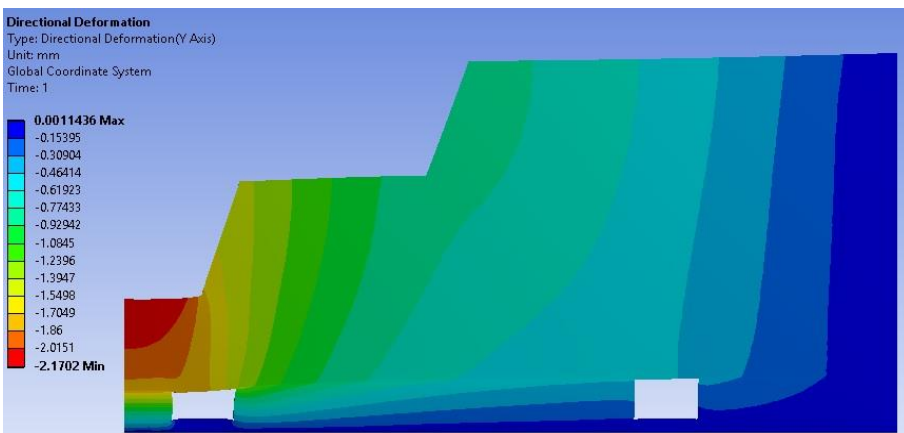
Fig. 3.44F Variation of deformation in slope of angle of 70°

Fig. 3.44 Modeling of slope angle based on field conditions

Deformation values at points 'A', 'B' and 'C' lying above the old underground galleries were obtained from models and tabulated in Table 3.12.

Table 3.12 Variation in deformation at different monitoring points along slope using numerical modeling

Slope Angle (Degrees)	Partition thickness(m)	Deformation(mm)		
		Monitoring Point-A	Monitoring Point-B	Monitoring Point-C
49	5.82	1.78	1.63	1.30
65	5.91	1.77	1.61	1.28
64	6.26	1.75	1.59	1.27
70	6.47	1.70	1.54	1.23
62	6.86	1.65	1.51	1.22
68	6.95	1.63	1.50	1.21

3.3.2.2 Modeling with various parameters

In addition to the modeling of field conditions, models were also developed to assess the influence of geometric dimensions, rock properties and external load on the stability of old underground galleries. The geometric dimensions are gallery width, gallery height, pillar width, partition thickness, slope angle and berm width. Rock properties are density, compressive strength of sandstone and coal. External load includes the load of shovel and dumper combination. Vertical deformation, strain and Factor of Safety (FOS) were observed at the surface centers ('R' and 'S') over old galleries and roof centers ('P' and 'Q') of gallery1 and gallery2 (Fig. 3.45).
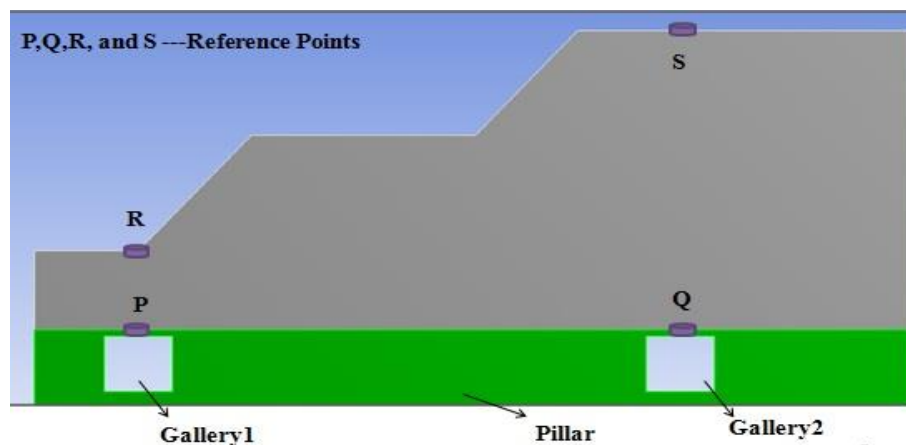
Fig. 3.45 Reference points for output in the model

Geometrical dimensions included gallery widths of 3.0m, 3.6m, 4.2m and 4.8m were considered as per Reg. No. 111 of CMR – 2017 (Table 3.13). Pillar widths were considered with respect to the gallery width and incremented by 1m. Gallery height values were ranging from 2.4m to 3.4m with an increment of 0.2m. Partition thickness was considered from 4m to 12m with increment of 2m. Berm width of 5m to 10m with an increment of 1m was considered. Slope angle of 50º to 75º with an increment of 5º was considered. In total, 20,736 models were developed by varying different parameters (Table 3.14).

Table 3.13 Dimensions of pillars and galleries at different working depths as per Reg. No. 111 of CMR – 2017

Depth of seam from the surface	Where width of gallery does not exceed 3.0m	Where width of gallery does not exceed 3.6m	Where width of gallery does not exceed 4.2m	Where width of gallery does not exceed 4.8m
	The distance between centers of adjacent pillars shall not be less than			
	m	m	m	m
Not exceeding 60m	12.0	15.0	18.0	19.5
Exceeding 60m but not exceeding 90m	13.5	16.5	19.5	21.0
Exceeding 90m but not exceeding 150m	16.5	19.5	22.5	25.5
Exceeding 150m but not exceeding 240m	22.5	25.5	30.5	34.5
Exceeding 240m but not exceeding 360m	28.5	34.5	39.5	45.0
Exceeding 360m	39.5	42.0	45.0	48.0

Table 3.14 Number of numerical models developed for assessment of stability of old underground coal workings

No. of Models for External load of 300t (Shovel-Dumper Combination Load)										
Geometrical Dimensions						Rock Properties				
						Sandstone		Coal		
Gallery Width (m)	Pillar Width (m)	Gallery Height (m)	Partition thickness (m)	Berm width (m)	Slope angle (Degree)	Density (kg/m³)	Compressive Strength (MPa)	Density (kg/cm³)	Compressive Strength (MPa)	Total No. of Models
3	22.5	2.4 to 3.4	4 to 12	5 to 10	50 to 75	2100 to 2500	25 to 85	1100 to 1500	15 to 45	6,912
	23.5									
	24.5									
3.6	25.5									
	26.5									
	27.5									
4.2	30.5									
	31.5									
	32.5									
4.8	34.5									
	35.5									
	36.5									
Total										6,912
External Load (t)			300 to 700 with increment of 200t							X 3
Grand Total										20,736

Influence of partition thickness

Overburden or partition thickness was varied by keeping other parameters such as gallery height, gallery width, pillar width, berm width, slope angle, rock properties and external load as constant. Partition thicknesses of 4m, 6m, 8m, 10m and 12m were considered to assess the influence of partition thickness on stability of old underground galleries. Multi-colored output results from ANSYS for the partition thickness of 4m, 6m, 8m, 10m and 12m are shown in the Figure 3.46. The results of directional deformation for different partition thicknesses over gallery 1 and gallery 2, when the gallery width is 4.2m, gallery height is ranging from 2.4m to 3.4m, slope angle is 55^0, berm width is 5m and pillar widths are about 30.5m, 31.5m and 32.5m, are given in Table 3.15 and 3.16. The results of FOS for different partition thicknesses over gallery 1 and gallery 2 are given Table 3.17.
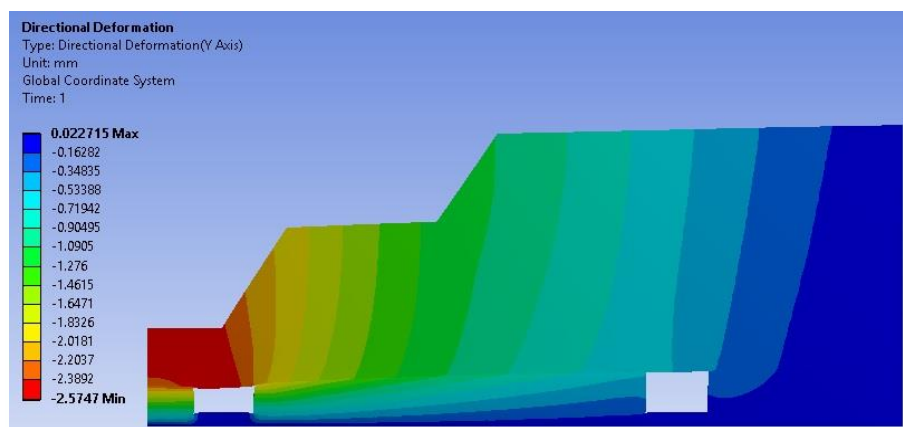
Fig. 3.46A Vertical deformation contours over old galleries for partition thickness of 4m
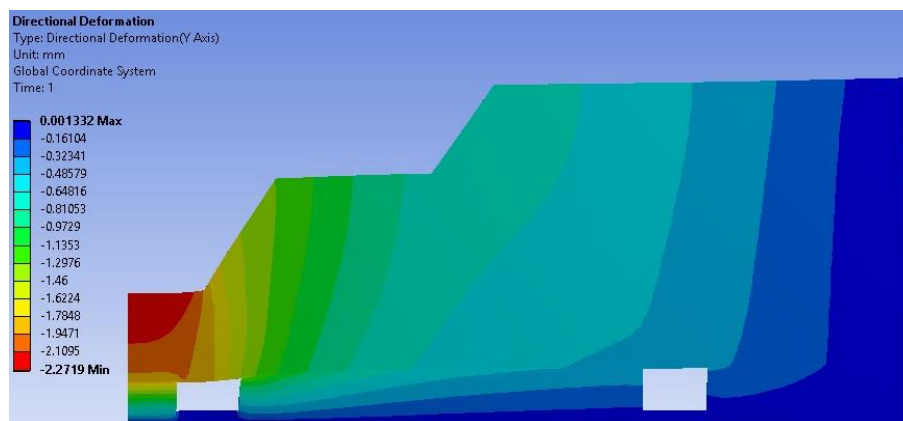
Fig. 3.46B Vertical deformation contours over old galleries for partition thickness of 6m
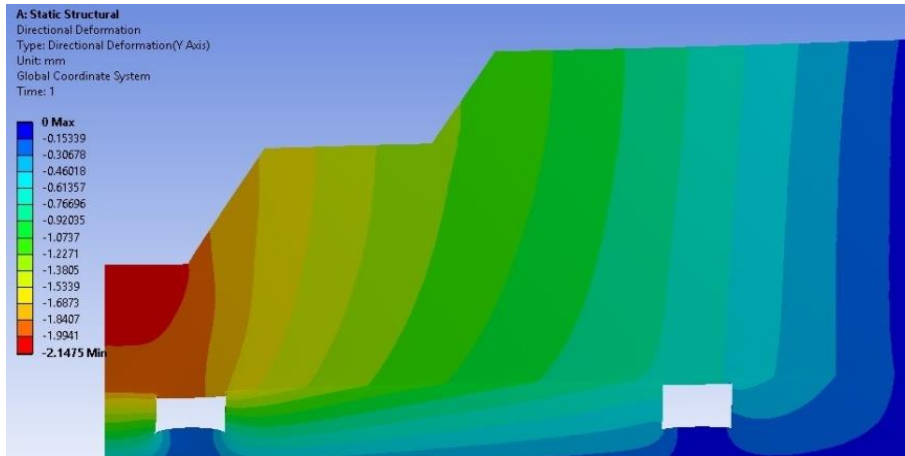
Fig. 3.46C Vertical deformation contours over old galleries for partition thickness of 8m
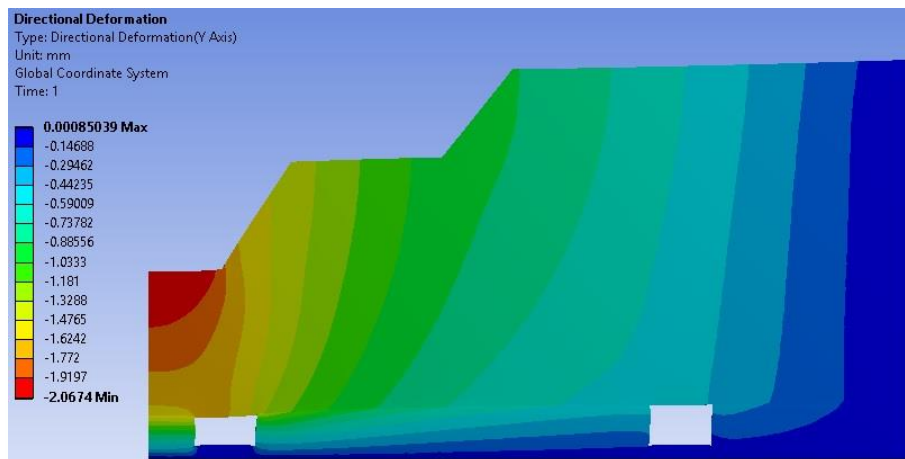
Fig. 3.46D Vertical deformation contours over old galleries for partition thickness of 10m
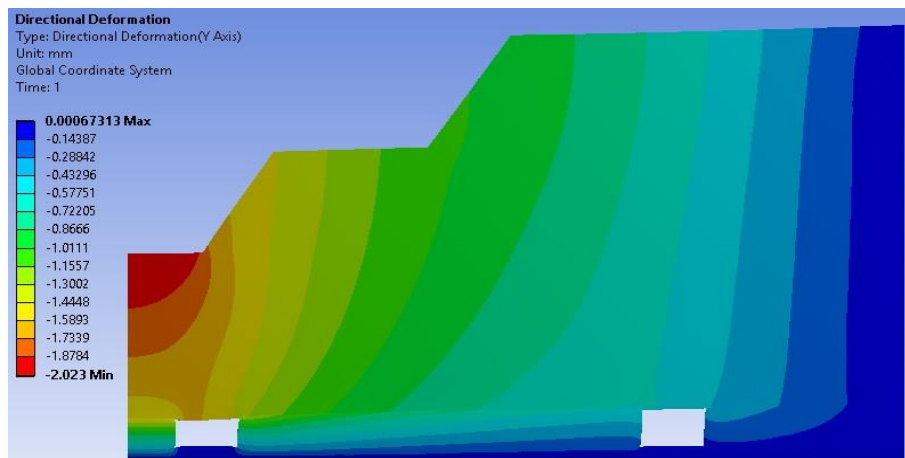
Fig. 3.46E Vertical deformation contours over old galleries for partition thickness of 12m

Fig. 3.46 The results for variation of partition thickness based on modeling studies

Table 3.15 Variation in directional deformation at points 'P' and 'R' of gallery1 for gallery width of 4.2m

Partition thickness(m) above gallery1	Pillar width(m)	Deformation (mm) at different gallery height (m) and gallery width=4.2m											
		Roof center of gallery 1 (Point P)						Surface center of gallery1 (Point R)					
		2.4	2.6	2.8	3.0	3.2	3.4	2.4	2.6	2.8	3.0	3.2	3.4
4	30.5	2.12	2.16	2.20	2.24	2.28	2.32	2.45	2.49	2.53	2.57	2.61	2.65
	31.5	2.04	2.08	2.12	2.16	2.20	2.24	2.37	2.41	2.45	2.49	2.53	2.57
	32.5	1.96	2.00	2.04	2.08	2.12	2.16	2.29	2.33	2.37	2.41	2.45	2.49
6	30.5	1.81	1.85	1.89	1.93	1.97	2.01	2.14	2.18	2.22	2.26	2.30	2.34
	31.5	1.73	1.77	1.81	1.85	1.89	1.93	2.06	2.10	2.14	2.18	2.22	2.26
	32.5	1.65	1.69	1.73	1.77	1.81	1.85	1.98	2.02	2.06	2.10	2.14	2.18
8	30.5	1.69	1.73	1.77	1.81	1.85	1.89	2.02	2.06	2.10	2.14	2.18	2.22
	31.5	1.61	1.65	1.69	1.73	1.77	1.81	1.94	1.98	2.02	2.06	2.10	2.14
	32.5	1.53	1.57	1.61	1.65	1.69	1.73	1.86	1.90	1.94	1.98	2.02	2.06
10	30.5	1.61	1.65	1.69	1.73	1.77	1.81	1.94	1.98	2.02	2.06	2.10	2.14
	31.5	1.53	1.57	1.61	1.65	1.69	1.73	1.86	1.90	1.94	1.98	2.02	2.06
	32.5	1.45	1.49	1.53	1.57	1.61	1.65	1.78	1.82	1.86	1.90	1.94	1.98
12	30.5	1.57	1.61	1.65	1.69	1.73	1.77	1.90	1.94	1.98	2.02	2.06	2.10
	31.5	1.49	1.53	1.57	1.61	1.65	1.69	1.82	1.86	1.90	1.94	1.98	2.02
	32.5	1.41	1.45	1.49	1.53	1.57	1.61	1.74	1.78	1.82	1.86	1.90	1.94

Table 3.16 Variation in directional deformation at points 'Q' and 'S' of gallery-2 for gallery width of 4.2m

Partition thickness(m) above gallery1	Pillar width(m)	Deformation (mm) at different gallery heights (m) and gallery width=4.2m											
		Roof center of gallery 2 (Point Q)						Surface center of gallery2 (Point S)					
		2.4	2.6	2.8	3.0	3.2	3.4	2.4	2.6	2.8	3.0	3.2	3.4
4	30.5	1.32	1.36	1.40	1.44	1.48	1.52	1.55	1.59	1.63	1.67	1.71	1.75
	31.5	1.24	1.28	1.32	1.36	1.40	1.44	1.47	1.51	1.55	1.59	1.63	1.67
	32.5	1.16	1.20	1.24	1.28	1.32	1.36	1.39	1.43	1.47	1.51	1.55	1.59
6	30.5	1.01	1.05	1.09	1.13	1.17	1.21	1.24	1.28	1.32	1.36	1.40	1.44
	31.5	0.93	0.97	1.01	1.05	1.09	1.13	1.16	1.20	1.24	1.28	1.32	1.36
	32.5	0.85	0.89	0.93	0.97	1.01	1.05	1.08	1.12	1.16	1.20	1.24	1.28
8	30.5	0.89	0.93	0.97	1.01	1.05	1.09	1.12	1.16	1.20	1.24	1.28	1.32
	31.5	0.81	0.85	0.89	0.93	0.97	1.01	1.04	1.08	1.12	1.16	1.20	1.24
	32.5	0.73	0.77	0.81	0.85	0.89	0.93	0.96	1.00	1.04	1.08	1.12	1.16
10	30.5	0.81	0.85	0.89	0.93	0.97	1.01	1.04	1.08	1.12	1.16	1.20	1.24
	31.5	0.73	0.77	0.81	0.85	0.89	0.93	0.96	1.00	1.04	1.08	1.12	1.16
	32.5	0.65	0.69	0.73	0.77	0.81	0.85	0.88	0.92	0.96	1.00	1.04	1.08
12	30.5	0.77	0.81	0.85	0.89	0.93	0.97	1.00	1.04	1.08	1.12	1.16	1.20
	31.5	0.69	0.73	0.77	0.81	0.85	0.89	0.92	0.96	1.00	1.04	1.08	1.12
	32.5	0.61	0.65	0.69	0.73	0.77	0.81	0.84	0.88	0.92	0.96	1.00	1.04

Table 3.17 Variation in FOS at points 'P' of gallery1 and 'Q'of gallery2

Partition thickness(m) above gallery1	Pillar width(m)	Deformation (mm) at different gallery height (m) and gallery width=4.2m											
		Roof center of gallery 1 (Point P)						Roof center of gallery 2 (Point Q)					
		2.4	2.6	2.8	3.0	3.2	3.4	2.4	2.6	2.8	3.0	3.2	3.4
4	30.5	1.58	1.50	1.42	1.34	1.26	1.18	8.84	8.76	8.68	8.60	8.52	8.44
	31.5	1.80	1.72	1.64	1.56	1.48	1.40	9.06	8.98	8.90	8.82	8.74	8.66
	32.5	1.88	1.80	1.72	1.64	1.56	1.48	9.14	9.06	8.98	8.90	8.82	8.74
6	30.5	1.99	1.91	1.83	1.75	1.67	1.59	8.84	8.76	8.68	8.60	8.52	8.44
	31.5	2.21	2.13	2.05	1.97	1.89	1.81	9.06	8.98	8.90	8.82	8.74	8.66
	32.5	2.43	2.35	2.27	2.19	2.11	2.03	9.14	9.06	8.98	8.90	8.82	8.74
8	30.5	2.20	2.12	2.04	1.96	1.88	1.80	9.46	9.38	9.30	9.22	9.14	9.06
	31.5	2.42	2.34	2.26	2.18	2.10	2.02	9.68	9.60	9.52	9.44	9.36	9.28
	32.5	2.64	2.56	2.48	2.40	2.32	2.24	9.90	9.82	9.74	9.66	9.58	9.50
10	30.5	2.31	2.23	2.15	2.07	1.99	1.91	9.57	9.49	9.41	9.33	9.25	9.17
	31.5	2.53	2.45	2.37	2.29	2.21	2.13	9.79	9.71	9.63	9.55	9.47	9.39
	32.5	2.75	2.67	2.59	2.51	2.43	2.35	10.01	9.93	9.85	9.77	9.69	9.61
12	30.5	2.39	2.31	2.23	2.15	2.07	1.99	9.65	9.57	9.49	9.41	9.33	9.25
	31.5	2.61	2.53	2.45	2.37	2.29	2.21	9.87	9.79	9.71	9.63	9.55	9.47
	32.5	2.83	2.75	2.67	2.59	2.51	2.43	10.09	10.01	9.93	9.85	9.77	9.69

Influence of gallery width

Studies were carried out to investigate the influence of gallery width on the stability of old underground coal workings. Gallery width of 3.0m, 3.6m, 4.2m and 4.8m were considered by keeping all other parameters such as partition thickness, gallery height, slope angle, rock properties, external load, berm width, pillar width, etc., as constant. Models developed and multi-colored output results from ANSYS for different gallery widths are shown in the Fig. 3.47.
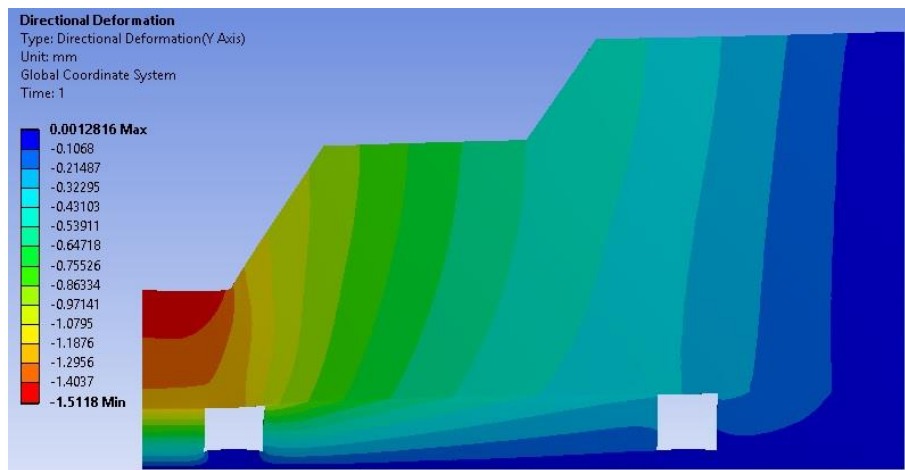
Fig. 3.47A Vertical deformation contours over old galleries for gallery width of 3.0m
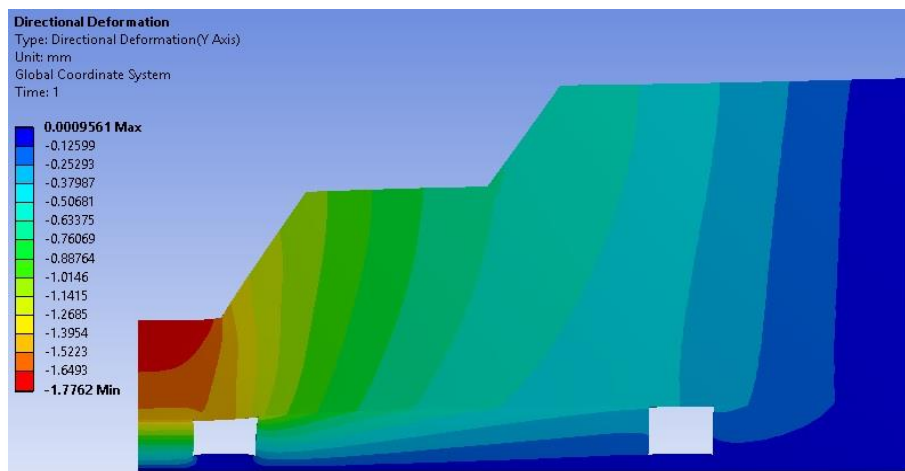
Fig. 3.47B Vertical deformation contours over old galleries for gallery width of 3.6m
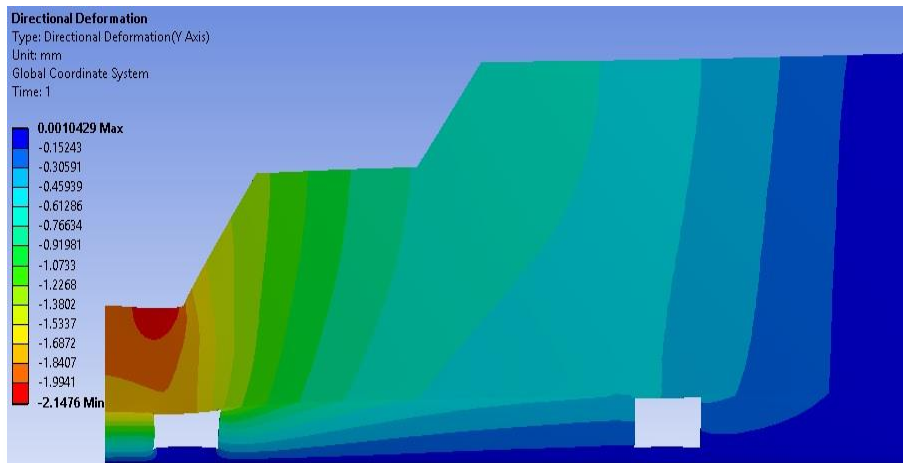
Fig. 3.47C Vertical deformation contours over old galleries for gallery width of 4.2m
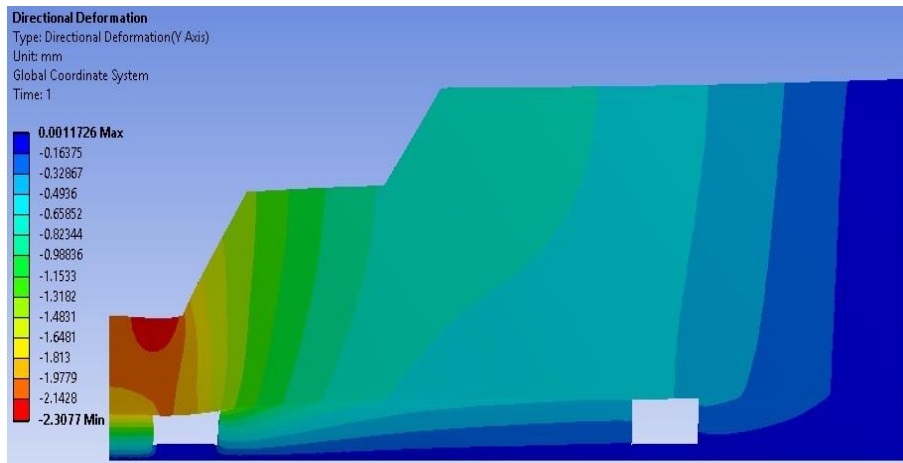
Fig. 3.47D Vertical deformation contours over old galleries for gallery width of 4.8m

Fig. 3.47 The results for variation of gallery width based on numerical modeling studies

The results of vertical deformation at reference points 'P' and 'R' for different gallery widths with respect to the pillar widths, partition thickness of 4m to 12m, gallery height of 2.4m, slope angle of 55°, berm width of 5m are given in Table 3.18.

Table 3.18 Variation in deformation at points 'P' and 'R' of gallery-1 for different gallery widths

Gallery Width (m)	Pillar width (m)	Deformation (mm)									
		Roof center of gallery 1 (Point P)					Surface center of gallery1 (Point R)				
		4	6	8	10	12	4	6	8	10	12
3.0	22.5	1.52	1.21	1.09	1.01	0.97	1.82	1.51	1.39	1.31	1.27
3.6	25.5	1.78	1.47	1.35	1.27	1.23	2.09	1.78	1.66	1.58	1.54
4.2	30.5	2.12	1.81	1.69	1.61	1.57	2.45	2.14	2.02	1.94	1.90
4.8	34.5	2.30	1.99	1.87	1.79	1.75	2.61	2.30	2.18	2.10	2.06

Influence of pillar width

The influence of pillar width on the stability of old underground galleries was analyzed in this case. Different pillar widths were considered with respect to the gallery width. For gallery width of 3.0m, pillar widths of 22.5m, 23.5m and 24.5m were considered. Similarly, Pillar widths of 25.5m, 26.5m and 27.5m for gallery width of 3.6, pillar width of 30.5m, 31.5m and 32.5m for gallery width of 4.2m and pillar widths of 34.5m, 35.5m and 36.5m for gallery width of 4.8m were considered in this study. Pillar width was varied by keeping other parameters as constant.

The results of Deformation at reference points 'P', 'Q', 'R' and 'S' and FOS at 'P' and 'Q' over old galleries when gallery width is 4.2m for different pillar widths of 30.5m, 31.5m and 32.5m, gallery heights of 2.4m, 2.6m, 2.8m, 3.0m, 3.2m and 3,4m, partition thicknesses of 4m, 6m, 8m, 10m and 12m, slope angle of 55° and berm width of 5m are given in Tables 3.15, 3.16 and 3.17 respectively.

Influence of gallery height

The objective of this study is to investigate the influence of gallery height on the stability of old underground coal workings. Different gallery heights were considered such as 2.4m, 2.6m, 2.8m, 3.0m, 3.2m and 3.4m for simulating field conditions. Gallery height was varied by keeping other parameters such as gallery width, partition thickness, pillar width, berm width, slope angle, rock properties and external load as constant.

The results of deformation values at reference points 'P', 'Q', 'R' and 'S' and FOS at 'P' and 'Q' over old galleries when gallery width is 4.2m for pillar widths of 30.5m, 31.5m and 32.5m, gallery height of 2.4m, 2.6m, 2.8m, 3.0m, 3.2m and 3,4m, partition thicknesses of 4m, 6m, 8m, 10m and 12m, slope angle of 55° and berm width of 5m are presented in Tables 3.15, 3.16 and 3.17 respectively.

Influence of slope angle

The influence of slope angle on the stability of old galleries was studied. Slope angle of 50° to 75° with an increment of 5° was considered for developing models. Slope angle was varied by keeping all other parameters such as gallery width, gallery height, partition thickness, pillar width, berm width, rock properties and external load as constant.

The results of vertical deformation at points 'P' and 'R' over galleries for slope angle of 50°, 55°, 60°, 65°, 70° and 75° when gallery width of 4.2m, pillar width of 30.5m, partition thickness of 6m, gallery height of 2.4m to 3.4m and berm width of 5m are tabulated in Table 3.19.

Table 3.19 Variation in deformation due to change in slope angle at point 'P' and 'R' over gallery1 width of 4.2m and pillar width of 30.5m

| Slope Angle (Deg) | Deformation (mm) at different gallery height (m) and gallery width=4.2m, Partition Thickness=6m | | | | | | | | | | | |
| | Roof center of gallery 1 (Point P) | | | | | | Surface center of gallery1 (Point R) | | | | | |
	2.4	2.6	2.8	3.0	3.2	3.4	2.4	2.6	2.8	3.0	3.2	3.4
50	1.79	1.83	1.87	1.91	1.95	1.99	2.12	2.16	2.20	2.24	2.28	2.32
55	1.81	1.85	1.89	1.93	1.97	2.01	2.14	2.18	2.22	2.26	2.30	2.34
60	1.83	1.87	1.91	1.95	1.99	2.03	2.16	2.20	2.24	2.28	2.32	2.36
65	1.85	1.89	1.93	1.97	2.01	2.05	2.18	2.22	2.26	2.30	2.34	2.38
70	1.87	1.91	1.95	1.99	2.03	2.07	2.20	2.24	2.28	2.32	2.36	2.40
75	1.89	1.93	1.97	2.01	2.05	2.09	2.22	2.26	2.30	2.34	2.38	2.42

Influence of berm width

The influence of berm width on the stability of old galleries was studied. Berm width of 5m to 10m with an increment of 1m was considered for developing models. Berm width was varied by keeping all other parameters as constant. In this section, the directional deformation values observed at points 'P' and 'R' over galleries when gallery width of 4.2m, pillar width of 30.5m, slope angle of 55°, partition thicknesses of 4m to 12m with an increment of 2m and gallery height of 2.4m to 3.4m are tabulated in the Tables 3.20 and 3.20.

Table 3.20 Variation in deformation due to change in berm width at point P over gallery1 width of 4.2m and pillar width of 30.5m

Partition thickness (m)	Gallery Height (m)	Deformation(mm) at point 'P' of gallery1 of width 4.2m					
		Berm Width(m)					
		5	6	7	8	9	10
4	2.4	2.12	2.11	2.10	2.09	2.08	2.07
	2.6	2.16	2.15	2.14	2.13	2.12	2.11
	2.8	2.20	2.19	2.18	2.17	2.16	2.15
	3.0	2.24	2.23	2.22	2.21	2.20	2.19
	3.2	2.28	2.27	2.26	2.25	2.24	2.23
	3.4	2.32	2.31	2.30	2.29	2.28	2.27
6	2.4	1.81	1.80	1.79	1.78	1.77	1.76
	2.6	1.85	1.84	1.83	1.82	1.81	1.80
	2.8	1.89	1.88	1.87	1.86	1.85	1.84
	3.0	1.93	1.92	1.91	1.90	1.89	1.88
	3.2	1.97	1.96	1.95	1.94	1.93	1.92
	3.4	2.01	2.00	1.99	1.98	1.97	1.96
8	2.4	1.69	1.68	1.67	1.66	1.65	1.64
	2.6	1.73	1.72	1.71	1.70	1.69	1.68
	2.8	1.77	1.76	1.75	1.74	1.73	1.72
	3.0	1.81	1.80	1.79	1.78	1.77	1.76
	3.2	1.85	1.84	1.83	1.82	1.81	1.80
	3.4	1.89	1.88	1.87	1.86	1.85	1.84
10	2.4	1.61	1.60	1.59	1.58	1.57	1.56
	2.6	1.65	1.64	1.63	1.62	1.61	1.60
	2.8	1.69	1.68	1.67	1.66	1.65	1.64

Partition thickness (m)	Gallery Height (m)	Deformation(mm) at point 'P' of gallery1 of width 4.2m					
		Berm Width(m)					
		5	6	7	8	9	10
	3.0	1.73	1.72	1.71	1.70	1.69	1.68
	3.2	1.77	1.76	1.75	1.74	1.73	1.72
	3.4	1.81	1.80	1.79	1.78	1.77	1.76
12	2.4	1.57	1.56	1.55	1.54	1.53	1.52
	2.6	1.61	1.60	1.59	1.58	1.57	1.56
	2.8	1.65	1.64	1.63	1.62	1.61	1.60
	3.0	1.69	1.68	1.67	1.66	1.65	1.64
	3.2	1.73	1.72	1.71	1.70	1.69	1.68
	3.4	1.77	1.76	1.75	1.74	1.73	1.72

Table 3.21 Variation in deformation due to change in berm width at point 'R' over gallery1 width of 4.2m and pillar width of 30.5m

Partition thickness (m)	Gallery Height (m)	Deformation(mm) at point 'R' of gallery1 of width 4.2m					
		Berm Width(m)					
		5	6	7	8	9	10
4	2.4	2.45	2.44	2.43	2.42	2.41	2.40
	2.6	2.49	2.48	2.47	2.46	2.45	2.44
	2.8	2.53	2.52	2.51	2.50	2.49	2.48
	3.0	2.57	2.56	2.55	2.54	2.53	2.52
	3.2	2.61	2.60	2.59	2.58	2.57	2.56
	3.4	2.65	2.64	2.63	2.62	2.61	2.60
6	2.4	2.14	2.13	2.12	2.11	2.10	2.09
	2.6	2.18	2.17	2.16	2.15	2.14	2.13
	2.8	2.22	2.21	2.20	2.19	2.18	2.17
	3.0	2.26	2.25	2.24	2.23	2.22	2.21
	3.2	2.30	2.29	2.28	2.27	2.26	2.25
	3.4	2.34	2.33	2.32	2.31	2.30	2.29
8	2.4	2.02	2.01	2.00	1.99	1.98	1.97
	2.6	2.06	2.05	2.04	2.03	2.02	2.01
	2.8	2.10	2.09	2.08	2.07	2.06	2.05
	3.0	2.14	2.13	2.12	2.11	2.10	2.09
	3.2	2.18	2.17	2.16	2.15	2.14	2.13
	3.4	2.22	2.21	2.20	2.19	2.18	2.17
10	2.4	1.94	1.93	1.92	1.91	1.90	1.89

Partition thickness (m)	Gallery Height (m)	Deformation(mm) at point 'R' of gallery1 of width 4.2m					
		Berm Width(m)					
		5	**6**	**7**	**8**	**9**	**10**
	2.6	1.98	1.97	1.96	1.95	1.94	1.93
	2.8	2.02	2.01	2.00	1.99	1.98	1.97
	3.0	2.06	2.05	2.04	2.03	2.02	2.01
	3.2	2.10	2.09	2.08	2.07	2.06	2.05
	3.4	2.14	2.13	2.12	2.11	2.10	2.09
12	**2.4**	1.90	1.89	1.88	1.87	1.86	1.85
	2.6	1.94	1.93	1.92	1.91	1.90	1.89
	2.8	1.98	1.97	1.96	1.95	1.94	1.93
	3.0	2.02	2.01	2.00	1.99	1.98	1.97
	3.2	2.06	2.05	2.04	2.03	2.02	2.01
	3.4	2.10	2.09	2.08	2.07	2.06	2.05

Influence of rock properties

As rock properties play a major role in stability analysis, they were varied in the modeling study by keeping other parameters as constant. The rock properties considered are density and compressive strength of sandstone and coal. Density of sandstone was ranging from 2100kg/m^3 to 2500kg/m^3.

Compressive strength was ranging from 25MPa to 100MPa. Similarly, density of coal was ranging from 1100kg/m^3 to 1500kg/m^3 and compressive strength was ranging from 15MPa to 45MPa.

Influence of external load

External load was taken as shovel-dumper combination load. A combination of shovel and dumper is used to transport the muck pile after the blasting activity. The shovel bucket capacity of 9.5m^3 to 12m^3 with gross weight of 185t is used and the dumper gross weight of 165t is used (BEML India, 2018). Shovel and dumper combination load of 350t was considered as external load for this study. So, to assess the influence of

external load, it was varied between 300t to 700t with increment of 200t by keeping other parameters as constant.

3.4 Regression Analysis

Regression analysis is a set of statistical processes for estimating the relationship among variables. Data obtained from both field and numerical modeling studies were analyzed using multiple regression analysis. Multiple regression analysis is used when the prediction value of a variable based on the value of two or more other variables. Regression analysis was carried out in three stages:

- Regression Coefficient (R^2) for the equations and standard error of the estimate were calculated. These parameters are measured to know how well the regression model describes the data.
- Analysis of variance (ANOVA) was performed for significance test (F). 'F' value gives the significance of the independent variables with respect to the dependent variable.
- Finally, regression analysis was performed to obtain the relationship between the independent variables and dependent variables.

In this study, directional deformation, strain and FOS depend on many independent variables such as gallery height and width, pillar width, partition thickness, slope angle and berm width. Independent variables were subjected to parametric evaluation by taking account of variability in input data. The output from numerical modeling was subjected to regression analysis. Multiple regression is considered to establish a relationship between the independent (predictor) variables and a dependent (criterion) variable in the study and is defined by the following equation:

$$Y = b_1 X_1 + b_2 X_2 + b_3 X_3 + \ldots + b_n X_n \qquad \ldots (3.1)$$

Where,

X_n = Number of independent variables involved in the analysis.

b_n = Regression coefficients

In the above equation, the regression coefficients (or 'b' coefficients) represent the independent contributions of each independent variable to the prediction of the dependent variable. The signs (plus or minus) of coefficients (b) can interpret direction of the relationship between variables. If 'b' is positive, relationship of independent variable with dependent variable is positive otherwise the relationship is negative.

Regression analysis was carried out by Statistical Package for Social Sciences (SPSS) software. SPSS is a software package used for statistical analysis. SPSS is a windows based program that can be used to perform data entry, analysis and to create tables and graphs. SPSS is capable of handling large amount of data and can perform the analysis covered in the text and much more. In this study, SPSS is used for multiple regression analysis. Figure. 3.48 shows the steps followed in SPSS software to develop mathematical models for deformation and strain. The discussions of results obtained from these studies are presented in results and analysis section.

Fig. 3.48A Importing input data into worksheets of SPSS
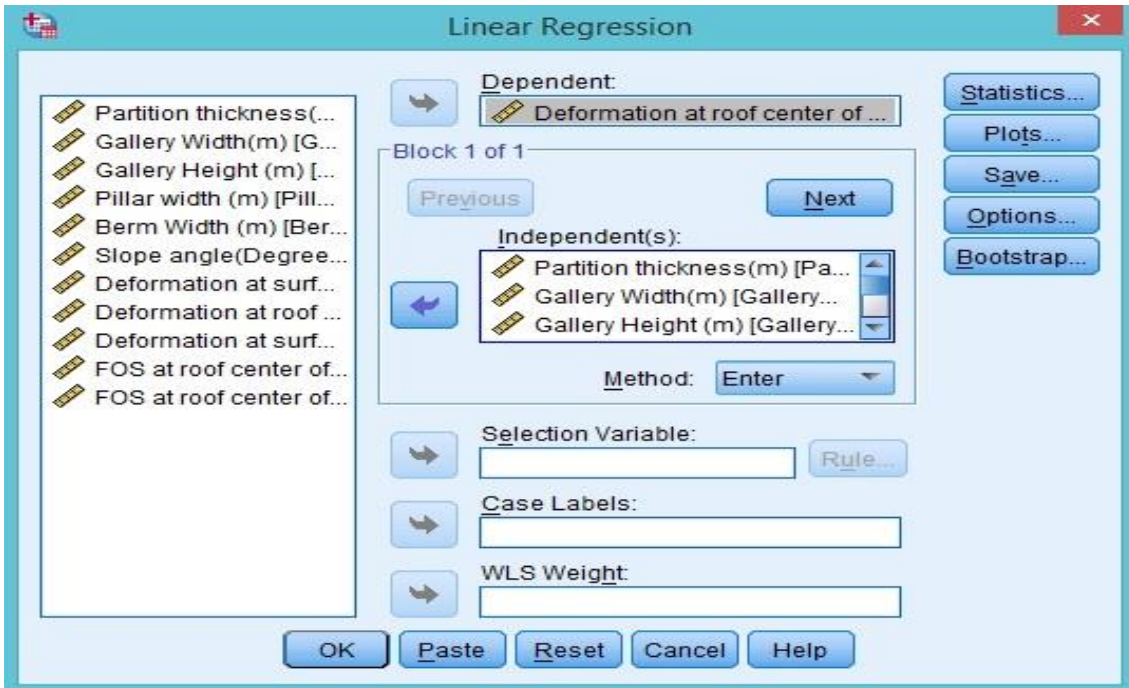
Fig. 3.48B Selection of input and output variables
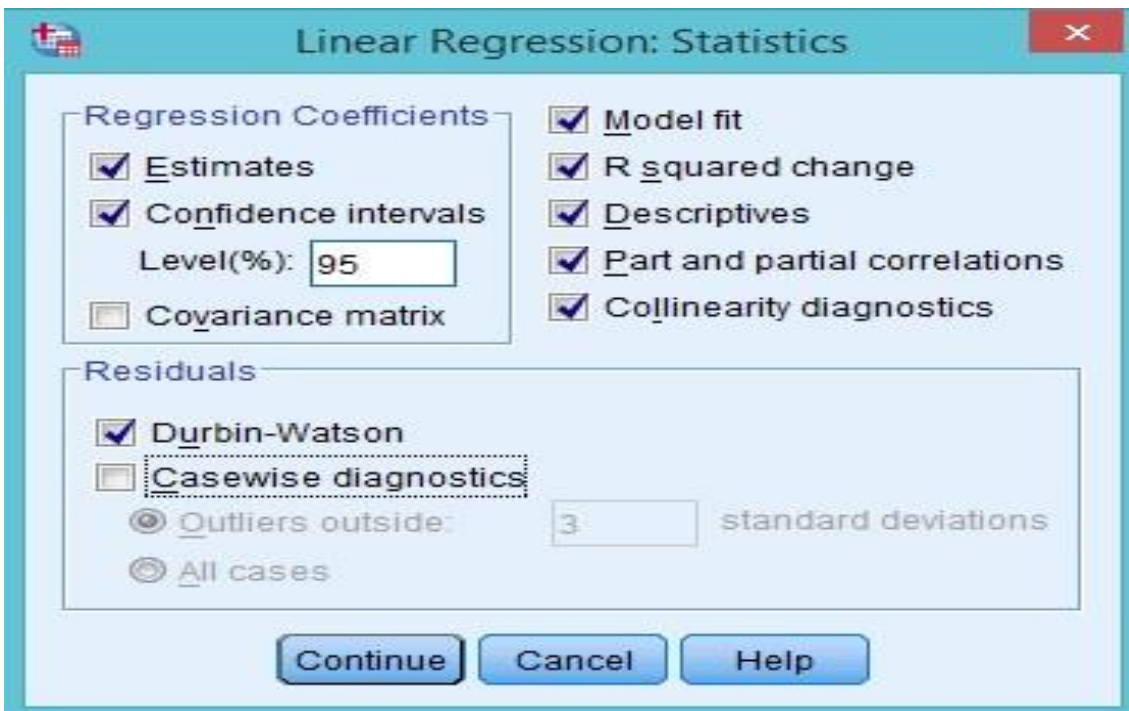
Fig. 3.48C Statistical models in SPSS
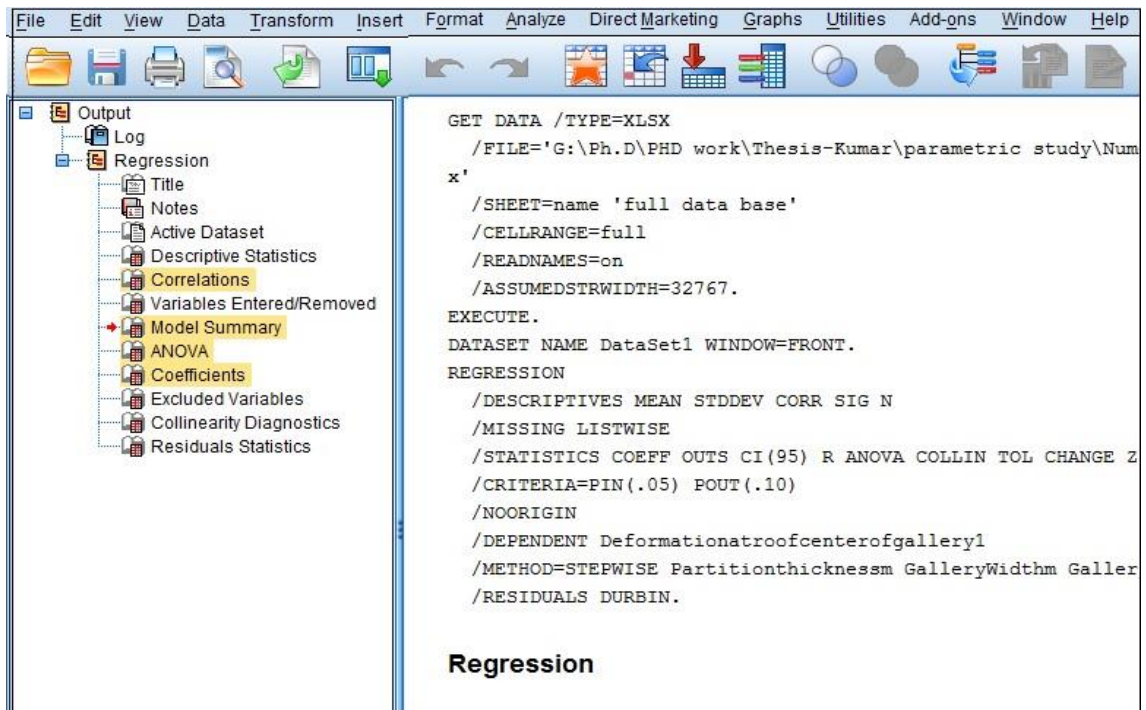
Fig. 3.48D Results of SPSS software

Fig. 3.48 Snap shots of results of regression analysis based on numerical data

3.5 Development of Design Guidelines

The design guidelines for the safe extraction of coal from old underground workings by opencast mining method were developed using field investigations and numerical modeling studies. Vertical deformation and strain were observed at P, Q, R and S over the old galleries. Factor of Safety (FOS) was observed at P and Q over old galleries based on Mohr-Coulomb yield criterion. A design methodology was developed by using FOS. The safety factors used by some researchers for the design of opencast mine, design of pillars in underground workings methods like bord and pillar and longwall extraction methods are given Table 3.22.

Based on above investigations, recommendations made by DME (1999), Wesseloo and Read (2009), FOS was categorized as unsafe, moderately safe and highly safe. If FOS was more than '2.0', the model considered as highly safe. If FOS was in between '1.5'

111

to '2.0', the model considered as moderately safe. If FOS is below '1.5', it was considered as unsafe.

Table 3.22 Range of safety factors used by various researchers

Author	Year	Range
Holland	1964	1.7-2.0
CMR	1964	2
Obert and Duvall	1967	2.4 (Short term), 4-8
Salamon	1967	1.31-1.88
Choi and McCain	1979	1.3
Carr et al.	1984	1-1.4
Mark	1992	1.3-1.5
Morsy and Peng	2003	1.3
Sheorey	2001	2

Based on FOS, optimum partition thickness and slope angle are suggested with respect to the geometrical dimensions (gallery width, pillar width and gallery height), rock properties and external load for safe extraction of old underground workings by surface mining operations. In order to use guidelines in simple a manner, it is proposed to develop a software package. A flow chart for the software development is given in the Figure 3.49. The software package consists of three modules. They are optimum partition thickness, optimum slope angle and Factor of Safety (FOS). Each module takes the input parameters as gallery width, pillar width, gallery height, berm width, rock properties and external load.
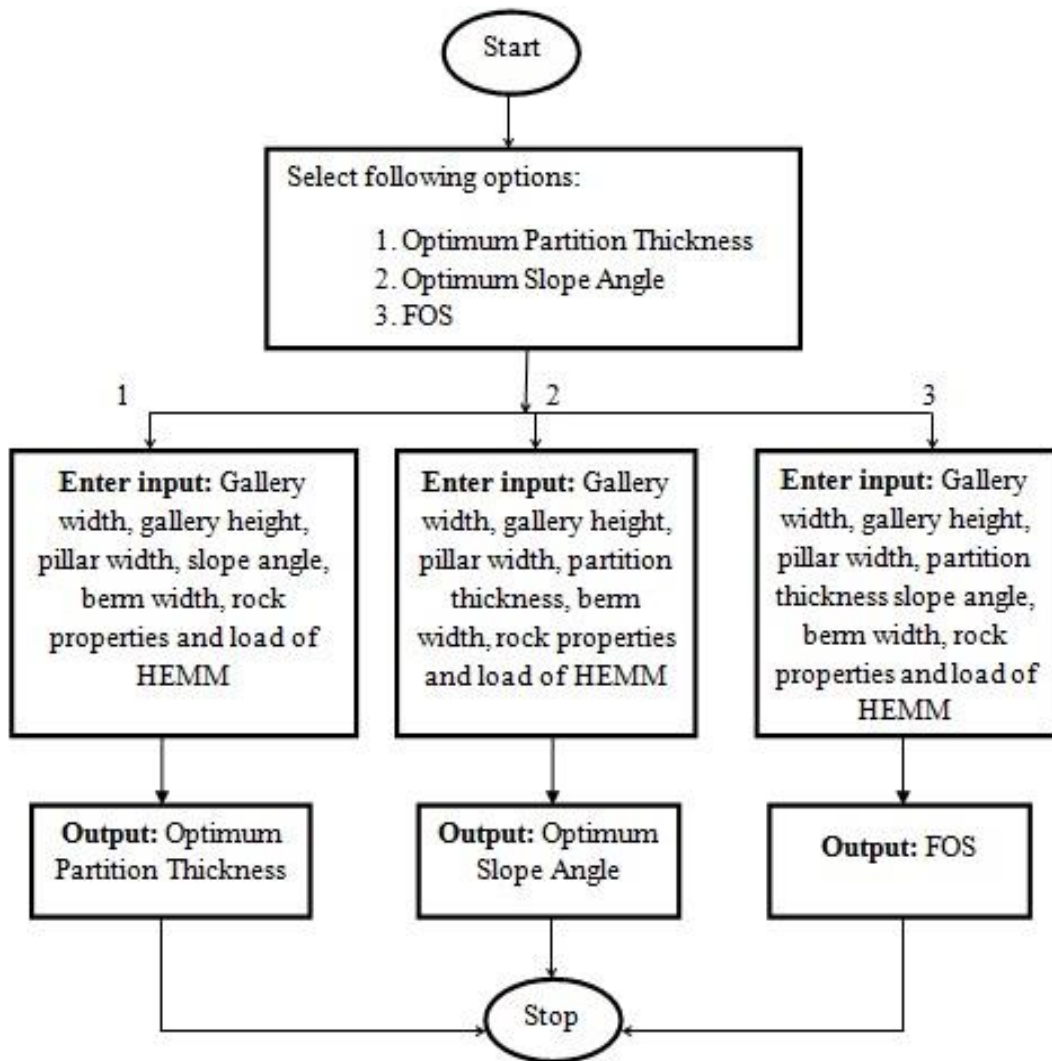
Fig. 3.49 Flowchart for developing a software package based on design guidelines

RESULTS AND ANALYSIS

Results obtained from field investigations, numerical modeling studies and statistical analysis are presented in this chapter. This chapter is arranged in the following sequence.

- Investigations

    Field investigations

        Investigations based on zigbee based WDAQ

        Investigations based on conventional data logger

    Numerical modeling

        Modeling based on field conditions

        Modeling with different parameters

            Influence of partition thickness

            Influence of gallery width

            Influence of pillar width

            Influence of gallery height

            Influence of berm width

            Influence of slope angle

            Influence of rock properties

    Comparison of field results with modeling results

- Parametric Study

    Comparison of statistical analysis of field results with modeling results

    Influence of parameters on the stability of old galleries

- Design Guidelines

    Development of design guidelines

    Development of a user-friendly software

4.1 Investigations

This section deals with the results obtained from both field investigations and numerical modeling studies.

4.1.1 Field investigations

Field monitoring was carried out by using zigbee based WDAQ and conventional data logger in the RGOCP-I and RGOCP-III of The Singareni Collieries Company Limited, Ramagundam, Peddapalli District of Telangana State. In total, 144 locations in partition and slope were monitored and at each location, data was captured about 5hours to 8hours under field conditions. Each analysis is described below.

4.1.1.1 Investigations based on Zigbee based WDAQ

Zigbee based WDAQ was installed on the partition and along slope to observe the deformation and strain. In case of partition monitoring, partition thicknesses of 4.12m, 5.91m, 6.86m, 7.91m, 10.21m and 12.10m over the gallery were considered as per field conditions. Deformation and strain were captured at different monitoring points, namely, point 'A' is the left edge of the gallery, whereas point 'B' and 'C' are above the center and the right edge of the gallery respectively in the partition as shown in Fig. 3.15.

Deformation at different monitoring points A, B and C in partition is shown in Fig. 4.1. From Fig. 4.1, it is clear that the deformation decreased with increase in partition thickness. The maximum deformation of 2.41mm was observed for 4.12m partition thickness and for partition thickness of 5.91m to 12.10m, the deformation decreased gradually at the monitoring point B. Similar trend was observed at point A and C also.
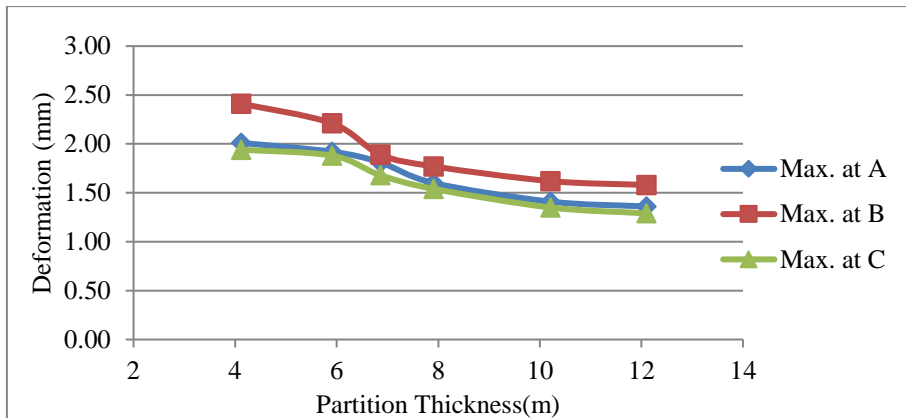
Fig. 4.1 Variation in deformation in the partition using zigbee based WDAQ

Variation of strain values at different monitoring points A, B and C in partition is shown in Fig. 4.2. Maximum strain at point A, B and C was 387με, 350με and 342με respectively for 4.12m partition thickness. From 5.91m to 12.10m thickness, almost there was almost no change in strain. The strain decreased with increased partition thickness at the points A, B and C.
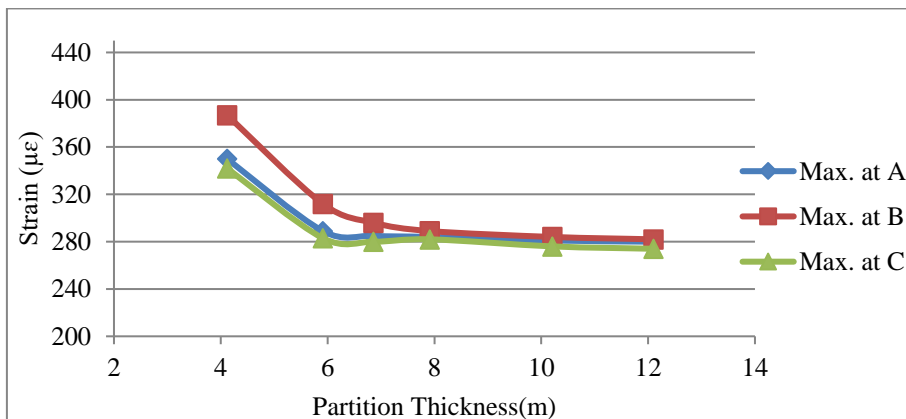
Fig. 4.2 Variation in strain in the partition using zigbee based WDAQ

It shows that the deformation and strain are decreased with increased partition thickness and vice versa. This could be due to increased partition thickness offers more resistance to the external load.

In case of slope monitoring, deformation and strain were observed at different monitoring points, namely, point 'E' is the toe of the slope above the gallery, point 'F'

116

lying above the center and 'G' at the crest of slope as shown in the Fig. 3.16. Fig. 4.3 shows the vertical deformation values observed at the monitoring points 'E', 'F' and 'G'. The maximum deformation observed at the point 'E' for slope angle of 49° is 1.90mm. And also the deformation decreased with increased partition thickness.
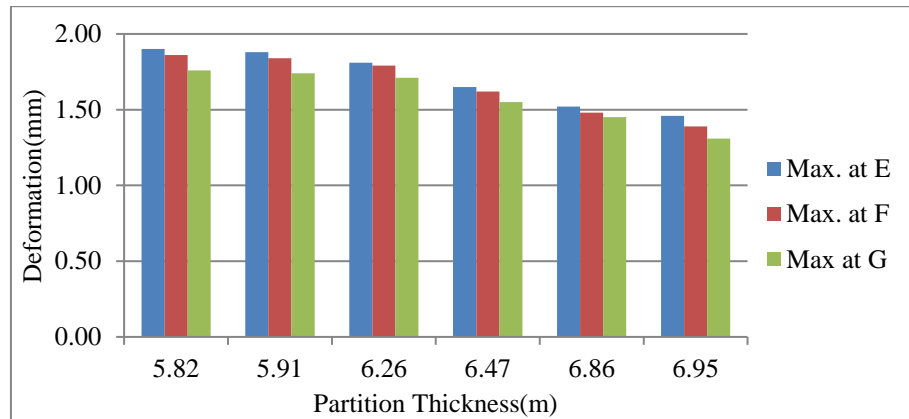
Fig. 4.3 Variation in deformation in slope using zigbee based WDAQ

The maximum strain values at the monitoring points 'E', 'F' and 'G' are shown in Fig. 4.4. Maximum strain values observed at point 'E', 'F' and 'G' were 185με, 156με and 132με respectively for 49° slope angle and partition thickness of 5.82m.

It is observed that deformation and strain values in slope decreased with increase in partition thickness and vice versa. In each case, maximum deformation and strain were observed at the monitoring point 'E' (toe). As the thickness of overburden increases, stability increases as the deformation decreases.
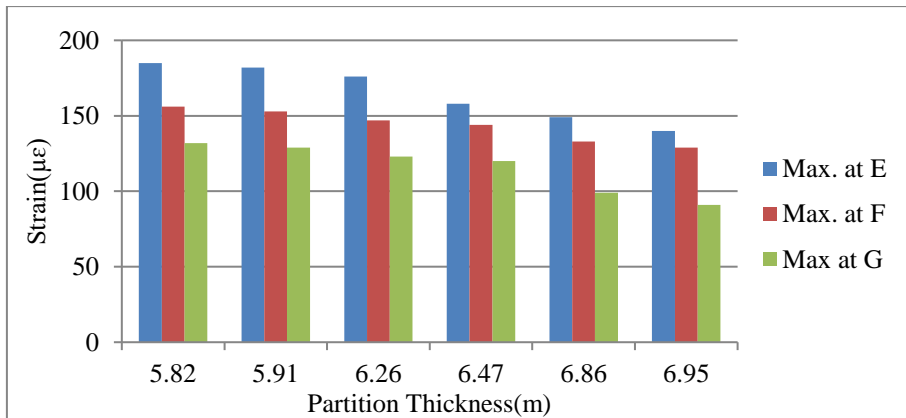
Fig. 4.4 Variation in strain in slope using zigbee based WDAQ

4.1.1.2 Investigations based on conventional data logger

Inorder to validate the data which was generated by zigbee based WDAQ, The Conventional data logger with similar set of sensors were installed on the partition and slope to observe the deformation and strain under the field conditions as similar to the Zigbee based WDAQ.

In case of partition monitoring, deformation and strain were observed at different monitoring points, namely, point 'A' is the left edge of the gallery, point 'B' lying above the center and 'C' lying on the right edge of the gallery as shown in the Fig. 3.15. A large quantity of data was captured from which maximum deformation values observed at monitoring points A, B and C as shown in Fig. 4.5. A maximum deformation of 2.31mm was observed for 4.12m partition thickness. It is also observed that the deformation gradually decreased from partition thickness of 5.91m to 12.10m at point A. Similarly, the same trend is observed at point B and C also.
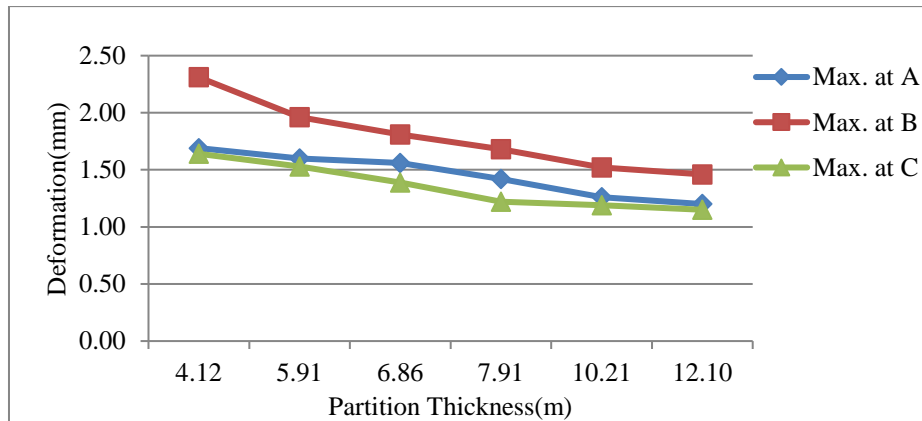
Fig. 4.5 Variation in deformation in the partition using Data Logger

Fig. 4.6 shows the maximum strain values observed at A, B and C for different partition thicknesses. Maximum strain observed at point A, B and C are 331με, 293με and 275με respectively for 4.12m partition. For the partition ranging from 5.91m to 12.10m, it was observed that the change in strain is negligible. The strain decreased with increase in partition thickness at all points A, B and C.

Data generated at different monitoring points in partition thicknesses using conventional data logger reveal that the deformation and strain values were decreased with increased parition thickness. The observation shows that increase in parition thickness offers more stability above the gallery.
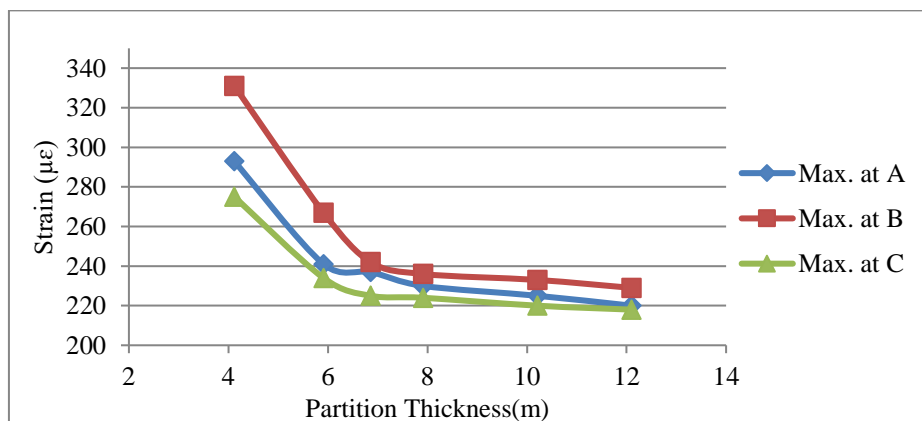
Fig. 4.6 Variation in strain in the partition using Data Logger

119

In case of slope monitoring, deformation and strain values were observed at different monitoring points, namely, point 'E' is the toe of the slope above the gallery, point 'F' lying above the center and 'G' lying at the crest of slope as shown in Fig. 3.16.

Various slope angles were considered and monitored under field conditions. Data was captured and from which maximum deformation values observed at the monitoring points 'E', 'F' and 'F' are shown in Fig. 4.7. The maximum deformation observed at point 'E' for 5.82m and 49° is 1.65mm. For the partition thickness ranging from 5.91m to 6.95m, the deformation decreased gradually at all monitoring points.
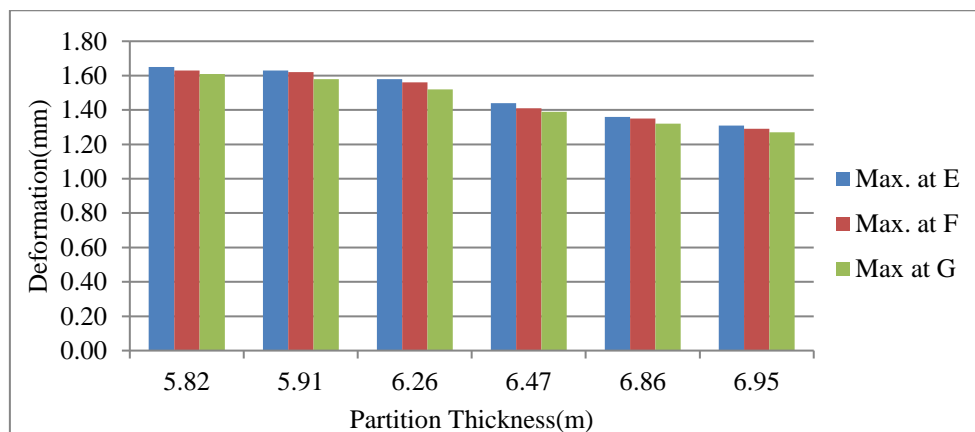
Fig. 4.7 Variation in deformation in slope using Data Logger

Fig. 4.8 shows that maximum strain values found at the monitoring points 'E', 'F' and 'G'. Maximum strain values observed at point 'E' are 172με, 168με , 154με, 149με, 140με and 138με for partition thicknesses of 5.82m, 5.92m, 6.26m, 6.47m, 6.86m and 6.95m respectively. The Strain values decreased with increase in partition thickness at all monitoring points E,F and G.

120
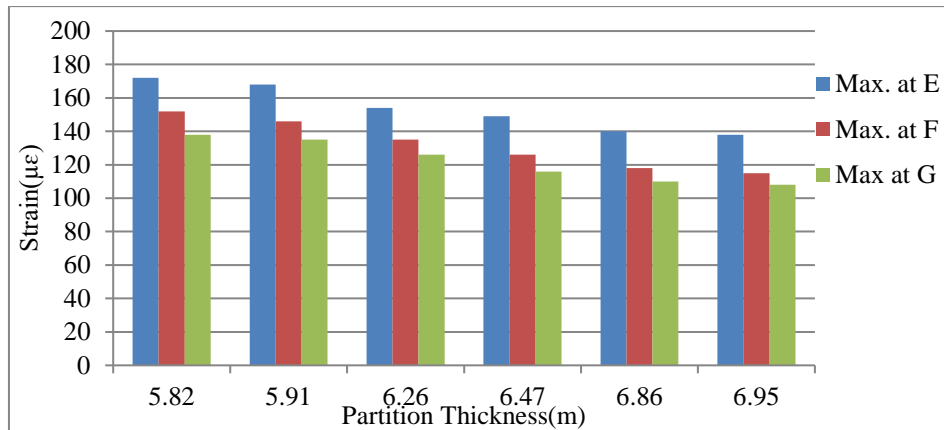
Fig. 4.8 Variation in strain in slope using Data Logger

It is observed that deformation and strain decreased with increase in partition thickness and vice versa. The stability of overburden increased with increase in partition thickness due to which deformation and strain are drecreased.

4.2 Numerical Modeling

Numaerical Modeling was carried out in two phases. In first phase, modeling studies were carried out exactly based on the field conditions. In the second phase, models were developed for assessment of the influence of geometrical dimensions, rock properties and external load on the stability of old galleries. ANSYS Workbench was used for developing models. This section deals with the results obtained from modeling studies.

4.2.1 Modeling based on field studies

Models were developed to validate the data generated by the Zigbee based WDAQ and conventional Data Logger. Input parameters for modeling like rock properties, bench configurations and old galleries dimensions were collected during field visits.

Field conditions were simulated for partition thicknesses of 4.12m, 5.91m, 6.86m, 7.91m, 10.21m and 12.10m and the results of deformation values observed in partition at different monitoring points 'A', 'B' and 'C' are shown in Fig. 4.9. It shows that the maximum deformation was 2.52mm at point 'B' for partition thickness of 4.12m. The

maximum deformation was observed at the point 'B' for each case. It is also observed that The deformation decreased with increase in partition thickness and vice versa.

Similarly, slope angles of 49º, 65º, 64º, 70º, 62º and 68º, and partition thicknesses of 5.82m, 5.92m, 6.26m, 6.47m, 6.86m and 6.95m were simulated under field conitions. Figure 4.10 shows deformation values observed in slope at different monitoring points 'E', 'F' and 'G'.
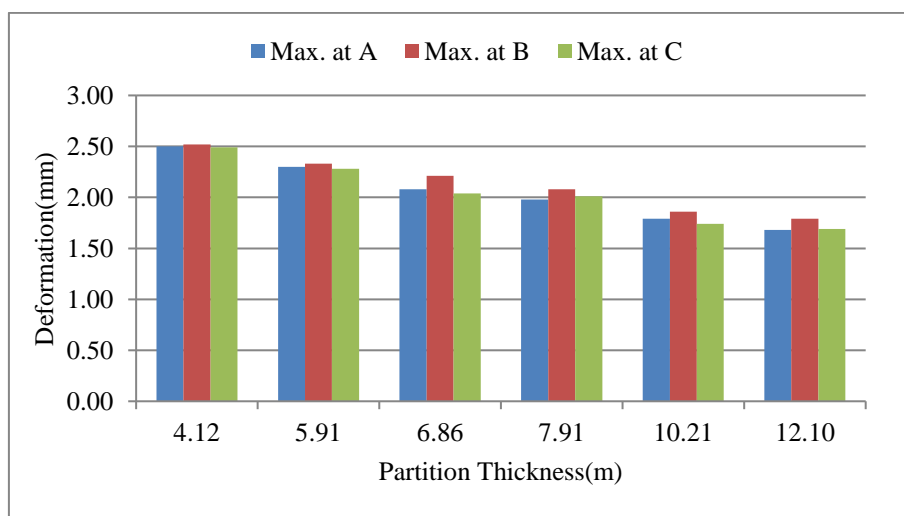
Fig. 4.9 Variation in deformation in partition by numerical modeling

Maximum deformation observed at point 'E' and values of deformation observed at the monitoring point 'E' were 1.78mm, 1.77mm, 1.75mm, 1.70mm, 1.65mm and 1.63mm for different slope angles of 49º, 65º, 64º, 70º, 62º and 68º and partition thickness of 5.82m, 5.92m, 6.26m, 6.47m, 6.86m and 6.95m respectively. It is also observed that deformation decreased with increase in partition thickness and vice versa.

In both cases, vertical deformation decreased with increased partition thickness as similar to the Zigbee based WDAQ and Conventional Data Logger. Owing to increase in partition thickness, the stability of overburden increases as deformation decreases.
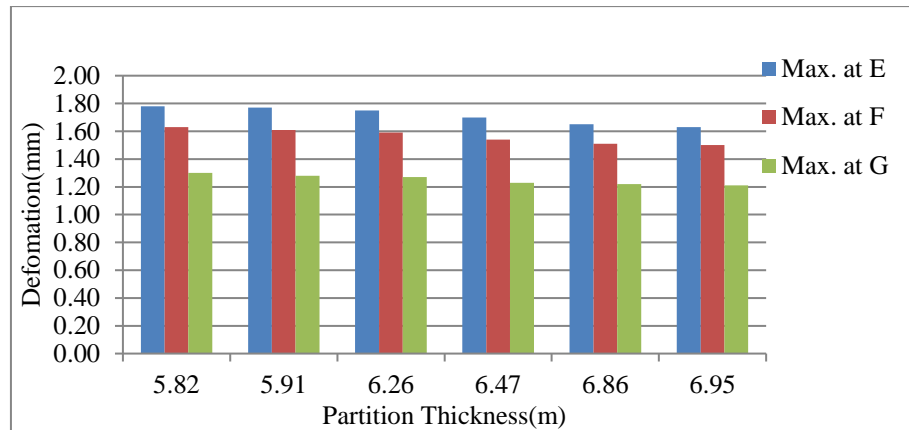
Fig. 4.10 Variation in deformation in slope by numerical modeling

4.2.2 Modeling with varied parameters

Numerical modeling studies were carried out to simulate and assess the influence of the geometrical dimensions, rock properties and external load on the stability of old underground coal workings. The results of these modeling studies are discussed in the following sections.

4.2.2.1 Influence of partition thickness

Models were developed to assess the influence of partition thicknesses on the stability of old underground galleries. Partition thickness of 4m, 6m, 8m, 10m and 12m were considered for this study. In this, partition thickness was varied by keeping all other parameters as constant. Vertical deformation was obtained at the reference points P, Q, R and S over old underground galleries (Fig. 3.45). The results of vertical deformation at point 'R' (surface center) above the gallery-1 for different partition thicknesses, gallery width of 4.2m, pillar width of 30.5m, slope angle of 55° and berm width of 5m are shown in Fig. 4.11. A maximum vertical deformation of 2.65mm was observed for partition thickness of 4m and gallery height of 3.4m. A minimum vertical deformation of 1.90mm was observed for partition thickness of 12m and gallery height of 2.4m.
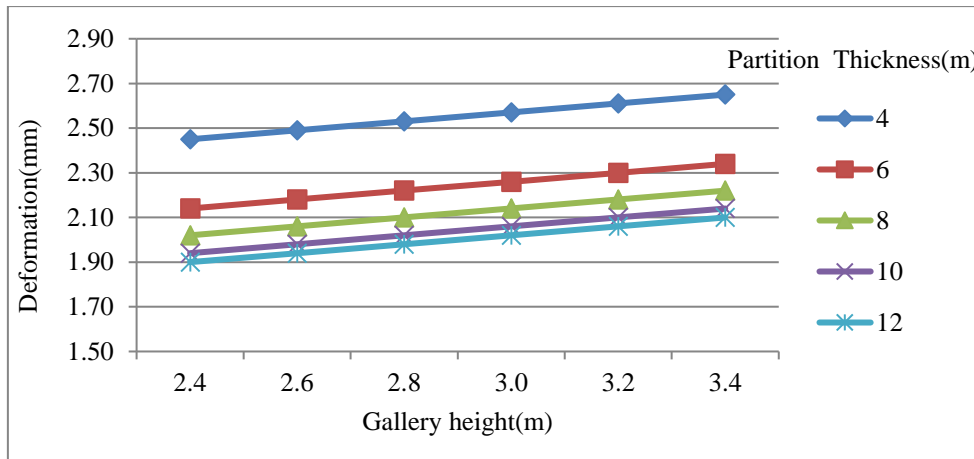
Fig. 4.11 Deformation at surface center (point 'R') of gallery1 for different partition thickness when gallery width of 4.2m and pillar width of 30.5m

Fig. 4.12 shows the results of vertical deformation at point 'S' (surface center) above the gallery-2 for different partition thicknesses gallery width of 4.2m, pillar width of 30.5m, slope angle of 55° and berm width of 5m. It is observed that the deformation values for partition thickness of 4m to 12m are 1.55mm, 1.24mm, 1.12mm, 1.04mm and 1.00mm respectively.
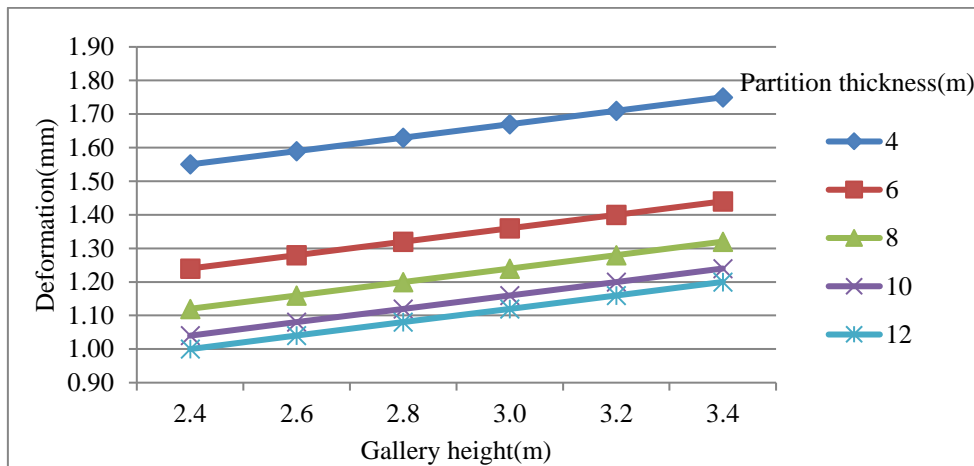
Fig. 4.12 Deformation at surface center (point 'S') of gallery2 for different partition thickness when gallery width of 4.2m and pillar width of 30.5m

Variation of FOS at point 'P' (roof center) above the gallery-1 for different partition thicknesses, and when gallery width of 4.2m, pillar width of 30.5m, slope angle of 55° and berm width of 5m is shown in Fig. 4.13.
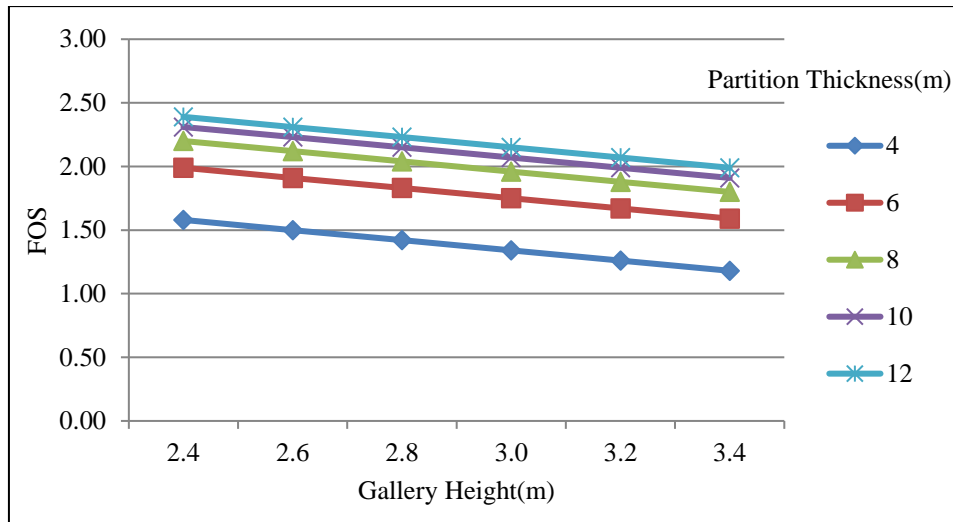
Fig. 4.13 FOS at roof center (point 'P') of gallery1 for different partition
thickness when gallery width of 4.2m and pillar width of 30.5m

It reveals that FOS increased with increase in partition thickness and the deformation decreased with increase in partition thickness and vice versa. As the thickness of overburden increases, stability increases due to which the deformation decreases.

4.2.2.2 Influence of gallery width

Influence of gallery width of 3.0m, 3.6m, 4.2m and 4.8m was simulated by keeping all other parameters constant. Vertical deformation obtained at the reference points P, Q, R and S over old underground galleries (Fig. 3.45). The results of vertical deformation at point 'P' of the gallery-1 for different gallery widths with respect to the partition thicknesses are shown in Fig. 4.14. The maximum and minimum deformation values were observed for gallery width of 4.8m and 3.0m respectively. The deformation values for gallery width of 3.0m and partition thickness of 4m to 12m are 1.52m, 1.21m, 1.09m, 1.01m and 0.97m (Fig. 4.14).
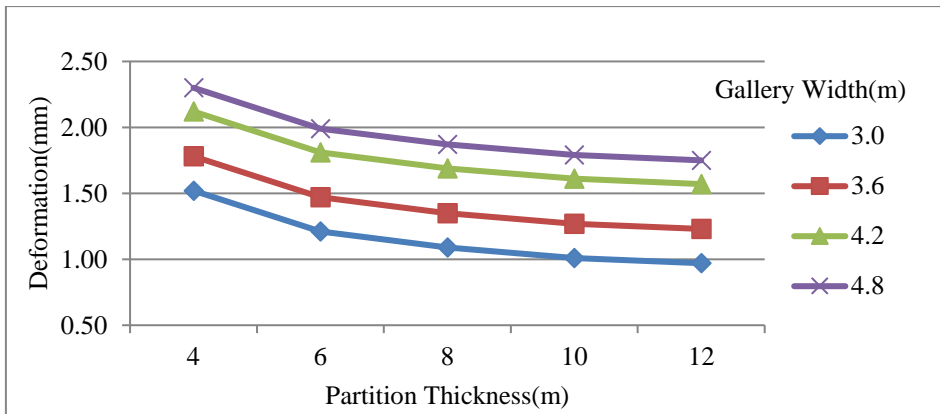
Fig. 4.14 Deformation at roof center (point 'P') of gallery1 for different gallery widths

Vertical deformation was obtained at the reference point 'R' for different gallery widths with respect to the partition thicknesses are shown in Fig. 4.15. The deformation values were obtained for partition thickness of 4m and 12m with respect to the gallery width of 3.0m, 3.6m, 4.2m and 4.8m. The deformation values for partition thickness of 4m, gallery widths of 3.0m, 3.6m, 4.2m and 4.8m are 1.52mm, 1.78mm, 2.12mm and 2.30mm respectively.

It is clear indication that there is influence of gallery width on stability of old galleries as vertical deformation increased with increase in gallery width. It is of increase in gallery width, overburden stability decreases as deformation increases.
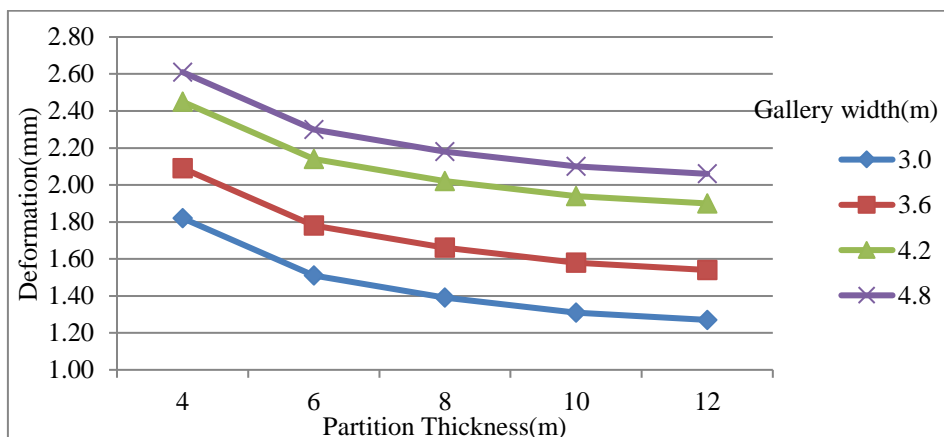
Fig. 4.15 Deformation at surface center (point 'R') of gallery1 for different gallery widths

4.2.2.3 Influence of pillar width

Models were developed to study the vertical deformation due to change in pillar width. Different pillar widths were considered as per Reg. No. 111 of CMR – 2017 (Table 3.13). Pillar width was varied by keeping all other parameters constant. Vertical deformation was obtained at the reference points P, Q, R and S over old underground galleries (Fig. 3.45). Vertical deformation due to change in pillar width was assessed and results at points 'P' and 'R' over the gallery-1 are shown in Fig. 4.16 and 4.17. The maximum deformation values at point 'P' over gallery-1 for pillar widths of 30.5m, 31.5m and 32.5m, gallery width of 4.2m, partition thickness of 4m and gallery height 3.4m are 2.32mm, 2.24mm and 2.16mm respectively as shown in Fig. 4.16.
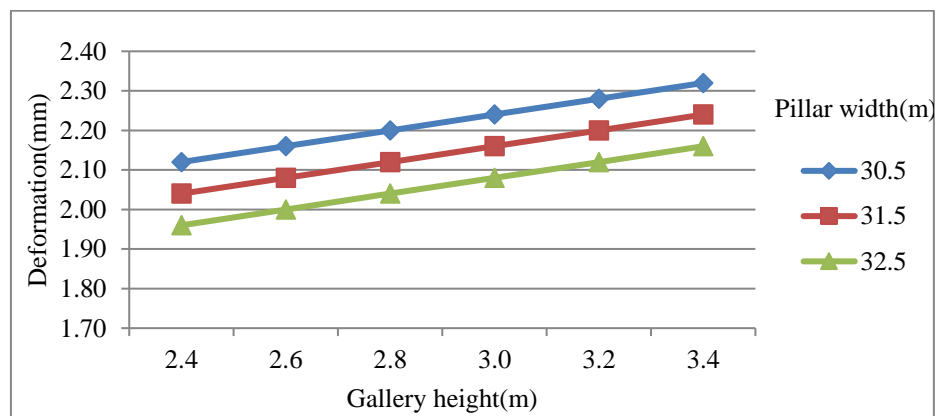
Fig. 4.16 Deformation at roof center (point 'P') of gallery1 for different pillar widths when gallery width of 4.2m

From Fig. 4.17, it can be observed that the maximum deformation values at point 'R' over gallery-1 for pillar width of 30.5m, gallery width of 4.2m, partition thickness of 4m and gallery height of 2.4, 2.6m, 2.8m, 3.2m and 3.4m are 2.45mm, 2.49mm, 2.53mm, 2.57mm, 2.61mm and 2.65mm respectively.
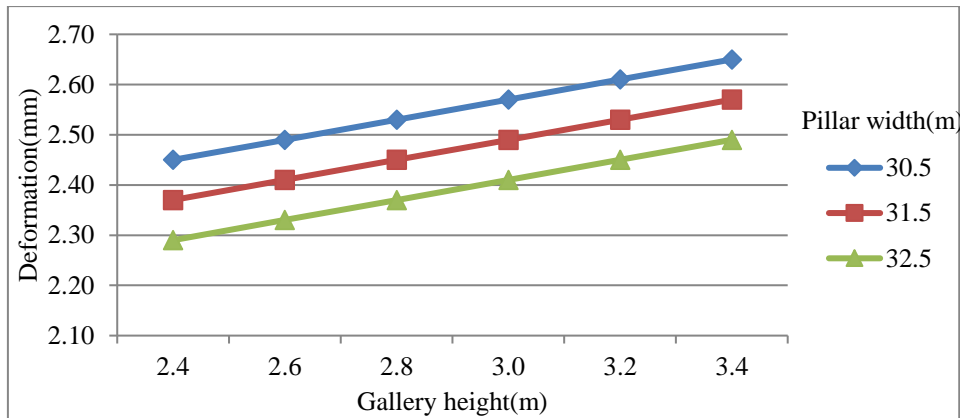
Fig. 4.17 Deformation at surface center (point 'R') of gallery1 for different
pillar widths when gallery width of 4.2m

Variation of FOS at point 'P' (roof center) above the gallery-1 for different pillar widths, gallery width of 4.2m, partition thickness of 6m, slope angle of 55° and berm width of 5m is shown in Fig. 4.18. This study states that FOS increased with increase in pillar width and decreased with increase in gallery height and the defromation decreased with increase in pillar width and vice versa. It indicates the stability of overburden and galleries increase with increase in pillar width as deformation decreases.
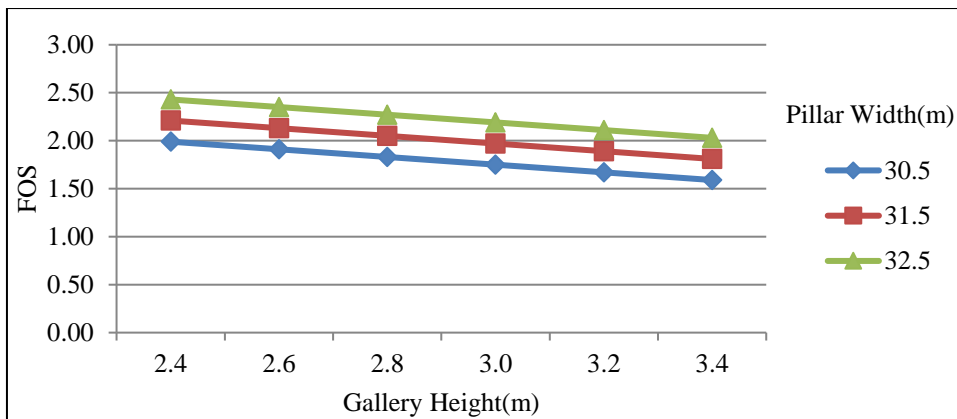
Fig. 4.18 FOS at roof center (point 'P') of gallery1 for different
pillar widths when gallery width of 4.2m

128

4.2.2.4 Influence of gallery height

Models were developed to study the directional deformation along the y-axis due to change in gallery height. Gallery height was varied by keeping all other parameters constant. Gallery height of 2.4m, 2.6m, 2.8m, 3.0m, 3.2m and 3.4m were considered for this study. Vertical deformation at point 'P' for different gallery heights are shown in Fig. 4.19. Maximum deformation values observed for gallery heights of 2.4m, 2.6m, 2.8m, 3.0m, 3.2m and 3.4m, partition thickness of 4m, pillar width of 30.5m are 2.12mm, 2.16mm, 2.20mm, 2.24mm, 2.28mm and 2.32mm respectively.

The results of Vertical deformation at points 'R' over the gallery-1 having different gallery heights are shown in Fig. 4.20. It is observed that maximum deformation values at point 'R' over gallery-1 for gallery heights of 3.4m, partition thickness of 4m to 12m, pillar width of 30.5m are 2.65mm, 2.34mm, 2.22, 2.14 and 2.10mm respectively.
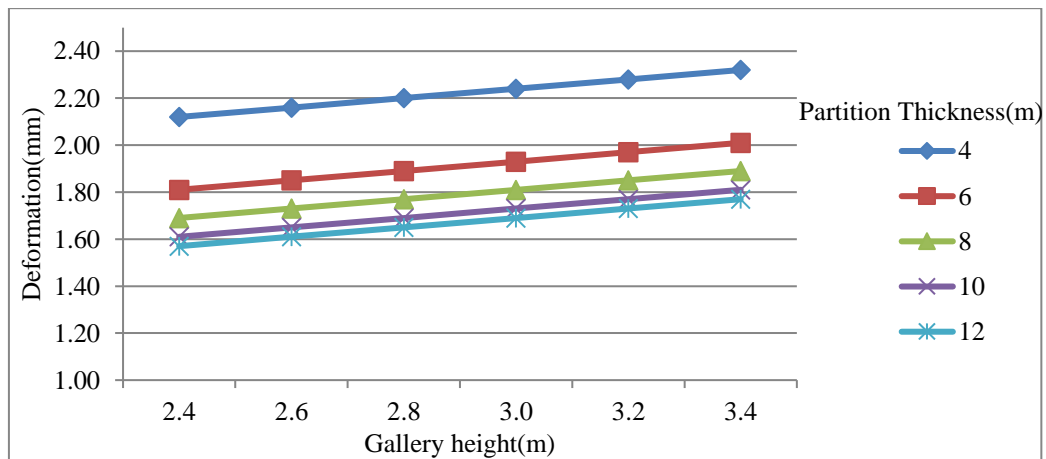
Fig. 4.19 Deformation at roof center (point 'P') over gallery1 for different gallery heights when gallery width of 4.2m
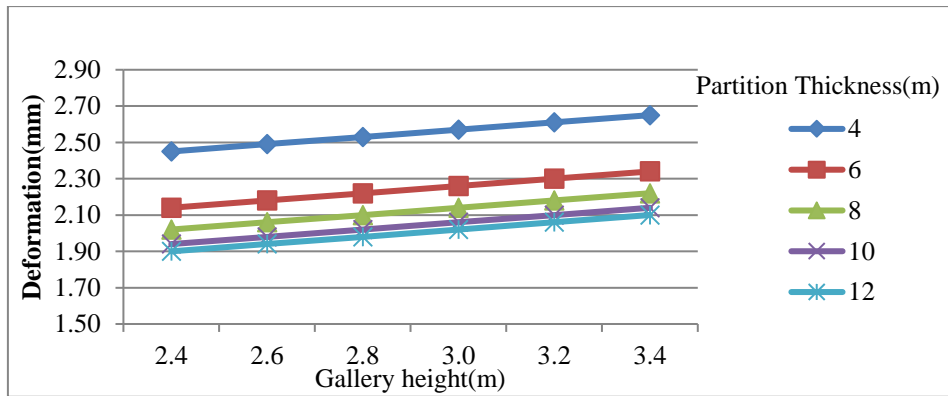
Fig. 4.20 Deformation at surface center (point 'R') over gallery1 for different gallery heights when gallery width of 4.2m

These results show that the deformation increased with increase in gallery height and vice versa. As the gallery height increases, the stability of overburden and gallery decreases due to which deformation increases.

4.2.2.5 Influence of berm width

Models were developed to assess the influence of berm width on the stability of old underground galleries. Berm widths from 5m to 10m with an increment of 1m, were considered for this study. The results of vertical deformation at point 'P' over gallery1 for different berm widths are shown in Fig. 4.21. From Fig. 4.21, it can be observed that the maximum deformation occurred for different berm widths of 5m to 10m, gallery width of 4.2m, gallery height of 3.4m and partition thicknesses of 4m and the values are 2.32mm, 2.31mm, 2.30mm, 2.29mm, 2.28mm and 2.27mm respectively.
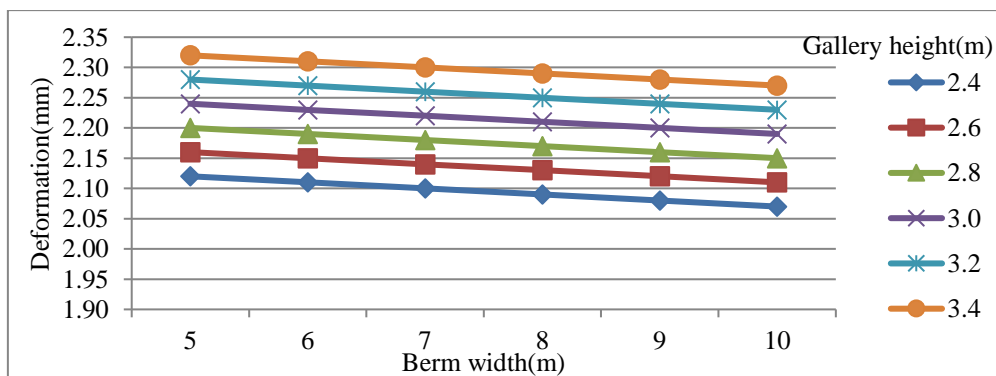
Fig. 4.21 Deformation at roof center (point 'P') over gallery1 for different berm widths when gallery width of 4.2m

130

Fig. 4.22 is plotted based on the results of vertical deformation at point 'R' over the gallery-1 for different berm widths. Maximum deformation values for different berm widths of 5m to 10m, gallery width of 4.2m, gallery height of 3.4m and partition thicknesses of 4m are 2.65mm, 2.64mm, 2.63mm, 2.62mm, 2.61mm and 2.60mm respectively.
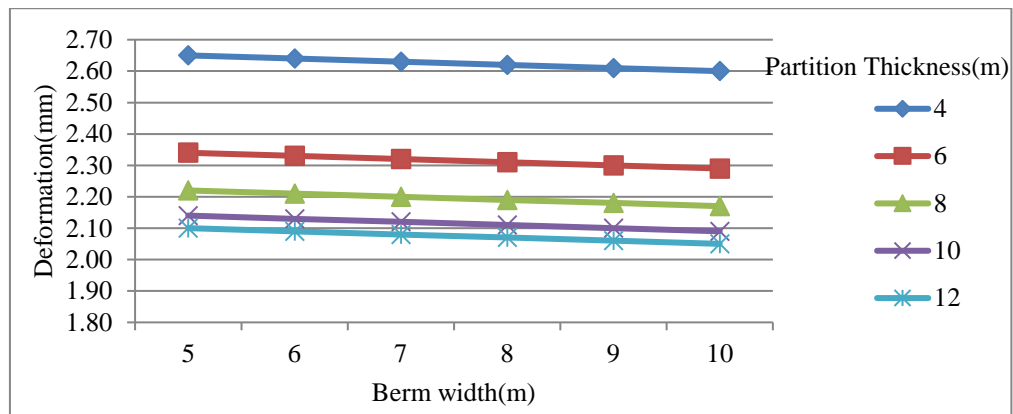
Fig.4.22 Deformation at surface center (point 'R') over gallery1 for different berm widths when gallery width of 4.2m

It is also observed that deformation decreased with increase in berm width and vice versa. The same trend is observed for the remaining gallery heights and partition thicknesses also. This could be due to increase in berm width with respect to the partition thickness and gallery height offers more resistance as deformation decreases.

4.2.2.6 Influence of slope angle

The objective of this study is to assess the influence of slope angle on the stability of old underground galleries. Slope angles of 50°, 55°, 60°, 65°, 70° and 75° were considered for this study. Slope angle was varied by keeping other parameters as constants.

Slope angel was simulated and values of vertical deformation obtained. The data plotted for different slope angles with respect to the gallery heights as shown in the Fig. 4.23. It shows that maximum deformation occurred for slope angles of 50° to 75°, gallery

131

width of 4.2m, gallery height of 3.4m, partition thicknesses of 6m are 1.99mm, 2.01mm, 2.03mm, 2.05mm, 2.07mm and 2.09mm respectively. It is also observed that deformation increased with increase in slope angle and vice versa. The same trend is observed for the remaining gallery heights also. As slope angle increases stability of slope decreases as deformation increases (Robertson and Mac, 1971; Gundewar, 2014).
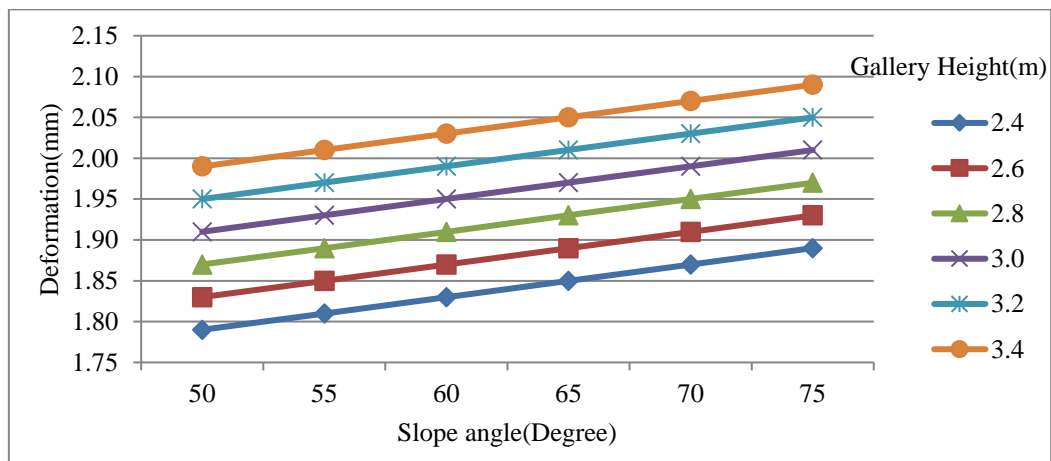
Fig. 4.23 Deformation at roof center (point 'P') over gallery1 for different slope angles when gallery width of 4.2m

4.2.2.6 Influence of rock properties

Models were developed to assess the influence of rock properties on the stability of old underground galleries. Density and compressive strength of sandstone and coal were considered for this study. The results of vertical deformation at point 'P' over gallery1 for density and compressive strength of sandstone and coal are shown in Tables. 4.1, 4.2, 4.3 and 4.4 respectively.

From Table 4.1, it can be observed that the maximum deformation occurred at density of sandstone of 2150 kg/m^3 for partition thickness of 4m to 12m, gallery width of 4.2m, gallery height of 3.0m, pillar width of 30.5, berm width of 5m and slope angle of 55° and the values are 2.27mm, 2.94mm, 2.82mm, 2.71mm, 2.28mm and 2.70mm respectively.

132

Table 4.1 Variation in deformation at roof center (point 'P') over gallery1 for density of sandstone when gallery width of 4.2m

Patition thickness(m)	Deformation(mm)			
	Density-Sandstone(Kg/m^3)			
	2150	2250	2350	2450
4	2.27	2.26	2.25	2.24
6	1.94	1.95	1.94	1.93
8	1.82	1.83	1.82	1.81
10	1.71	1.72	1.74	1.73
12	1.70	1.71	1.70	1.69

The results of vertical deformation at point 'P' over gallery1 for different compressive strength of sandstone are shown in the Table 4.2. From the Table 4.2, it can be found that the maximum deformation occurred for partition thickness of 4m, gallery width of 4.2m, gallery height of 3.0m, slope angle of 55°, berm width of 5m and pillar width of 30.5 and the values are 2.25mm, 1.94mm, 1.81mm, 1.72mm, and 1.68mm respectively.

Table 4.2 Variation in deformation at roof center (point 'P') over gallery1 for compressive strength of sandstone when gallery width of 4.2m

Patition Thickness(m)	Deformation(mm)			
	compressive strength-Sandstone(Mpa)			
	37	40	43	46
4	2.25	2.24	2.23	2.22
6	1.94	1.93	1.92	1.91
8	1.81	1.81	1.80	1.79
10	1.72	1.73	1.72	1.71
12	1.68	1.69	1.68	1.67

Density of coal was varied as 1200kg/m^3 to 1500kg/m^3 by keeping other parameters as constant and values of vertical deformation obtained. The data plotted for different density of coal values with respect to the partition thicknesses as shown in the Table 4.3. It shows that maximum deformation occurred for partition thickness of 4m to 12m, slope angles of 55°, gallery width of 4.2m, gallery height of 3.0m, pillar width of 30.5 and bem width of 5m are 2.25mm, 1.94mm, 1.82mm, 1.71mm and 1.70mm respectively.

Table 4.3 Variation in deformation at roof center (point 'P') over gallery1 for density of coal when gallery width of 4.2m

Patition Thickness(m)	Deformation(mm)			
	Density-Coal (Kg/m³)			
	1200	1300	1400	1500
4	2.25	2.25	2.24	2.24
6	1.94	1.94	1.93	1.93
8	1.82	1.82	1.81	1.81
10	1.71	1.71	1.70	1.73
12	1.70	1.70	1.69	1.69

The results of vertical deformation at point 'P' over gallery1 for different compressive strength of coal are shown in the Table 4.4. From the Table 4.4, it can be found that the maximum deformation occurred for partition thickness of 4m, gallery width of 4.2m, gallery height of 3.0m, slope angle of 55°, berm width of 5m and pillar width of 30.5 and the values are 2.25mm, 1.94mm, 1.82mm and 1.74mm respectively.

Table 4.4 Variation in deformation at roof center (point 'P') over gallery1 for compressive strength of coal when gallery width of 4.2m

Patition Thickness(m)	Deformation(mm)			
	compressive strength-Coal(Mpa)			
	19	22	25	28
4	2.25	2.24	2.24	2.23
6	1.94	1.93	1.93	1.92
8	1.82	1.81	1.81	1.80
10	1.74	1.73	1.73	1.72
12	1.68	1.69	1.69	1.68

It is observed that deformation decreased with increase in density and compressive strength of sandstone and coal and vice versa. The same trend is observed for the remaining partition thicknesses also. As density and compressive strength increases stability of overburden increases as deformation increases. Similarly, models were developed and data was analysed for remaining dimensions, and external load.

4.3 Comparison of Field Results with Modeling Results

Maximum deformation values for different slope angles at different monitoring points 'E', 'F' and 'G' over slope above old underground galleries of height 3m and gallery width of 4.2m from Zigbee based WDAQ (ZWDAQ), Data Logger (DL) and Numerical Modeling (NM) are given in Table 4.5. Comparison of different monitoring methods is shown in Figure 4.24.

Table 4.5 Comparison of maximum deformation observed in slope by different
         monitoring methods

Slope angle (Degree)	Partition thickness (m)	Deformation (mm)			Percentage of variation		
		ZWDAQ	DL	NM	ZWDAQ Vs. DL	ZWDAQ Vs. NM	DL Vs. NM
49	5.82	1.90	1.65	1.78	13.16	6.32	7.30
65	5.91	1.88	1.63	1.77	13.30	5.85	7.91
64	6.26	1.81	1.58	1.75	12.71	3.31	9.71
70	6.47	1.65	1.44	1.70	12.73	-3.03	15.29
62	6.86	1.52	1.36	1.65	10.53	-8.55	17.58
68	6.95	1.46	1.31	1.63	10.27	-11.64	19.63
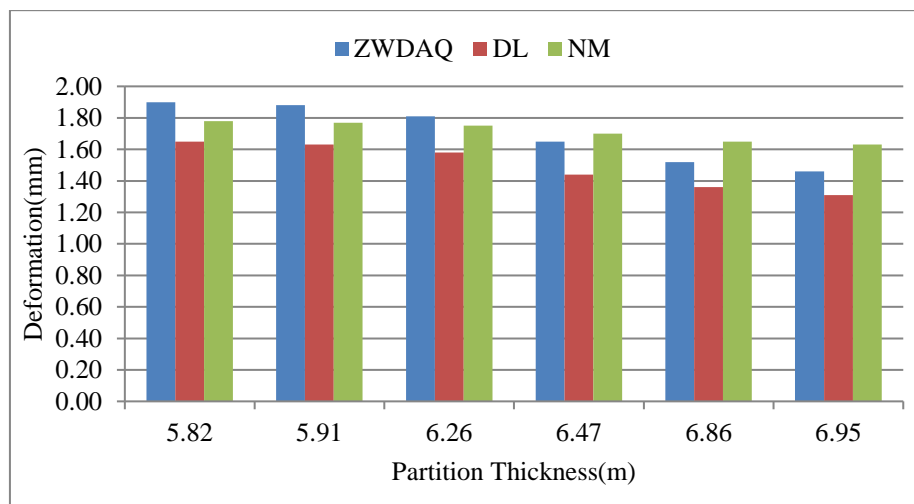
Fig. 4.24 Comparison of different slope monitoring methods

Maximum deformation values using NM, ZWDAQ and DL are 1.78mm, 1.90mm and 1.65mm for slope angles of 49º and partition thickness of 5.82m respectively. Similarly, minimum deformation values using NM, Zigbee WDAQ and DL are 1.63mm, 1.88mm and 1.65mm for slope angle of 68º and partition thickness of 6.95m respectively. The variation between ZWDAQ and DL is around 10.27% to 13.30%. The variation in between ZWDAQ and NM is around -3.03% to 6.32% and NM to DL is 7.30% to 19.63%. However, the data obtained using ZWDAQ is in close to the other two methods, indicating ZWDAQ monitoring method is reliable. It is observed that the trend of deformation in slope is decreased with increase in partition thickness and vice versa.

4.4 Parametric Study

This section consists two phases. In the first phase, comparison of data obtained by field investigations and numerical modeling studies were discussed. In the second phase, a detailed analysis was carried out for simulating various various parameters that affect the stability of old galleries using numerical modeling method. Parametric study was done by using Statistical Package for the Social Sciences (SPSS). Further, the influence of various parameters over the stability of old galleries was discussed.

4.4.1 Comparison of statistical analysis of field results with modeling results

Statistical analysis was carried to assess the regression coefficient which finds the relation between field and numerical modeling studies and influence of different parameters on the stability of old underground galleries.

Results of regression analysis such as R^2, un-standardized coefficients of regression, standardized coefficient and results of a significance test for deformation and strain for different slope angles are given in Tables 4.6 and 4.7.

The values of "t" and "p" from significance test were above '1' and below '0.05' respectively, which shows that the results are significant for both field investigations

and numerical modeling studies. Standardized coefficient, obtained from multiple regression analysis, represents the influence of the corresponding input variable in the analysis. Standardized coefficient can be positive or negative.

In the present study, the negative value of standardized coefficient of an independent variable (parameter) indicated that the deformation decreased with increase in partition thickness. Similarly, strain in partition decreased with increase in partition thickness, when standardized coefficient of variable is negative.

Table 4.6 Results of regression analysis of deformation determined based on zigbee based WDAQ with data logger and numerical modeling

Parameter	R^2	Un-standardized coefficient		Standardized coefficient (Beta)	Significance test	
		B	Std. Error		t	p
Constant	0.891	0.318	0.115	-	2.354	0.03
Deformation by DL		0.642	0.095	0.950	6.064	0
Constant	0.898	0.627	0.095	-	6.604	0.003
Deformation by NM		0.427	0.075	0.953	4.512	0.003

Table 4.7 Results of regression analysis of strain determined based on zigbee based WDAQ with data logger and numerical modeling

Parameter	R^2	Un-standardized coefficient		Standardized coefficient (Beta)	Significance test	
		B	Std. Error		t	p
Constant	0.901	34.302	10.591	-	1.845	0.001
Strain by DL		0.722	0.112	0.955	6.446	0.003
Constant	0.881	49.989	11.799	-	2.976	0.05
Strain by NM		0.551	0.101	0.939	5.437	0.006

R^2 value obtained for deformation values of Zigbee based WDAQ to data logger is 0.891 and Zigbee based WDAQ to numerical modeling is 0.898, which shows that there is a good correlation between field observations and modeling studies. Similarly, R^2 value obtained for strain values of Zigbee based WDAQ to data logger is 0.901 and Zigbee based WDAQ to numerical modeling is 0.881. It also shows that there is a good correlation between field observations and modeling studies.

4.4.2 Influence of various parameters on the stability of old galleries

This stage of investigations deals with parameters which influence the stability of old underground coal workings during surface mining operations. The parameters are geometrical dimensions, rock properties and external load. Geometrical dimension considered were partition thickness, gallery width and height, pillar width, slope angle and berm width. Rock properties were density and compressive strength of coal and sandstone. External load was taken as shovel and dumper combination load.

In order to study the stability of old underground galleries, in total of 20,736 models were developed. Output results from the models were obtained in the form of directional deformation and strain at points 'P', 'Q', 'R' and 'S', and FOS at points 'P' and 'Q' above the galleries. Regression analysis and significance tests were conducted on input and output parameters to assess the influence of each parameter on the stability of old galleries.

Results of regression analysis for different parameters with respect to the deformation, strain and FOS are presented in Tables 4.8, 4.9 and 4.10 respectively. The regression coefficients (R^2) obtained for deformation, strain and FOS at roof center (point 'P') of gallery1 were 0.883, 0.813 and 0.891 respectively. The parameters including external load were found to have an influence on the stability of old galleries as 't' value and 'p' values were greater than '1' and below '0.05' respectively.

Results have revealed that standardized coefficients of gallery width were 0.257, 0.376 and -0.365 for deformation, strain and FOS respectively. Deformation and strain at point 'P' over gallery1 increased with increasing gallery width since standardized coefficient was found to be positive. FOS was decreased with incresed with gallery width as standardized coefficient was found to be negative.

Table 4.8 Results of regression analysis to assess the deformation at roof center of gallery1

Parameter	R^2	Un-standardized coefficient		Standardized coefficient (Beta)	Significance test	
		B	Std. Error		t	p
Constant		-2.099	0.016		-131.303	0
Gallery width		0.211	0.004	0.257	53.484	0
Partition thickness		-0.650	0.0001	-0.318	-172.710	0
Gallery Height		0.139	0.003	0.089	48.153	0
Pillar Width		-0.037	0.001	-0.325	-62.539	0
Berm width	0.883	-0.010	0.001	-0.031	-16.911	0
Slope angle		0.004	0.0001	0.061	33.216	0
External Load		4.9E-07	0.00001	0.600	323.077	0
DensitySS		-0.001	0.00001	-0.022	-84.734	0
CSSS		-0.003	0.0000642	-0.013	-51.889	0
DensityCL		-0.0001	0.0001859	-0.011	-42.367	0
CSCL		-0.002	0.0001859	-0.009	-8.967	0

DensitySS-Density of Sandstone, CSSS-Compressive strength of Sandstone, DensityCL-Density of Coal, CSCL-Compressive Strength of Coal.

Table 4.9 Results of regression analysis to assess the strain at roof center of gallery1

Parameter	R^2	Un-standardized coefficient		Standardized coefficient (Beta)	Significance test	
		B	Std. Error		t	p
Constant		-213.277	1.374		-155.229	0
Gallery width		44.871	0.339	0.376	132.354	0
Partition thickness		-9.500	0.032	-0.321	-295.169	0
Gallery Height		16.869	0.248	0.074	68.034	0
Pillar Width		-9.687	0.051	-0.538	-189.720	0
Slope Angle	0.813	0.600	0.011	0.061	56.282	0
Berm Width		-2.000	0.053	-0.041	-37.521	0
External Load		7.8E-06	0.0001	0.650	345.0125	0
DensitySS		-0.010	0.0001	-0.010	-62.523	0
CSSS		-0.333	0.009	-0.006	-38.288	0
DensityCL		-0.005	0.0001	-0.005	-31.262	0
CSCL		-0.155	0.0001	-0.0001	-16.142	0

DensitySS-Density of Sandstone, CSSS-Compressive strength of Sandstone, DensityCL-Density of Coal, CSCL-Compressive Strength of Coal.

Table 4.10 Results of regression analysis to assess the FOS at roof center of gallery1

Parameter	R²	Un-standardized coefficient		Standardized coefficient (Beta)	Significance test	
		B	Std. Error		t	p
Constant		7.679	0.22		351.789	0
Gallery width		-0.548	0.005	-0.365	-101.664	0
Partition thickness		0.102	0.001	0.358	200.336	0
Gallery Height		-0.270	0.004	-0.123	-88.556	0
Pillar Width		0.029	0.001	0.385	35.341	0
Slope Angle	0.891	-0.012	0.0001	-0.113	-71.450	0
Berm Width		0.040	0.001	0.085	47.713	0
External Load		-5.4E-07	0.0001	-0.467	-259.534	0
DensitySS		0.0002	0.0001	0.025	69.716	0
CSSS		0.006	0.0001	0.015	42.692	0
DensityCL		0.0001	0.0001	0.012	34.858	0
CSCL		0.005	0.0001	0.009	26.568	0

DensitySS-Density of Sandstone, CSSS-Compressive strength of Sandstone, DensityCL-Density of Coal, CSCL-Compressive Strength of Coal

Standardized coefficient of partition thickness was -0.318, -0.321 and 0.358 for deformation, strain and FOS respectively. Deformation and strain were decreased with increased partition thickness as standardized coefficient was found to be negative whreas FOS was increased with incresed with partition thickness since standardized coefficient was found to be positive.

In the case of gallery height, standardized coefficients were found to be 0.089, 0.074, -0.123 for deformation, strain and FOS respectively. Standardized coefficients for pillar width were found to be -0.325, -0.538, 0.385 for for deformation, strain and FOS respectively. Standardized coefficients for slope angles were found to be 0.061, 0.061,-0.113 for deformation, strain and FOS respectively. In case of berm width, standardized coefficients were be -0.031, -0.041, 0.085 for deformation, strain and FOS respectively. Results have revealed that standardized coefficients of external load were 0.6, 0.65 and

- 0.467 for deformation, strain and FOS respectively. Deformation and strain at point 'P' over gallery1 increased with increased external load since standardized coefficient was found to be positive. FOS was decreased with incresed with external load as standardized coefficient was found to be negative.

Results indicated that deformation and strain were decreased with increased density and compressive strength of coal and sandstone at point 'P' over gallery1. Incase of density of sandstone, standardized coefficients were -0.022, -0.010 and 0.025 for deformation, strain and FOS. Standardized coefficients of compressive strength of sandstone were -0.013, -0.006 and 0.015 for deformation, strain and FOS. Similarly, standardized coefficients of density of coal were -0.011, -0.005 and 0.012 for deformation, strain and FOS. Standardized coefficients of compressive strength of coal were -0.009, -0.0001 and 0.009 for deformation, strain and FOS. Research results based on investigations carried out by SPSS software indicated that all the independent variables influenced the stability of old underground coal workings. Order of influence of different variables was determined based on the standardized coefficient of regression obtained during analysis (Table 4.11).

Table 4.11 Order of influence of various parameters obtained from regression analysis

Parameter	standardized coefficient			Order of influence
	Deformation (mm)	Strain($\mu\varepsilon$)	FOS	
External Load	0.600	0.650	-0.467	1
Pillar width	-0.325	-0.538	0.385	2
Gallery width	0.321	0.376	-0.368	3
Partition thickness	-0.318	-0.321	0.358	4
Gallery Height	0.089	0.074	-0.123	5
Slope angle	0.061	0.061	0.113	6
Berm width	-0.031	-0.041	0.085	7
Density of Sandstone	-0.022	-0.010	0.025	8
Compressive strength of Sandstone	-0.013	-0.006	0.015	9
Density of Coal	-0.011	-0.005	0.012	10

Compressive Strength of Coal	-0.009	-0.0001	0.009	11

Results also revealed that external load was found to be the most influencing parameter on the stability of old underground galleries. Pillar width and gallery width were found to be second and third most important parameters. Partition thickness increased the stability of old galleries and was found to be the fourth most influencing parameter. Gallery height, Slope angle and berm width were found to be fifth, sixth and seventh most important parameters respectively. Density of sandstone was found to be eighth most important parameter and followed by compressive strength of sandstone. Similarly, density of coal was found to be tenth and eleventh position to influence the stability of old galleries.

From the tables 4.8, 4.9 and 4.10 a relationship was established for deformation, strain and FOS at roof center (point 'P') of gallery1 to other parameters (gallery width, pillar width, partition thickness, gallery height, slope angle, berm width, rock properties and external load) as given in equation 4.1, 4.2 and 4.3 respectively. These equation were developed based on un-standardized coefficient (B value) of each parameter. Equation for deformation (Y_{def}) is developed using un-standardized coefficient (B value) from the table 4.8. Similarly, Equations for strain (Y_{strain}) and FOS are developed using B value from the tables 4.9 and 4.10.

Y_{def} =-2.099 +0.211 *(GW) - 0.650*(PT) + 0.139*(GH)-0.037* (PW) + 0.004*(SA) - 0.01*(BW) +4.9E-07*(EL)-0.001*(DS)- (0.003)*(CSSS)-0.0001*(DCL)- 0.002*(CSCL) -- (4.1)

Y_{strain} = -213.277 +44.871 *(GW) – 9.5*(PT) +16.869*(GH)-9.687* (PW) +0.6*(SA) –2*(BW)+7.8E-06*(EL)- 0.01*(DSS)- (0.333)*(CSSS)-0.005*(DCL)- 0.155*(CSCL) -- (4.2)

FOS = 7.679 -0.548 *(GW) + 0.102*(PT) - 0.270*(GH)+0.029* (PW) - 0.012*(SA) +0.04* (BW)-5.4E07*(EL)+0.0002*(DSS)+(0.006)*(CSSS)+0.0001*(DCL)+ 0.005* (CSCL) -- (4.3)

Where,

Y_{def} = Deformation at point 'P' of gallery1 (mm)

Y_{strain}	=	Strain at point 'P' of gallery1 ($\mu\varepsilon$)
FOS	=	Factor of Safety of gallery1
GW	=	Gallery Width (m)
PT	=	Partition Thickness (m)
GH	=	Gallery Height (m)
PW	=	Pillar Width (m)
SA	=	Slope Angle (Degree)
BW	=	Berm Width (m)
EL	=	External Load (N)
DSS	=	Density of Sandstone (kg/m^3)
DCL	=	Density of Coal (kg/m^3)
CSSS	=	Compressive Strength of Sandstone (MPa)
CSCL	=	Compressive Strength of Coal (MPa)

4.5 Design Guidelines

This section deals with the development of design guidelines and details of a user-friendly software.

4.5.1 Development of design guidelines

Based on the field investigations, numerical modeling studies and statistical analysis, design guidelines are prepared for safe extraction of old underground coal workings by opencast workings. Design guidelines were developed based on FOS, which was determined using Mohr-Coulomb theory in numerical modeling studies.

In this study, FOS was categorized as unsafe, moderately safe and highly safe. If FOS was more than '2.0', the model considered as highly safe. If FOS was in between '1.5' to '2.0', the model considered as moderately safe. If FOS is below '1.5', it was considered as unsafe. FOS having the va1ue of 1 ("highly safe") and 2 ("moderately safe") with respect to the input parameters were considered as a design methodology for different gallery widths. Therefore, the design guidelines recommended that the partition

thickness with respect to the slope angle for different gallery widths, pillar widths, gallery heights, berm width, rock properties, external load was based on FOS of "highly safe" and "moderately safe".

A design methodology was developed by using the results of FOS. The results of FOS at point 'P' over gallery1 for partition thickness of 6m, slope angle of 50° to 75°, gallery height of 2.4m to 3.4m, pillar width of 30.5m and gallery width of 4.2m are given in Table 4.12. It can be observed that partition thickness of 6m, slope angle of 50°, gallery height of 2.4m for pillar width of 30.5m is highly safe as the value of FOS was found to be 2.05 and it was indicated as '1'. Similarly, remaining FOS categorical values are given in Table 4.13. Therefore, partition thickness of 6m and slope angle of 50° were considered as "highly safe" when pillar width of 30.5m and gallery height of 2.4m for safe extraction of old galleries with width of 4.2m. It observed that remaining FOS values for pillar width of 30.5m were '2', which indicated as "moderately safe". Gallery height of 3.0m and 3.4m, slope angle of 65° to 75° for pillar width of 30.5m and partition thickness of 6m were found to be "unsafe" as FOS was '3'. Above procedure was applied to the gallery widths of 3.0m, 3.6m, 4.2m and 4.8m. FOS values for gallery width of 4.2m are given in Table 4.14.

Table 4.12 FOS values at point 'P' of partition thickness of 6m for gallery1 width of 4.2m

Partition Thickness (m)	Slope Angle (Degree)	Pillar Width(m)/Gallery Height(m)					
		30.5					
		2.4	2.6	2.8	3.0	3.2	3.4
6	50	2.05	1.97	1.89	1.81	1.73	1.65
	55	1.99	1.91	1.83	1.75	1.67	1.59
	60	1.93	1.85	1.77	1.69	1.61	1.53
	65	1.87	1.79	1.71	1.63	1.55	1.47
	70	1.81	1.73	1.65	1.57	1.49	1.41
	75	1.75	1.67	1.59	1.51	1.43	1.35

Table 4.13 Category of FOS values of partition thickness of 6m for gallery1 width of 4.2m

Partition Thickness (m)	Slope Angle (Degree)	Pillar Width(m)/Gallery Height(m)					
		30.5					
		2.4	2.6	2.8	3.0	3.2	3.4
6	50	1	2	2	2	2	2
	55	2	2	2	2	2	2
	60	2	2	2	2	2	2
	65	2	2	2	2	2	3
	70	2	2	2	2	3	3
	75	2	2	2	2	3	3

1-Highly safe, 2-Moderately safe, 3-Unsafe

Partition thickness of 4m and slope angle of 50º was found to be suitable for gallery width of 3.0m, gallery height of 2.4m and pillar width of 22.5m as FOS for given data was '1'. Similarly, partition thicknesses of 4m and slope angle of 50º were found to be suitable for pillar width of 22.5m and gallery height of 2.6m, 2.8m, 3.0m, 3.2m and 3.4m as shown in Table 4.15. The recommended guidelines for gallery width of 3.0m with respect to the other dimensions when FOS of '2' are given in Table 4.16.

In case of galley width of 3.6m, partition thickness of 4m and slope angle of 50º was found to be suitable for gallery height of 2.4m and pillar width of 25.5m as given in Table 4.17. Partition thicknesses of 4m, 6m, 6m, 6m, 6m and slope angle of 50º were found to be suitable for pillar width of 25.5m and gallery height of 2.6m, 2.8m, 3.0m, 3.2m and 3.4m respectively as FOS for given data was '1'. The maximum recommended partition thickness was 8m for slope angle changing from 65º to 75º and 75º, pillar width of 30.5m and gallery height of 3.4m and 3.2m. The recommended guidelines for gallery width of 3.6m with respect to the other dimensions when FOS of '2' are given in Table 4.18.

The recommended partition thicknesses with respect to the slope angle for gallery width of 4.2m is given in Table 4.19. Partition thickness of 6m and slope angle of 50º was found to be suitable for gallery height of 2.4m and pillar width of 30.5m as FOS for

given data was '1'. Similarly, partition thicknesses of 8m, 8m, 8m, 10m and 12m, and slope angle of 50° were found to be suitable for pillar width of 30.5m and gallery height of 2.6m, 2.8m, 3.0m, 3.2m and 3.4m respectively. As the bench height is 8m, partition thickness above 12m for different slope angles is not feasible for mine operations. The recommended guidelines for gallery width of 4.2m with respect to the other dimensions when FOS of '2' are given in Table 4.20.

Partition thickness of 10m and slope angle of 50° were found to be suitable for, gallery width of 4.8m gallery height of 2.4m and pillar width of 34.5m as shown in Table 4.21. Partition thicknesses of 10m, 10m and 12m, and slope angle of 50° were found to be suitable for pillar width of 34.5m and gallery height of 2.4m, 2.6m and 2.8m respectively. As the bench height is 8m, partition thickness above 12m for different slope angles is not feasible for mine operations. The recommended guidelines for gallery width of 4.2m with respect to the other dimensions when FOS of '2' are given in Table 4.22.

Table 4.14 FOS categorical values for gallery1 width of 4.2m

Partition Thickness (m)	Slope Angle (Degree)	Pillar Width(m)/Gallery Height(m)																	
		30.5						31.5						32.5					
		2.4	2.6	2.8	3.0	3.2	3.4	2.4	2.6	2.8	3.0	3.2	3.4	2.4	2.6	2.8	3.0	3.2	3.4
4	50	2	2	3	3	3	3	2	2	2	2	2	3	2	2	2	2	2	2
	55	2	2	3	3	3	3	2	2	2	2	3	3	2	2	2	2	2	3
	60	2	3	3	3	3	3	2	2	2	2	3	3	2	2	2	2	2	3
	65	3	3	3	3	3	3	2	2	2	3	3	3	2	2	2	2	3	3
	70	3	3	3	3	3	3	2	2	3	3	3	3	2	2	2	3	3	3
	75	3	3	3	3	3	3	2	3	3	3	3	3	2	2	3	3	3	3
6	50	1	2	2	2	2	2	1	1	1	1	2	2	1	1	1	1	1	1
	55	2	2	2	2	2	2	1	1	1	2	2	2	1	1	1	1	1	1
	60	2	2	2	2	2	2	1	1	2	2	2	2	1	1	1	1	1	2
	65	2	2	2	2	2	3	1	1	2	2	2	2	1	1	1	1	2	2
	70	2	2	2	2	3	3	1	2	2	2	2	2	1	1	1	1	2	2
	75	2	2	2	2	3	3	2	2	2	2	2	2	1	1	1	2	2	2
8	50	1	1	1	1	2	2	1	1	1	1	1	1	1	1	1	1	1	1
	55	1	1	1	2	2	2	1	1	1	1	1	1	1	1	1	1	1	1
	60	1	1	2	2	2	2	1	1	1	1	1	2	1	1	1	1	1	1
	65	1	2	2	2	2	2	1	1	1	1	2	2	1	1	1	1	1	1
	70	1	2	2	2	2	2	1	1	1	2	2	2	1	1	1	1	1	1
	75	2	2	2	2	2	2	1	1	1	2	2	2	1	1	1	1	1	2
10	50	1	1	1	1	1	2	1	1	1	1	1	1	1	1	1	1	1	1
	55	1	1	1	1	2	2	1	1	1	1	1	1	1	1	1	1	1	1
	60	1	1	1	1	2	2	1	1	1	1	1	1	1	1	1	1	1	1
	65	1	1	1	2	2	2	1	1	1	1	1	1	1	1	1	1	1	1
	70	1	1	2	2	2	2	1	1	1	1	1	2	1	1	1	1	1	1
	75	1	2	2	2	2	2	1	1	1	1	2	2	1	1	1	1	1	1
12	50	1	1	1	1	1	1	1	1	1	1	1	1	1	1	1	1	1	1
	55	1	1	1	1	1	2	1	1	1	1	1	1	1	1	1	1	1	1
	60	1	1	1	1	1	2	1	1	1	1	1	1	1	1	1	1	1	1
	65	1	1	1	1	2	2	1	1	1	1	1	1	1	1	1	1	1	1
	70	1	1	1	2	2	2	1	1	1	1	1	1	1	1	1	1	1	1
	75	1	1	2	2	2	2	1	1	1	1	1	2	1	1	1	1	1	1

Table 4.15 Recommended design guidelines for gallery width 3.0m (FOS>1.5= "Moderately Safe")

Slope Angle (Degree)	Recommended Partition Thickness(m) and Slope Angles																	
	Pillar Width(m)/Gallery Height(m)																	
	22.5						23.5						24.5					
	2.4	2.6	2.8	3.0	3.2	3.4	2.4	2.6	2.8	3.0	3.2	3.4	2.4	2.6	2.8	3.0	3.2	3.4
50	4	4	4	4	4	4	4	4	4	4	4	4	4	4	4	4	4	4
55	4	4	4	4	4	4	4	4	4	4	4	4	4	4	4	4	4	4
60	4	4	4	4	4	4	4	4	4	4	4	4	4	4	4	4	4	4
65	4	4	4	4	4	4	4	4	4	4	4	4	4	4	4	4	4	4
70	4	4	4	4	4	4	4	4	4	4	4	4	4	4	4	4	4	4
75	4	4	4	4	4	4	4	4	4	4	4	4	4	4	4	4	4	4

Table 4.16 Recommended design guidelines for gallery width 3.0m (FOS>2="Highly Safe")

Slope Angle (Degree)	Recommended Partition Thickness(m) and Slope Angles																	
	Pillar Width(m)/Gallery Height(m)																	
	22.5						23.5						24.5					
	2.4	2.6	2.8	3.0	3.2	3.4	2.4	2.6	2.8	3.0	3.2	3.4	2.4	2.6	2.8	3.0	3.2	3.4
50	4	4	4	4	4	4	4	4	4	4	4	4	4	4	4	4	4	4
55	4	4	4	4	4	4	4	4	4	4	4	4	4	4	4	4	4	4
60	4	4	4	4	4	4	4	4	4	4	4	4	4	4	4	4	4	4
65	4	4	4	4	4	6	4	4	4	4	4	4	4	4	4	4	4	4
70	4	4	4	4	6	6	4	4	4	4	4	4	4	4	4	4	4	4
75	4	4	4	4	6	6	4	4	4	4	4	4	4	4	4	4	4	4

Table 4.17 Recommended design guidelines for gallery width 3.6m (FOS>1.5="Moderately Safe")

Slope Angle (Degree)	Recommended Partition Thickness(m) and Slope Angles																	
	Pillar Width(m)/Gallery Height(m)																	
	25.5						26.5						27.5					
	2.4	2.6	2.8	3.0	3.2	3.4	2.4	2.6	2.8	3.0	3.2	3.4	2.4	2.6	2.8	3.0	3.2	3.4
50	4	4	4	4	4	4	4	4	4	4	4	4	4	4	4	4	4	4
55	4	4	4	4	4	4	4	4	4	4	4	4	4	4	4	4	4	4
60	4	4	4	4	4	4	4	4	4	4	4	4	4	4	4	4	4	4
65	4	4	4	4	4	4	4	4	4	4	4	4	4	4	4	4	4	4
70	4	4	4	4	4	4	4	4	4	4	4	4	4	4	4	4	4	4
75	4	4	4	4	4	6	4	4	4	4	4	4	4	4	4	4	4	4

Table 4.18 Recommended design guidelines for gallery width 3.6m (FOS>2="Highly Safe")

Slope Angle (Degree)	Recommended Partition Thickness(m) and Slope Angles																	
	Pillar Width(m)/Gallery Height(m)																	
	25.5						26.5						27.5					
	2.4	2.6	2.8	3.0	3.2	3.4	2.4	2.6	2.8	3.0	3.2	3.4	2.4	2.6	2.8	3.0	3.2	3.4
50	4	4	6	6	6	6	4	4	4	4	4	6	4	4	4	4	4	4
55	4	4	6	6	6	6	4	4	4	4	6	6	4	4	4	4	4	6
60	4	6	6	6	6	6	4	4	4	4	6	6	4	4	4	4	4	6
65	6	6	6	6	6	8	4	4	4	6	6	6	4	4	4	4	6	6
70	6	6	6	6	6	8	4	4	6	6	6	6	4	4	4	6	6	6
75	6	6	6	6	8	8	4	6	6	6	6	6	4	4	6	6	6	6

Table 4.19 Recommended design guidelines for gallery width 4.2m (FOS>1.5="Moderately Safe")

Slope Angle (Degree)	Recommended Partition Thickness(m) and Slope Angles																	
	Pillar Width(m)/Gallery Height(m)																	
	30.5						31.5						32.5					
	2.4	2.6	2.8	3.0	3.2	3.4	2.4	2.6	2.8	3.0	3.2	3.4	2.4	2.6	2.8	3.0	3.2	3.4
50	4	4	6	6	6	6	4	4	4	4	4	6	4	4	4	4	4	4
55	4	6	6	6	6	6	4	4	4	4	6	6	4	4	4	4	4	6
60	4	6	6	6	6	6	4	4	4	6	6	6	4	4	4	4	6	6
65	6	6	6	6	6	8	4	4	4	6	6	6	4	4	4	4	6	6
70	6	6	6	6	8	8	4	4	6	6	6	6	4	4	4	6	6	6
75	6	6	6	6	8	8	4	6	6	6	6	6	4	4	6	6	6	6

Table 4.20 Recommended design guidelines for gallery width 4.2m (FOS>2="Highly Safe")

Slope Angle (Degree)	Recommended Partition Thickness(m) and Slope Angles																	
	Pillar Width(m)/Gallery Height(m)																	
	30.5						31.5						32.5					
	2.4	2.6	2.8	3.0	3.2	3.4	2.4	2.6	2.8	3.0	3.2	3.4	2.4	2.6	2.8	3.0	3.2	3.4
50	6	8	8	8	10	12	6	6	6	6	8	8	6	6	6	6	6	6
55	8	8	8	10	12	>12	6	6	6	8	8	8	6	6	6	6	6	6
60	8	8	10	10	12	>12	6	6	8	8	8	10	6	6	6	6	6	8
65	8	10	10	12	>12	>12	6	6	8	8	10	10	6	6	6	6	8	8
70	8	10	12	>12	>12	>12	6	8	8	10	10	12	6	6	6	6	8	8
75	10	12	>12	>12	>12	>12	8	8	8	10	12	>12	6	6	6	8	8	10

>12 indicates not feasible for mine operation

Table 4.21 Recommended design guidelines for gallery width 4.8m (FOS>1.5=”Moderately Safe”)

Slope Angle (Degree)	Recommended Partition Thickness(m) and Slope Angles																	
	Pillar Width(m)/Gallery Height(m)																	
	34.5						35.5						36.5					
	2.4	2.6	2.8	3.0	3.2	3.4	2.4	2.6	2.8	3.0	3.2	3.4	2.4	2.6	2.8	3.0	3.2	3.4
50	6	6	6	6	8	8	4	6	6	6	6	6	4	4	6	6	6	6
55	6	6	6	8	8	8	4	6	6	6	6	6	4	4	6	6	6	6
60	6	6	8	8	8	10	6	6	6	6	6	8	4	6	6	6	6	6
65	6	6	8	10	10	10	6	6	6	6	8	8	6	6	6	6	6	6
70	6	8	8	10	10	12	6	6	6	6	8	8	6	6	6	6	6	6
75	8	8	8	10	12	>12	6	6	6	8	8	10	6	6	6	6	6	6

>12 indicates not feasible for mine operation

Table 4.22 Recommended design guidelines for gallery width 4.8m (FOS>2="Highly Safe")

Slope Angle (Degree)	Recommended Partition Thickness(m) and Slope Angles																	
	Pillar Width(m)/Gallery Height(m)																	
	34.5						35.5						36.5					
	2.4	2.6	2.8	3.0	3.2	3.4	2.4	2.6	2.8	3.0	3.2	3.4	2.4	2.6	2.8	3.0	3.2	3.4
50	10	10	12	>12	>12	>12	8	8	8	10	12	>12	6	6	8	8	8	8
55	10	12	>12	>12	>12	>12	8	8	10	10	12	>12	6	6	8	8	8	10
60	12	>12	>12	>12	>12	>12	8	10	10	12	>12	>12	6	6	8	8	10	10
65	>12	>12	>12	>12	>12	>12	8	10	12	>12	>12	>12	6	8	8	10	10	12
70	>12	>12	>12	>12	>12	>12	10	12	>12	>12	>12	>12	8	8	8	10	12	>12
75	>12	>12	>12	>12	>12	>12	10	12	>12	>12	>12	>12	8	8	10	12	>12	>12

>12 indicates not feasible for mine operation

4.5.2 Development of user-friendly software package

A user-friendly software package is developed, which provides access to the design guidelines in an easy way. It consists of three modules, namely, Factor of Safety (FOS), Partition Thickness and Slope Angle. Each module takes input data as gallery width, gallery height, pillar width, berm width, rock properties and external load. The following are screenshots of the software module (Fig. 4.25).

Description of software package:

Software package starts with login in page, which allows the user/admin to enter into "Home" page by providing user name and password (Fig.4.25A).

Fig. 4.25A Login page of guidelines software

After successfully logged in, the user is allowed to access the Home page, which is named as "Guidelines for Safe Extraction of Old Underground Coal Workings". Home page consists of three modules, Factor of Safety (FOS), Partition Thickness and Slope Angle as

156

shown in the Fig. 4.25B. Apart from these modules, Home has two menus such as 'About' and 'Logout' menus in Menu bar. 'About' menu gives the details of hierarchy of software. Logout menu is used to traverse from Home page to login page. FOS, partition thickness and slope angle modules can be accessed through Home page. By clicking on Factor of Safety (FOS) in Home page, user can be traversed to the Factor of Safety module. In this module, input data is categorized into various sections such as old underground working dimensions, opencast bench configurations, rock properties and external load. After successful entering of input data the output is displayed by clicking "Factor of Safety" button in the module (Fig. 4.25C). Similarly, Partition thickness and slope angles modules can be accessed(Fig.4.25D and 4.25E). Finally, reports will be generated after successful execution of module (Fig. 4.25F).
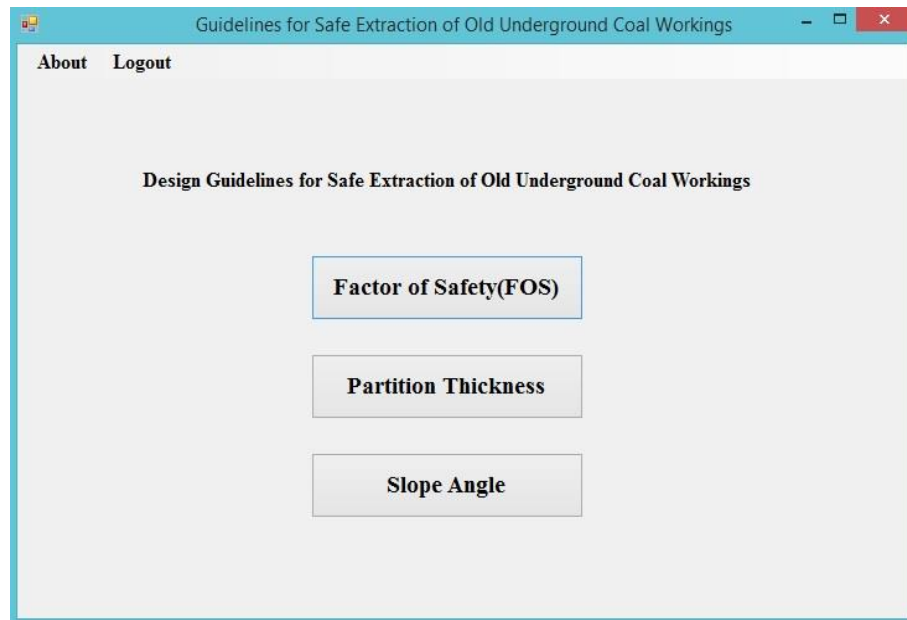
Fig. 4.25B Modules in software package

Fig. 4.25C Factor of Safety module

Fig. 4.25D Partition thickness module

Fig. 4.25E Slope angle module
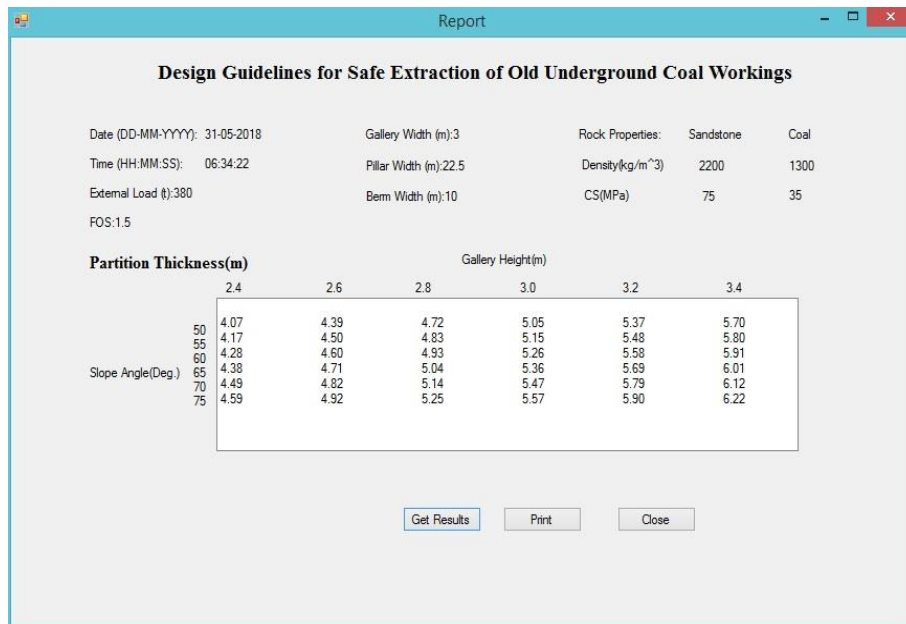
Fig. 4.25F Interface of report module

Fig. 4.25 Screen shots of modules of guidelines software

5 Conclusions and Recommendations

This chapter deals with conclusions drawn from research studies, and recommendations for future scope of work. The details are given as follows.

5.1 Conclusions

State-of-the-art Zigbee based Wireless DAQ is developed for monitoring deformation and strain in partition and slope above old underground coal workings. Field investigations were carried out in Ramagundam Opencast Project-I (RGOCP-I) and Ramagundam Opencast Project-III (RGOCP-III) of The Singareni Collieries Company Limited, Ramagundam, Peddapalli District of Telangana State, India. Zigbee based WDAQ and conventional data logger were deployed for monitoring deformation and strain in partition and slope above the old underground workings that are being converted into opencast mine. The following are the main conclusions drawn from the research study:

- State of the art system Zigbee based WDAQ was developed and deployed in the field, and validated with conventional data logger and modeling studies. The data obtained using ZWDAQ is in close to the other two methods, indicating ZWDAQ monitoring method is reliable.
- Maximum strain observed by data logger was 387με, whereas 331με was observed by Zigbee based WDAQ for 4.12m partition thickness. Maximum deformation observed by data logger was 2.31mm, whereas 2.41mm was observed by Zigbee based WDAQ for 4.12m partition thickness, gallery width of 4.2m and height of 3m under field conditions.
- Maximum strain, in slope observed by data logger was 172με, whereas 185με was observed by Zigbee based WDAQ for of 49° slope angle and partition thickness of 5.82m. Maximum deformation observed by data logger was

1.65mm, whereas 1.90mm was observed by Zigbee based WDAQ gallery width of 4.2m and height of 3m under field conditions.

- Maximum deformation observed in partition and slope was 2.52mm and 1.90mm for partition thickness of 4.12m and 5.82m respectively by using numerical modeling studies.

- From field studies, it can be observed that strain and deformation were decreased with increased partition thickness and vice versa.

- The variation between Zigbee based WDAQ and data logger is around 10.27% to 13.30%. The variation in between Zigbee based WDAQ and numerical modeling is around 3.03% to 6.32% and numerical modeling to data logger is 7.30% to 19.63%. However, the data obtained using Zigbee based WDAQ is in close to the other two methods. As rock is non-homogeneous, such variation can be considered as within acceptable limits.

- A total of 20,736 models were developed and simulated for different gallery dimension, rock properties and external load to assess the stability of old underground coal workings using ANSYS workbench software.

- Numerical modeling analysis results indicated that strain and deformation were decreased with increased partition thickness, pillar width, berm width, density, external load and compressive strength of sandstone and coal. Strain and deformation were increased with increased gallery width, gallery height and slope angle.

- SPSS based analysis was done for both field investigations and numerical modeling studies. Regression coefficient (R^2) values obtained for deformation-Zigbee based WDAQ to the data logger and numerical modeling were 0.891, 0.898 and strain- Zigbee based WDAQ to the data logger and numerical modeling were 0.901 and 0.881 respectively. These results show good relation between field observations and modeling studies.

- Statistical analysis results revealed that the order of influence of input parameters on the stability of old galleries.

  External Load
  Pillar width

Gallery width

Partition thickness

Gallery Height

Slope angle

Berm width

Density of Sandstone

Compressive strength of Sandstone

Density of Coal

Compressive Strength of Coal

- The design guidelines were developed based on field and numerical modeling investigations. These guidelines are categorized based on FOS value as highly safe, moderately safe and unsafe. Optimum partition thickness, slope angle and Factor of Safety were suggested for given geometrical dimensions, rock properties and external load.

- The User-friendly software was developed to use the guidelines in simple way. The input parameters are geometrical dimensions, rock properties and external load. Optimum partition thickness, slope angle and FOS are output parameters for given input.

5.2 Recommendations

Research work was focused on the real-time monitoring of stability of old underground coal workings by using Zigbee based Wireless Data Acquisition System (WDAQ). Numerical modeling studies were carried out and design guidelines were recommended for the safe extraction of old galleries. The following suggestions are made for future research on the subject.

- In the present work, Zigbee based WDAQ was implemented. In future work, it can be extended to the Internet of Things (IOT) for connecting several of devices such as machinery, handheld systems and other smart instruments available in the field.

162

- At present, numerical modeling was done with two galleries and two benches. Hence, further research work can be considered more than two galleries and benches for better assessment of the stability of old galleries.
- Impact of blasting can also be studied for further research work.

REFERENCES

Abramson, L.W., Lee, T.S., Sharma, S. and Boyce, G.M. (2002). "Slope stability and stabilization methods." *Second Edition, John Wiley & Sons, Inc.*, New York, USA, 329-339.

Ali, N., Drieberg, M. and Sebastian, P. (2012). "Development of wireless sensor network for slope monitoring." *4th Int. Conference on Intelligent and Advanced Systems (ICIAS2012)*, 1(4), 285–290.

Akyildiz, I., Su, W., Sankarasubramaniam, Y. and Cayirci, E. (2002). "Wireless sensor networks: a survey." *Computer Networks*, 38(4), 393–422.

Anon. (2017). "Provisional coal statistics-2016-17." *Ministry of Coal*, India, 1–89. http://www.coalcontroller.gov.in/writereaddata/files/download/provisionalcoalstat /ProvisionalCoalStat2016-17.pdf (Nov. 25, 2017).

Anon. (2017). "Energy statistics." *Central Statistics Office, Ministry of Statistics and Programme Implementation,* Government of India, New Delhi, 1-121.

BP statistics (2018). "BP statistical review of world energy."1-56 https://www.bp.com/content/dam/bp/en/corporate/pdf/energy-economics/statistical-review-2017/bp-statistical-review-of-world-energy-2018-full-report.pdf (Aug.20, 2018).

Anon. (2017). "Indian coal and lignite resources." *Geological survey of India,* 1-46. https://gsi.gov.in/cs/groups/public/documents/document/b3zp/mtyx/~edisp/dcport 1gsigovi161863.pdf (Dec. 25, 2017)

Ashkan, V., Moore, L. and Ali, H. (2010). "Monitoring systems for warning impending failures in slopes and open pit mines." *Natural Hazards*, 55(2), 501–512.

Azzam, R., Arnhardt, C. and Fernandez-Steeger T. M. (2010). "Monitoring and early warning of slope instabilities and deformations by sensor fusion in self-organized wireless ad-hoc sensor networks." *J. SE Asian Appl. Geol.*, 2(3), 163–169.

Azizi, M.A., Kramadibrata, S., Wattimena, R.K. and Sidi, I.D. (2013). "Probabilistic Analysis of Physical Models Slope Failure." *Procedia Earth and Planetary Science6,* 411 – 418.

Baronti, P., Pillai, P., Chook, V. W. C., Chessa, S., Gotta, A. and Hu, Y. F. (2007). "Wireless sensor networks: a survey on the state of the art and the 802.15.4 and zigbee standards." *Computer Communications*, 30(7), 1655–1695.

Berardino, P., Costantini, M., Franceschetti, G., Iodice, A., Pietranera, L. and Rizzo, V. (2003). "Use of differential sar interferometry in monitoring and modelling large slope instability at maratea (basilicata, italy), *Engineering Geology*, 68, 31–51.

Bond, J., Kim, D., Langley, R.B. and Chrzanowski, A. (2003). "An investigation on the use of GPS for deformation monitoring in open pit mines." *Proc., of the Fourth Int. Conference on Computer Applications in the Minerals Industries (CAMI)*, Canada, 1–13.

Bond, J., Kim, D., Chrzanowski, A. and Szostak-Chrzanowski, A. (2007). "Development of a fully automated, GPS based monitoring system for disaster prevention and emergency preparedness: PPMS+RT." *Sensors*, 7(7), 1028–1046.

Casademont, J., Lopez-aguilera, E., Paradells, J., Rojas, A., Cotrina, J., Calveras, A. and Barcelo, F. (2004). "Wireless technology applied to GIS." *Computers & Geosciences*, 30, 671–682.

Chen, Y., He, X., Ding, X. and Sang, W. (2005). "Steep-slope monitoring: GPS multiple-antenna system at Xiaowan Dam." *Jl. of geodetic science*, 16(11), 20-25.

Chrzanowski, A. (1994). "The deformable world-problems and solutions." *Proc., of Perelmuter Workshop on Dyn,* Deformation Models, Workshop Organizing Com- mittee, Technion City, Israel, 8–28.

Clough, R.W. (1960). "The finite element method in plane stress analysis." *Proc., of Second ASCE Conference Electronic Computations*, Pittsburg, 345-378.

Cundall, P.A. (1971). "A computer model for simulating progressive large scale movements in blocky rock systems." *Proc., Int. Symp. on Rock Fracture*, Nancy, 2-8.

Dave Ta, T. C., Yuh-Show, T. and Kai-Chun, Y. (2013). "Study of real-time slope stability monitoring system using wireless sensor network." *TELKOMNIKA*, 11(3), 1478-1488.

Desai, U. B. and Jain, B. N. (2007). "Wireless sensor networks : technology roadmap." *A Project supported by Department of Information Technology, Ministry of Information and Communication Technology*, India,19-22.

Ding, X., Swindells, C.F., Montgomery, S.B., Ren, D. and Chen, X. (1995). "An overview of geotechnical instrumentation for deformation monitoring in Australian open pit mines." *Proc., 5th South East Asian and 36th Australian Surveyors Congress*, 539–550.

Ding, X., Montgomery, S.B., Tsakiri, M., Swindells, C.F. and Jewell, R.J. (1998). "Integrated monitoring systems for open pit wall deformation." *Minerals and Energy Research Institute of Western Australia*, Perth, 1-186.

Dowding, C.H., Su, M.B. and O'Connor, K.M. (1989). "Measurement of rock mass deformation with grouted coaxial antenna cables." *Rock Mechanics and Rock Engineering*, 22, 1-23.

Eberhardt, E. (2003). "Rock slope stability analysis-utilization of advanced numerical techniques." *Int. Jl. of Geological Engineering/Earth and Ocean Sciences,*17-32.

Garich, E.A. (2007). "Wireless, automated monitoring for potential landslide hazards." MS *Dissertation*, Texas A&M University,1-48.

Farina, P., Leoni, L., Babboni, F., Coppi, F., Mayer, L. and Ricci, P. (2011). "IBIS-M, an innovative radar for monitoring slopes in open-pit mines." *Int. Symp. on Rock Slope Stability in Open Pit Mining and Civil Engineering*, Vancouver, Canada, 793-801

Farina, P. and Coli, N. (2013). "Efficient real time stability monitoring of mine walls : the çollolar mine case study." *Int. Mining Congress and Exhibition of Turkey*, 111–117.

Francioni, M., Salvini, R., Stead, D., Giovannini, R., Riccucci, S., Vanneschi, C. and Gullì, D.(2015). "An integrated remote sensing-gis approach for the analysis of an open pit in the carrara marble district, italy, slope stability assessment through kinematic and numerical method." *Computers and Geotechnics*, 67, 46–63.

Girard, J. M., Mayerle, R. T. and McHugh, E. L. (1998). "Advances in remote sensing techniques for monitoring rock falls and slope failures." *Proc., of the 17th Int. Conference on Ground Control in Mining*, NIOSHTIC-2, No 20000186, 326-331.

Girard, J.M. and McHugh, E. (2000). "Detecting problems with mine slope stability." *In 31st Annual Institute on Mining Health, Safety and Research*, Roanoke, NIOSHTIC Report-No.10006193, 8-20.

Guangming, B., Jauan, C. and Zhigang, L. (2014). "Analysis of open-pit to underground mining slope stability." *Applied Mechanics and Materials*, 599-603.

Gundewar, C.S. (2014). "Application of rock mechanics in surface and underground mining." *Indian Bureau of Mines*, Government of India Ministry of Mines, 53-73.

Harries, N., Noon, D. and Rowley, K. (2003). "Case studies of slope stability radar used in open cut mines." *The South African Institute of Mining and Metallurgy Int. Symp. on Stability of Rock Slopes in Open Pit Mining and Civil Engineering*, South Africa, 335–342.

Hunter, G., Cox, C. and Kremer, J. (2006). "Development of a commercial laser scanning mobile mapping system - street-mapper." *The Int. Archives of the Photogrammetry, Remote Sensing and Spatial Information Sciences,* 36-56.

Hussain Qaisar, Ȧ. S. and Aquil Ahmad, Ȧ. M. (2014). "Production, consumption and future challenges of coal in India." *Int. Jl. of Current Engineering and Technology*, 5, 3437–3440.

Hsu-yang, k., jing-shiuan, h. and chaur-tzuhn, c. (2006). "Drought forecast model and framework using wireless sensor networks." *Jl. of Information Science and Engineering*, 22(4), 751-769.

Hawwash, A.A., Abdel-rahman, A.K., Nada, S.A. and Ookawara, S. (2017). "Numerical investigation and experimental verification of performance enhancement of flat plate solar collector using nanofluids."*Applied Thermal Engineering*, 130, 363–374.

Jiang, T. and Yang, Z. (2011). "Research on mine safety monitoring system based on WSN." *Procedia Engineering*, 26, 2146–2151.

Jingusui, M., Sena-cruz, J., Czaderski, C. and Motavalli, M. (2013). "Structural strengthening with prestressed cfrp strips with gradient." *Journal of Composites for Construction*, 17(5), 651-661.

Kane, W. F., Beck, T. J., Anderson, N. O. and Perez, H. (1996). "Remote monitoring of unstable slopes using time domain reflectometry." *The 11th Thematic Conference and Workshops on Applied Geologic Remote Sensing*, Las Vegas, Nevada, 431-440.

Kane, W.F. and Beck, T.J. (1999). "Advances in slope instrumentation: TDR and remote data acquisition systems." *Field Measurements in Geomechanics, 5th International Symposium on Field Measurements in Geomechanics*, Singapore, 101-105.

Kane, W.F., Novotny, C., Owen, J. and Anbessaw, A. (2007). "Automated slope monitoring of a large unstable slope." *50th Annual Meeting, Association of Environmental and Engineering Geologists.*

Kasraoui, M., Cabani, A. and Mouzna, J. (2013). "Zbr-M: a new zigbee routing protocol", *Int. Jl. of Computer Science and Application*, 10(2), 15–32.

Kayesa, G. (2006). "Prediction of slope failure at letlhakane mine with the geomos slope monitoring system." *Proc. Int. Symp. on Stability of Rock Slopes in Open Pit Mining and Civil Engineering Situations*, Series S44, South Africa,605-622.

Kalyana, T., Mehta, P., Bansal, R., Parekh, C., Merchant, S. N. and Desai, U. B. (2006). "Routing protocols for landslide prediction using wireless sensor networks." *Fourth Int. Conference on Intelligent Sensing and Information Processing*, 43–47.

Kliche, C. (1999). "Rock slope stability." *Society for Mining, Metallurgy and Explorations*, 303-344.

Kumar, D. and Ram Chandar, K. (2016). "Application of wireless sensor networks in slope stability monitoring – a critical review." *The Indian Mining & Engineering Journal*, 55(3), 29-32.

Kumar, D. and Ram Chandar, K. (2017). "Computer aided slope stability monitoring." *Disaster Advances*, 10(12),37-51.

Kyoon-Tai, K. and Jae-Goo, H. (2008). "Design and implementation of a real-time slope monitoring system based on ubiquitous sensor network." *The 25th Int. Symp. on Automation and Robotics in Construction*, 330–336.

Little, M.J. (2006). "Slope monitoring strategy at pprust open pit operations." *International Symposium on Stability of Rock Slopes in Open Pit Mining and Civil Engineering*, The South African Institute of Mining and Metallurgy, 44, 211-230.

Mahto T. (2015). "Safe extraction of developed pillars by opencast method – a challenge for mining engineers: a case study." http://www.slideshare.net/tikeshwarmahto5/extraction-of-developed-pillars-by-opencast-mine-acase-study (Dec. 5, 2015).

Marconcin, L. R., Machado, R. D. and Marino, M. A. (2010). "Numerical modeling of steel-concrete composite beams Modelagem numérica de vigas mistas aço-concreto." *IBRACON Structures and Materials Journal*, 3(4), 449–462.

McHugh, E.L., Dwyer, J., David, G., Long, D.G. and Sabine, C. (2006). "Applications of ground-based radar to mine slope monitoring." *Centers for Disease Control and Prevention National Institute for Occupational Safety and Health*, 1-39.

Morris, R. and Clough, W.D. (1985). "The opencast mining of previously underground mined coal seams." *Jl. of the South African Institute of Mining and Metallurgy*, 435-439.

Morris, R and W.D. Clough. (1986). "Effects of underground workings on the slope stability of an opencast mine." *Deetlefs (ed.) The planning and operation of open pit and ship mines*. Johannesburg, SAIMM, 55-61.

Nunoo, S., Tannant, D. D. and Newcomen, H. W. (2015). "Slope monitoring practices at open pit porphyry mines in British Columbia, Canada." *Int. Jl. of Mining, Reclamation and Environment*, 0930, 1–12.

Pakzad, S.N., Fenves, G.L., Kim, S. and Culler, D.E. (2008). "Design and implementation of scalable wireless sensor network for structural monitoring." *Journal of Infrastructure Systems*, 14(1), 89–101.

Patikova, A. (2004). "Digital photogrammetry in the practice of open pit mining." *The Int. Archives of the Photogrammetry, Remote Sensing and Spatial Information Sciences*, 1-34.

Perrone, N. and Kao, R. (1975). "A general finite difference method for arbitrary meshes." *Computers and Structures*, 5, 45-58.

Prasad, A. N. (1986). "Coal industry of India." *Problems of Coal Industry: Some New Challenges, South Asia Books*, 325-326.

Prakshep, M., Deepthi, C., Shahim, M., Kalyana, T., Merchant, S. N. and Desai, U. B. (2007). "Distributed detection for landslide prediction using wireless sensor network." *First Int. Global Information Infrastructure Symp. (GIIS) 2007*, 2, 195 – 198.

Raj kumar, B., Balanagu, P. and Babu, N. S. (2012). "Zigbee based mine safety monitoring system with GSM*." International Journal of Computer & Communication Technology*, 3(5), 63–67.

Ramesh, M. V. (2009). "Real-time wireless sensor network for landslide detection." *Proc., 3rd Int. Conference on Sensor Technologies and Applications, SENSORCOMM 2009*, 405–409.

Ramesh, M. V. (2014). "Design, development, and deployment of a wireless sensor network for detection of landslides." *Ad Hoc Networks*, *13*(PART A), 2–18.

Ram Chandar, K. and Gowtham Kumar, B. (2014). "Effect of width of highwall mining gallery on stability of highwall." *Int. Jl. Mining and Mineral Engineering*, 5(3), 212-228.

Ram Chandar, K., Chiranth, H., Mohan, Y. and Gowtham Kumar, B. (2015). "Classification of stability of highwall during highwall mining: a statistical adaptive learning approach." *Int. J. Geotechnical & Geological Engineering*, 33(1), 511-521.

Reeves, B., Noon, D.A., Stickley, G.F. and Longstaff, D. (2001). "Slope stability radar for monitoring mine walls." *Proc., of the international society for optics and photonics (SPIE)*, 57–67.

Robertson, A. and Mac, G. (1971), "Determination of stability of slopes in jointed rock with particular reference to the determination of strength parameters and mechanism of failure." *Ph. D. dissertation*, University of the Witwatersrand,106-126.

Rui, T. and Fangwei, H. (2012). "Stability analysis of open-pit slope in rock movement zone based on simulation and BP network." *Int. Conference on Industrial Control and Electronics Engineering*, 2040–2042.

Sakurai, S. and Shimizu, N. (2003). "Monitoring the stability of slopes by GPS." *The South African Institute of Mining and Metallurgy Int. Symp. on Stability of Rock Slopes in Open Pit Mining and Civil Engineering*, Construction Engineering Research Institute Foundation, Japan, 353–360.

Sastry, V.R. and Ram Chandar, K. (2014). "Effect of berm width on stability of slopes- a case study." *Minetech Journal*.

Satyanarayana, I. (2012). "Extraction of developed pillars by opencast method." http://www.slideshare.net/isnindian/extraction-of-developed-pillars (Jul. 22, 2015).

Scaioni, M., Lu, P., Chen, W. and Wu, H. B. (2012). "Wireless sensor network based monitoring on a landslide simulation platform." *8th Int. Conference on Wireless Communications, Networking and Mobile Computing*, Shanghai, China, 1–4.

Shizhuang, L., Jingyu, L., Yanjun, F. and Wuhan, U.W. (2007). "Zigbee based Wireless Sensor Networks and Its applications in industrial." *Int. Conference on Automation and Logistics*, Jinan, China, 1979-1983.

Singh, T.N. and Singh, D.P. (1992). "Prediction of instability of slope in opencast mine over old surface and underground workings." *Int. Jl. of Surface Mining and Reclamation 6*, 81-89.

Singer, J., Thuro, K. and Festl, J. (2010). "Development and testing of a time domain reflectometry (tdr) monitoring system for subsurface deformations." *Taylor & Francis Group*, London, 613–616.

170

Singhroy, V. and Molch, K. (2004). "Characterizing and monitoring rockslides from SAR techniques, *Advances in Space Research*, 33(3), 290–295.

Somani, N.A. and Patel, Y. (2012). "Zigbee: a low power wireless technology for industrial." *Int. Jl. of Control Theory and Computer Modelling (IJCTCM)*, 2(3),27-33.

Terzis, A., Anandarajah, A., Moore, K. and Wang, I.J. (2006). "Slip surface localization in wireless sensor networks for landslide prediction." *5th Int. Conference on Information Processing in Sensor Networks*, Nashville, TN, USA,109-116

Tolk, A., Diallo, S.Y., King, R.D., Turnitsa, C.D. and Padilla, J.J. (2010). "Conceptual modeling for composition of model-based complex systems." *Publisher: CRC Taylor & Francis*, 355–381.

Waltters, R.J. and Finn, D. and Coulthard, J. (1989). "Pit slope instability problems induced by disused underground mine workings." *Proc., of the 25th Symp. on Engineering Geology and Geotechnical Engineering*, 101-106.

Walton, G. and Taylor, R.K. (1977). "Likely constraints on the stability of excavated slopes due to underground coal workings." *Int. Jl. of Rock Mechanics and Mining Sciences & Geo Mechanics Abstracts*, 14, 5-6.

Wang, J., Gao, J., Liu, C. and Wang, J. (2010). "High precision slope deformation monitoring model based on the gps/pseudolites technology in open-pit mine." *Mining Science and Technology*, 20(1), 126–132.

Wei, Y., Chen, Z., Deng, J., Zhu, H., Deng, F. and Liu, Z. (2015). "Numerical method for subsea wellhead stability analysis in deep water drilling." *Ocean Engineering*, *98*, 50–56.

Wheaton, J.M., Garrard, C., Whitehead, K. and Volk, C.J. (2012). "A simple, interactive GIS tool for transforming assumed total station surveys to real world coordinates - the champ transformation tool." *Computers and Geosciences*, 42, 28–36.

Wilkins, R., Bastin, G., Chrzanowski, A., Newcomen, H. W. and Shwydiuk, L. (2003). "A fully automated system for monitoring pit wall displacements." *SME Annual Meeting and Exhibit*, Cincinnati, OH,1-7.

Yu, B., Liu, G., Li, Z., Zhang, R., Jia, H., Wang, X. and Cai, G. (2013). "Subsidence detection by terrasar-x interferometry on a network of natural persistent scatterers and artificial corner reflectors, *Computers and Geosciences*, 58, 126–136.

Zan, L., Latini, G., Piscina, E., Polloni, G. and Baldelli, P. (2002). "Landslides early warning monitoring system." *IEEE Int. Geoscience and Remote Sensing Symp.,* Toronto, Ontario, Canada, Canada, 1(C), 188–190.

Zheng, H., Liu, D. F. and Li, C. G. (2005). "Slope stability analysis based on elasto-plastic finite element method." *Int. Conference on Computer Application and System Modeling (ICCASM)*, 1871–1888.

APPENDIX – I

SOURCE CODE OF ZIGBEE BASED WDAQ

I.1 SOURCE CODE OF WISMS SOFTWARE OF ZIGBEE BASED WIRELESS DATA ACQUISITION SYSTEM

```
#include <EEPROM.h>
#include <dht.h>
#define data 11
#define clk 12
#define PDWNPIN 10
#define cal_sw 9
#define led 13
#define DHT11_PIN 2dht  DHT;
int sum = 0;
int sum1 = 0;
char buf[22];
char buf1[20];

struct MyObject
{
   int cal;
};

int i,j;
int val,val1,val2,val3;
int c_data;

void setup()
{
 Serial.begin(9600);
 pinMode(clk, OUTPUT);
 pinMode(data, INPUT);
 pinMode (PDWNPIN,OUTPUT);
 pinMode(led,OUTPUT);
 analogReference(INTERNAL);
 digitalWrite(clk,LOW);
 reset_adc();
 MyObject cal_data;    //Variable to store custom object read from EEPROM.
 EEPROM.get( 0,cal_data);
 c_data = cal_data.cal_;
Serial.println(c_data);
}

void loop()
{
 digitalWrite(led,HIGH);
```

```
 read_adc();
 lvdt();
 DHT_();
digitalWrite(led,LOW);
if(digitalRead(cal_sw)==LOW)
{
 cal();
}
 Serial.println();
 Serial.println();
 delay(1000);
}

void read_adc()
{
 if(digitalRead(data) == LOW)
  {
   for(i=0;i<21;i++)
    {
        digitalWrite(clk,HIGH);
      __asm__("nop\n\t");
      if(digitalRead(data)==1)
       {
        buf[i]='1';
       }
    else
       {
        buf[i]='0';
       }

    __asm__("nop\n\t");

     digitalWrite(clk,LOW);
      }
    }

  conv();
}

void conv()
{
 int k;
 for(k=0;k<19;k++)
  {
```

```
    buf1[k]=buf[k];
   }

   bin2dec(buf1);
   sum1=sum;
   sum = c_data - sum;
   Serial.println("Strain Gauge Output");
  Serial.println(sum);
   delay(1000);
}

void reset_adc()
{
 digitalWrite(PDWNPIN, LOW);
 delayMicroseconds(26);
digitalWrite(PDWNPIN, HIGH);
}

void drdy_wait()
{
 delayMicroseconds(.10);
}

void bin2dec(char binary[])
{
   int power = pow(2,18-1);
   sum=0;
   int i;
   for (i=0; i<18; ++i)
   {
     if ( i==0 && binary[i]!='0')
     {
           sum = power * 1;
      }
     else
      {
      sum += (binary[i]-'0')*power;//The -0 is needed
      }
    power /= 2;
    }
 }
```

```
void cal() // Strain Gauge Module
{
  int l;
  Serial.println("Strain gauge calibration start");
   for(l=0;l<7;l++)
   EEPROM.write(l,'\0');
   delay(1000);
  MyObject  cal_data = {sum1 };
  EEPROM.put(0, cal_data);
  Serial.println("calibration done");
  delay(1000);
  c_data = sum1;
}
void lvdt()  // LVDT Module
{
  val = analogRead(4); // read the input pin
  delay(1000);
  Serial.println("Deformation (mm)");
  val2=val/30.00;
  val1=map(val2,3,25,0,25);
  Serial.println(val1);  // debug value
  delay(1000);
}
```

Flow Chart for WISMS Software Code

```
                    ┌──────────┐
                    │  Start   │
                    └──────────┘
                         │
                         ▼
              ╱───────────────────────╲
             ╱  Setup and Inialize the ╲
             ╲  WISMS Software         ╱
              ╲───────────────────────╱
                         │
                         ▼
                    ◇ Is
         NO ←────── Connection
                    Established ◇
                         │ YES
                         ▼
              ┌───────────────────────┐
              │ Call-LVDT module      │
              │                       │
              │ Call-Strain Gauge module │
              └───────────────────────┘
                         │
                         ▼
                    ◇ Is data
                    received ◇ ──── NO
                         │ YES
                         ▼
              ┌───────────────────────┐
              │ Call-Analg-to-Digital Converter │
              └───────────────────────┘
                         │
                         ▼
              ╱───────────────────────╲
             ╱  Display Data           ╱
              ╲───────────────────────╱
                         │
                         ▼
                    ┌──────────┐
                    │  Stop    │
                    └──────────┘
```
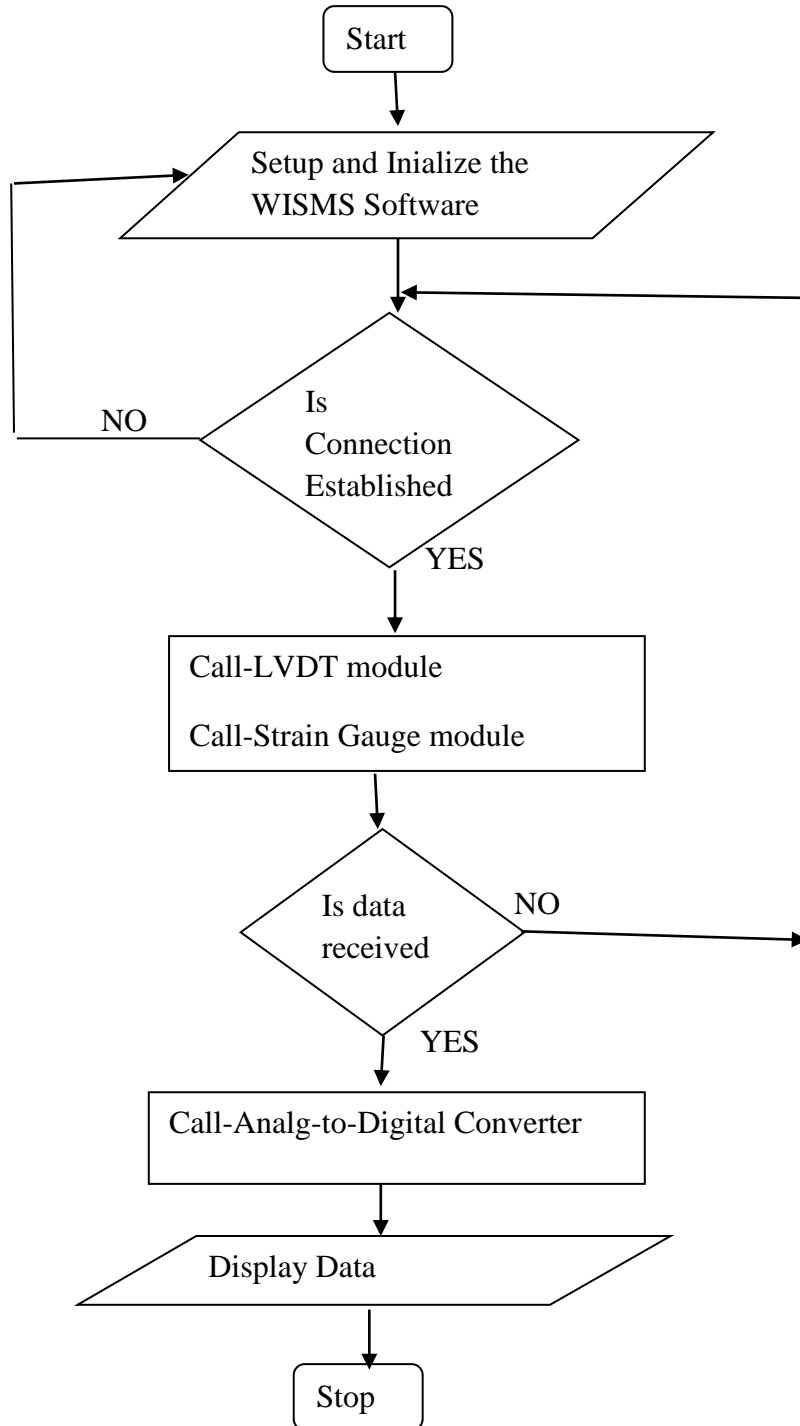
APPENDIX – II

DATA RELATED TO THE NUMERICAL MODELING

Table II.1 Variation in directional deformation at points 'P' and 'R' of gallery-1 for gallery width of 3.0m

Partition thickness(m)	Pillar width(m)	Deformation (mm) at different gallery height (m) and gallery width=3.0m											
		Roof center of gallery 1 (Point P)						Surface center of gallery1 (Point R)					
		2.4	2.6	2.8	3.0	3.2	3.4	2.4	2.6	2.8	3.0	3.2	3.4
4	22.5	1.52	1.56	1.60	1.64	1.68	1.72	1.85	1.89	1.93	1.97	2.01	2.05
	23.5	1.44	1.48	1.52	1.56	1.60	1.64	1.77	1.81	1.85	1.89	1.93	1.97
	24.5	1.36	1.40	1.44	1.48	1.52	1.56	1.69	1.73	1.77	1.81	1.85	1.89
6	22.5	1.21	1.25	1.29	1.33	1.37	1.41	1.54	1.58	1.62	1.66	1.70	1.74
	23.5	1.13	1.17	1.21	1.25	1.29	1.33	1.46	1.50	1.54	1.58	1.62	1.66
	24.5	1.05	1.09	1.13	1.17	1.21	1.25	1.38	1.42	1.46	1.50	1.54	1.58
8	22.5	1.09	1.13	1.17	1.21	1.25	1.29	1.42	1.46	1.50	1.54	1.58	1.62
	23.5	1.01	1.05	1.09	1.13	1.17	1.21	1.34	1.38	1.42	1.46	1.50	1.54
	24.5	0.93	0.97	1.01	1.05	1.09	1.13	1.26	1.30	1.34	1.38	1.42	1.46
10	22.5	1.01	1.05	1.09	1.13	1.17	1.21	1.34	1.38	1.42	1.46	1.50	1.54
	23.5	0.93	0.97	1.01	1.05	1.09	1.13	1.26	1.30	1.34	1.38	1.42	1.46
	24.5	0.85	0.89	0.93	0.97	1.01	1.05	1.18	1.22	1.26	1.30	1.34	1.38
12	22.5	0.97	1.01	1.05	1.09	1.13	1.17	1.30	1.34	1.38	1.42	1.46	1.50
	23.5	0.89	0.93	0.97	1.01	1.05	1.09	1.22	1.26	1.30	1.34	1.38	1.42
	24.5	0.81	0.85	0.89	0.93	0.97	1.01	1.14	1.18	1.22	1.26	1.30	1.34

Table II.2 Variation in directional deformation at points 'P' and 'R' of gallery-1 for gallery width of 3.6m

Partition thickness(m)	Pillar width(m)	Deformation (mm) at different gallery height (m) and gallery width=3.6m											
		Roof center of gallery 1 (Point P)						Surface center of gallery1 (Point R)					
		2.4	2.6	2.8	3.0	3.2	3.4	2.4	2.6	2.8	3.0	3.2	3.4
4	25.5	1.78	1.82	1.86	1.90	1.94	1.98	2.10	2.14	2.18	2.22	2.26	2.30
	26.5	1.70	1.74	1.78	1.82	1.86	1.90	2.02	2.06	2.10	2.14	2.18	2.22
	27.5	1.62	1.66	1.70	1.74	1.78	1.82	1.94	1.98	2.02	2.06	2.10	2.14
6	25.5	1.47	1.51	1.55	1.59	1.63	1.67	1.79	1.83	1.87	1.91	1.95	1.99
	26.5	1.39	1.43	1.47	1.51	1.55	1.59	1.71	1.75	1.79	1.83	1.87	1.91
	27.5	1.31	1.35	1.39	1.43	1.47	1.51	1.63	1.67	1.71	1.75	1.79	1.83
8	25.5	1.35	1.39	1.43	1.47	1.51	1.55	1.67	1.71	1.75	1.79	1.83	1.87
	26.5	1.27	1.31	1.35	1.39	1.43	1.47	1.59	1.63	1.67	1.71	1.75	1.79
	27.5	1.19	1.23	1.27	1.31	1.35	1.39	1.51	1.55	1.59	1.63	1.67	1.71
10	25.5	1.27	1.31	1.35	1.39	1.43	1.47	1.59	1.63	1.67	1.71	1.75	1.79
	26.5	1.19	1.23	1.27	1.31	1.35	1.39	1.51	1.55	1.59	1.63	1.67	1.71
	27.5	1.11	1.15	1.19	1.23	1.27	1.31	1.43	1.47	1.51	1.55	1.59	1.63
12	25.5	1.23	1.27	1.31	1.35	1.39	1.43	1.55	1.59	1.63	1.67	1.71	1.75
	26.5	1.15	1.19	1.23	1.27	1.31	1.35	1.47	1.51	1.55	1.59	1.63	1.67
	27.5	1.07	1.11	1.15	1.19	1.23	1.27	1.39	1.43	1.47	1.51	1.55	1.59

Table II.3 Variation in directional deformation at points 'P' and 'R' of gallery-1 for gallery width of 4.2m

Partition thickness(m)	Pillar width(m)	Deformation (mm) at different gallery height (m) and gallery width=4.2m											
		Roof center of gallery 1 (Point P)						Surface center of gallery1 (Point R)					
		2.4	2.6	2.8	3.0	3.2	3.4	2.4	2.6	2.8	3.0	3.2	3.4
4	30.5	2.12	2.16	2.20	2.24	2.28	2.32	2.45	2.49	2.53	2.57	2.61	2.65
	31.5	2.04	2.08	2.12	2.16	2.20	2.24	2.37	2.41	2.45	2.49	2.53	2.57
	32.5	1.96	2.00	2.04	2.08	2.12	2.16	2.29	2.33	2.37	2.41	2.45	2.49
6	30.5	1.81	1.85	1.89	1.93	1.97	2.01	2.14	2.18	2.22	2.26	2.30	2.34
	31.5	1.73	1.77	1.81	1.85	1.89	1.93	2.06	2.10	2.14	2.18	2.22	2.26
	32.5	1.65	1.69	1.73	1.77	1.81	1.85	1.98	2.02	2.06	2.10	2.14	2.18
8	30.5	1.69	1.73	1.77	1.81	1.85	1.89	2.02	2.06	2.10	2.14	2.18	2.22
	31.5	1.61	1.65	1.69	1.73	1.77	1.81	1.94	1.98	2.02	2.06	2.10	2.14
	32.5	1.53	1.57	1.61	1.65	1.69	1.73	1.86	1.90	1.94	1.98	2.02	2.06
10	30.5	1.61	1.65	1.69	1.73	1.77	1.81	1.94	1.98	2.02	2.06	2.10	2.14
	31.5	1.53	1.57	1.61	1.65	1.69	1.73	1.86	1.90	1.94	1.98	2.02	2.06
	32.5	1.45	1.49	1.53	1.57	1.61	1.65	1.78	1.82	1.86	1.90	1.94	1.98
12	30.5	1.57	1.61	1.65	1.69	1.73	1.77	1.90	1.94	1.98	2.02	2.06	2.10
	31.5	1.49	1.53	1.57	1.61	1.65	1.69	1.82	1.86	1.90	1.94	1.98	2.02
	32.5	1.41	1.45	1.49	1.53	1.57	1.61	1.74	1.78	1.82	1.86	1.90	1.94

Table II.4 Variation in directional deformation at points 'P' and 'R' of gallery-1 for gallery width of 4.8m

Partition thickness(m)	Pillar width(m)	Deformation (mm) at different gallery height (m) and gallery width=4.8m											
		Roof center of gallery 1 (Point P)						Surface center of gallery1 (Point R)					
		2.4	2.6	2.8	3.0	3.2	3.4	2.4	2.6	2.8	3.0	3.2	3.4
4	34.5	2.30	2.34	2.38	2.42	2.46	2.50	2.65	2.69	2.73	2.77	2.81	2.85
	35.5	2.22	2.26	2.30	2.34	2.38	2.42	2.57	2.61	2.65	2.69	2.73	2.77
	36.5	2.14	2.18	2.22	2.26	2.30	2.34	2.49	2.53	2.57	2.61	2.65	2.69
6	34.5	1.99	2.03	2.07	2.11	2.15	2.19	2.34	2.38	2.42	2.46	2.50	2.54
	35.5	1.91	1.95	1.99	2.03	2.07	2.11	2.26	2.30	2.34	2.38	2.42	2.46
	36.5	1.83	1.87	1.91	1.95	1.99	2.03	2.18	2.22	2.26	2.30	2.34	2.38
8	34.5	1.87	1.91	1.95	1.99	2.03	2.07	2.22	2.26	2.30	2.34	2.38	2.42
	35.5	1.79	1.83	1.87	1.91	1.95	1.99	2.14	2.18	2.22	2.26	2.30	2.34
	36.5	1.71	1.75	1.79	1.83	1.87	1.91	2.06	2.10	2.14	2.18	2.22	2.26
10	34.5	1.79	1.83	1.87	1.91	1.95	1.99	2.14	2.18	2.22	2.26	2.30	2.34
	35.5	1.71	1.75	1.79	1.83	1.87	1.91	2.06	2.10	2.14	2.18	2.22	2.26
	36.5	1.63	1.67	1.71	1.75	1.79	1.83	1.98	2.02	2.06	2.10	2.14	2.18
12	34.5	1.75	1.79	1.83	1.87	1.91	1.95	2.10	2.14	2.18	2.22	2.26	2.30
	35.5	1.67	1.71	1.75	1.79	1.83	1.87	2.02	2.06	2.10	2.14	2.18	2.22
	36.5	1.59	1.63	1.67	1.71	1.75	1.79	1.94	1.98	2.02	2.06	2.10	2.14

APPENDIX – III

OUTPUTS RELATED TO THE NUMERICAL SIMULATION RESULTS
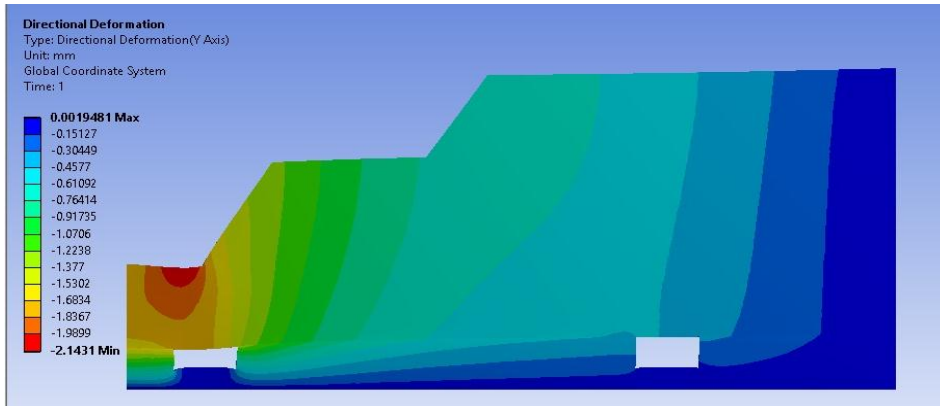
Fig. III-1 Variation of vertical deformation for galley height of 2.4m

Fig. III-2 Variation of vertical deformation for galley height of 2.6m

Fig. III-3 Variation of vertical deformation for galley height of 2.8m
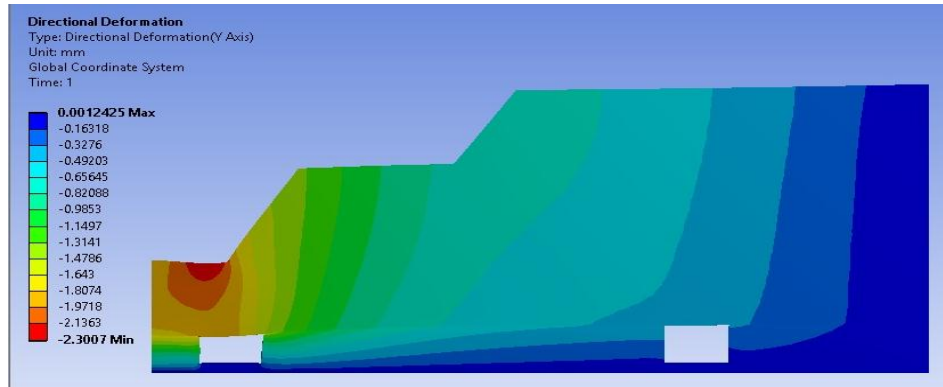
Fig. III-4 Variation of vertical deformation for galley height of 3.0m
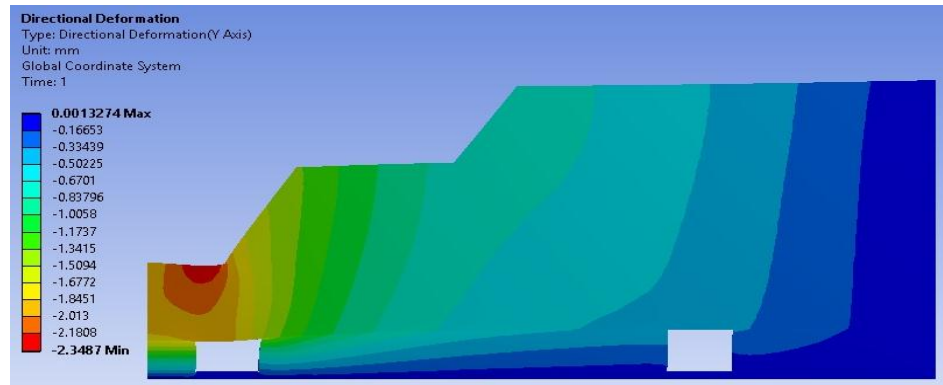
Fig. III-5 Variation of vertical deformation for galley height of 3.2m

Fig. III-6 Variation of vertical deformation for galley height of 3.4m

Fig. III-7 Variation of vertical deformation for pillar width of 30.5m

Fig. III-8 Variation of vertical deformation for pillar width of 31.5m
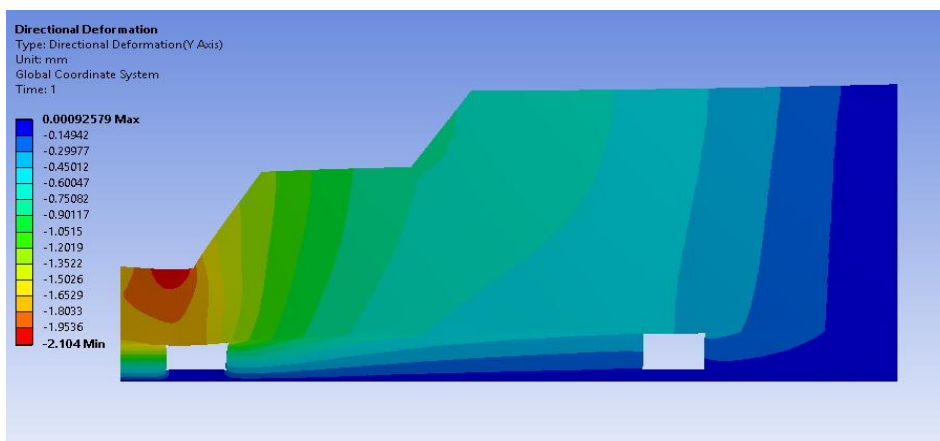
Fig. III-9 Variation of vertical deformation for pillar width of 32.5m
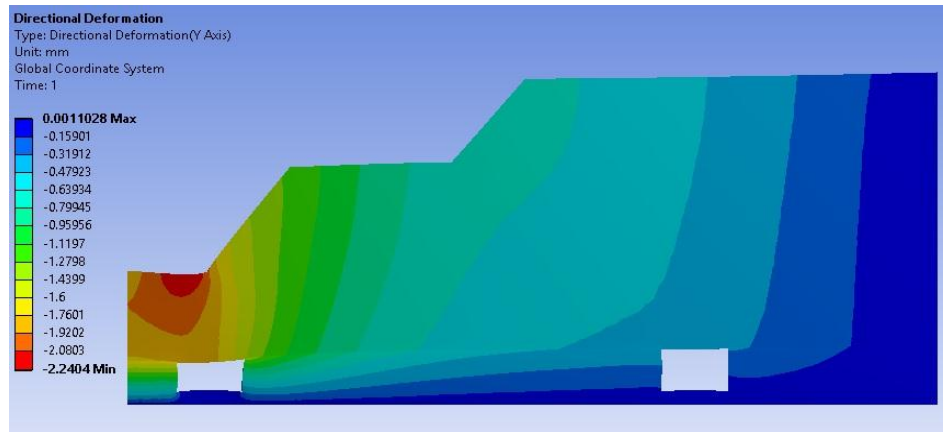
Fig. III-10 Variation of vertical deformation for slope angle of 50°
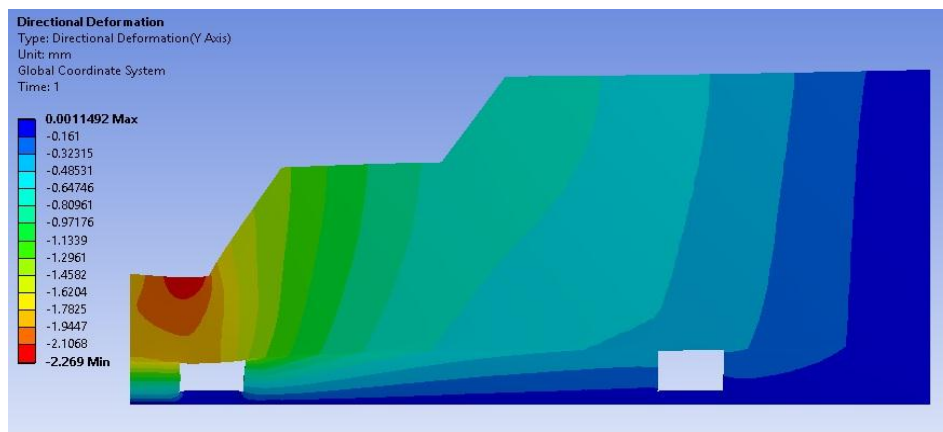
Fig. III-11 Variation of vertical deformation for slope angle of 55°
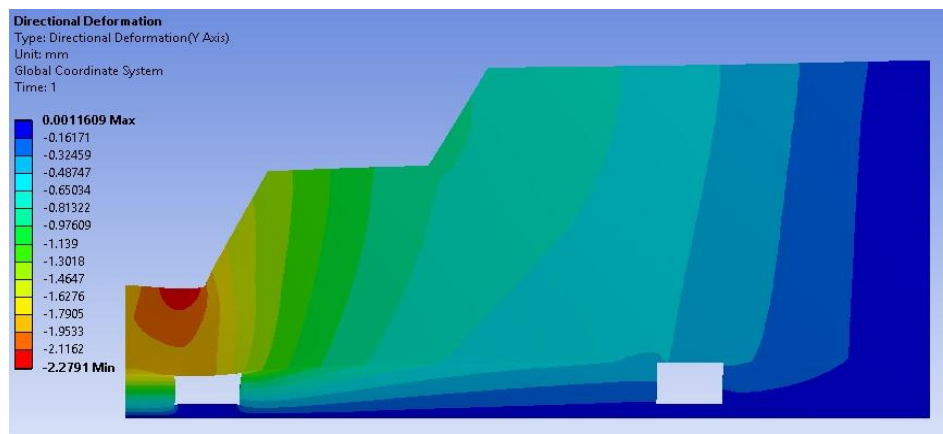
Fig. III-12 Variation of vertical deformation for slope angle of 60°
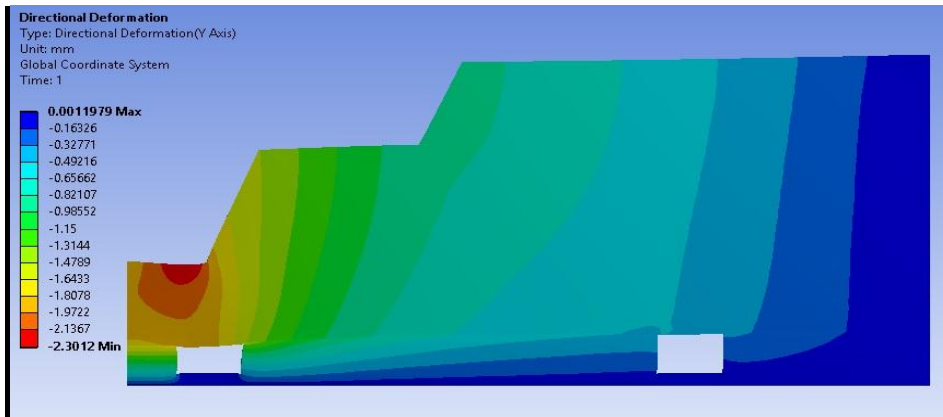
Fig. III-13 Variation of vertical deformation for slope angle of 65º
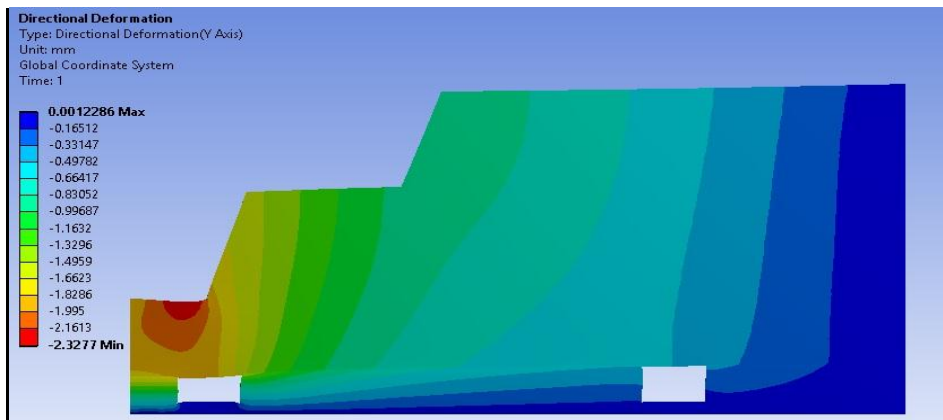
Fig. III-14 Variation of vertical deformation for slope angle of 70º
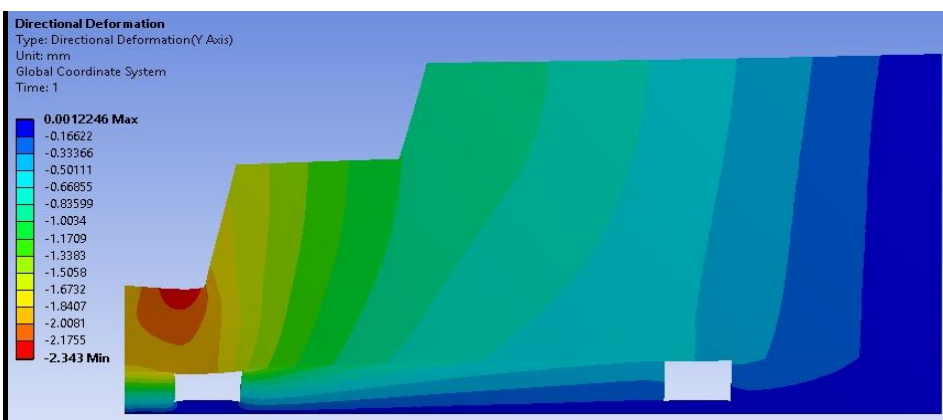
Fig. III-15 Variation of vertical deformation for slope angle of 75º
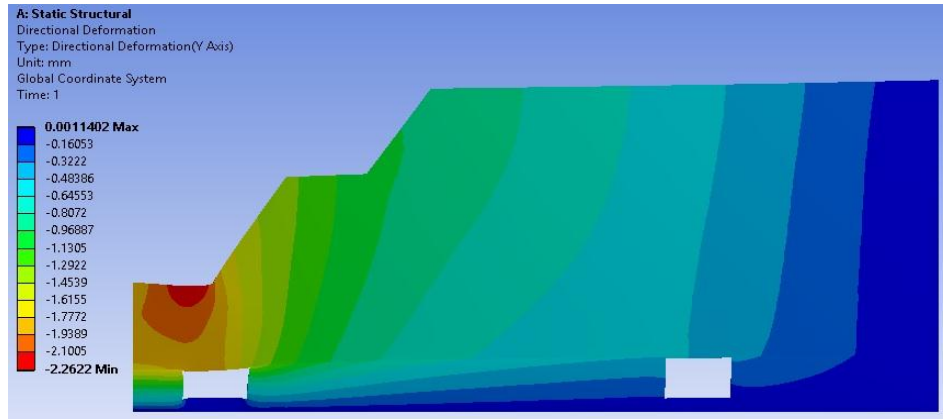
Fig. III-16 Variation of vertical deformation for berm width of 5m
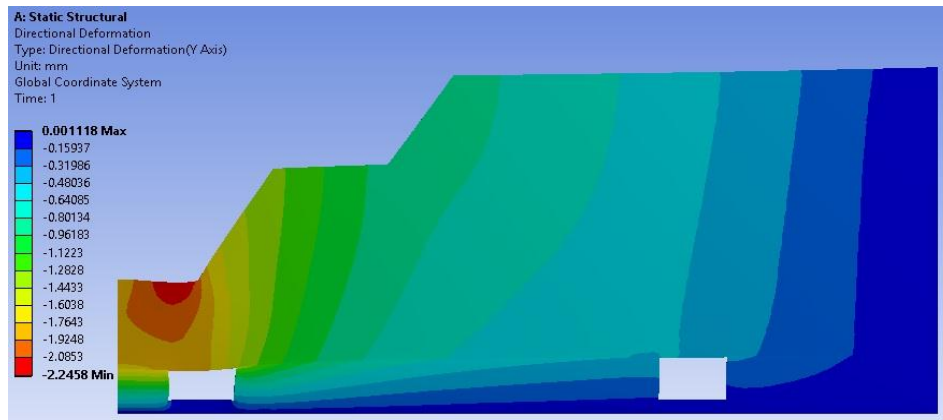
Fig. II-17 Variation of vertical deformation for berm width of 6m
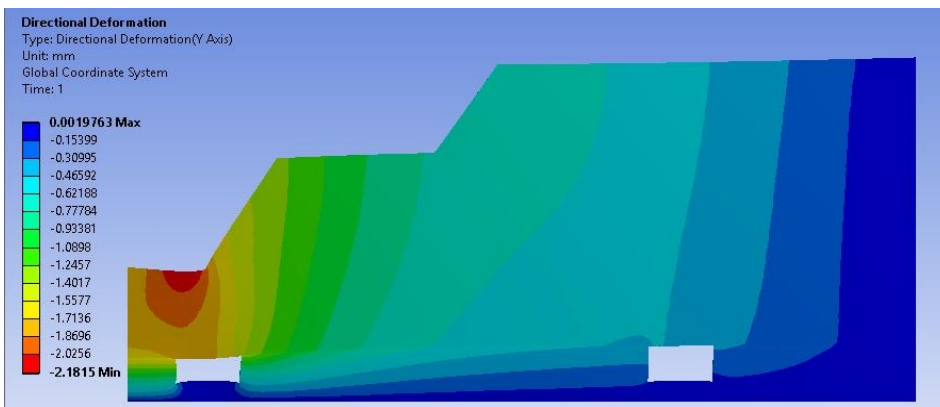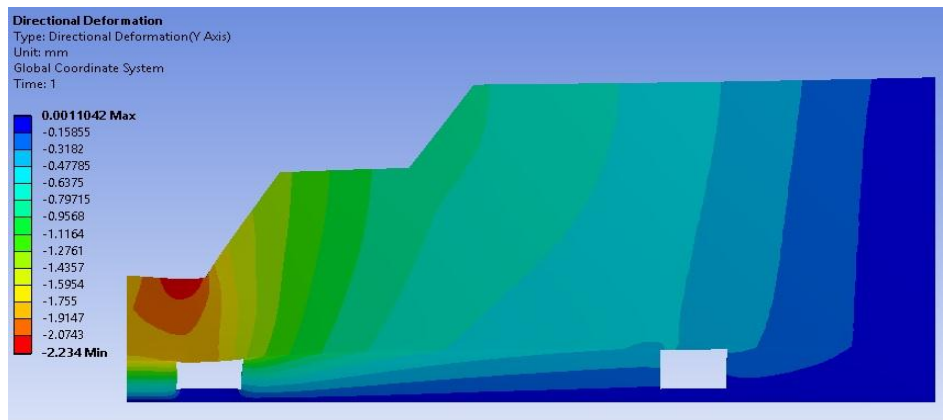

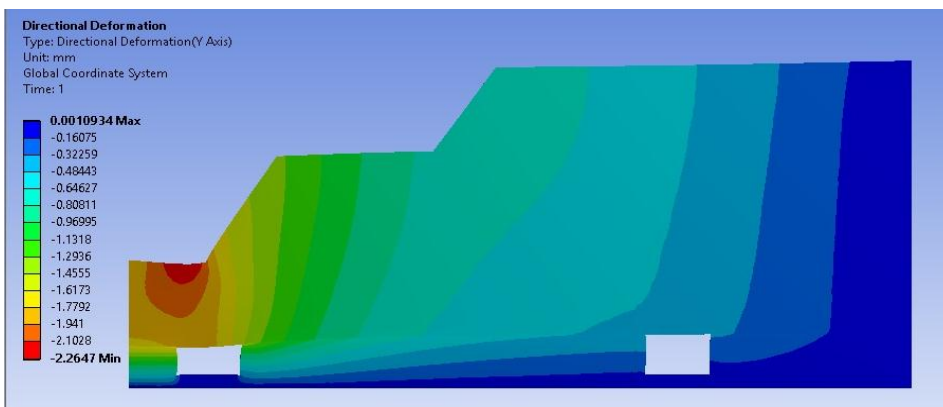Fig. III-18 Variation of vertical deformation for berm width of 7m
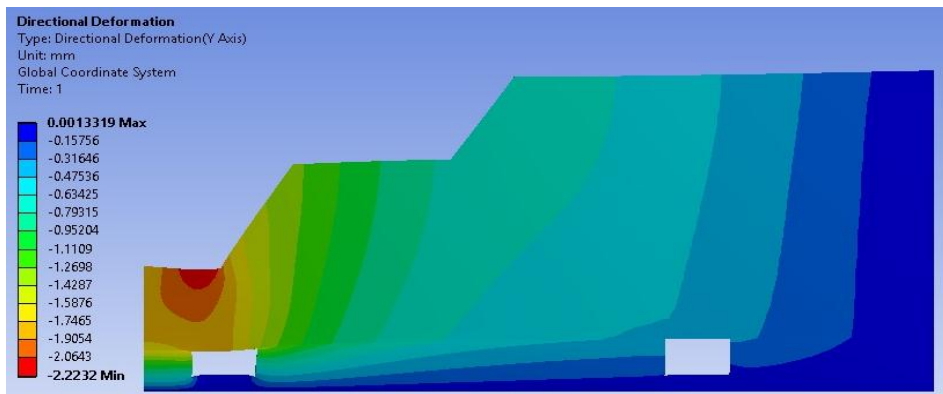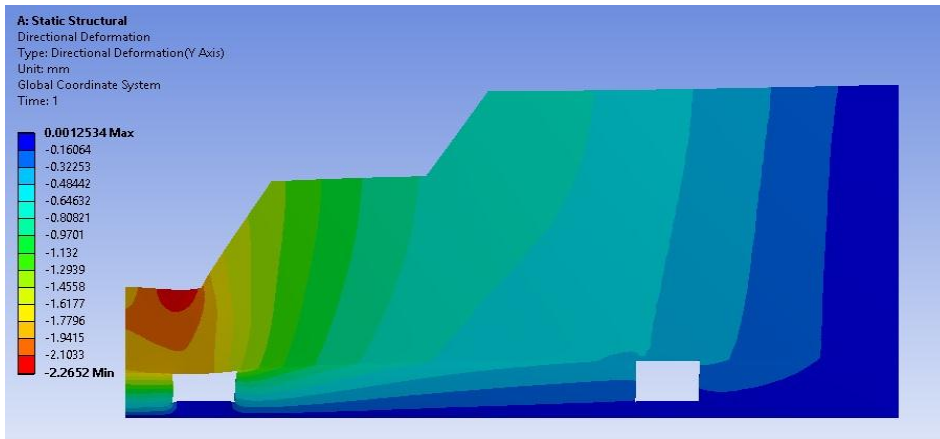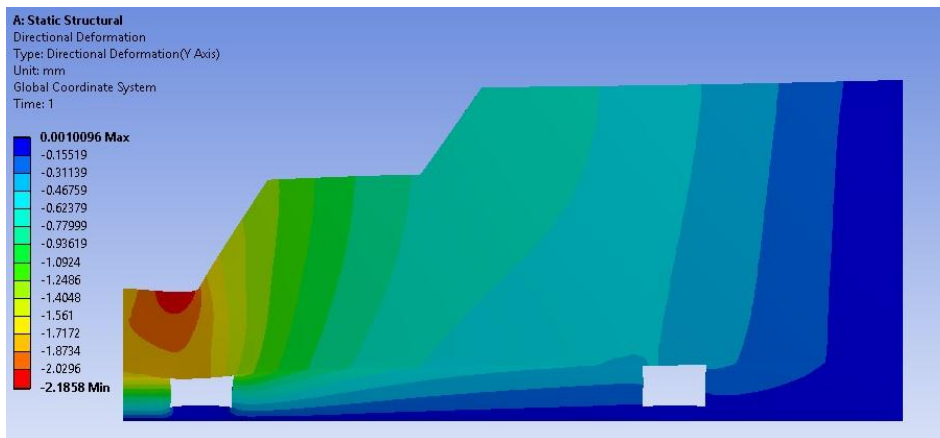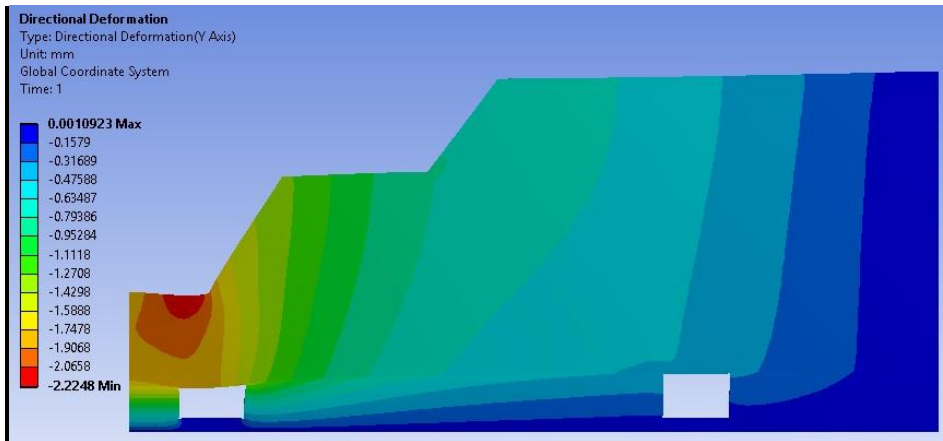
Fig. III-19 Variation of vertical deformation for berm width of 8m
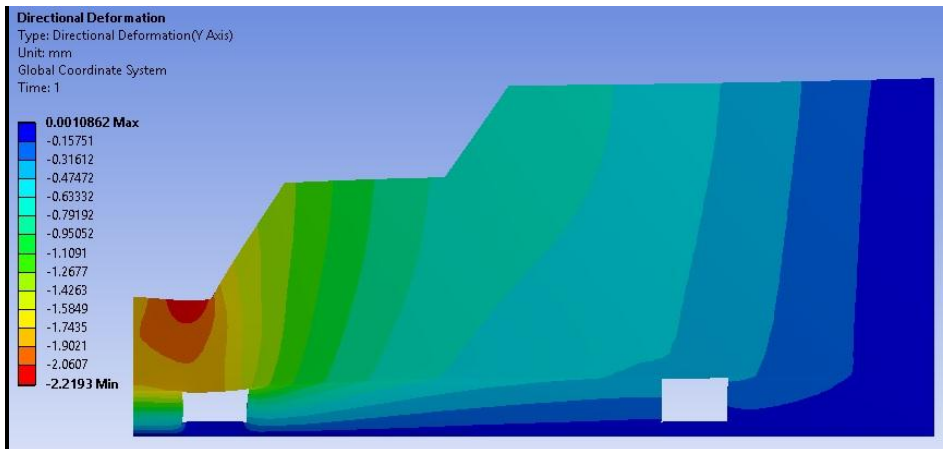
Fig. III-20 Variation of vertical deformation for berm width of 9m
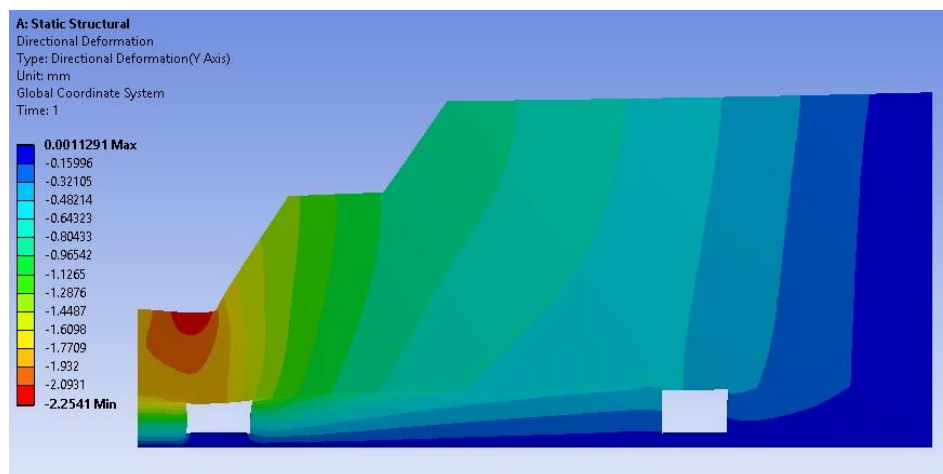
Fig. III-21 Variation of vertical deformation for berm width of 10m

# APPENDIX – IV

SOURCE CODE OF DESIGN GUIDELINES

SOFTWARE PACKAGE

VISUAL BASIC CODE WAS USED FOR DEVELOPMENT OF SOFTWARE

#LOGIN MODULE

```vb
Public Class login

    Private Sub Button1_Click(ByVal sender As System.Object, ByVal e As
System.EventArgs) Handles Button1.Click
        If TextBox1.Text = My.Settings.Username And TextBox2.Text =
My.Settings.Password Then
            mainmenu.Show()
            Me.Hide()
        Else
            MessageBox.Show("Enter Valid User Name and Password")
        End If
    End Sub
    Private Sub Button2_Click(ByVal sender As System.Object, ByVal e As
System.EventArgs) Handles Button2.Click
        TextBox1.Text = ""
        TextBox2.Text = ""
    End Sub

    Private Sub LinkLabel1_LinkClicked(ByVal sender As System.Object,
ByVal e As System.Windows.Forms.LinkLabelLinkClickedEventArgs) Handles
LinkLabel1.LinkClicked
        Form1.Show()
        Me.Hide()
    End Sub
End Class

Public Class Form1

    Private Sub Button1_Click(ByVal sender As System.Object, ByVal e As
System.EventArgs) Handles Button1.Click
        My.Settings.Username = TextBox1.Text
        My.Settings.Password = TextBox2.Text
        My.Settings.Save()
        MsgBox("Registration successful")
        login.Show()
        Me.Hide()

    End Sub

    Private Sub Button2_Click(ByVal sender As System.Object, ByVal e As
System.EventArgs) Handles Button2.Click
        TextBox1.Text = ""
        TextBox2.Text = ""

    End Sub
End Class
```

191

#MAIN MENU MODULE

```vb
Public Class mainmenu
    Private Sub AboutToolStripMenuItem1_Click(ByVal sender As
System.Object, ByVal e As System.EventArgs) Handles
AboutToolStripMenuItem1.Click
        login.Show()
        Me.Dispose()
    End Sub

    Private Sub AboutToolStripMenuItem_Click(ByVal sender As
System.Object, ByVal e As System.EventArgs) Handles
AboutToolStripMenuItem.Click
        about.show()
        Me.Hide()
    End Sub

    Private Sub Button1_Click(ByVal sender As System.Object, ByVal e As
System.EventArgs) Handles Button1.Click
        FOS.Show() ''call module FoS
        Me.Dispose()
    End Sub

    Private Sub Button2_Click(ByVal sender As System.Object, ByVal e As
System.EventArgs) Handles Button2.Click
        OPT.Show() ''call module Partition thickness
        Me.Dispose()
    End Sub

    Private Sub Button3_Click(ByVal sender As System.Object, ByVal e As
System.EventArgs) Handles Button3.Click
        OSA.Show() ''call module slope angle
        Me.Dispose()
    End Sub

    Private Sub HEMMToolStripMenuItem_Click(ByVal sender As
System.Object, ByVal e As System.EventArgs) Handles
HEMMToolStripMenuItem.Click
        HEMM.Show()
    End Sub
End Class

Public Class About

    Private Sub Button2_Click(ByVal sender As System.Object, ByVal e As
System.EventArgs) Handles Button2.Click
        mainmenu.Show()
        Me.Hide()
    End Sub
```

```vb
    Private Sub About_Load(ByVal sender As System.Object, ByVal e As
System.EventArgs) Handles MyBase.Load
        Label1.Text = "Copy Right © 2018, NITK Surathkal. All Rights
Reserved."
    End Sub
End Class


Public Class HEMM

    Private Sub HEMM_Load(ByVal sender As System.Object, ByVal e As
System.EventArgs) Handles MyBase.Load

    End Sub

    Private Sub Button1_Click(ByVal sender As System.Object, ByVal e As
System.EventArgs) Handles Button1.Click
        Me.Dispose()
    End Sub
End Class
```

#PARTITION THICKNESS MODULE

```vb
Imports System.Math
Public Class OPT
    Dim GW As Decimal
    Dim GH As Decimal
    Dim PW As Decimal
    Dim BW As Decimal
    Dim PT As Decimal
    Dim SA As Decimal
    Dim FOS As Decimal
    Dim DS As Integer
    Dim DC As Integer
    Dim UCSS As Integer
    Dim UCSC As Integer
    Dim EL As Integer

    Private Sub OPT_Load(ByVal sender As System.Object, ByVal e As
System.EventArgs) Handles MyBase.Load
        Me.ComboBox1.Text = "select"
        Me.ComboBox2.Text = "select"
        Me.ComboBox3.Text = "select"


    End Sub
    Private Sub ComboBox1_SelectedIndexChanged(ByVal sender As
System.Object, ByVal e As System.EventArgs) Handles
ComboBox1.SelectedIndexChanged
        If ComboBox1.SelectedItem = "3.0" Then
            Me.ComboBox2.Text = "select"
            ComboBox2.Items.Clear()
            ComboBox2.Items.Add("22.5")
            ComboBox2.Items.Add("23.5")
```

193

```vb
            ComboBox2.Items.Add("24.5")

        ElseIf ComboBox1.SelectedItem = "3.6" Then
            Me.ComboBox2.Text = "select"
            ComboBox2.Items.Clear()
            ComboBox2.Items.Add("25.5")
            ComboBox2.Items.Add("26.5")
            ComboBox2.Items.Add("27.5")
        ElseIf ComboBox1.SelectedItem = "4.2" Then
            Me.ComboBox2.Text = "select"
            ComboBox2.Items.Clear()
            ComboBox2.Items.Add("30.5")
            ComboBox2.Items.Add("31.5")
            ComboBox2.Items.Add("32.5")

        ElseIf ComboBox1.SelectedItem = "4.8" Then
            Me.ComboBox2.Text = "select"
            ComboBox2.Items.Clear()
            ComboBox2.Items.Add("34.5")
            ComboBox2.Items.Add("35.5")
            ComboBox2.Items.Add("36.5")
        End If

    End Sub
    Private Sub Button1_Click(ByVal sender As System.Object, ByVal e As
System.EventArgs) Handles Button1.Click

        GW = Val(ComboBox1.Text)
        PW = Val(ComboBox2.Text)
        GH = Val(ComboBox3.Text)
        BW = Val(TextBox7.Text)
        SA = Val(TextBox1.Text)
        FOS = Val(TextBox2.Text)
        DS = Val(TextBox3.Text)
        UCSS = Val(TextBox4.Text)
        DC = Val(TextBox5.Text)
        UCSC = Val(TextBox6.Text)
        EL = Val(TextBox10.Text)


        If (BW > 10) Or (BW < 5) Then
            MsgBox("Enter berm width in given range")
            TextBox7.Text = ""
        ElseIf (SA > 75) Or (SA < 50) Then
            MsgBox("Enter slope angle in given range")
            TextBox1.Text = ""
        ElseIf (FOS > 2.5) Or (FOS < 1.3) Then
            MsgBox("Enter FOS in given range")
            TextBox2.Text = ""
        ElseIf (DS > 2500 Or DS < 2100) Then
            MsgBox("Enter density of sandstone in given range")
            TextBox3.Text = ""
        ElseIf (UCSS > 100 Or UCSS < 25) Then
```

194

```
            MsgBox("Enter Compressive strength of sandstone in given
                    range")
            TextBox4.Text = ""
        ElseIf (DC > 1500 Or DC < 1100) Then
            MsgBox("Enter density of coal in given range")
            TextBox5.Text = ""
        ElseIf (UCSC > 45 Or UCSC < 15) Then
            MsgBox("Enter Compressive strength of coal in given range")
            TextBox6.Text = ""

        ElseIf (EL >= 600) Then
            MsgBox("Load is too high")
            TextBox10.Text = ""
        ElseIf (EL < 250) Then
            MsgBox("Load is too low")
            TextBox10.Text = ""

        End If


    End Sub

    Public Sub PTCall()

        Dim x1 As Double
        Dim i As Double = 1.5
        ''Dim i1 As Double

        If GW = "3.0" Then

            x1 = ((1.5) - (1.314 - (0.1099 * GH) + (0.01099 * PW) +
(0.005 * BW) - (0.00162 * SA))) / (0.065)

            End If

        ElseIf GW = "3.6" Then

            x1 = ((1.5) - (1.272 - (0.1099 * GH) + (0.01099 * PW) +
(0.005 * BW) - (0.00162 * SA))) / (0.065)
            ''MsgBox(x1)

            ElseIf GW = "4.2" Then

            x1 = ((1.5) - (1.121 - (0.1099 * GH) + (0.01099 * PW) +
(0.005 * BW) - (0.00162 * SA))) / (0.065)


        ElseIf GW = "4.8" Then

            x1 = ((1.5) - (1.061 - (0.1099 * GH) + (0.01099 * PW) +
(0.005 * BW) - (0.00162 * SA))) / (0.065)

            Else
            PT = "Please enter valid input"
```

195

```vb
        End If

        PT = Math.Round(PT, 2)
        Label7.Text = ":" + Convert.ToString(PT)


    End Sub
    Private Sub Button2_Click(ByVal sender As System.Object, ByVal e As
System.EventArgs) Handles Button2.Click
        mainmenu.Show()
        Me.Hide()
    End Sub

    Private Sub Button3_Click(ByVal sender As System.Object, ByVal e As
System.EventArgs) Handles Button3.Click
        clear()
    End Sub
    Public Sub clear()
        Me.ComboBox1.Text = "select"
        Me.ComboBox2.Text = "select"
        Me.ComboBox3.Text = "select"

        TextBox1.Text = ""
        TextBox2.Text = ""
        TextBox3.Text = ""
        TextBox4.Text = ""
        TextBox5.Text = ""
        TextBox6.Text = ""
        TextBox7.Text = ""
        TextBox10.Text = ""
        Label7.Text = ":"
    End Sub

    Private Sub Button6_Click(ByVal sender As System.Object, ByVal e As
System.EventArgs) Handles Button6.Click
        PTReport.Show()
    End Sub

    Private Sub LinkLabel1_LinkClicked(ByVal sender As System.Object,
ByVal e As System.Windows.Forms.LinkLabelLinkClickedEventArgs) Handles
LinkLabel1.LinkClicked
        HEMM.Show()
    End Sub

End Class
```

PARTITION THICKNESS REPORT

```vb
Public Class PTReport
    Dim GW As Decimal
    Dim GH As Decimal
    Dim PW As Decimal
    Dim BW As Decimal
    Dim PT As Decimal
```

```vb
    Dim SA As Decimal
    Dim FOS As Decimal
    Dim DS As Integer
    Dim DC As Integer
    Dim UCSS As Integer
    Dim UCSC As Integer
    Dim EL As Integer
    Private Sub Report_Load(ByVal sender As System.Object, ByVal e As
System.EventArgs) Handles MyBase.Load

        GW = Val(OPT.ComboBox1.SelectedItem())
        PW = Val(OPT.ComboBox2.SelectedItem())
        BW = Val(OPT.TextBox7.Text)
        FOS = Val(OPT.TextBox2.Text)

        DS = Val(OPT.TextBox3.Text)
        UCSS = Val(OPT.TextBox4.Text)
        DC = Val(OPT.TextBox5.Text)
        UCSC = Val(OPT.TextBox6.Text)
        EL = Val(OPT.TextBox10.Text)

        Label15.Text = Label15.Text + "" + Convert.ToString(GW)
        Label16.Text = Label16.Text + "" + Convert.ToString(PW)
        Label17.Text = Label17.Text + "" + Convert.ToString(BW)
        Label34.Text = Label34.Text + "" + Convert.ToString(FOS)

        Label18.Text = Label18.Text + "" + Convert.ToString(EL)
        Label26.Text = Label26.Text + "" + Convert.ToString(DS)
        Label27.Text = Label27.Text + "" + Convert.ToString(UCSS)
        Label28.Text = Label28.Text + "" + Convert.ToString(DC)
        Label29.Text = Label29.Text + "" + Convert.ToString(UCSC)

        Timer1.Enabled = True

    End Sub
    Private Sub Button1_Click(ByVal sender As System.Object, ByVal e As
System.EventArgs) Handles Button1.Click
        GW = Val(OPT.ComboBox1.SelectedItem())
        PW = Val(OPT.ComboBox2.SelectedItem())
        BW = Val(OPT.TextBox7.Text)
        FOS = Val(OPT.TextBox2.Text)

        DS = Val(OPT.TextBox3.Text)
        UCSS = Val(OPT.TextBox4.Text)
        DC = Val(OPT.TextBox5.Text)
        UCSC = Val(OPT.TextBox6.Text)
        EL = Val(OPT.TextBox10.Text)

        If (EL >= 550) And (EL < 600) Then
            FOS = FOS + 0.33
            rockcallss()
            rockcallcl()
            Dim GH1() As Double = {2.4, 2.6, 2.8, 3.0, 3.2, 3.4}
            Dim SA1() As Double = {50, 55, 60, 65, 70, 75}
```

197

```vb
    Dim GH11 As Double
    Dim SA11 As Double

    For Each GH11 In GH1
        For Each SA11 In SA1
            report1(GH11, SA11)
        Next
        ListView1.Items.Add(Environment.NewLine)
    Next
ElseIf EL >= 500 Then
    FOS = FOS + 0.31
    rockcallss()
    rockcallcl()
    Dim GH1() As Double = {2.4, 2.6, 2.8, 3.0, 3.2, 3.4}
    Dim SA1() As Double = {50, 55, 60, 65, 70, 75}
    Dim GH11 As Double
    Dim SA11 As Double

    For Each GH11 In GH1
        For Each SA11 In SA1
            report1(GH11, SA11)
        Next
        ListView1.Items.Add(Environment.NewLine)
    Next
ElseIf EL >= 460 Then
    FOS = FOS + 0.28
    rockcallss()
    rockcallcl()
    Dim GH1() As Double = {2.4, 2.6, 2.8, 3.0, 3.2, 3.4}
    Dim SA1() As Double = {50, 55, 60, 65, 70, 75}
    Dim GH11 As Double
    Dim SA11 As Double

    For Each GH11 In GH1
        For Each SA11 In SA1
            report1(GH11, SA11)
        Next
        ListView1.Items.Add(Environment.NewLine)
    Next
ElseIf EL >= 430 Then
    FOS = FOS + 0.22
    rockcallss()
    rockcallcl()
    Dim GH1() As Double = {2.4, 2.6, 2.8, 3.0, 3.2, 3.4}
    Dim SA1() As Double = {50, 55, 60, 65, 70, 75}
    Dim GH11 As Double
    Dim SA11 As Double

    For Each GH11 In GH1
        For Each SA11 In SA1
            report1(GH11, SA11)
        Next
        ListView1.Items.Add(Environment.NewLine)
    Next
```

198

```vb
ElseIf EL >= 410 Then
    FOS = FOS + 0.18
    rockcallss()
    rockcallcl()
    Dim GH1() As Double = {2.4, 2.6, 2.8, 3.0, 3.2, 3.4}
    Dim SA1() As Double = {50, 55, 60, 65, 70, 75}
    Dim GH11 As Double
    Dim SA11 As Double

    For Each GH11 In GH1
        For Each SA11 In SA1
            report1(GH11, SA11)
        Next
        ListView1.Items.Add(Environment.NewLine)
    Next
ElseIf EL >= 380 Then
    FOS = FOS + 0.15
    ''MsgBox(FOS)
    rockcallss()
    rockcallcl()
    Dim GH1() As Double = {2.4, 2.6, 2.8, 3.0, 3.2, 3.4}
    Dim SA1() As Double = {50, 55, 60, 65, 70, 75}
    Dim GH11 As Double
    Dim SA11 As Double

    For Each GH11 In GH1
        For Each SA11 In SA1
            report1(GH11, SA11)
        Next
        ListView1.Items.Add(Environment.NewLine)
    Next
ElseIf EL >= 350 Then
    ''MsgBox(FOS)
    rockcallss()
    rockcallcl()
    Dim GH1() As Double = {2.4, 2.6, 2.8, 3.0, 3.2, 3.4}
    Dim SA1() As Double = {50, 55, 60, 65, 70, 75}
    Dim GH11 As Double
    Dim SA11 As Double

    For Each GH11 In GH1
        For Each SA11 In SA1
            report1(GH11, SA11)
        Next
        ListView1.Items.Add(Environment.NewLine)
    Next
ElseIf EL >= 320 Then
    FOS = FOS - 0.1
    rockcallss()
    rockcallcl()
    Dim GH1() As Double = {2.4, 2.6, 2.8, 3.0, 3.2, 3.4}
    Dim SA1() As Double = {50, 55, 60, 65, 70, 75}
    Dim GH11 As Double
    Dim SA11 As Double
```

```vbnet
            For Each GH11 In GH1
                For Each SA11 In SA1
                    report1(GH11, SA11)
                Next
                ListView1.Items.Add(Environment.NewLine)
            Next
        ElseIf EL >= 300 Then
            FOS = FOS - 0.03
            rockcallss()
            rockcallcl()
            Dim GH1() As Double = {2.4, 2.6, 2.8, 3.0, 3.2, 3.4}
            Dim SA1() As Double = {50, 55, 60, 65, 70, 75}
            Dim GH11 As Double
            Dim SA11 As Double

            For Each GH11 In GH1
                For Each SA11 In SA1
                    report1(GH11, SA11)
                Next
                ListView1.Items.Add(Environment.NewLine)
            Next
        ElseIf EL >= 250 Then
            FOS = FOS - 0.07
            rockcallss()
            rockcallcl()
            Dim GH1() As Double = {2.4, 2.6, 2.8, 3.0, 3.2, 3.4}
            Dim SA1() As Double = {50, 55, 60, 65, 70, 75}
            Dim GH11 As Double
            Dim SA11 As Double

            For Each GH11 In GH1
                For Each SA11 In SA1
                    report1(GH11, SA11)
                Next
                ListView1.Items.Add(Environment.NewLine)
            Next

        End If

    End Sub
    Public Sub report1(ByVal x, ByVal y)
        GH = x
        SA = y

        Dim x1 As Double
        Dim i As Double = 1.5

        If GW = "3.0" Then

            x1 = ((1.5) - (1.314 - (0.1099 * GH) + (0.01099 * PW) +
(0.005 * BW) - (0.00162 * SA))) / (0.065)

        ElseIf GW = "3.6" Then
```

```vb
            x1 = ((1.5) - (1.272 - (0.1099 * GH) + (0.01099 * PW) +
(0.005 * BW) - (0.00162 * SA))) / (0.065)
            ElseIf GW = "4.2" Then

            x1 = ((1.5) - (1.121 - (0.1099 * GH) + (0.01099 * PW) +
(0.005 * BW) - (0.00162 * SA))) / (0.065)

        ElseIf GW = "4.8" Then

            x1 = ((1.5) - (1.061 - (0.1099 * GH) + (0.01099 * PW) +
(0.005 * BW) - (0.00162 * SA))) / (0.065)

            Else
            MsgBox("invalid data") ''PT = "Please enter valid input"
        End If

        PT = Math.Round(PT, 2)
        ListView1.Items.Add(PT)

    End Sub

    Private Sub Button2_Click(ByVal sender As System.Object, ByVal e As
System.EventArgs) Handles Button2.Click

        If PrintDialog1.ShowDialog() = Windows.Forms.DialogResult.OK
Then

            Me.PrintForm1.PrinterSettings =
PrintDialog1.PrinterSettings
            Me.PrintForm1.PrintAction =
Printing.PrintAction.PrintToPreview
            Me.PrintForm1.Print()
        End If


    End Sub

    Private Sub Timer1_Tick(ByVal sender As System.Object, ByVal e As
System.EventArgs) Handles Timer1.Tick
        Label19.Text = Date.Now.ToString("dd-MM-yyyy")
        Label20.Text = Date.Now.ToString("hh:mm:ss")
    End Sub

    Private Sub Button3_Click(ByVal sender As System.Object, ByVal e As
System.EventArgs) Handles Button3.Click
        Me.Dispose()
    End Sub
End Class
```

201

KUMAR DORTHI

Personal Profile

Name	:	Kumar Dorthi
Permanent Address	:	S/o Rama Swamy
		5-124, Kunaram
		Kalva Srirampur,
		Peddapalli Dist.Telangana State, India -505174
		Mobile No.:9550944054,9490930371

ACADEMIC DETAILS:

- M.Tech. with **80.88%** First Class with Distinction in **Software Engineering**, in Kakatiya Institute of Technology & Science, Warangal Affiliated to Kakatiya University during 2009-11.

- B.Tech. with **77.80%** First Class with Distinction in **Computer Science and Engineering**, in Kakatiya Institute of Technology & Science, Warangal Affiliated to Kakatiya University during 2005-09.

- Intermediate with **93.10%** First Class with Distinction in **M.P.C** in Krishnaveni Jr. College, Kothagudem during 2003-05.

- Secondary School Certificate (SSC) with **89.66%** First Class with Distinction in A.P.S.W.R.SCHOOL, Koheda, Karimnagar in 2003.

EXPERIENCE:

- Worked as Lecturer in the Department of Computer Engineering in Singareni Collieries Polytechnic, CCC Naspur, Mancherial and Telangana State during 2012-14.

MEMBERSHIPS:

- Life Member of International Association of Engineers (IAENG). Membership ID: 121534.

- Associate member of Universal Association of Computer and Electronics Engineers (UACEE). Membership ID: AM10100052877.

- Member of International Computer Science and Engineering Society (ICSES). Membership ID: #621.

WORKSHOP/FDP:

- Attended 5 days short term course on "**Computer Application and Data Analysis in Mining and other Core Industries**" held during 12-16, March, 2018 at National Institute of Technology Karnataka, Surathkal.
- Attended 5 days short term course on "**Algorithmic Foundations of Wireless Sensor Networks with Applications**" held during 10-14, Dec, 2017 at National Institute of Technology Karnataka, Surathkal.
- Participated in National-level Faculty Development Program (FDP) on "**Data Analytics Using R**" held at REVA University, Bangalore during 24th -25th July, 2017.
- Participated in Meity, Govt of India, sponsored Faculty Development Program (FDP) on "**Machine Learning**" organized by E&ICT Academy, National Institute of Technology, Warangal, Nitte during 23rd -28th January, 2017.
- Attended one-day workshop on "**Virtualization: Foundation to Cloud Computing**" held at National Institute of Technology Karnataka, Surathkal, 9th January, 2017.
- Participated in "**National Workshop on Computing Systems Research**" held during 25-28, March, 2015 and funded by TEQIP-II at NMAMIT, Nitte.
- Attended 2-day National Level workshop focusing on" **Cloud Computing and Security Issues**" Organized by Cipher Cloud Pvt Software Solutions, Osmania University, Hyderabad, 2012.

PUBLICATIONS
Journals:

- Kumar D and Ram Chandar K (2017). "Zigbee based wireless data acquisition system for monitoring of partition stability above old underground coal workings", *Arabian Journal of Geosciences* (**Communicated-Under Review-SCI, Scoupus**).
- Kumar Dorthi and Ram Chandar K (2017). "Slope Stability Monitoring in Opencast Coal Mine based on Wireless Data Acquisition System- a Case Study", *International Journal of Engineering and Technology*(**Accepted-Scopus Indexed Journal**).

- Kumar, D., & Ram Chandar, K. (2017). "Computer aided slope stability monitoring: A critical review", *Disaster Advances,* Vol. 10(12), ISBN No.0974262X **(Scopus Indexed Journal)**.
- Kumar, D. and Ram Chandar, K. (2016). "Application of wireless sensor networks in slope stability monitoring – A critical review." *The Indian Mining & Engineering Journal*, Vol. 55, 29-32, ISSN No.0019-5944.

Conferences:

- Kumar, D. and Ram Chandar, K. (2016). "Stability analysis of old underground coal workings using Wireless Sensor Networks (WSNs)", *International Conference on Recent Advances in Rock Engineering***,** DOI:10.2991/rare-16.2016.14., Bengaluru, India. **(International Society for Rock Mechanics (ISRM) Specialized Conference)**.
- Kumar, D., Ram Chandar, K. and Alston D'Souza. (2016). "Effect of partition of overburden on stability of old underground workings." *Proc. INDOROCK-16***, IIT Bombay**, 17-18, June, 950-970. (Sponsored by **International Society for Rock Mechanics (ISRM)**).